

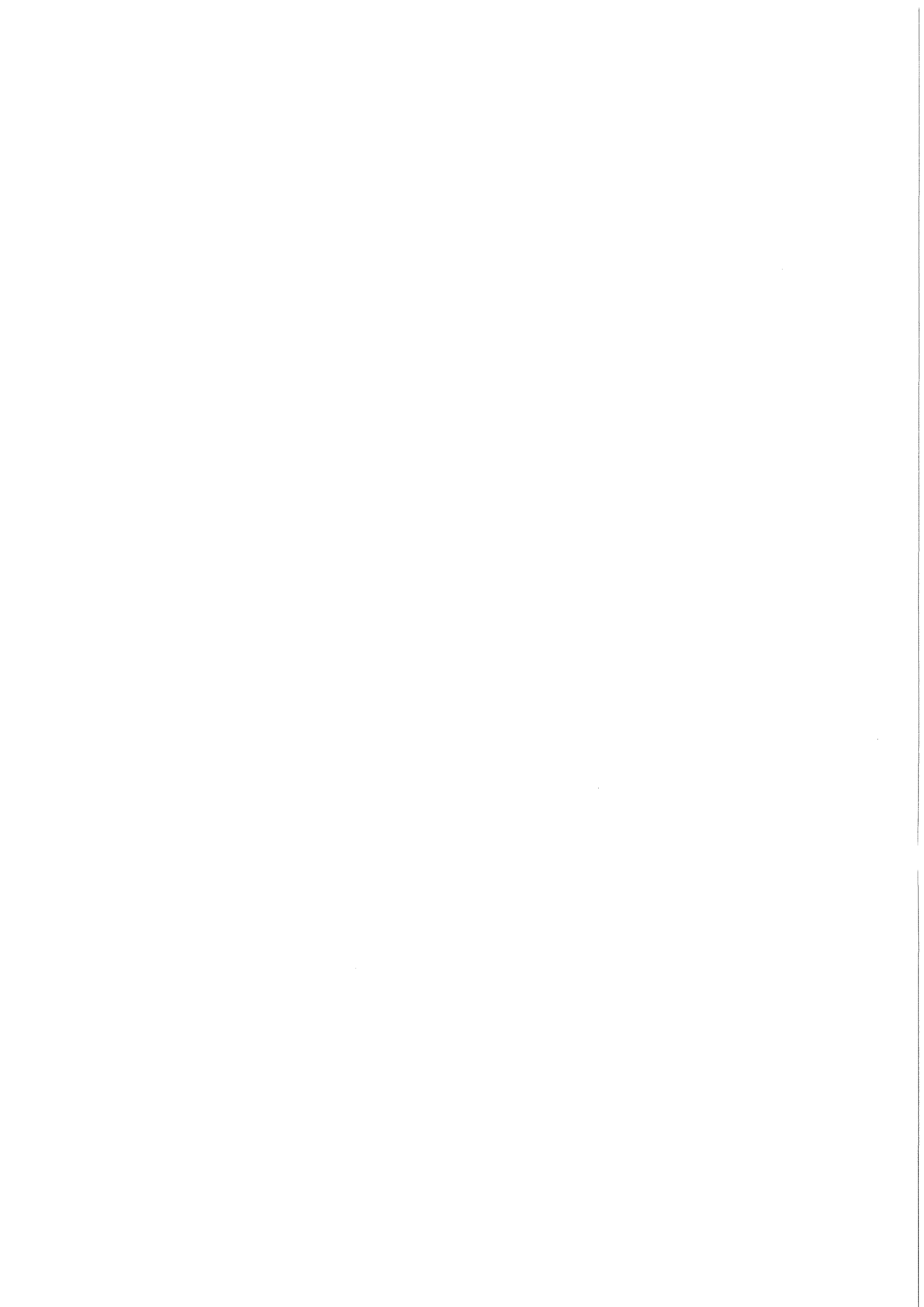
KfK 4355
November 1987

NET Model Coil Test Possibilities

Final Study Report, November 1987

**J. Erb, A. Grünhagen, W. Herz, I. Horvath, K. Jentsch,
P. Komarek, K. Kwasnitza, E. Lotz, S. Malang, C. Marinucci,
W. Maurer, G. Nöther, G. Pasztor, A. Peters, A. Roeterdink,
C. Sborchia, A. Ulbricht, A. Vogt, P. Weymuth, G. Zahn**
Projekt Kernfusion

Kernforschungszentrum Karlsruhe



KERNFORSCHUNGSZENTRUM KARLSRUHE

PROJEKT KERNFUSION

KfK 4355

NET Model Coil Test Possibilities

Final Study Report, November 1987

J. Erb¹, A. Grünhagen¹, W. Herz¹, I. Horvath², K. Jentzsch¹, P. Komarek¹,
K. Kwasnitza², E. Lotz¹, S. Malang¹, C. Marinucci², W. Maurer¹, G. Nöther¹,
G. Pasztor², A. Peters³, A. Roeterdink³, C. Sborchia², A. Ulbricht¹, A. Vogt¹,
P. Weymuth², G. Zahn¹

Contract No.	238/86-6/FU-CH/NET
	239/86-6/FU-NL/NET
	240/86-6/FU-D /NET

-
- 1 Kernforschungszentrum Karlsruhe
 - 2 Schweizerisches Institut für Nuklearforschung
 - 3 Stichting Energieonderzoek Centrum Nederland

Kernforschungszentrum Karlsruhe GmbH, Karlsruhe

Als Manuskript vervielfältigt
Für diesen Bericht behalten wir uns alle Rechte vor

Kernforschungszentrum Karlsruhe GmbH
Postfach 3640, 7500 Karlsruhe 1

ISSN 0303-4003

Abstract

A single full size coil for NET/INTOR represents an investment of the order of 40 MUC (Million Unit Costs). Before such an amount of money or even more for the 16 TF coils is invested as much risks as possible must be eliminated by a comprehensive development programme. In the course of such a programme a coil technology verification test should finally prove the feasibility of NET/INTOR TF coils. This study report is almost exclusively dealing with such a verification test by model coil testing. These coils will be built out of two Nb₃Sn-conductors based on two concepts already under development and investigation. Two possible coil arrangements are discussed:

- A cluster facility, where two model coils out of the two Nb₃Sn-TF-conductors are used, and the already tested LCT-coils producing a background field.
- A solenoid arrangement, where in addition to the two TF model coils another model coil out of a PF-conductor for the central PF-coils of NET/INTOR is used instead of LCT background coils.

Technical advantages and disadvantages are worked out in order to compare and judge both facilities. Costs estimates and the time schedules broaden the base for a decision about the realisation of such a facility.

Testmöglichkeiten für NET Modellspulen

Zusammenfassung

Eine Einzelspule für NET/INTOR stellt eine Investition in der Größenordnung von 40 MUC (Millionen Kosteneinheiten) dar. Bevor solch ein Betrag oder noch mehr für die 16 TF-Spulen insgesamt investiert wird, müssen mit Hilfe eines umfassenden Entwicklungsprogramms so viele Risiken wie möglich eliminiert werden. Im Verlauf eines solchen Programms muß die Machbarkeit der NET/INTOR Spulen in einem Technologietest verifiziert werden. Diese Studie befaßt sich fast ausschließlich mit solch einem Verifikationstest mit Hilfe von Modellspulen.

Diese werden aus zwei Nb₃Sn-Leitern gebaut, die beide bereits in der konzeptionellen Entwicklungsphase untersucht werden. Zwei mögliche Spulenanordnungen werden diskutiert:

- eine Cluster-Anlage, bei der zwei Modellspulen aus den beiden Nb₃Sn-TF-Leitern und bereits getestete LCT Spulen zur Erzeugung eines Hintergrundfeldes benutzt werden und
- eine Solenoidanordnung, bei der zusätzlich zu den beiden TF-Modellspulen noch eine Modellspule aus einem PF-Leiter für die zentralen Solenoide von NET/INTOR benutzt wird.

Technische Vor- und Nachteile werden ausgearbeitet, um beide Anordnungen vergleichen und beurteilen zu können. Kostenabschätzungen und Zeitpläne verbreitern die Basis für eine Entscheidung über die Realisierung einer solchen Anlage.

TABLE OF CONTENTS

	Page
1. Introduction	1
2. The Goals of the Test	
2.1 NET Development Programme	4
2.2 Description of the TF-Conductors	5
2.3 Description of Conductors for pulsed Solenoids	14
2.4 General Objectives of the Model Coil Test Programme	17
2.5 NET Test Requirements	18
2.5.1 Test Requirements of the TF Coils	19
2.5.2 Test Requirements of the OH Coils	20
3. Cluster Test Facility	
3.1 Introduction	23
3.2 Development of a useful Cluster Configuration by parametric Calculations	24
3.3 Restrictions and Consequences of the Constraint to use the existing Vacuum Vessel	33
3.3.1 Reduction of the minimum Bending Radius	33
3.3.2 Enhancement of operational Current in EU-LCT	33
3.3.3 Enhancement of the Current in the NET-Test Coils	40
3.4 Testing of OH-Conductor in the Cluster Test Facility	40
3.5 Further Reduction of the Bending Radius	40
3.6 Summary	46

4.	Solenoid Test Facility	
4.1	Introduction	49
4.2	Development of a Solenoid Test Facility S1	49
4.3	Description of the Solenoid Test Configuration S1	55
4.4	Solenoid Test Facility with 1m Bending Radius	60
5.	Forces and Stresses in the Model - Coils	
5.1	Forces and Stresses in the Cluster Test Facility	66
5.1.1	Stresses in the TF-Model Coils	71
5.1.2	Stresses in the EU-LCT Coil	98
5.1.3	Structural Feasibility of the Swiss LCT Coil	103
5.2	Forces and Stresses in the Solenoid Test Facility	112
5.2.1	TF - Model Coils	112
5.2.2	OH - Model Coil	115
5.2.3	Comparison of the numerical Result	119
5.2.4	Discussion and Conclusion	122
6.	Installation of the Test - Rig	
6.1	Cluster Configuration	126
6.1.1	Cluster Configuration C3 with a minimum Bending Radius of 1.2 m	126
6.1.2	Cluster Configuration C6 with a minimum Bending Radius of 1.0 m	129
6.2	Installation of the Solenoid Configuration	135

7.	Cooling Considerations	138
7.1	Cluster Facility	139
7.1.1	Cooling of the LCT - Coils at 3.5 K	139
7.1.2	An 1.8 K Cooling option for the LCT - Coils	143
7.2	Cooling Considerations of the Solenoid Facility	146
7.3	Summary	151
8.	Costs Estimate	
8.1	Costs of the Cluster Configuration C6	153
8.2	Costs of the Solenoid Configuration S3	157
9	Time Schedule	162
9.1	Time Schedule for the Cluster Facility	163
9.2	Time Schedule for the Solenoid Facility	164
9.3	Comparison of Time Schedule of M 7	165
10.	Model Coil Test Programme (NET)	
10.1	Design Approach	166
10.1.1	Test Programme for the TF - Model Coils in TOSKA-Upgrade	166
10.1.2	Test Procedure	167
10.1.3	Instrumentation and Quench Detection	169
11.	Further Use of TOSKA	
11.1	Magnet Test Facility	172
11.2	Blanket Test Facility	172
11.3	Non Nuclear Component Test Stand	176

12.	Other Possibilities for Testing	
12.1	Solitary OH - Model Coil Test	178
12.2	Pancake Tests in SULTAN III	179
12.2.1	Introduction	179
12.2.2	Assumptions and Calculations	179
12.2.3	Budget (in kSFr.)	181
12.2.4	Time Schedule	183
13.	Technical Comparison of the Cluster and Solenoid Test Facilities	191
14.	Conclusions and Proposals	
14.1	General	201
14.2	Conclusions	202
14.3	A Proposal to meet the Test Goals	203

1. Introduction

One major task in the area of the fusion technology programme is to develop a toroidal field (TF) magnet system for NET/INTOR with superconducting coils of about 8 x 11 m bore, generating a maximum field of 11 - 12 Tesla, highly reliable in the Tokamak environment at a stored energy level of tens of Gigajoules. A significant present step in this task is the International Large Coil Task Project (LCT), initiated in 1977 as a joint effort by the USA and its partners EURATOM, Japan and Switzerland. The Large Coil Task, however, will not give the final answer to all problems of the toroidal field system for the next step. The field in LCT is limited to about 8 T due to the use of NbTi superconductors except one coil. The next step, however, will have 11 to 12 T fields requiring the Nb₃Sn technology for TF coils. LCT coils are about one third of the size for NET/INTOR, a size which allows the extrapolation of the coil manufacturing technique.

A single full size coil for NET/INTOR represents an investment of the order of 40 MUC (Million Unit Costs). A fully relevant operational test is only possible with at least three such coils forming a torus segment requiring structural and cryogenic installation comparable to the corresponding final components of NET/INTOR itself. Therefore, it is very probable that full size coil fabrication and tests will only be possible as first phase of the final commissioning of NET/INTOR, with the sequence of coil fabrication being influenced by successive performance tests of the first set of coils. For such an undertaking prior of final design as much risks as possible must be eliminated by implementation of a comprehensive development programme closing the gap from LCT to NET in several areas such as:

- design studies (covered by NET/INTOR studies)
- high field conductor development
- full size conductor test
- full size and/or subsize pancake test
- coil technology verification test.

The European fusion technology programme covers in the area of magnets the development of high field superconductors and the feasibility demonstration of the superconducting coils for the NET device. The major programme steps defined and partially already under execution for the TF-coils of NET are:

- LCT coil tests (task M1);
- Construction of SULTAN facility and application of A15 conductors in medium size magnets (task M2);
- Development and testing of short samples (few meters) of the NET conductor (16 kA rated current at 11 T) (tasks M2 and M3);
- Industrial fabrication of prototype lengths of the NET conductor (~ two or three pieces of about 1 km length) (task M5);
- TF model coil manufacturing and testing (tasks M6 and M7), with the conductors made available in task M5.

This study report is exclusively dealing with the last programme item, namely the TF model coil testing. It was undertaken in order to define a most suited and relevant test arrangement for such model coils. It is assumed that these model coils will be built out of two Nb₃Sn-conductors, based on concepts under development and investigation now (task M3). Winding and cooling conditions should be as in the later full size NET coils in order to be relevant.

As a first arrangement a so-called "Cluster Test Facility" was investigated. It uses the both European LCT coils as background field coils and existing equipment at KfK, as the TOSKA-facility, used for the domestic LCT-coil tests and the POLO-tests (M4).

As an alternate arrangement, a so-called "Solenoid Test Facility" was proposed by the NET-team in June 1986 [1.1] and studied as well. It combines the test of the two TF-conductor model coils together with an OH-conductor coil as a common high field solenoid. It is based on the assumption, that in the PF-coil development programme such a large OH-winding test is requested (task M13). Aim of the study was to evaluate these arrangements in detail for the same boundary conditions as minimum conductor bending radius, use of existing TOSKA-vacuum vessel etc.. For both cases solutions could be found, which can be realized from an engineering point of view. For the relevance of NET, the technical difficulties, costs and time frame, and differences have been identified.

The study represents the common effort of the three associated Euratom laboratories ECN, SIN and KfK. The work has been performed under the NET contracts numbers 238/86-6/FU-CH/NET, 239/86-6/FU-NL/NET, and 240/86-

6/FU-D/NET. The basis of the study was Annex A [1.2] to the above mentioned contracts. It should provide a solid basis for further decisions concerning the programme step "NET-TF model coil testing" (tasks M6/M7).

References to Chapt. 1:

- [1.1] R. Pöhlchen, Minutes of the "Pancake Test Meeting" at KfK on the 27th of June 1986, private communication.
- [1.2] R. Pöhlchen, Technical Specification for the Study of the NET TF Pancake Test, private communication.

2. The Goals of the Test

2.1 NET Development Programme

The main steps of the development programme for the TF conductors are given in the following tasks:

M3: Conductor Development (until 1987)

- stability, current sharing of subscale conductors
- fabrication and test of NET subscale and 1:1 prototype conductors

M5: Conductor Fabrication (until 1990)

- conductor fabrication (handling) of unit winding length(s)
- short sample tests
- accompanying laboratory measurements

The outcome of an industrial development contract will be pieces of conductors with lengths representative for the production line and NET coil winding lengths.

Quality assurance covers the materials and components up to short conductor samples. For further handling, applied manufacturing techniques and the integration of other components in the winding will have an impact on the overall performance of conductor and coil. Therefore it is proposed to manufacture model coils from these conductor pieces. The programme for this is:

M6: Model Coil Fabrication (1991)

- conductor handling and winding experience for double pancakes
- assembling and impregnation experience
- ground and pancake to pancake insulation
- joints of conductors

M7: Tests of Model Coils (1992)

- stresses in comparison with FEM-calculations
- quench and stability characteristics
- nuclear heat and AC-load simulation if necessary
- cooling conditions e.g. helium mass flow and pressure drop

In parallel to this development programme there are some components which have to be developed during this time e.g. vapour cooled leads for 25 kA having low losses, pulse coils for AC-loss effects, joints, specific devices for additional mechanical loads.

A similar development programme for PF coils is underway (M4, M8). The steps are:

M4: NET relevant conductor and coil development

- Low AC-losses
- Stability
- High voltage
- Design and construction of a model coil
- Test in TOSKA

M8: PF-coil for TORE-SUPRA

- Design and construction of a PF coil with a diameter of about 8 m
- Test of the coil in TORE-SUPRA

The conductors developed so far for PF coils are NbTi-conductors. However, Nb₃Sn conductors are also under study.

2.2 Description of the TF-Conductors

References 2.1 and 2.2 contain the design procedure and the description of the TF-conductors. The latest design is given in Figs. 2.1-1, 2.1-2. and 2.1-3. The conductors are built up by a superconducting cable core, two electrical stabilizer units and a steel conduit. The SIN and ECN TF conductor designs are quite similar. The current density differs only by 3 %. The choice of the characteristic data of the SIN conductors for the calculation and design of the SULTAN-Test Coil is arbitrarily and was agreed among the collaboration.

The main characteristic data of the SIN conductor are:

<u>Outer conductor dimensions</u> (without insulation)	25.2 x 26.1 mm ²
Insulation thickness	0.8 mm
Critical current at 11,1 T/4.5 K	39.2 kA
Rated current at 12 T	16 kA
Nominal current density	2180 A/cm ²

Strand

Diameter	0.125 mm
Filament number	306
Filament size	4 μm
(Cu + Sn) to Nb ratio	2.26

Flat cable

Dimensions (after reaction)	6.6 x 19.8 mm ²
Superconducting strand number	19 x 5 x 4 x 12
Bronze core dimensions	0.65 x 15.9 mm ²
Pitch lengths	
1. stage	8 mm
2. stage	25 mm
3. stage	45 mm
4. stage	160 mm

Stabilizer (Cu + CuNi)

Dimensions	63 x 20.1 mm ²
Cooling channel dimensions	3.2 x 4.0 mm ²
CuNi to Cu ratio	1 : 3.6
Twist pitch	100 cm

Steel jacket (316 LN)

Thickness	3 mm
-----------	------

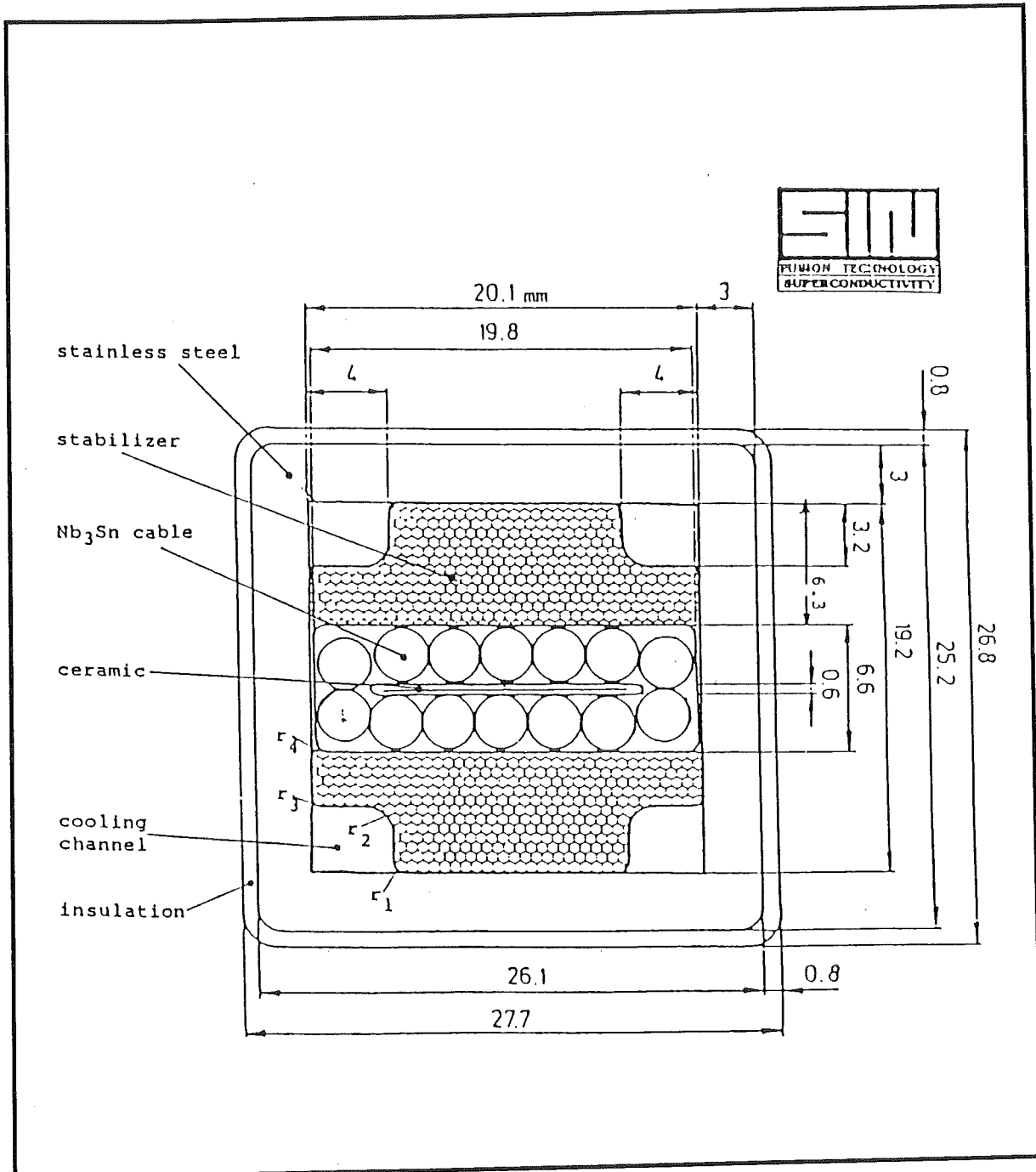


Fig. 2.1-1: Cross Section of the SIN-Conductor (all lengths in mm)

The main characteristic data of the ECN conductor are:

Specification ECN NET TF-conductor (16 kA, 11 T, 4.5 K)

1. Strand material

Wire diameter	0.85 mm
Number of filaments	1014
Composition (vol. %)	
copper	52.2 %
niobium	36.9 %
powder	10.9 %
Filaments diameter	
niobium	19 μm
powder unreacted	9 μm
Nb ₃ Sn reacted	13 μm
Twist pitch (left hand pitch)	25 mm
RRR value	> 120
Critical current at 4.2 K and 11 T	> 400 A (10 ⁻¹⁴ Ωm criterion)

2. First stage cable

Composition	1 x Cu (0.6 mm diameter) 5 x Nb ₃ Sn (0.85 mm diameter)
Outer diameter	2.3 mm
Twist pitch (left hand pitch)	16 mm
Copper core	half hard OFHC copper RRR value > 120
Critical current at 4.2 K and 11 T	> 1900 A

3. Rutherford cable (2nd stage)

Number of 1st stage cables	20
Dimensions Rutherford cable	
width	23.3 mm
height	4.8 mm
twist pitch (left hand pitch)	263 mm
Core strip	
width	18.5 mm
height	0.6 mm
(including ceramic insulation)	
Reaction heat treatment	96 hrs at 700°C in argon atmosphere
Impregnation	soft solder PbSn (40/60) after heat treatment
Critical current at 4.2 K and 11 T	> 36000 A

4. Stabilizator

Basic material	Cu wires with CuNi (70/30) cladding
Material to be produced by cabling followed by cold work.	
Dimension	15.6 x 5.6 right hand pitch
All cables impregnated with PbSn (40/60) solder.	
Twist angle cables	approx. 11°

5. CuNi barrier strips

Material CuNi	30 % Ni, 70 % Cu
Temper	soft
Dimensions	24 x 0.5 mm ²

6. Stainless steel jacket

- a) 2 x 22 mm x 2.5 mm
- b) 2 x 24 mm x 2.5 mm
- c) 4 x 5.6 mm x 1.0 mm

Material	AISI 316 LN
Temper	annealed

7. Weldments

Stainless steel casing:	TIG or laser-welded
Stainless steel strips:	SPOT-welded

8. Soldered joints

Rutherford cable to CuNi barriers

CuNi barriers to stabilizator

} PbSn (40/60) as solder

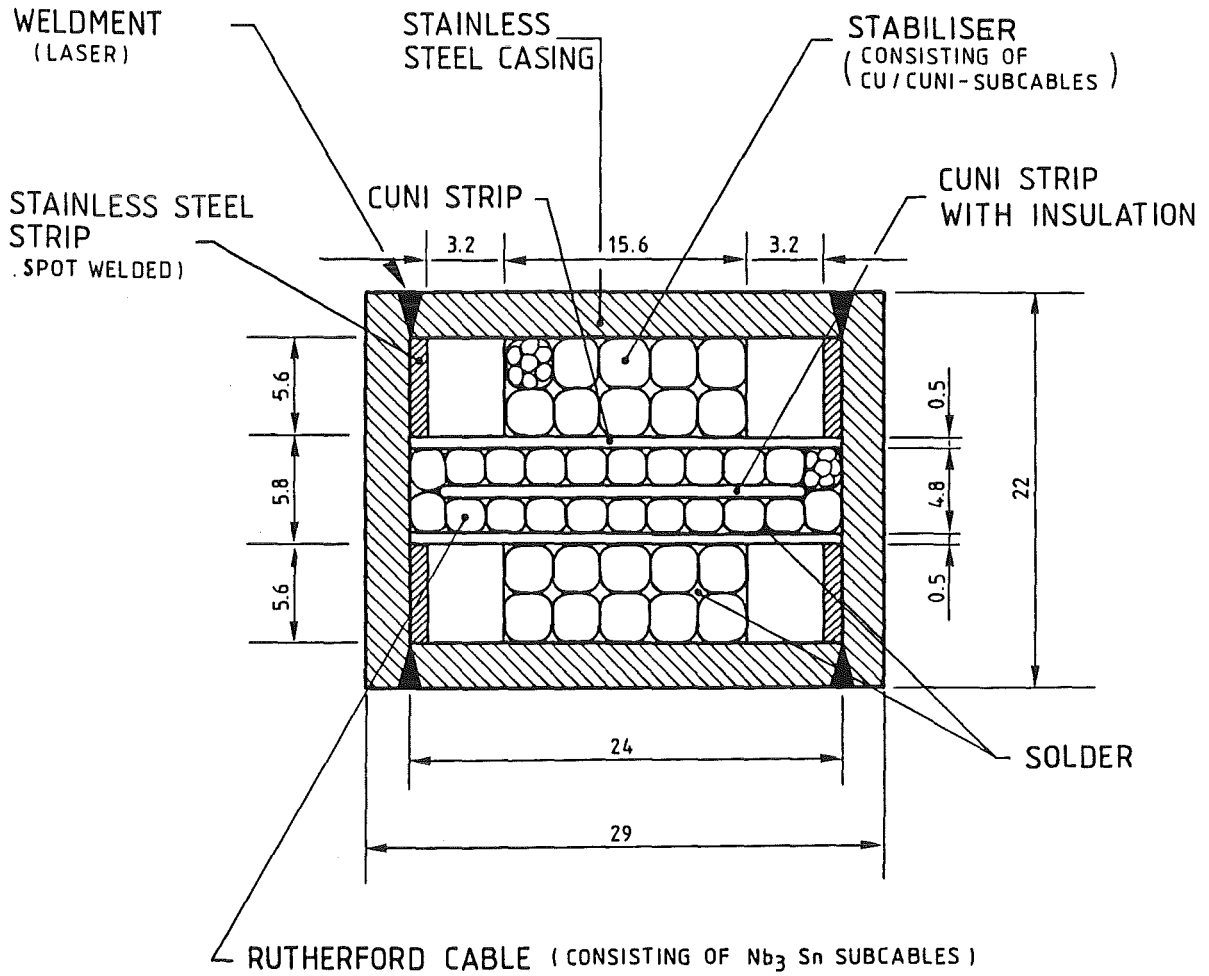


Fig. 2.1-2: Cross Section of the ECN-Conductor (all lengths in mm)

The main characteristic data of the KfK conductor are (End of 1986):

Outer conductor dimensions 37.0 x 16.5 mm²
(without insulation)

Insulation thickness 0.5 mm

Critical current at 12 T/4.2 K 35 kA

Nominal current at 12 T 16 kA

Nominal current density 2406 A/cm²

Delivery in multiples of
either 800 m
or 1600 m

Superconducting cable core

Dimensions including CuNi sections 30.6 x 5.1 mm²

29 strands each 1.92 mm diameter

Transposition length 600 mm

Ceramic coated strip 25.1 x 0.5 mm²

Thickness of coating ~50 μm

Dimensions of CuNi10-U sections 30.2 x 4.7 mm²

U sections are slit with slit dimensions 2 x 4,7 mm²

Stabilizer unit

Outer dimensions 30.6 x 4.2 mm²

Stainless steel core 0.5 x 24.6 mm²

Kapton foil in between 0.05 x 20.0 mm²

13 rectangular wires (sections)
with 3.0 x 1.6 mm each, made out of
1/4 hard copper. The transposition
length is 600 mm.

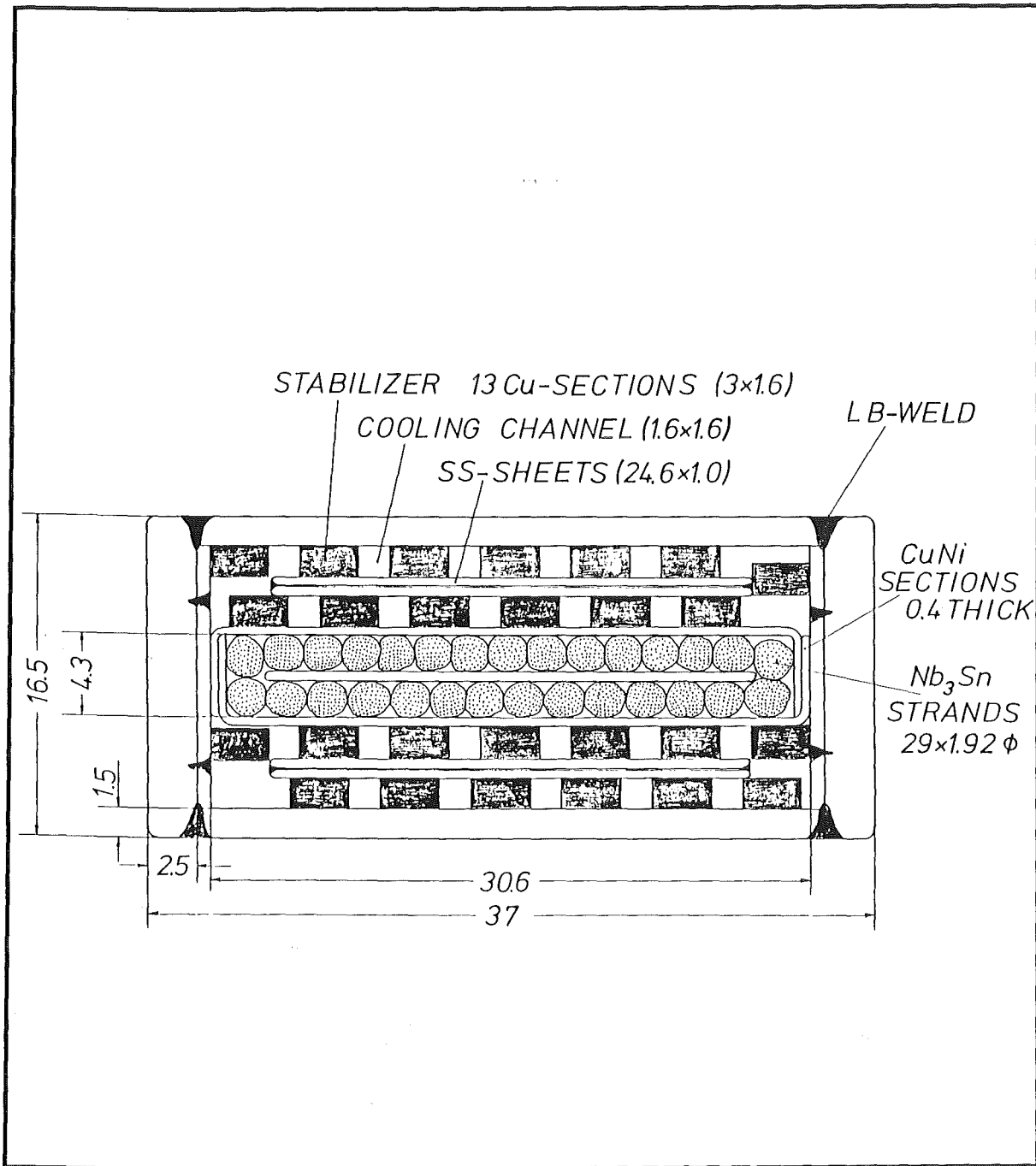


Fig. 2.1-3: Cross Section of KfK-Conductor (all lengths in mm)

Strands

Superconducting material	Nb ₃ Sn (or (Nb-7Ta) ₃ Sn)
Processing	Bronze process
Strand diameter	1.92 mm
Bronze / Nb ratio	3.1 : 1
Stabilization of strands	internal Cu (23 %), separated from the bronze by a Ta (4 %) barrier
Number of filaments in strand	~ 56.000
Size of filament	~ 4 μm
Twist pitch	50 mm
*J _c (non copper) at 12 T / 4.2 K	5.5 x 10 ⁴ A/cm ²
*J _c (overall strand) at 12 T / 4.2 K	4.2x 10 ⁴ A/cm ²
* without degradation	

2.3 Description of Conductors for pulsed Solenoids

During the study the NET-team proposed to investigate also the possibility of testing an OH conductor for the central solenoid (CS) of the NET machine. Fig. 2.1-4 shows a cross section delivered by the NET team. This type of conductor is studied by BBC, Switzerland [2.3], and it is similar to the conductor used in the Westinghouse coil in the International Fusion Superconducting Magnet Test Facility (IFSMTF) in Oak Ridge, USA [2.4]. For calculation purposes an insulation thickness of 1 mm is assumed. The nominal conductor current is 40 kA, therefore the nominal current density is 2.4 kA/cm².

The outer pulsed coils of NET may have NbTi conductors. The proposed conductor type is shown in Fig. 2.1-5. This concept is already developed and will be tested in TOSKA with a model coil of about 3 m diameter [2.5].

Another study [2.6] considers NbTi conductors subcooled to 1.8 K. This allows to enhance the maximum field to about 11 T. It is proposed to use the conductor type discussed in [2.6] for both coil systems, for the PF-coils as well as the TF-coils.

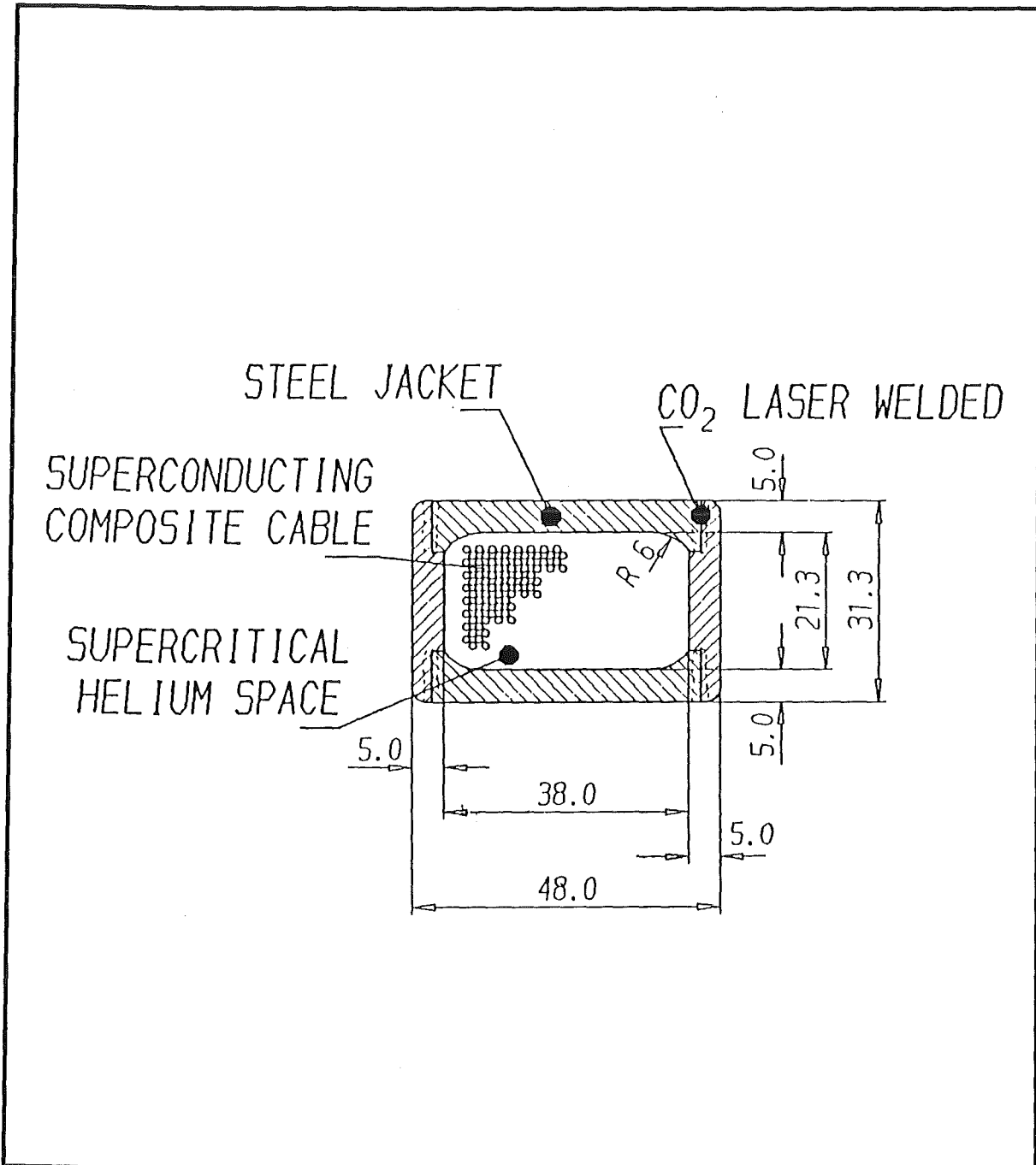


Fig. 2.1-4: Cross Section of OH-Conductor (all lengths in mm)
(Insulation thickness is supposed to be 1 mm.)

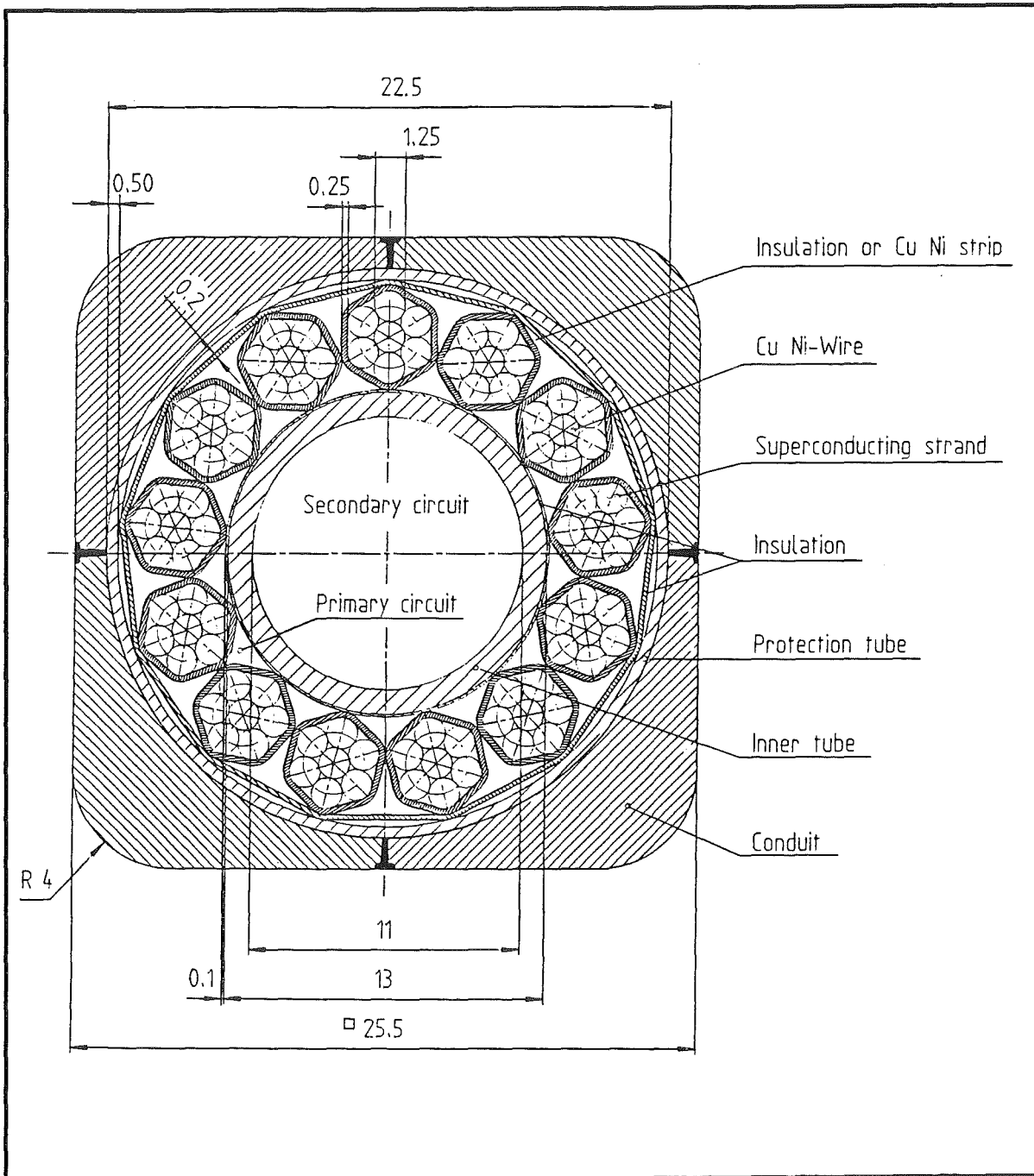


Fig. 2.1-5: Conductor Type for outer poloidal Field Coils

2.4 General Objectives of the Model Coil Test Programme

The primary goals of the model coil test programme include [2.7]

- development of the entire coil manufacturing process including coil winding of double pancakes, conductor termination and joints, coil insulation, assembly, vacuum impregnation, current leads, feed throughs and instrumentation,
- verification of the success of the industrial manufacturing process by testing the coils under operation as close as possible to NET conditions,
- validation of design codes for stress analysis and quench behaviour and validation of predictions of performance made on the basis of sub-size component tests,
- performance of tests that can only be made in a large coil test and that may point up synergistic effects,
- selection among the conductor options based upon test performance, manufacturing evaluation, and cost evaluation.

The model coils shall have geometrical dimensions which are representative for NET coils in certain limits. In its test bed the model coil shall reach field and stress values which are either identical with those of the NET coils or allow a scaling. The model coils shall demonstrate in its test bed that the manufacturing techniques of conductor and coil is ruled by engineering standards and is reproducible.

The general goals mentioned above in the section covered a quantity of objectives which have in the sum to demonstrate the availability of the developed technology for application.

The objectives can be divided into two major groups: direct and indirect test objectives.

- Direct test objectives:

The direct test objectives are determined by the specifications of the final product: the model coil. The specifications are measurable facts characterizing the model coils. Some of them are verified by the use of special equipment. These will be discussed in detail in the following sections.

There are components which can't be tested sufficiently without the model coil or which are needed for the operation of the model coil. All electrical and thermohydraulic protection systems of the model coils belong to these objectives. The dynamic behaviour of such systems is strongly correlated to the coil and the arrangement of the coils. Another item is the optimization of thermohydraulic operation parameters which are needed for the design of an economic cryogenic system for the NET magnets.

- indirect test objectives:

The manufacturing of the conductor and the coils requires an extended development programme in order to obtain a reproducible production process which is then handled by the quality assurance program. The model coil manufacturing is partly a test of the process for the NET coil production. Therefore this process is indirectly tested if the model coil reaches its specifications.

2.5 NET Test Requirements [2.7]

Tests for both the TF and OH coils can generally be divided into two categories, namely tests at standard NET operating conditions and tests to determine the limits of operation. Given the different missions of the two coil types, the specific test requirements for each type will be different. The tests should simulate as close as possible the actual NET operating conditions including magnetic field, current, strain and transient operation.

The coils should be designed and instrumented to extract as much information as possible. However, the experimental nature of these coils and the imposed instrumentation should not interfere with the safe operation of the coils or otherwise compromise the chances for a successful mission.

All test requirements for the model coils are based upon the assumption that a significant basis of knowledge of conductor performance and parameters has been determined by exhaustive tests on sub-size components and full-size conductors in short lengths. Results of tests that should be available for the prototype conductor and components include (but are not limited to):

- critical current as a function of magnetic field, temperature and strain (longitudinal, transverse, bending) ideally for the full-size conductor
- complete characterization of the AC loss as a function of \dot{B} , B , ΔB and I for three field orientations (2 transverse, 1 longitudinal) and various combinations thereof
- stability measurements as a function of mass flow rate, temperature, current, magnetic field and energy disturbance length and duration for the TF conductor and maximum current and field ramp rates (or AC operation) for the OH conductor
- quench and recovery behaviour as a function of operating current, field, temperature and mass flow rate including measurement of maximum pressure and temperature and quench propagation velocity as a function of dump delay time, and dump time constant.

To the extent these tests can't be completed, it becomes imperative that they be carried out in the model coil test. For example, it might be difficult to get sufficient data on quench behaviour from a sub-size test facility thus requiring more extensive testing in the model coil.

2.5.1 Test Requirements of the TF Coils

- The coils should be operated at the nominal NET conditions including current (16 kA), peak magnetic field (11,4 T), and global winding pack peak stress levels. The requirement to operate near NET stress levels may require the use of an external loading structure.
- Strain measurements should be used for comparison with results of FEM calculations for verification of the codes and measured or estimated global winding pack parameters.
- The DC limits of operation should be determined by measuring the critical current as a function of magnetic field and temperature.
- AC loss calculations and measurements should be verified by exposing the coil to AC or pulsed magnetic fields either self-generated or created by an external source.

- Stability calculations and measurements should be verified by exposing the coil to sudden energy inputs to discover the limits of stable operation.
- Quench tests should be performed in order to verify the quench codes, test the coil insulation system, test the quench detection and dump system, and cold helium recovery system.

2.5.2 Test Requirements of the OH Coils

- The coil should be energized in the AC mode ideally following the NET OH coil operating cycle including peak fields of 11.5 T at 40 kA. Measurements should verify AC loss calculations and measurements. The minimum requirement is for fast ramped or discharge operation.
- Strain measurements should be made for verification of FEM calculations and estimated or measured global winding pack parameters.
- The DC limits of operation should be determined by measuring the critical current as a function of magnetic field and temperature.
- The limits to stable AC operation should be determined by increasing the rates of field change until the coil quenches within the limits of the power supplies, dump circuits, and design voltages. Alternatively, energy perturbations can be superimposed on the normal operating cycle to determine the stability limits.
- Coil behaviour should be measured while quenching during AC operation with a parameter being the time during the cycle when the quench is initiated.
- Protection system verification test under operation conditions.

Table 2.1: Target Test Values

TF - COILS (TF-Conductors)

Parameter	Value
Maximum Field at Conductor (T)	11.4
Operating Current (kA)	16
Peak Winding Pack Stresses	
- Radial (MPa)	-40
- Toroidal (MPa)	-140
- Hoop (MPa)	140
- Shear (MPa)	30
Maximum Rate of Field Change	
- Normal Operation (T/s)	0.55
- Plasma Disruption (T/s)	1.0*
Nuclear Heating in Winding Pack	
- Average (mW/cm ³)	0.05
- Peak (mW/cm ³)	0.3

* Estimate, to be confirmed by further analysis.

CS - COILS (OH-Conductors)

Parameter	Value
Maximum Field at Conductor (T)	11.5
Operating Current (kA)	40
Peak Winding Pack Stresses	
- Radial (MPa)	10
- Toroidal (MPa)	100
- Hoop (MPa)	200
- Shear (MPa)	30
Maximum Rate of Field Change	
- Normal Operation (T/s)	2.4
- Plasma Disruption (T/s)	3.0*

* Estimate, to be confirmed by further analysis.

References to Chapt. 2:

- [2.1] Flükiger et al, An A15 Conductor Design and its Implication for the NET-II TF-Coils, Final Study Report, KfK Report 3937, June 1985.
- [2.2] C. Marinucci, P. Bruzzone, I. Horvath, B. Jakob, K. Kwasnitza, G. Pasztor, G. Vecsey, C. Wassermann, P. Weymuth, "NET toroidal field coil design studies. Final Report" - SIN-Report KRYO-87.3 (1987).
- [2.3] R. Pöhlchen, E. Salpietro, private communication.
- [2.4] L. Dresner et al., First Tests of the Westinghouse Coil in the International Fusion Superconducting Magnet Test Facility (IFSMTF). Applied Superconductivity Conference ASC-86, Baltimore, Maryland, USA, Sept. 28 - Oct. 3, 1986.
- [2.5] S. Förster et al., A 2 MJ 150 T/s pulsed Ring Coil. Status of the Design and the Test Arrangements. Magnet Technology, 9th Internat. Conf., September 9 - 13, 1985, Zürich, Switzerland.
- [2.6] B. Turck, J.L. Duchâteau, Forced Flow subcooled HeII Superconducting Coils for the Central Solenoids of NET, TS/44-87-03.
- [2.7] J. Minervini, NET-team, NET/87/TE-100-R-04, 29.06.1987.

3. Cluster Test Facility

3.1 Introduction

A first layout of a TOSKA Test Facility for the verification testing of superconducting coils made of toroidal field (TF) coil conductors is already discussed in [3.1]. The conductors to be tested are described in Chapter 2.

Test conditions in the earlier discussed facility [3.1] were:

- a nominal current of 20 kA and about 11 T at the Nb₃Sn conductor
- a minimum bending radius of 1.5 m for the Nb₃Sn conductor,
- a peak field of not more than 8.4 T at the NbTi conductor of background field coils.
- use of the least amount of Nb₃Sn conductor in the test for cost reasons.

These constraints would be fulfilled, but the arrangement of the coils required a new vacuum vessel in the KfK-TOSKA-Facility.

The investigations now, which started in January 1986, are made under the constraint to use as much as possible the existing facility, especially the installed vacuum vessel, and keep low the modification and installation work. The aim was to find a solution and the restrictions of this at the realization and to undertake a comparison with respect to costs, physics restrictions, installation work, maintenance, repair work, and expense for exchange of test coils, if necessary.

In addition, the test facility should allow the simultaneous testing of both conductors for the NET-TF coils proposed by the SULTAN group and KfK. This facility where the LCT coils are prone to each other is called in the following Cluster Test Facility.

3.2 Development of a useful Cluster Configuration by parametric Calculations

The constraint of using the existing vacuum vessel led to a serious consequence for the minimum bending radius of the conductor. Table 3.2-1 contains the main parameters of a parameter study (until June 86) for four different cases. The LCT coils are operated at 13 kA for the first three cases; this is the nominal current of the CH-LCT-coil and 14% higher than the nominal current of the EURATOM-LCT-coil (11.4 kA). The NET-test coils are first considered to be operated at their nominal current at 16 kA instead of 20 kA which was decided in the mean time after some changes in the TF-conductor designs.

The starting configuration C1 is shown in Fig. 3.2-1 keeping the inner diameter of the test coils to 3 m corresponding to 1.5 m minimum bending radius. It should be mentioned that only the winding cross section (without casing) is drawn. This configuration has only 6 T at the conductor of the test coils, too low to fulfil the test requirement. Using this configuration as a starting one new configurations were developed by applying different means.

Table 3.2-1: Results of a Parameter Study for the Cluster Test Facility

CONFIGURATION:	C1	C2	C3	C4
<u>EU - LCT - COIL</u>				
CURRENT [kA] :	13	13	13	11.6
B max [T] :	8	7.7	8.8	8.0
TEMPERATURE [K] :	4.2	4.2	3.5	3.5
<u>CH - LCT - COIL</u>				
CURRENT [kA] :	13	13	13	11.6
B max [T] :	8	7.7	7.3	7.0
TEMPERATURE [K] :	4.2	4.2	3.5	3.5
<u>NET - KfK TEST COIL</u>				
CONDUCTOR :	KfK	KfK	KfK	KfK
NUMBER OF TURNS :	140	180	180	180
INNER DIAMETER [m] :	3	2.4	2.4	2.4
CURRENT [kA] :	16	22	22	22
B max [T] :	6	11	11.5	11.1
TEMPERATURE [K] :	4.2	4.2	4.2	4.2
<u>NET - SULTAN TEST COIL</u>				
CONDUCTOR :	SULTAN	SULTAN	SULTAN	SULTAN
NUMBER OF TURNS :	126	160	180	180
INNER DIAMETER [m] :	3	2.4	2.4	2.4
CURRENT [kA] :	16	22	22	22
B max [T] :	6	10.8	11.5	11.1
TEMPERATURE [K] :	4.2	4.2	4.2	4.2
Remarks :	B _{max} too low	B _{max} at test coils too low	Reference case June 86	

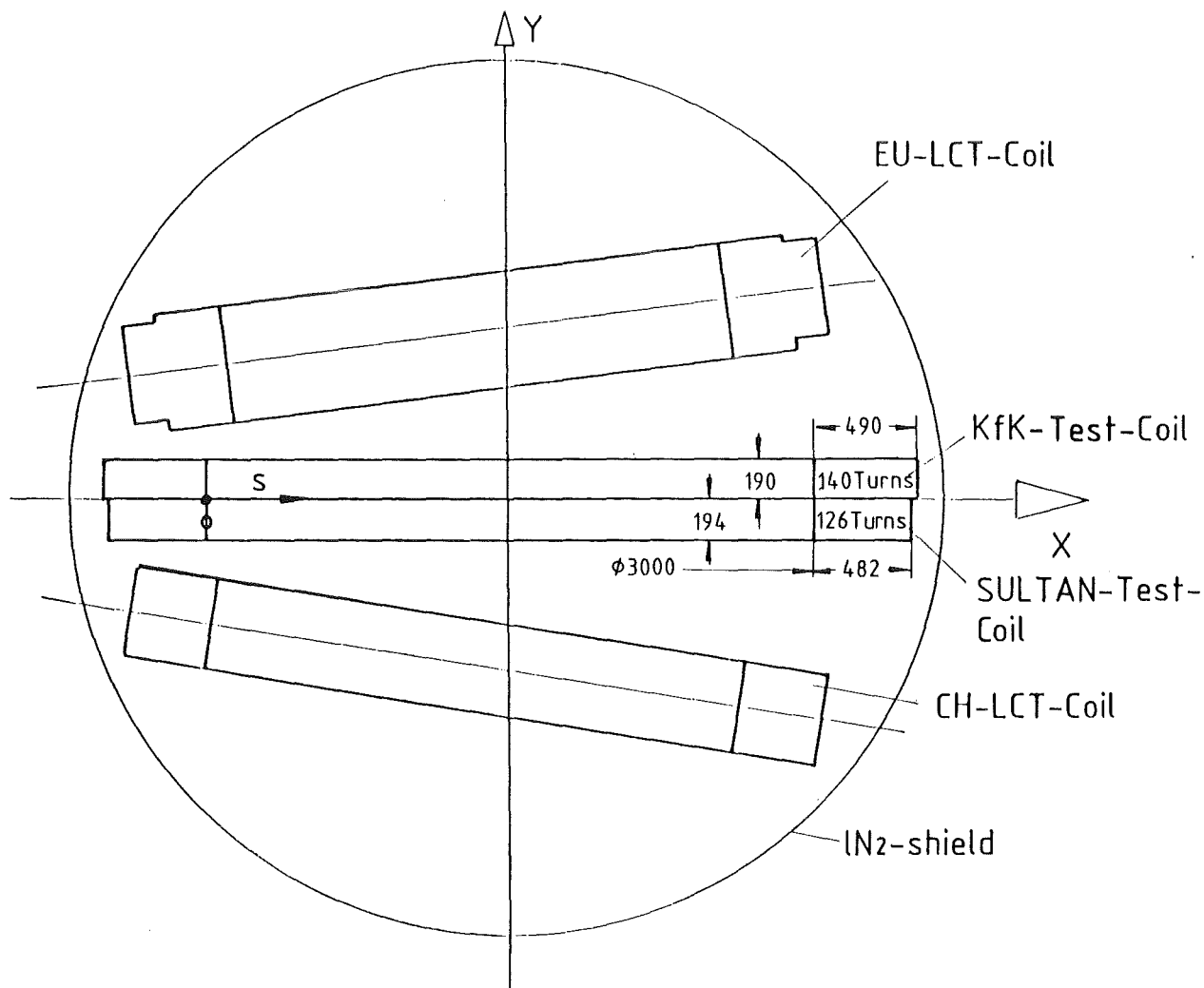


Fig. 3.2-1: Midplane of the starting Configuration C1. All Lengths in mm. The straight Section of the D-shaped LCT-Coils is located at the left Side.

To get an enhancement of the field at conductor of the test coils, the inner leg of the test coils (at the location of the straight section of the LCT-coils) is moved inward into the direction of the positive X-axis while keeping fixed the outer leg, in other words the bending radius is continuously decreased. Fig. 3.2-2 shows the result of this procedure, where B_{\max} at the test coils is drawn versus the distance s from the original position. At $s = 0.6$ m B_{\max} saturates at 7.5 T, i.e. the inner diameter of the test coil is reduced from 3 m to 2.4m. This means a reduction of the minimum bending radius from 1.5 m to 1.2m. This smaller bending radius is chosen for further considerations.

The maximum field of 7.5 T is still too low. To rise the field three changes were made:

- enhancement of the number of turns from 140 to 180 in the KfK-test coil and from 126 to 160 in the SULTAN-test coil
- change of position of the SULTAN- and KfK-test coils due to space reasons.
- enhancement of currents in the test coils from 16 kA to 22 kA.

This leads to configuration C2 in Fig. 3.2-3. But the field at the conductor is still slightly too low.

To get the case C3 for the Cluster Test Facility (Table 3.2-1, Fig. 3.2-4) the main change was to enhance the number of turns in the SULTAN-test coil from 160 to 180. This rises the maximum field to 11.5 T at the test coil. During the whole procedure discussed above the maximum field migrates from the straight section of the D-coils to the back of the coils and reaches 8.8 T at the Euratom-LCT coil, but is still below 8 T in the Swiss-LCT coil. By decreasing the current of the coils to 11.6 kA (to about the nominal value of the EU-LCT coil) the field at the coil decreases to 8 T at the EURATOM coil (Configuration C4 of Table 3.2-1).

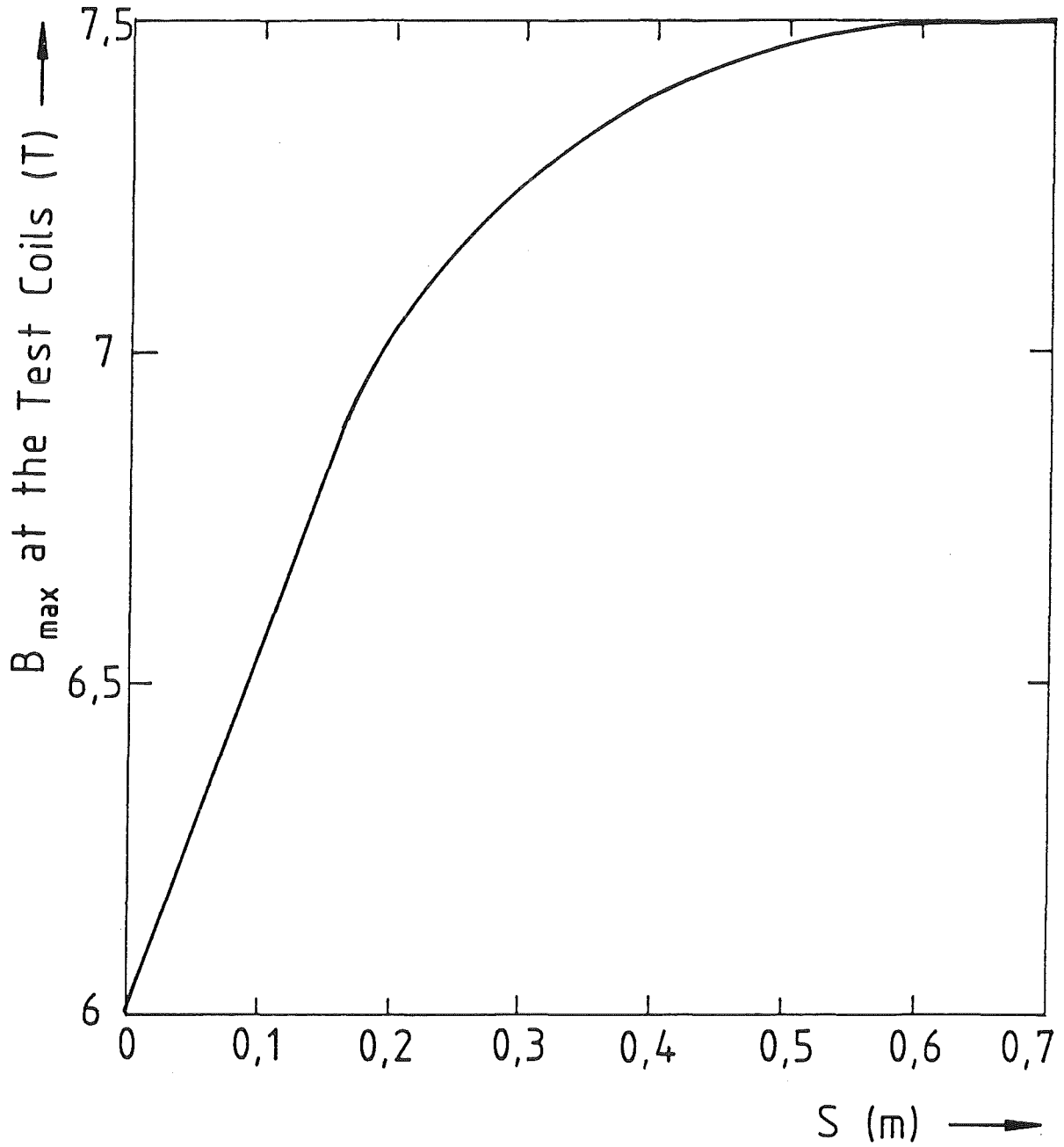


Fig. 3.2-2: B_{\max} at the Test Coils in Dependence on the moving Distance s .

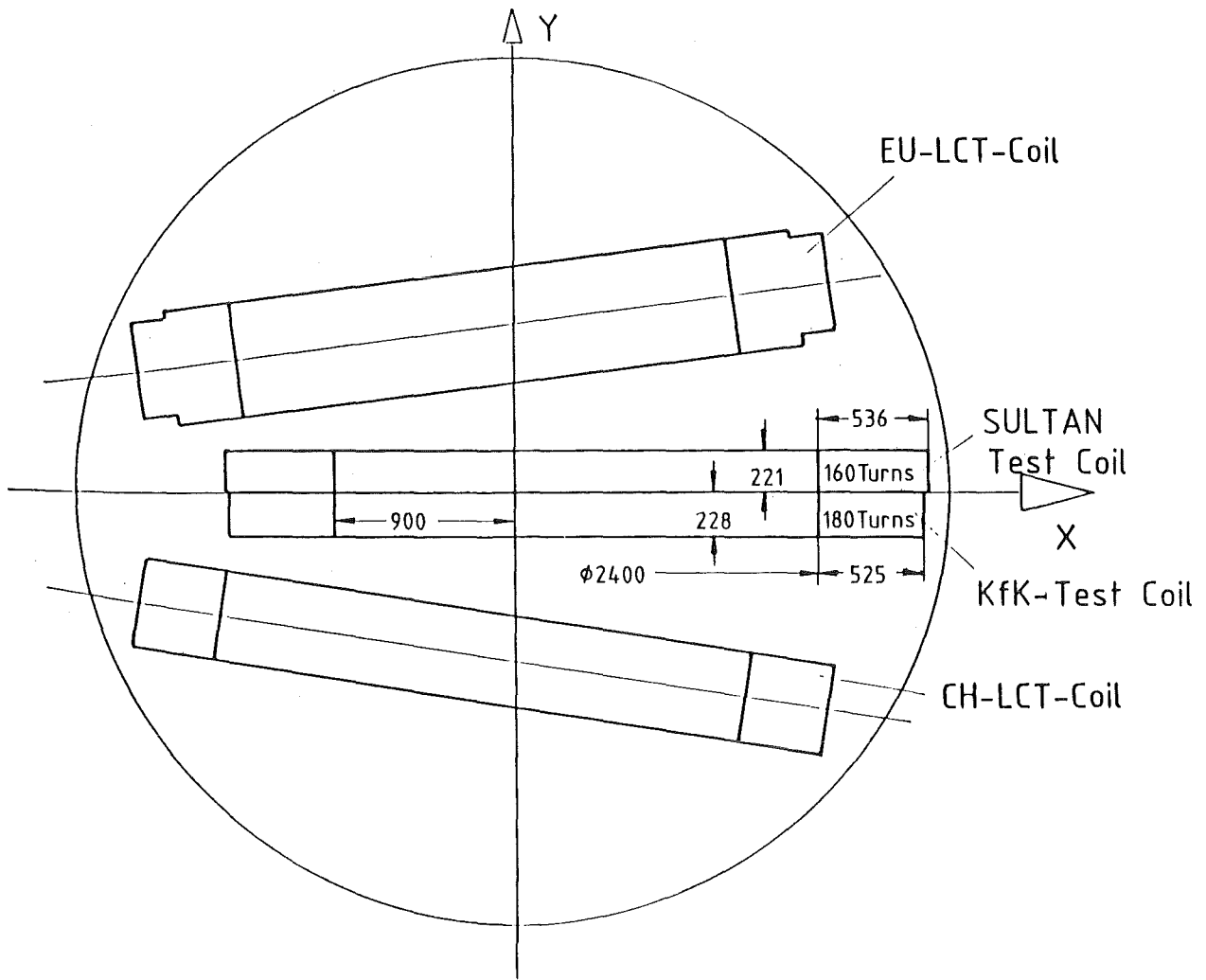


Fig. 3.2-3: Midplane of Configuration C2. All Lengths in mm. The straight Section of the D-shaped LCT-Coils is located at the left Side.

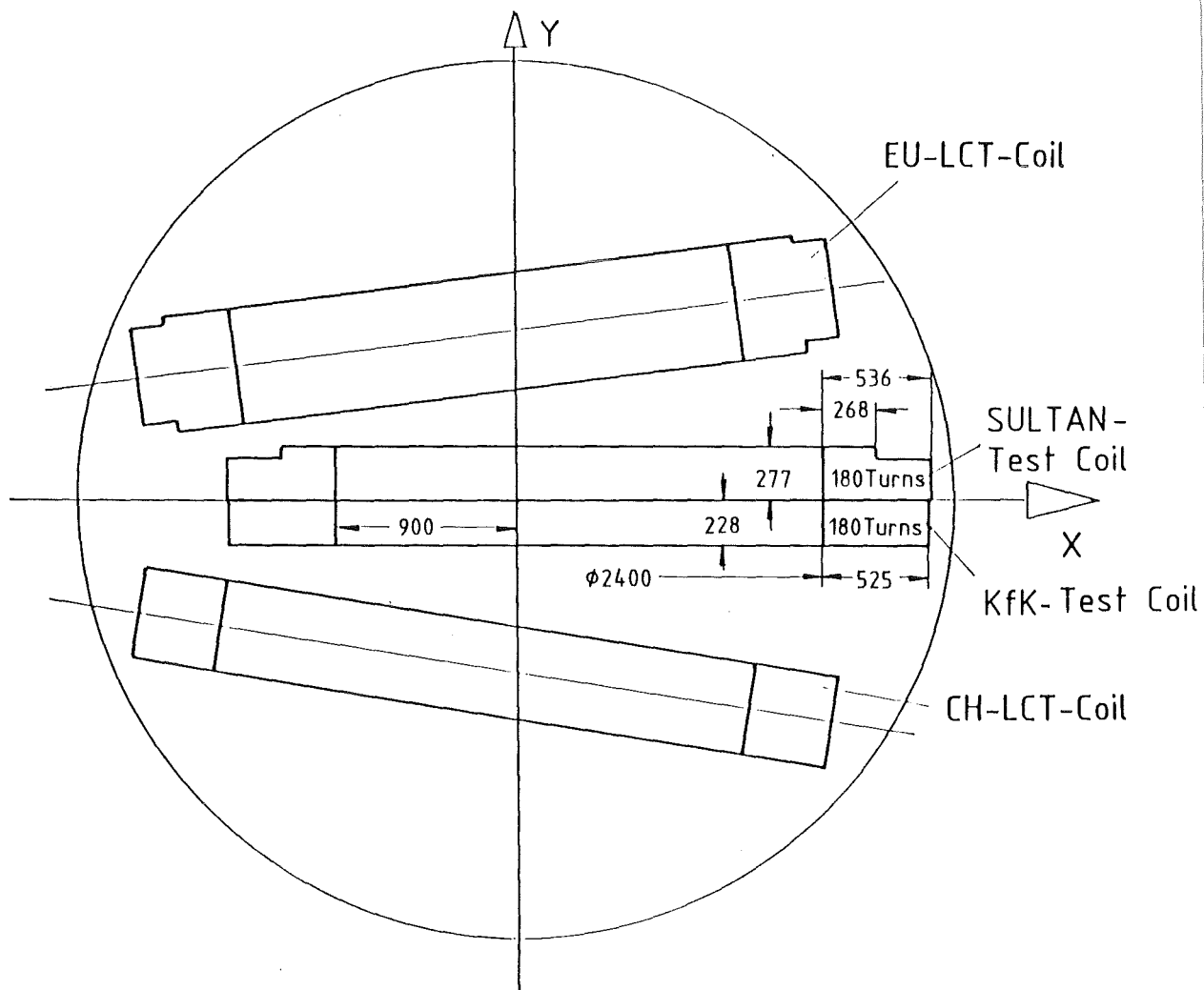


Fig. 3.2-4: Midplane of Configuration C3. All Lengths in mm. The straight Section of the D-shaped LCT-Coils is located at the left Side.

Table 3.2-2 contains the main characteristics of the NET-test coils in the Cluster Test Facility e.g. position of coil centre, conductor characteristics and winding characteristics for the configuration C3, defined as reference case June 86. It should be mentioned, that the division of the SULTAN-NET-test coil in an inner and outer coil is artificial, only due to computing reasons but the outer double pancake is smaller due to space restrictions. A double pancake winding is envisaged for both test coils.

Table 3.2-2: Main Characteristics of the NET-Test Coils in the Cluster Test Facility. Configuration C3.

	Unit	KfK-NET	SULTAN-NET	
			Inner Coil	Outer Coil
X-position of coil centre	m	0.3	0.3	
Y-position of coil centre	m	-0.114	0.13875	0.111
Conductor:				
Width	mm	38	27.7	
Thickness	mm	17.5	26.8	
Nominal current	kA	16	16	
Nominal current density	kA/cm ²	2.406	2.180	
Test coil current	kA	22	22	
Test coil current density	kA/cm ²	3.308	2.964	
Kind of winding		double pancake	winding	
Number of pancakes		6	10	8
Number of layers		30	10	10
Number of turns		180	100	80
Inner radius	m	1.2	1.2	1.468
Axial width	m	0.228	0.2775	0.222
Radial thickness	m	0.525	0.268	0.268
Average radius	m	1.4625	1.334	1.602
Average turn length	m	9.2	8.4	10.1
Total conductor length	m	1654	838	805
Coil cross section	m ²	0.12	0.075	0.06
Coil volume	m ³	1.1	0.623	0.6
Ampère meters	10 ⁶ Am	36.4	18.44	17.71
Coil current	10 ⁶ A	3.96	2.2	1.76

3.3 Restrictions and Consequences of the Constraint to use the existing Vacuum Vessel

3.3.1 Reduction of the minimum Bending Radius

The reduction of the minimum bending radius from 1.5 m to 1.2 m leads to an enhancement of the bending strain in the NET conductor. Table 3.3-1 shows the theoretical bending strain values ϵ in % and δ the maximum distance from the neutral bending axis, for both NET test coils (KfK-NET, SULTAN-NET). The values are given for both the superconductor and stainless steel jacket. The strain values are acceptable. The strain degradation of the current density is taken into account at the conductor design. The strain values of the superconductor can be reduced due to an adjustment of the reaction drum.

3.3.2 Enhancement of operational Current in EU-LCT

Fig. 3.3-1 shows the earlier measured values of the critical current in dependence on the magnetic field B at 4.2 K for 23-LCT-strands of the EU-LCT coil [3.2]. A measured value at 3.72 K is added to the diagram. It shows, that an operational current of 13 kA at 4.2 K is above the critical current for 8.8 T. Therefore the current in the LCT-coils was reduced to 11.6 kA leading to 8.0 T at the conductor. This gives a sufficient safety margin for operation. Fig. 3.3-2 shows the load lines of TOSKA-Upgrade for the EU-LCT-coil compared with that of the single coil. This diagram is based on actual test results obtained in TOSKA and IFSMTF [3.2]. Fig. 3.3-2 shows clearly that the EU-LCT coil has to be operated at 3.5 K due to the required safety margin at an operating current of 13 kA. The consequences of a 3.5 K operation are discussed in Chapter 7. The safety margin for the current of the CH-LCT-coil is larger compared with the EU-LCT-coil as given in Fig. 3.3-3. Fig. 3.3-4 and 3.3-5 show the loadlines of the KfK- and SULTAN-NET-test coils.

Table 3.3-1: Strain of the Nb₃Sn strands (SC) and of the steel jacket (SS)

	KfK-NET		SULTAN-NET	
	SC	SS	SC	SS
δ	2.15	8.25	3.3	12.6
R [m]	ϵ [%]	ϵ [%]	ϵ [%]	ϵ [%]
2	0.11	0.41	0.17	0.63
1.5	0.14	0.55	0.22	0.84
1.4	0.15	0.59	0.24	0.90
1.3	0.17	0.63	0.25	0.97
1.2	0.18	0.69	0.28	1.05
1.1	0.19	0.75	0.30	1.15
1.0	0.22	0.83	0.33	1.26

δ = Distance from the neutral bending axis in mm

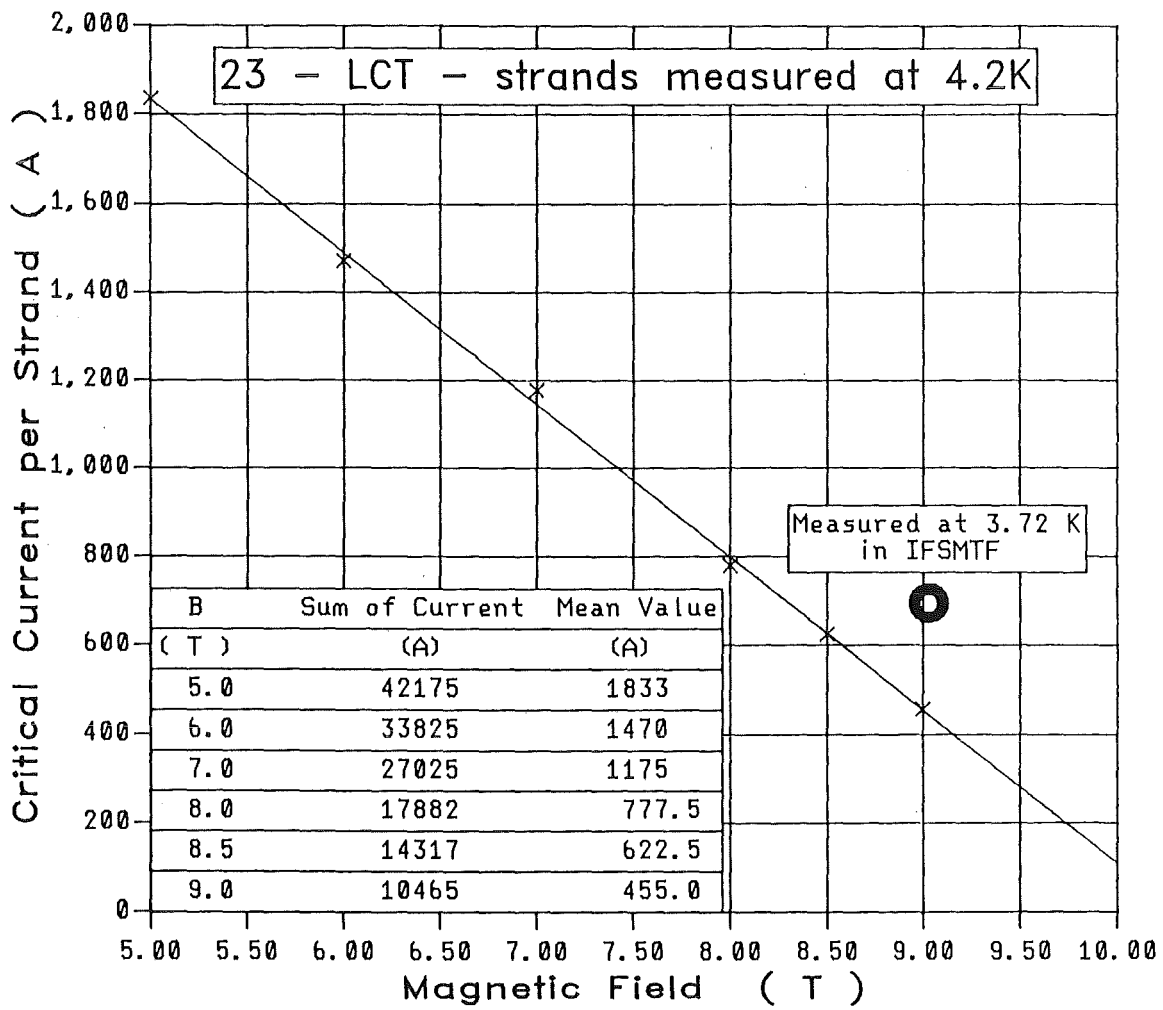


Fig. 3.3-1: Measured Values of critical Current in Dependence on magnetic Field for single Strands.

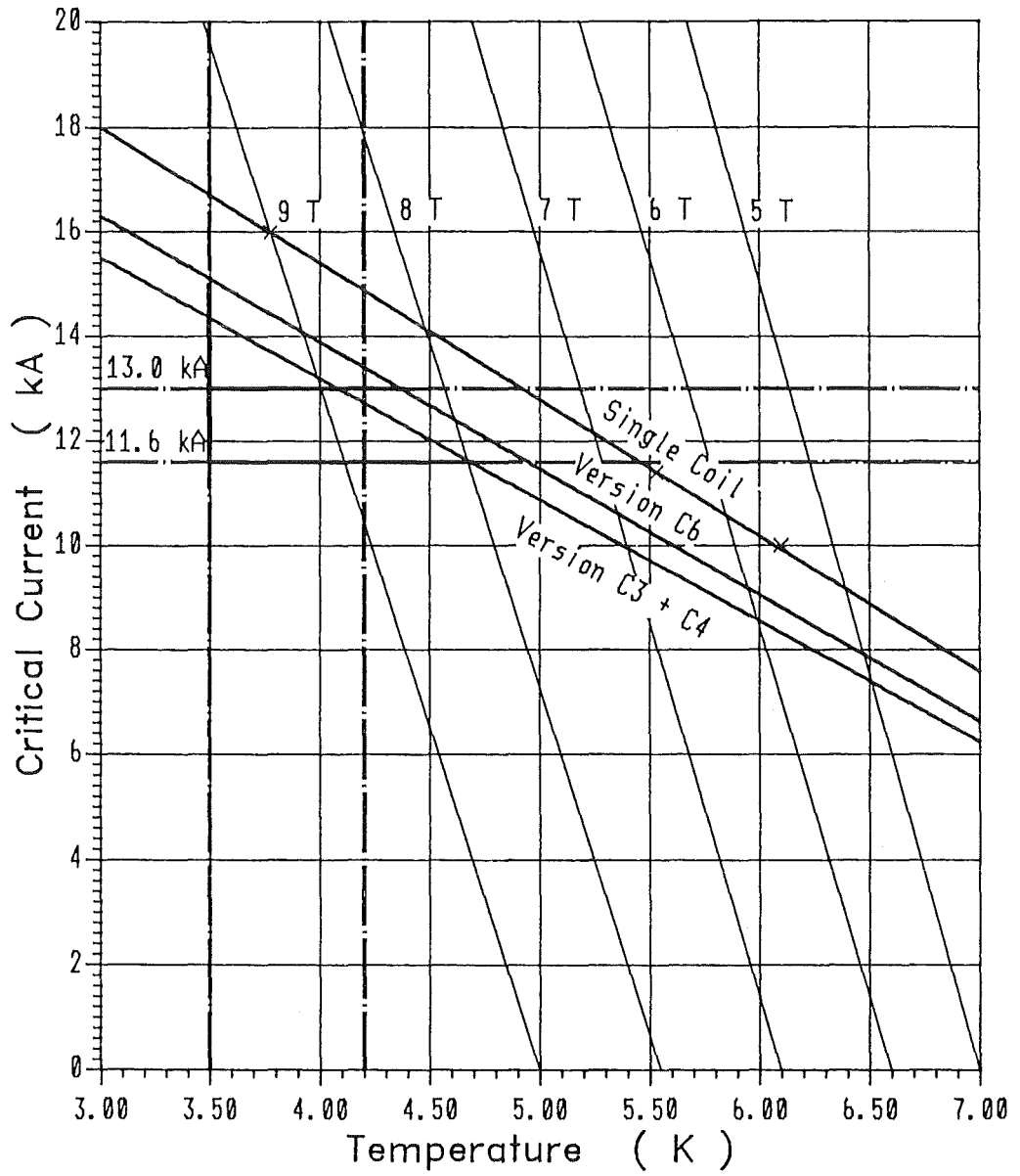


Fig. 3.3-2: Loadlines for the EU-LCT-Coil in TOSKA-Upgrade and Single Coil.

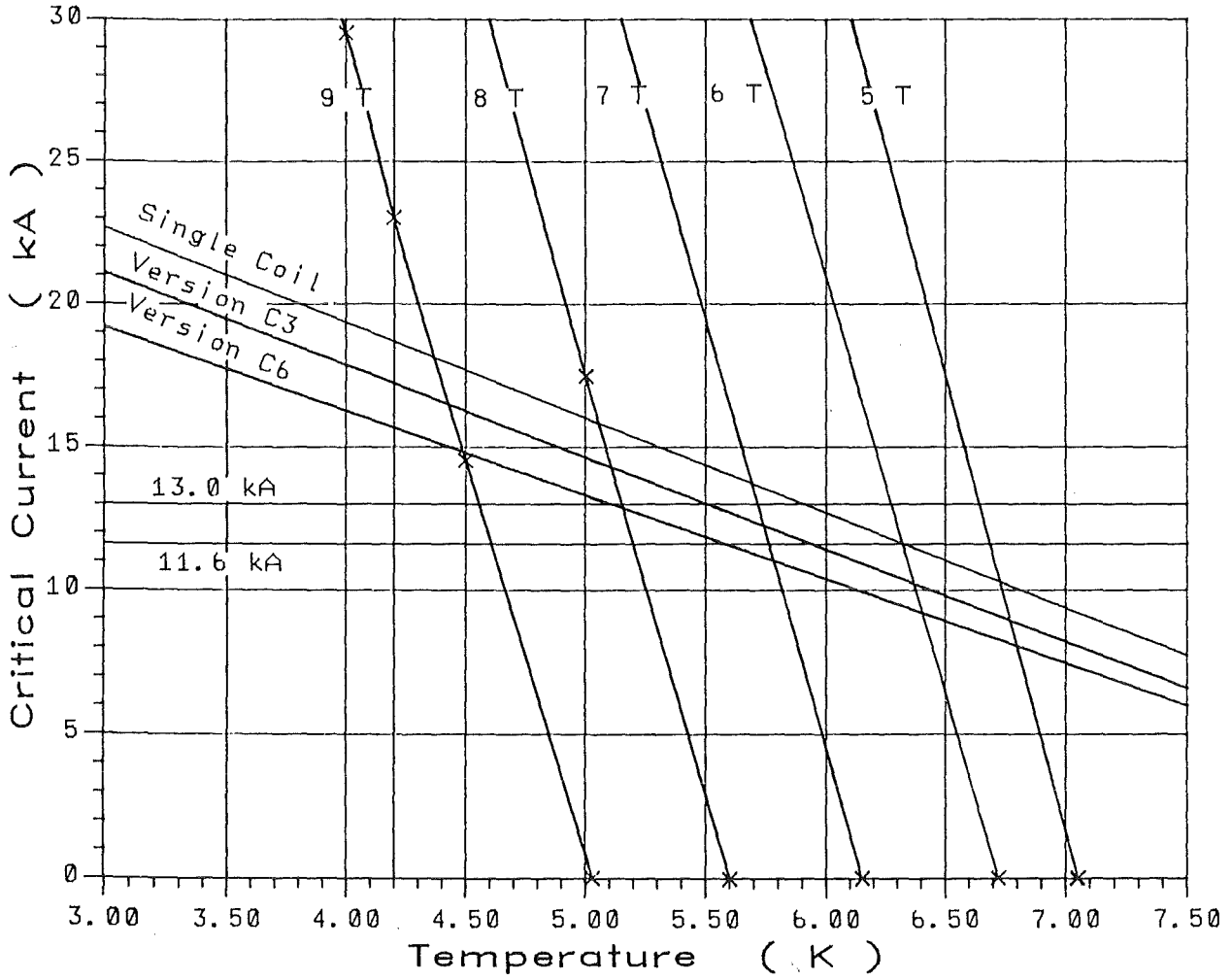


Fig. 3.3-3: Loadline for the CH-LCT-Coil in TOSKA-Upgrade and Single Coil. The critical Current is extrapolated from single Strands without Degradation.

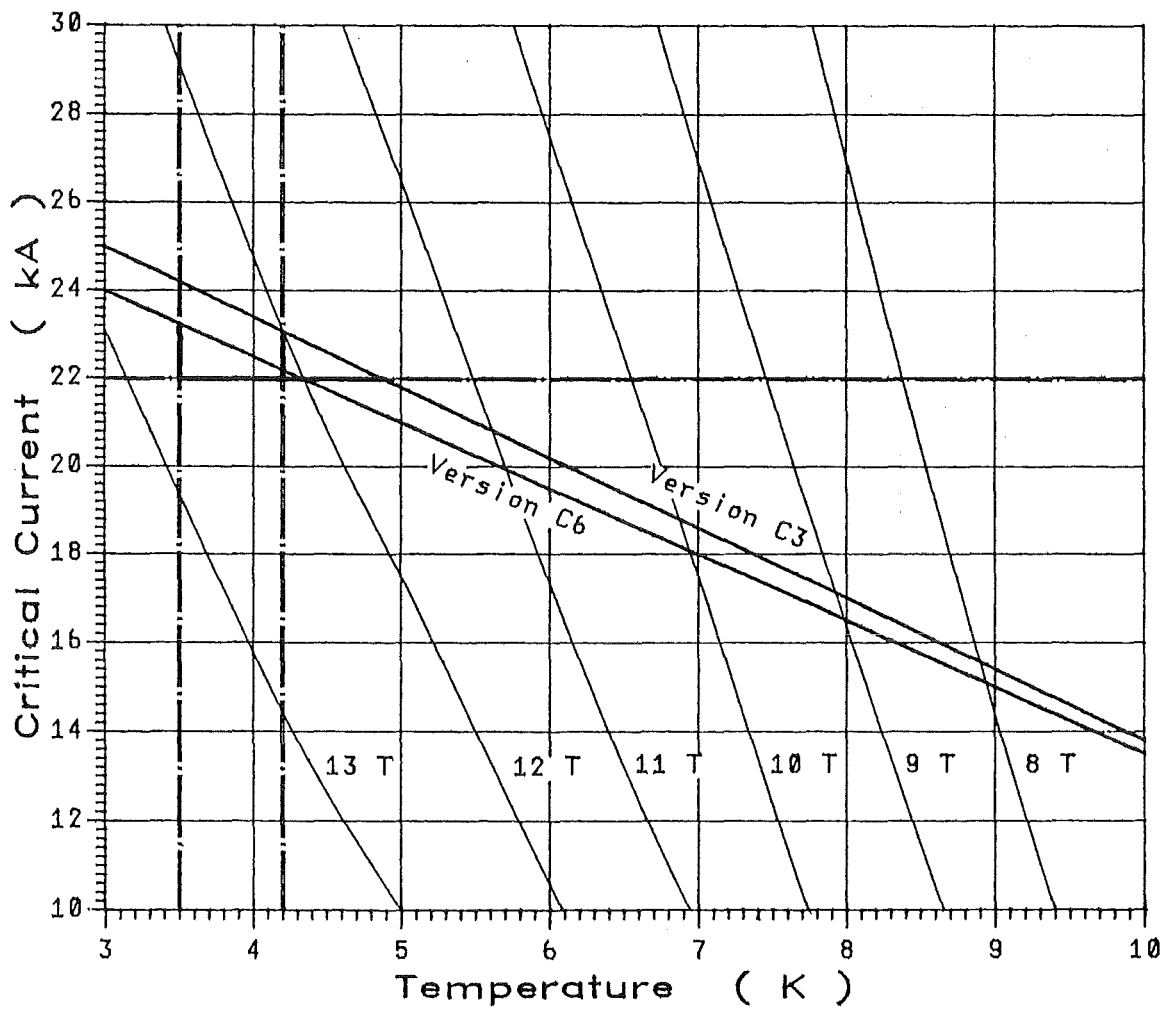


Fig. 3.3-4: Loadlines for the KfK-NET-Test Coil. A Degradation of 35 % is taken into Account for Handling, Bending and transverse Stresses.

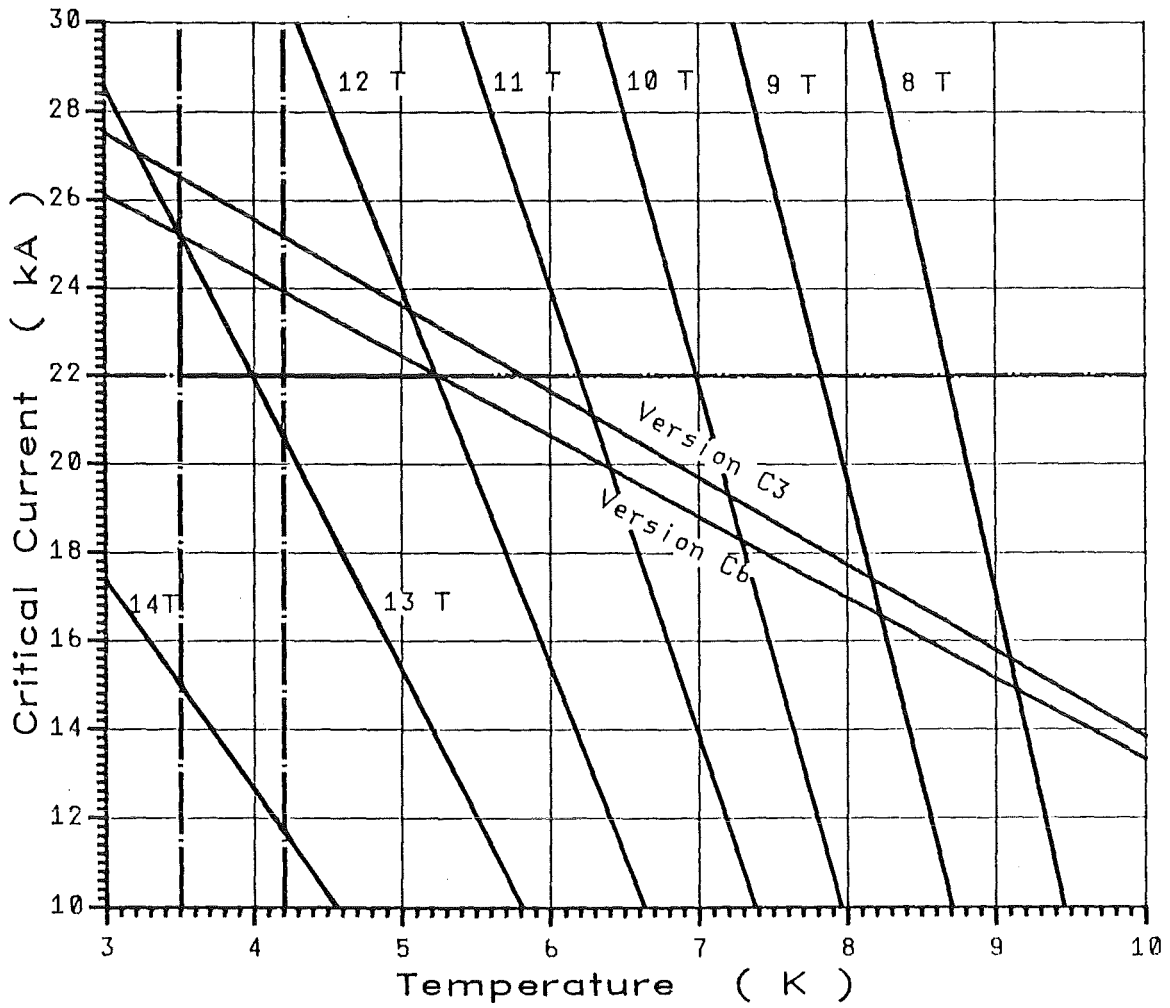


Fig. 3.3-5 Loadline for the SULTAN-NET-Test Coil. A Degradation of 30 % is taken into Account for Handling, Bending and transverse Stresses.

3.3.3 Enhancement of the Current in the NET-Test Coils

The enhancement of the current in the NET-Test coil from 16 kA to 22 kA leads to higher forces in the magnet arrangement. This is discussed in detail in Chapt. 5.

3.4 Testing of OH-Conductor in the Cluster Test Facility

If the KfK-NET- and SULTAN-NET test coils are replaced by a test coil out of the OH conductor, then the maximum magnetic field at conductor of the test coil is 11.4 T instead of 12.5 T. This is due to the fact that the current density of the OH test coil (3003 A/cm² at 50 kA) is lower than the TF-conductor current density averaged over both TF conductor test coils (3121 A/cm² at 22 kA). The OH conductor length is about 1500 m for the test coil.

The specification of dB/dt is 3 T/s for the OH coils compared with dB/dt = 1 T/s for the TF test coils [3.4] It has to be mentioned that it is very difficult to arrange a pulse coil for AC-loss testing in the cluster test facility. That is valid for both cases either OH conductor testing or TF conductor testing.

One question is still open whether the LCT coils can sustain the pulse load during testing. Test results for the EU-LCT-coil and for the Swiss-LCT-coil up to dB/dt = 0.16 T/s are available. It is difficult to extrapolate from dB/dt=0.16T/s to about 1T/s, but according to [3.5] a rise of the losses by a factor of about 6 is expected. If the background field LCT-coils do not sustain the pulse load, a test without energized LCT-coils is possible, but then the maximum field is only about 7,5 T at the test coil conductor. Whether this is sufficient, has to be discussed. In any case, a comprehensive conductor pulse test seems to be questionable in the Cluster Test Facility.

3.5 Further Reduction of the Bending Radius

An analysis of the required installation work, which is discussed in Chapt.6, led to the conclusion that installation is very expensive and time consuming for the configuration C3 and C4. Also pretests of components were excluded.

Another argument was a possible reduction of the conductor length for the test coils. Therefore it was decided to design test coils with 1 m minimum bending radius which leads according to Table 3.3.-1 to a strain in Nb₃Sn of 0.22% in the KfK test coil and to 0.33 % in the SULTAN test coil.

A gap of 2 cm between the test coil was introduced. This allows a case thickness of 1 cm on the sides of the test coils.

Considerations about the relevance of tests with the higher test coil current 22 kA instead of the 16 kA nominal NET current give rise to a preliminary design of two configurations C5 and C6. Common feature of the both is a minimum bending radius of 1 m for the test coils. The main difference is the current in both options, 16 kA in C5, the nominal current of NET, and 22 kA in C6. Table 3.5-1 contains the main characteristics of both configurations. Fig. 3.5-1 shows the arrangement of the coils. It is seen that the LCT-background field coils touch the ℓ N₂-shield (inner circle) of the existing vacuum vessel. The test coils are very huge due to the low current and consequently the conductor length exceeds the limits set for this test. Therefore the configuration C6 was developed. Fig. 3.5-2 shows the coil arrangement. The inner circle represents the ℓ N₂ shield of the existing vacuum vessel and the outer one the wall of the vessel. Fig. 3.5-3 shows B-contours for configuration C6. The inductive coupling in such an arrangement is very strong and has to be taken into account in the layout of the protection system. The total stored energy in configuration C6 is 512 MJ, although the sum of the stored self-energies of the four coils is only 296 MJ (SULTAN model coil = 38 MJ, KfK model coil = 34 MJ, CH-LCT = 90 MJ, EU-LCT = 134 MJ).

At a first glance the configuration C3 and C6 seems to be identical, but this is not true. One difference is the higher inclination angle (14 degrees instead of 7.4 degrees) of the EURATOM-LCT-coil in order to keep the maximum field at conductor below 8.3 T. Another difference is the change of the test coil position. This was done in order to balance the current densities. The Swiss-LCT-coil has a higher nominal current density than the EURATOM-LCT-coil. This is opposite for the NET-conductor test coils.

The configuration C6 requires small changes of the ℓ N₂-shield. That will be discussed in Chapt. 6.

Table 3.5-1: Cluster Configurations with 1 m Bending Radius of the Test Coils

CONFIGURATION:	C5	C6
<u>EU - LCT - COIL</u>		
CURRENT [kA] :	11.6	13
B max [T] :	8.0	8.3
TEMPERATURE [K] :	3.5	3.5
<u>CH - LCT - COIL</u>		
CURRENT [kA] :	11.6	13
B max [T] :	<8.0	8.1
TEMPERATURE [K] :	3.5	3.5
<u>NET - KfK TEST COIL</u>		
CONDUCTOR :	KfK	KfK
NUMBER OF TURNS :	400	204
INNER DIAMETER [m] :	2.0	2.0
CURRENT [kA] :	16	22
B max [T] :	11.7	12.1
TEMPERATURE [K] :	4.2	3.5
<u>NET - SULTAN TEST COIL</u>		
CONDUCTOR :	SULTAN	SULTAN
NUMBER OF TURNS :	330	220
INNER DIAMETER [m] :	2.0	2.0
CURRENT [kA] :	16	22
B max [T] :	11.5	12.0
TEMPERATURE [K] :	4.2	3.5

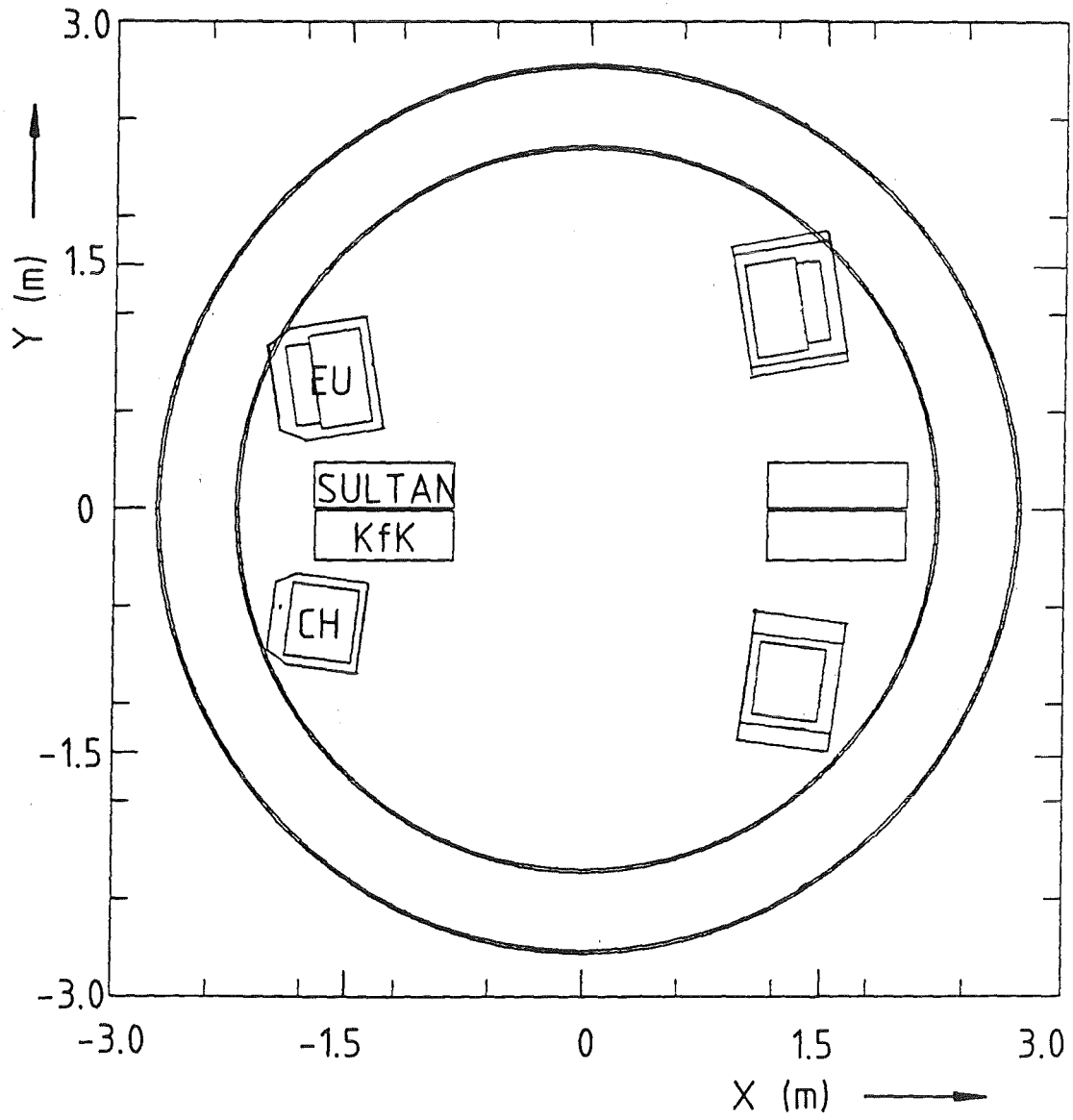


Fig. 3.5-1: Arrangement of the Cluster Test Configuration C5 with 16 kA Current in the Test Coils.

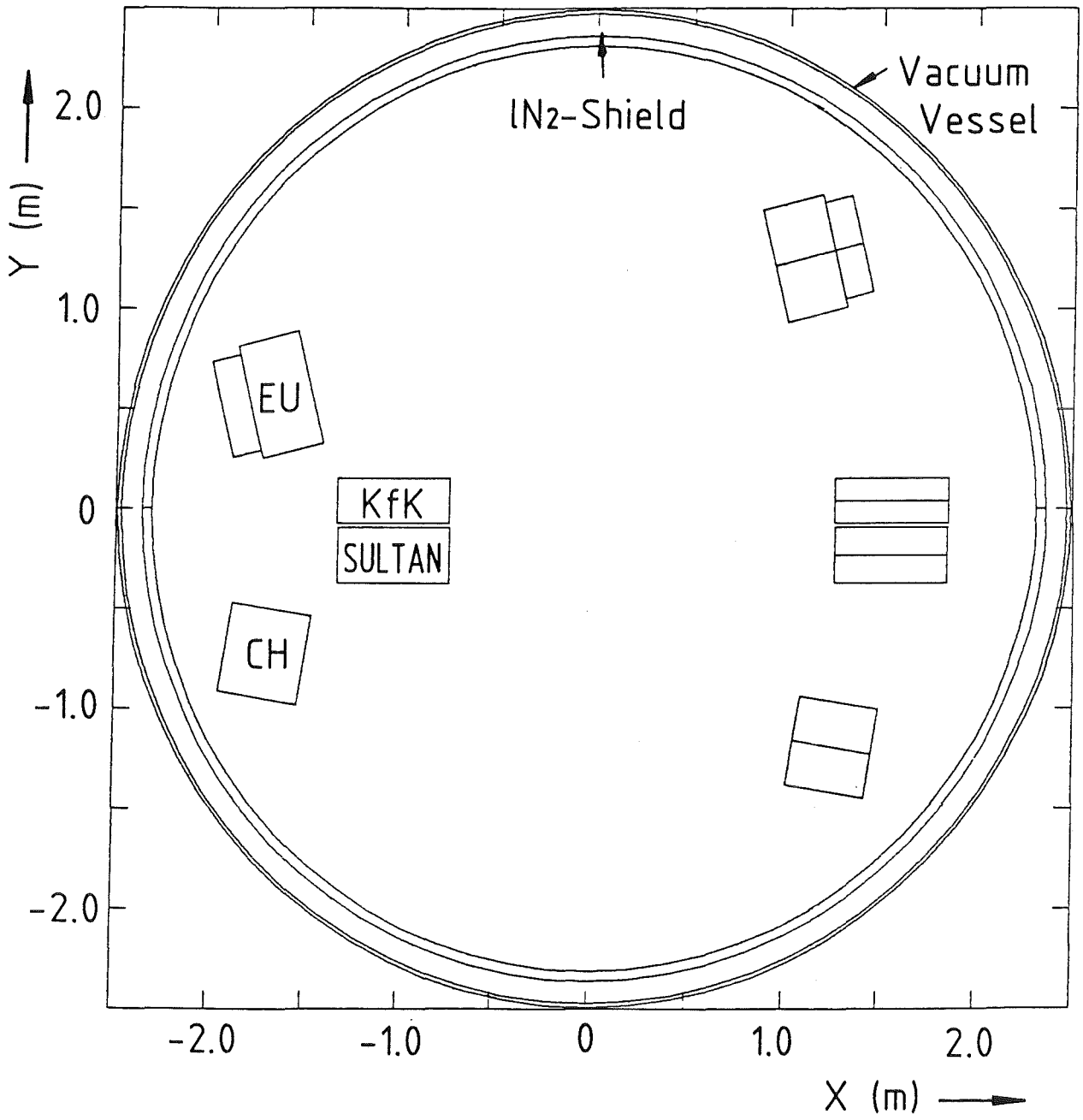


Fig. 3.5-2: Midplane of Configuration C6 with 22 kA in the Test Coils.

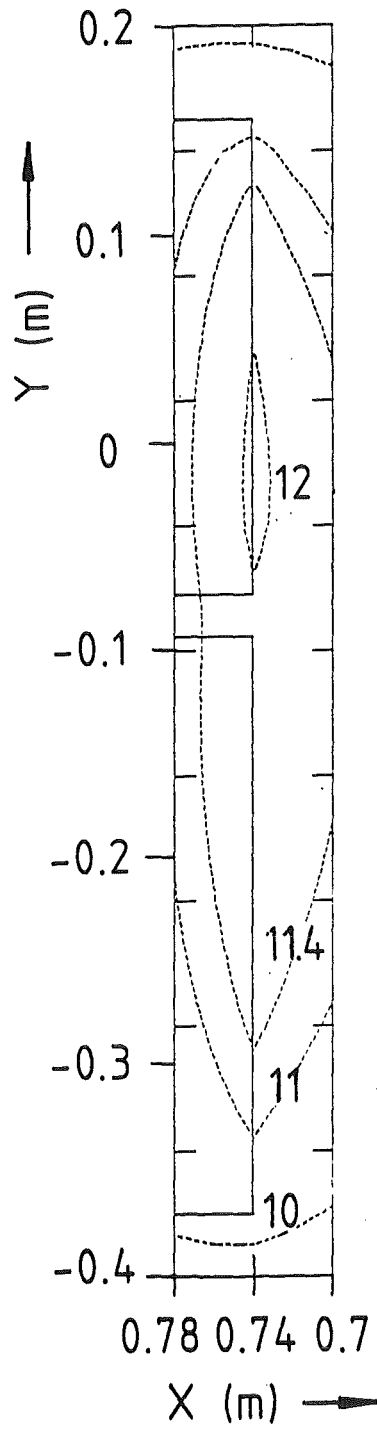


Fig. 3.5-3: B-contours for Configuration C6

3.6 Summary

The development of a useful Cluster Test Facility is described. Different constraints lead to a variety of design options. Table 3.6-1 contains the main technical characteristics for three different versions of the Cluster Test Facility. The configuration C6 is the most advanced one and is the base for a detailed design of a Cluster Test Facility.

Table 3.6-1: Comparison of Test Coil Characteristics for three different Versions of the Cluster Test Facility.

Winding pack characteristics	Unit	C3		C5		C6	
		KfK	SULTAN	KfK	SULTAN	KfK	SULTAN
Model coil current	kA	22	22	16	16	22	22
Current density	kA/cm ²	3.308	2.958	2.406	2.151	3.308	2.958
Kind of winding		double		pancake		winding	
Number of pancakes		2 x 3	2 x 5/2 x 4	2 x 4	2 x 5	2 x 3	2 x 5
Number of layers/pancake		30	10/10	50	33	34	22
Total number of turns		180	100/80	400	330	204	220
Inner radius, R _i	m	1.2	1.2	1.0	1.0	1.0	1.0
Axial winding width, DA	m	0.228	0.277/0.222	0.304	0.277	0.228	0.277
Radial winding thickness, DR	m	0.525	0.268/0.268	0.875	0.884	0.595	0.5896
Average winding radius, R _{av}	m	1.462	1.334/1.602	1.4375	1.442	1.2975	1.2948
Average turn length	m	9.189	8.382/10.06	9.05	9.06	8.15	8.14
Average pancake conductor length (= cooling length)	m	276	~ 200	451	290	277	179
Total conductor length *	m	1654	838/805	3613	2990	1664	1790
Winding cross section	m ²	0.120	0.0744/0.059	0.266	0.245	0.13566	0.16332
Winding volume	m ³	1.1	1.22	2.402	2.219	1.11	1.33
Estimated winding weight (ρ ~ 7 t/m ³)	t	7.7	8.54	16.8	15.5	7.8	9.3
Ampère-meters	10 ⁶ Am	36.4	18.44/17.71	57.92	47.84	36.608	39.38
Total coil current	10 ⁶ A	3.96	2.2/1.76	6.4	5.28	4.488	4.84
Stored Self Energy	MJ					34	38
B _{max}	T	11.5	11.5	11.7	11.5	12.1	12.0

* not including spare lengths for fabrication and joints (~ 10 %)

References to Chapter 3:

- [3.1] F. Arendt, B. Manes, A. Ulbricht, March 1985, unpublished
- [3.2] H. Krauth, VAC, private communication
A. Ulbricht, KfK, private communication
- [3.3] W. Herz et al., Testing of the Euratom-LCT-Coil, a Forced-Flow Cooled NbTi Coil, in the International Fusion Superconducting Magnet Test Facility (IFSMTF), Applied Superconductivity Conference ASC-86, Baltimore, Maryland, USA, Sep. 28.-Oct. 3, 1986
- [3.4] The NET Team, NET Status Report, NET Report 51, Dec. 1985
- [3.5] D. Tabarsi, Wechselfeldverlustverhalten von technischen Supraleitern, KfK 4074, Dez. 1986

4. Solenoid Test Facility

4.1 Introduction

Due to the engineering difficulties feared with the realization of the Cluster Test Facility, an alternative was studied as proposed by the NET-Team at the end of June 86. In this facility the test coils (solenoids) with the SULTAN- (SIN or ECN) and KfK-TF conductors and the OH-conductor foreseen for the central solenoid (CS) of NET provide the required field levels by themselves.

The conductor for the CS solenoids is described in Chapt. 2. The concept of the cable-in-conduit conductor made out of Nb₃Sn demands not only testing of conductor components and short samples but also real test coils of significant size. This statement is strongly corroborated by the test results of the Westinghouse coil in the IFSMTF [2.4]. The critical current of the Nb₃Sn/Cu conductor of that coil showed a serious degradation compared with short sample data. This is supposed to be due to strain degradation of the Nb₃Sn/Cu conductor suffered after reaction as a result of handling during coil fabrication and connecting.

At the time where the calculations started (July 86) the target magnetic field values were given by the NET-Team to be 11 T for TF-conductors and about 12 T for the OH conductor. With these values in mind and the experience gained during the development of the Cluster Test Facility, Configuration C3, the development of a Solenoid Test Facility, Configuration S1, was started.

4.2 Development of a Solenoid Test Facility S1

As a first idea the plan was to use the spare LCT-conductor available at KfK as it was done in the earliest Cluster Test Facility [4.1]. The lengths available are:

- 2 pieces of 75 m each,
- 4 pieces of 220 m each,
- 1 piece of 494 m,
- 1 piece of 400 m, and
- 1 piece of 145 m.

Obviously the pieces of 75 m and 145 m are not useable.

One possibility is to use the lengths of 494 m and 400 m as one double pancake and the four lengths of 220 m as two double pancakes. At each end of a piece 15 m are foreseen for handling during winding and joints. The data of the coils are given in Table 4.2-1. If we place both coils beside the KfK- and SULTAN-NET-test coils, as seen in Fig. 4.2-1, then we get 12.3 T at the OH-test coil in the midplane, but the field at the LCT conductor is then much too high (more than 9 T!). Also the field contribution to the maximum field of the coils made from LCT spare conductor is only 0.35 T.

Another possibility is to use the 2 pieces of 494 m and 400 m as 2 double pancakes similar to the use of the four 220 m pieces. The data of the coils are also given in Table 4.2-1. Both equal "LCT-coils" are placed in the back behind the KfK- and SULTAN-NET-test coils as seen in Fig. 4.2-2. The maximum field at the OH-conductor in the midplane is now about 12.5 T, and the contribution of the "LCT-coils" is 0.56 T. The "LCT-coils" are now in a field less than 5 T. We restricted the current in the "LCT-coils" in order to use the 10 kA power supply available in KfK.

Analyzing this configuration of Fig. 4.2-2 with respect to complexity, additional 10 kA current leads and amount of field contribution, it seems to be wise to renounce on the spare LCT-conductor which can be used otherwise. (Maybe such "LCT-coils" can be used to yield the background fields for turbomolecular pump test stands. Pumps operate normally in fringe fields. For NET these fields reach about 0.5 T, the order of magnitude which provided by the coils discussed above [4.2].) By adding up a few layers of conductor at the KfK and SULTAN-NET-test coils we get about 12.4 T at the OH-coil in the midplane. This configuration is further considered as reference case S1. Fig. 4.2-3 shows a field plot illustrating the contours of the magnetic field.

Table 4.2-1: Data of Coils made out of the LCT spare Conductor: "LCT-Coils".

		1st possibility		2nd possibility
	Units	"LCT 1"	"LCT 2"	2 equal coils
Conductor dimensions	mm x mm	40 x 10	40 x 10	40 x 10
Inner radius	m	1.2	1.2	1.7
Average radius	m	1.41	1.315	1.79
Axial width	m	0.08	0.16	0.16
Radial thickness	m	0.42	0.23	0.16
Current density	kA/cm ²	2.5	2.5	2.5
Current	kA	10	10	10
Turn number		2 x 42	4 x 23	4 x 16

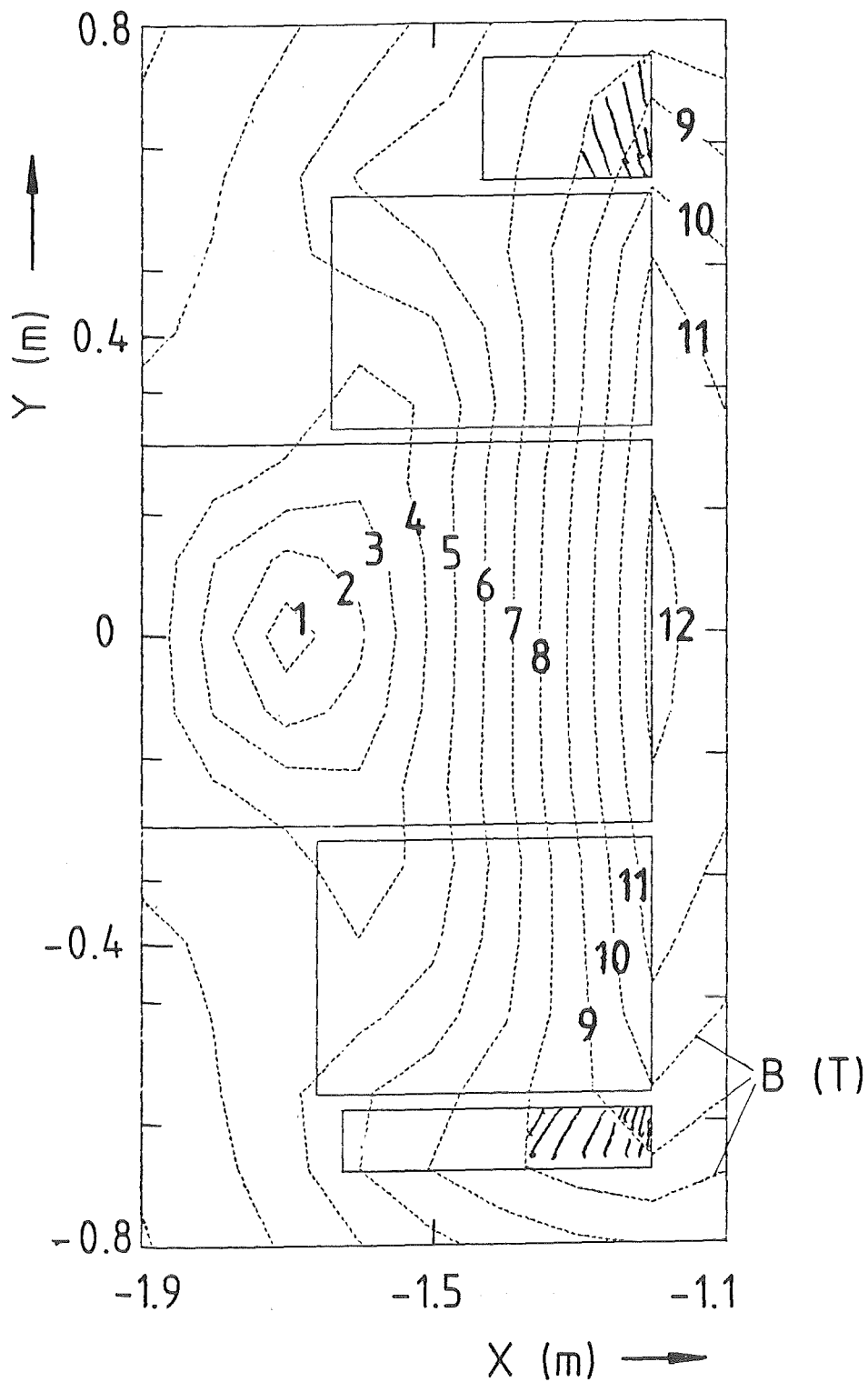


Fig. 4.2-1: Field Plot for Solenoid Test Configuration with LCT-spare Conductor Coils beside the Solenoids. (1st possibility)

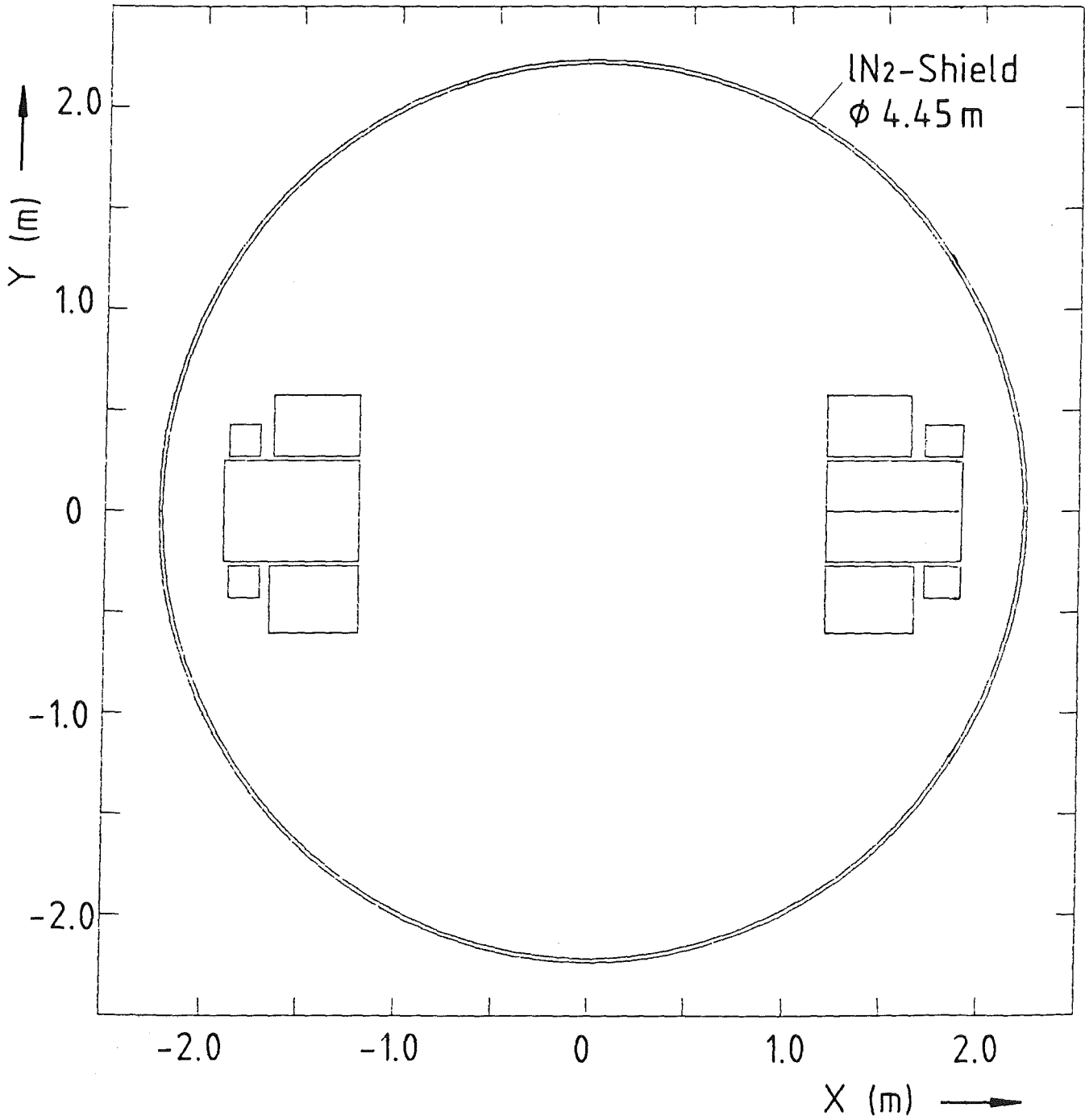


Fig. 4.2-2: Midplane Cross-section with LCT-spare Conductor Coils behind the Solenoids. (2nd possibility)

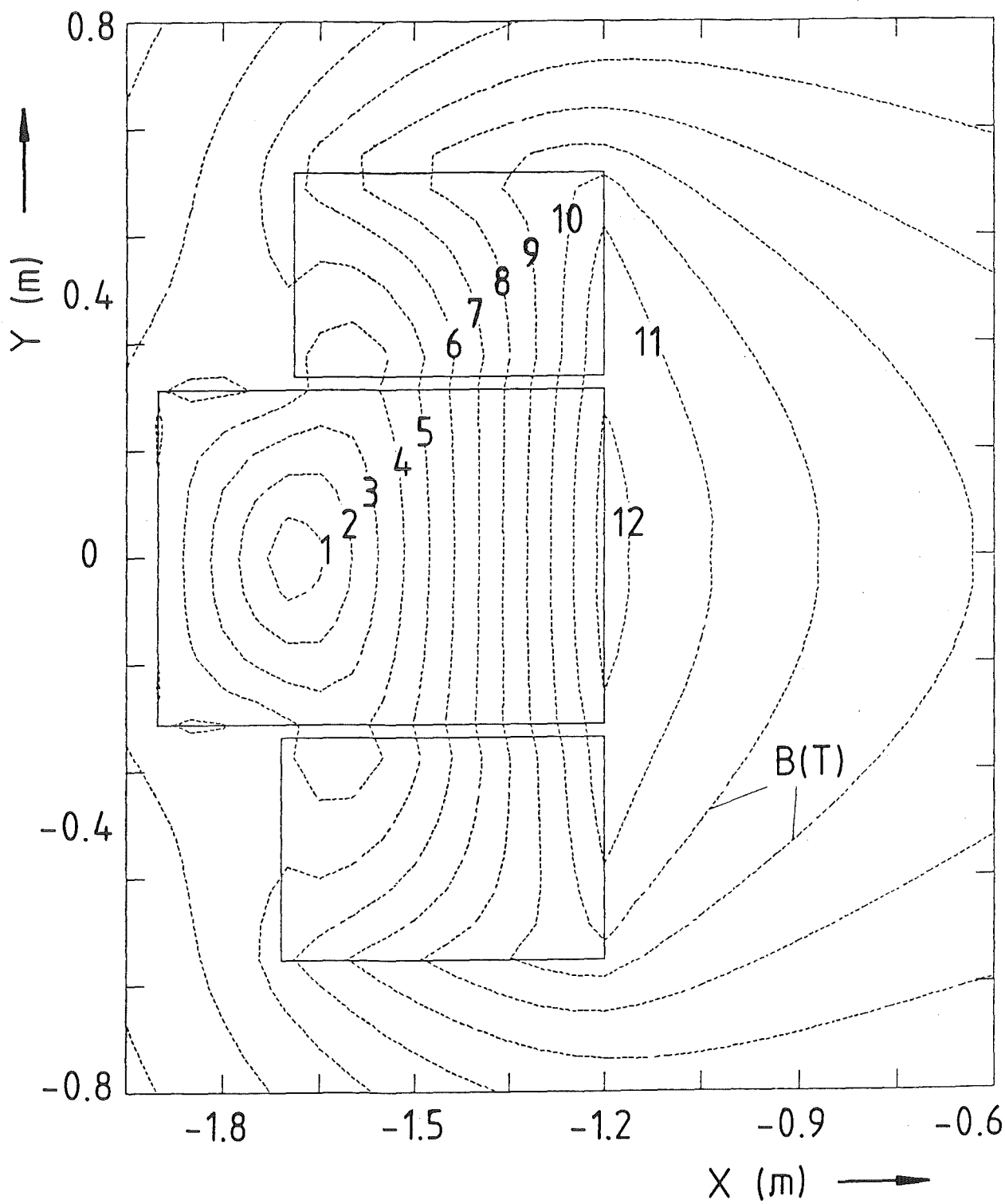


Fig. 4.2-3: Field Plot of Reference Case S1.

4.3 Description of the Solenoid Test Configuration S1

A cut of the three coils arrangement in the horizontal midplane ($XY, Z = 0$) is shown in Fig. 4.3-1. The three solenoids of inner radius R_i , axial width DA , and radial thickness DR stand upright in the existing vacuum vessel. The double circle represents the ℓN_2 shield inside the vacuum vessel. It should be mentioned, that only the winding cross section is shown. The space between winding and ℓN_2 shield is about 0.3 m at the narrowest distance, enough for casing and support structure and handling the coils.

Table 4.3-1 contains the main characteristics for the Solenoid Test Facility S1. This table is one basis of the comparison of both Test Facilities, which will be discussed in detail in chapter 13.

One feature of this coil arrangement should be outlined: the strong inductive coupling of the coils. Table 4.3-2 gives the inductance matrix. The stored self-energies are for KfK-NET 49 MJ, for OH-NET 100 MJ, and for SULTAN-NET 50 MJ. Due to the very strong inductive coupling the total stored energy at the test currents of the coils is 584 MJ. This is almost twice the value of the sum of the stored self-energies. The strong inductive coupling has to be taken into account in the layout of the protection system.

A force study was made in order to investigate how the forces build up in the pancakes of the test coils. Therefore the coils were subdivided into pancakes and the forces were calculated (The KfK coil has 8, the OH coil 10 and the SULTAN coil 12 pancakes). Table 4.3-3 contains the results. Small differences in the quoted figures are due to rounding errors, Using the geometry data of Table 4.3-1 the pressure of the KfK-NET-test coil on the OH-test coil is about 48 MPa. A similar value (46 MPa) is valid for the SULTAN-NET-test coil. The maximum pressure in the OH-coil is about 44 MPa. Radial acting forces were also calculated. The resulting radial pressure range from 55 MPa to about 65 MPa. The relevance of these data for NET is discussed lateron. Additional load can be applied as discussed in section 6.1.2.

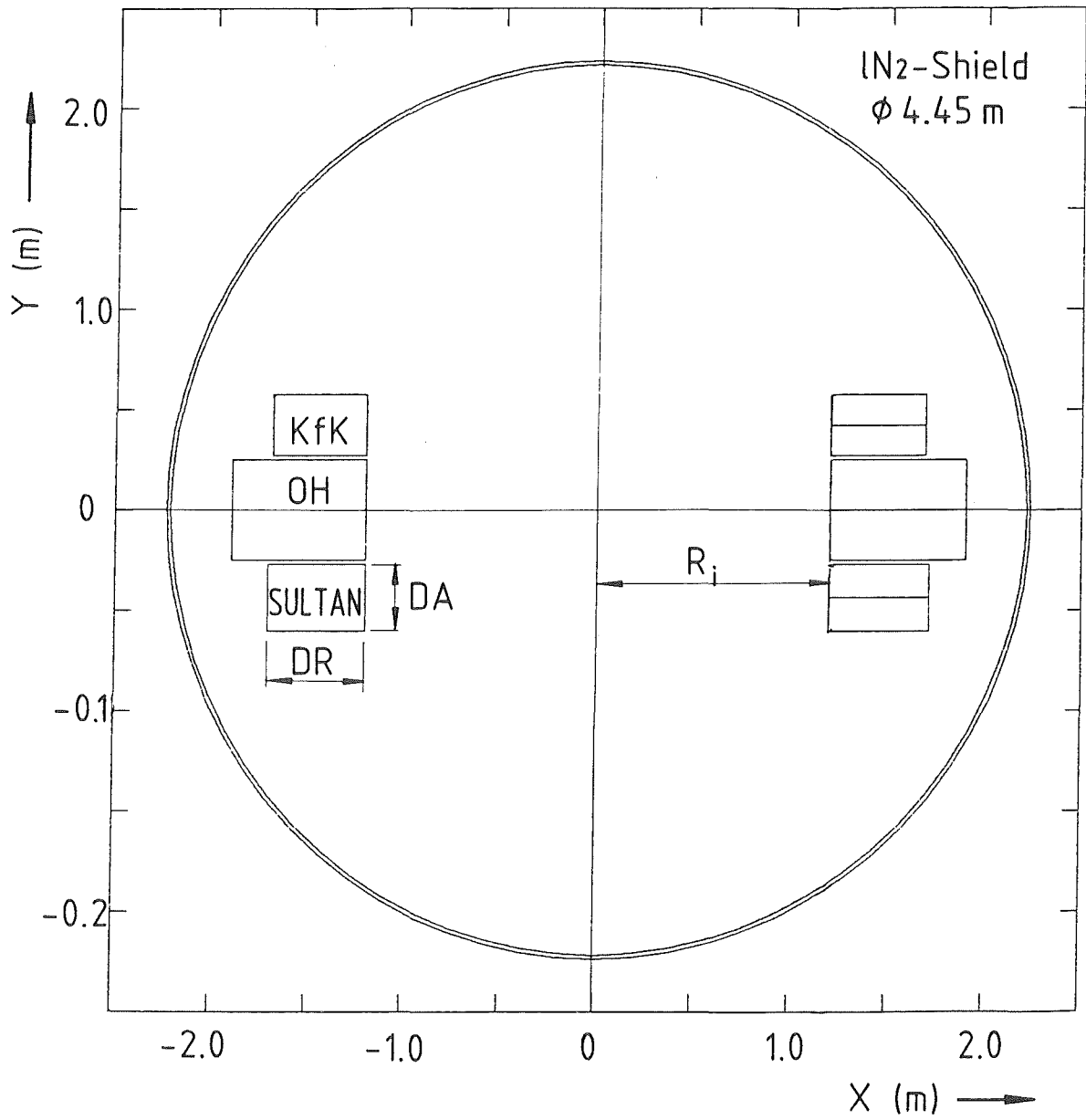


Fig. 4.3-1: Cut of the Reference Case S1 in the horizontal Midplane.

Table 4.3-1: Main characteristics for the Solenoid Test Facility, Configuration S1.

Version		S1		
Winding pack characteristics	Unit	KfK	OH	SULTAN
Model coil current	kA	22	50	22
Current density	kA/cm ²	3.308	3.003	2.958
Kind of winding		double	pancake	winding
Number of pancakes		2 × 4	2 × 5	2 × 6
Number of layers/pancake		28	21	19
Total number of turns		224	210	228
Inner radius, R _i	m	1.2	1.2	1.2
Axial winding width, DA	m	0.304	0.5	0.3324
Radial winding thickness, DR	m	0.49	0.6993	0.5092
Average winding radius, R _{av}	m	1.445	1.55	1.455
Average turn length	m	9.08	9.74	9.14
Average pancake conductor length (= cooling length)	m	255	205	174
Total conductor length *	m	2034	2045	2084
Winding cross section	m ²	0.149	0.35	0.17
Winding volume	m ³	1.353	3.405	1.547
Estimated winding weight (ρ ~ 7 t/m ³)	t	9.5	24	11
Ampère-meters	10 ⁶ Am	45	103	46
Total coil current	10 ⁶ A	4.93	10.5	5.02
Stored Self-Energy	10 ⁶ J	49	200	50
B _{max}	T	11.65	12.38	11.5

* not including spare lengths for fabrication and joints (~ 10 %)

Table 4.3-2: Inductance Matrix of the three Solenoids (Inductance unit = H)

Test-Coil	Number	1	2	3
KfK-NET	1	0.2	0.115	0.069
OH-NET	2	0.115	0.160	0.116
SULTAN-NET	3	0.069	0.116	0.21

Table 4.3-3: Axial Forces (F_y) on the NET-Test Coils in Configuration S1
 ($1t = 10^4$ N). (The sum of $F_{y \text{ total}}$ must be zero. Small differences are due to rounding errors.)

Name	F_y [10^4 N]	$F_{y \text{ total}}$ [10^4 N]
KfK 1	- 3860	- 21272
KfK 2	- 3455	
KfK 3	- 3095	
KfK 4	- 2766	
KfK 5	- 2459	
KfK 6	- 2167	
KfK 7	- 1881	
KfK 8	- 1589	
OH 1	- 3200	- 8689
OH 2	- 2429	
OH 3	- 1708	
OH 4	- 1015	
OH 5	- 337	
OH 6	+ 337	+ 8691
OH 7	+ 1015	
OH 8	+ 1709	
OH 9	+ 2430	
OH 10	+ 3200	
S 1	+ 1097	21265
S 2	+ 1212	
S 3	+ 1325	
S 4	+ 1437	
S 5	+ 1553	
S 6	+ 1672	
S 7	+ 1797	
S 8	+ 1929	
S 9	+ 2069	
S 10	+ 2221	
S 11	+ 2385	
S 12	+ 2568	

4.4 Solenoid Test Facility with 1 m Bending Radius

Similar to the Cluster Test Facility configurations with only 1 m bending radius were calculated. The results are given in Table 4.4-1 for comparison. The configuration S2 has 1 m bending radius and the nominal NET current of 16 kA for the TF conductors and 40 kA for the OH conductor, while configuration S3 has also 1 m bending radius but enhanced operational current of 22 kA and 50 kA respectively.

Going on from configuration S1 to S2 and S3 the target values for the TF and OH conductors were changed meanwhile. For the TF conductor it should be 11.4 T and only 11 T for the OH conductor. This effected a rearrangement of the coils as shown in Fig. 4.4-1. The main effect of this rearrangement is seen at the conductor lengths of S3 compared with S1.

Fig. 4.4-2 shows the loadlines for the KfK model coil in the configurations S1 and S3. Similar loadlines are given in Fig. 4.4-3 for the SIN-model coil.

A last change of the maximum field for the OH conductor by the NET team (see table 2.1 in Chapter 2) to be 11.5 T leads back to a configuration as in S1. The OH model coil with the highest field at conductor is in between the TF model coils.

Table 4.4-1: Comparison of the different Solenoid Test Configurations.

Configuration		S1			S2			S3		
Winding pack characteristics	Unit	KfK	OH	SULTAN	KfK	OH	SULTAN	KfK	OH	SULTAN
Model coil current	kA	22	50	22	16	40	16	22	50	22
Current density	kA/cm ²	3.308	3.003	2.958	2.406	2.435	2.18	3.308	3.003	2.958
Kind of winding		double	pancake	winding	double	pancake	winding	double	pancake	winding
Number of pancakes		2 x 4	2 x 5	2 x 6	2 x 6	2 x 4	2 x 10	2 x 5	2 x 4	2 x 7
Number of layers/pancake		28	21	19	40	21	26	30	16	20
Total number of turns		224	210	228	480	168	520	300	128	280
Inner radius, R _i	m	1.2	1.2	1.2	1.0	1.0	1.0	1.0	1.0	1.0
Axial winding width, DA	m	0.304	0.5	0.3324	0.456	0.4	0.554	0.38	0.4	0.3878
Radial winding thickness, DR	m	0.49	0.6993	0.5092	0.700	0.699	0.696	0.525	0.5328	0.536
Average winding radius, R _{av}	m	1.445	1.55	1.455	1.350	1.349	1.348	1.2625	1.2664	1.268
Average turn length	m	9.08	9.74	9.14	8.48	8.48	8.47	7.94	7,98	7.97
Average pancake conductor length (= cooling length)	m	255	205	174	339	178	220	238	127	160
Total conductor length *	m	2034	2045	2084	4070	1424	4400	2380	1019	2231
Winding cross section	m ²	0.149	0.35	0.17	0.32	0.28	0.39	0.2	0.213	0.208
Winding volume	m ³	1.353	3.405	1.547	2.71	2.37	3.30	1.584	1.7	1.66
Estimated winding weight (ρ ~ 7 t/m ³)	t	9.5	24	11	18.97	16.61	23.12	11.1	11.9	11.6
Ampère-meters	10 ⁶ Am	45	103	46	65	57	71	53	51	49
Total coil current	10 ⁶ A	4.93	10.5	5.02	7.68	6.72	8.32	6.6	6.4	6.16
Stored Self-Energy	10 ⁶ J	49	200	50				67	40	58
B _{max}	T	11.65	12.38	11.5	11.65	12.25	11.65	12.27	11.62	11.54

* not including spare lengths for fabrication and joints (~ 10 %)

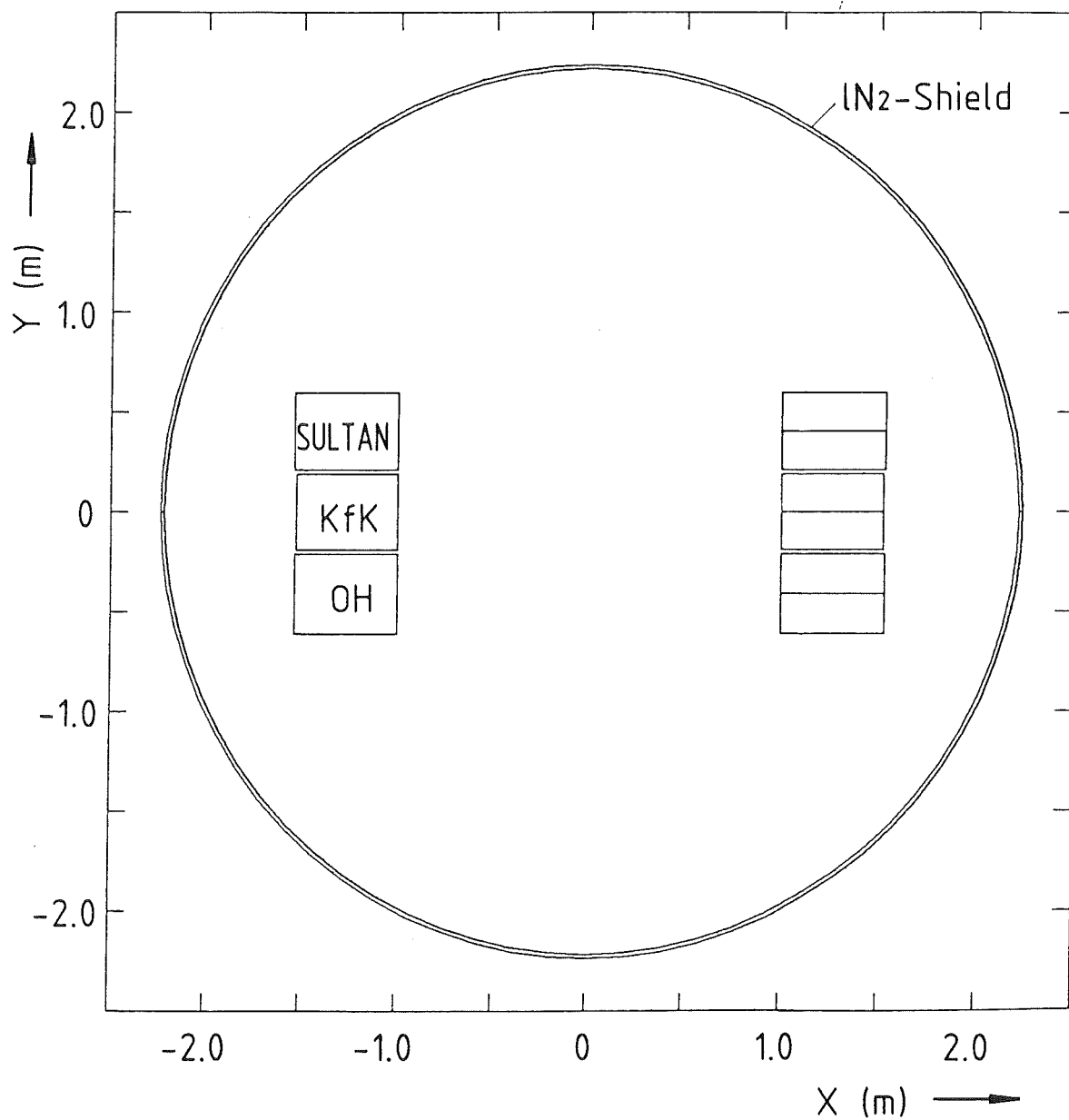


Fig. 4.4-1: Coil Arrangement for S3.

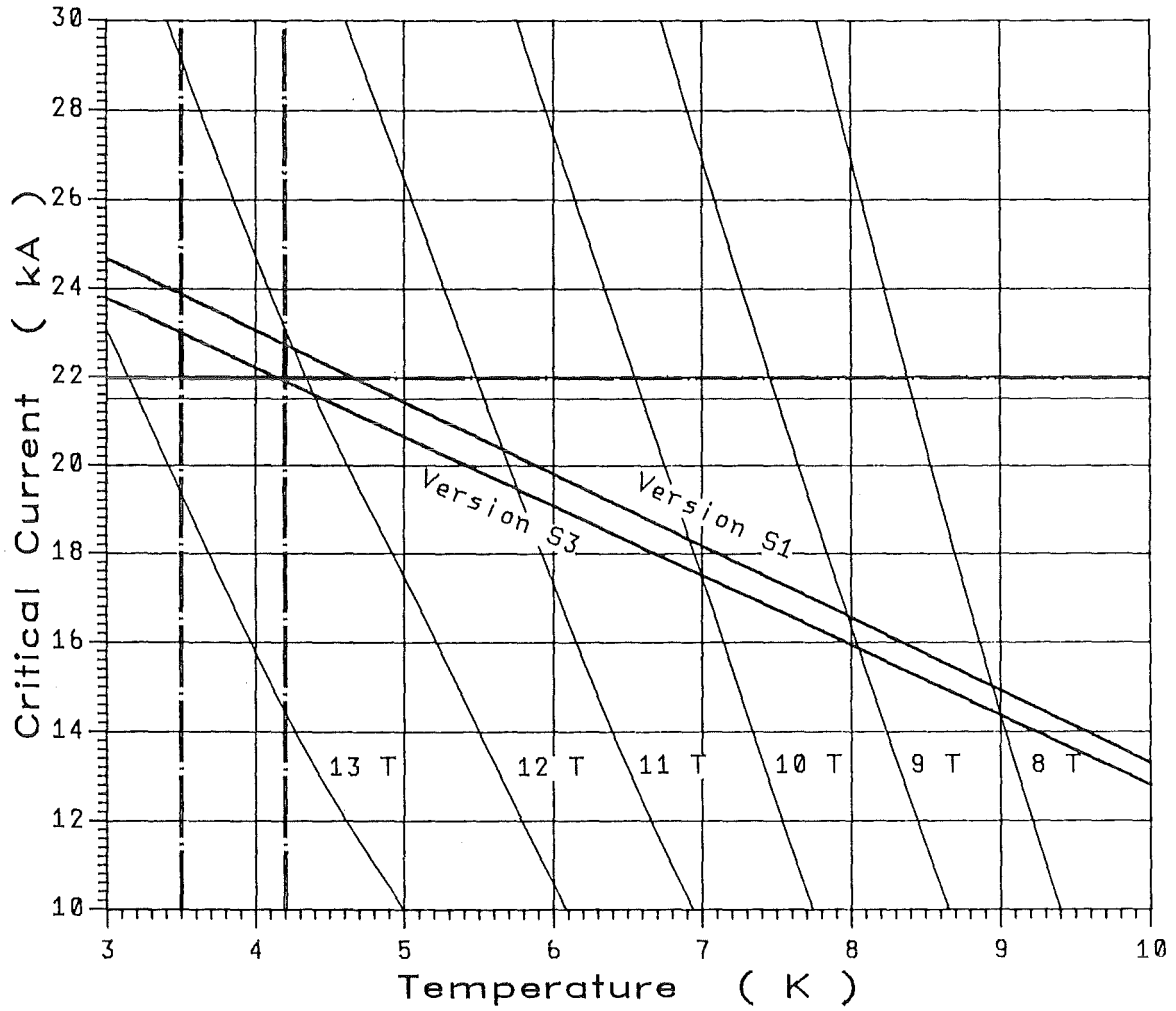


Fig. 4.4-2 Loadlines of the KfK NET Model Coil in the Solenoid Configurations S1 and S3. A Degradation of 35 % is taken into Account for Handling, Bending and transverse Stresses.

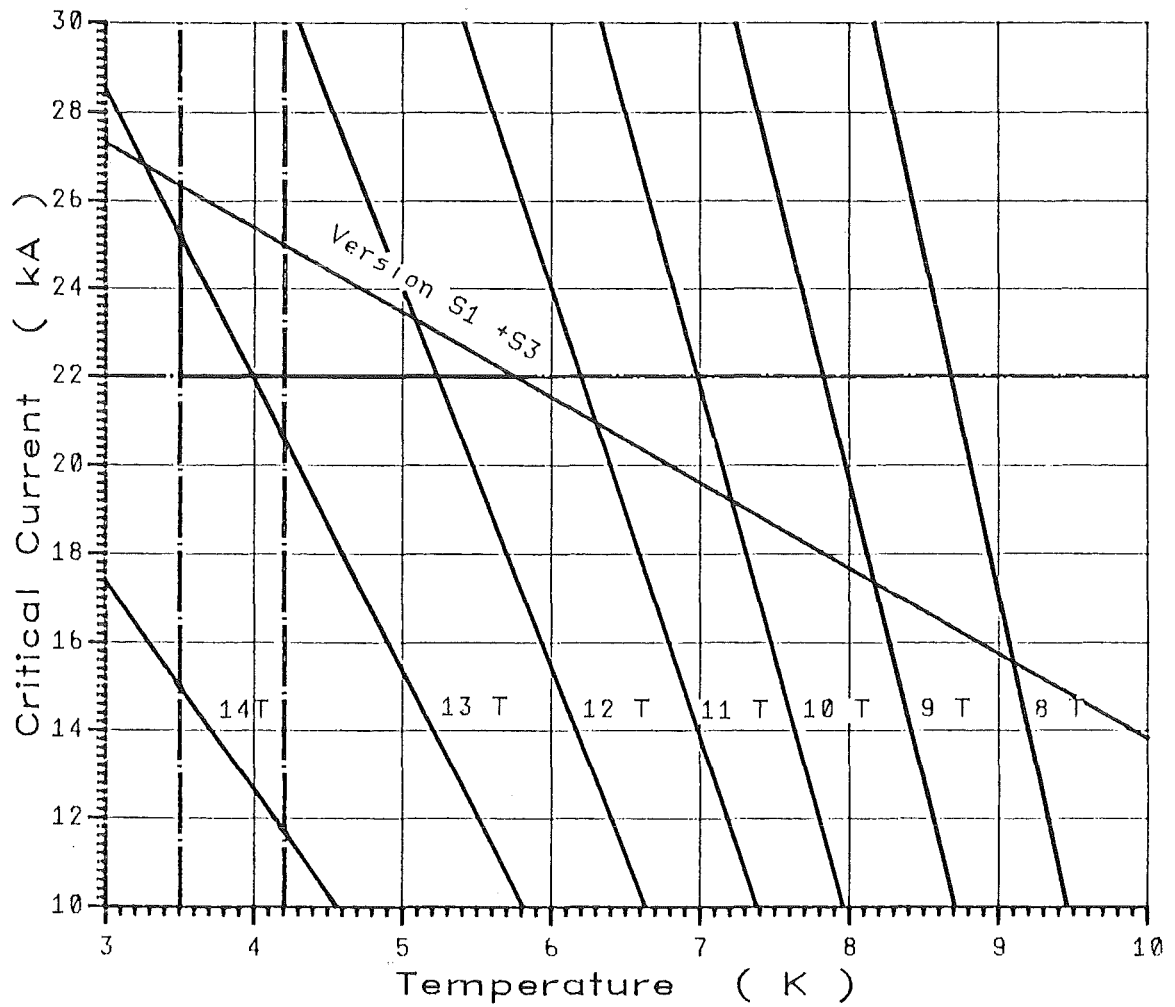


Fig. 4.4-3: Loadline for the SIN Model Coil. A Degradation of 30 % is taken into Account for Handling, Bending and transverse Stresses.

References to Chapter 4

[4.1] F.Arendt, B. Manes, A. Ulbricht, KfK, March 1985, unpublished

[4.2] J. Hanauer et al., KfK, Nov. 1985, unpublished

5. Forces and Stresses in the Model-Coils

5.1 Forces and Stresses in the Cluster Test Configuration

The enhancement of the current in the NET-Test coil from 16 kA to 22 kA leads to higher forces in the magnet arrangement. Fig. 5.1-1 shows these forces (total forces) for the test coil currents 22 kA and 13 kA in the LCT-coils. Figs. 5.1-2 and 5.1-3 show the total forces for $I_{CH} = 0$ or $I_{EU} = 0$. The highest lateral force experienced by the EU-LCT coil during the test in Oak Ridge was 26.6 MN. This is lower by a factor of about 4 compared with the values of Fig. 5.1.-1. The CH-LCT coil experienced a lateral force of about 18 MN which is a factor of about 5 lower than the value expected in TOSKA-Upgrade.

The forces calculated here are the electromagnetic ones (Lorentz Forces). Table 5.1-1 contains the values of the cluster configuration C6 and solenoid configuration S3 in comparison with NET values. To meet NET requirements additional means for force application are necessary, especially for axial and shear stresses. FEM calculations using a clamping rod for the solenoid configuration are reported below in section 5.2. Additional axial forces can be applied using a He pressure cylinder as described below in Chapt. 6.

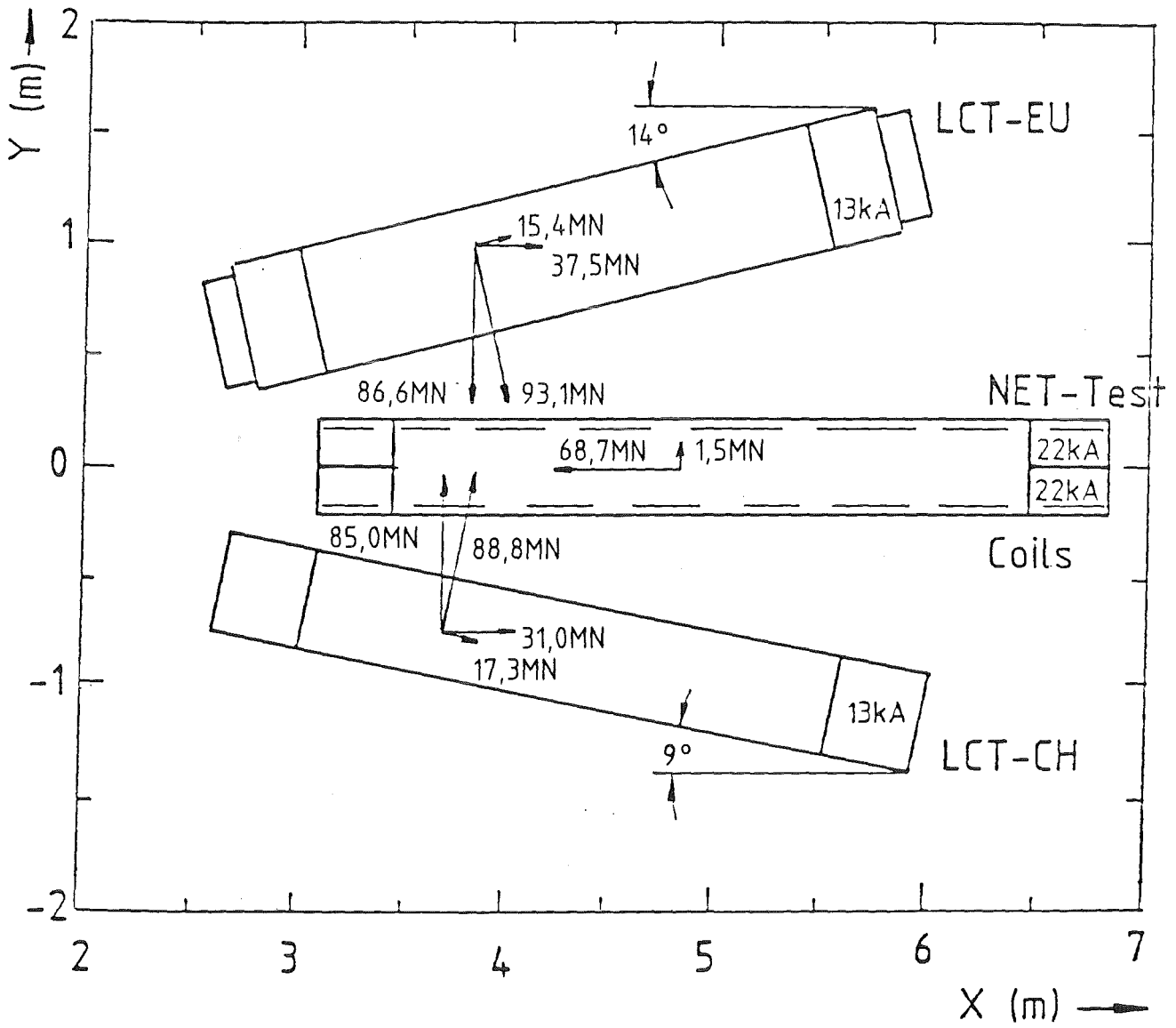


Fig. 5.1-1: Forces between the Coils for Configuration C6; 11T.

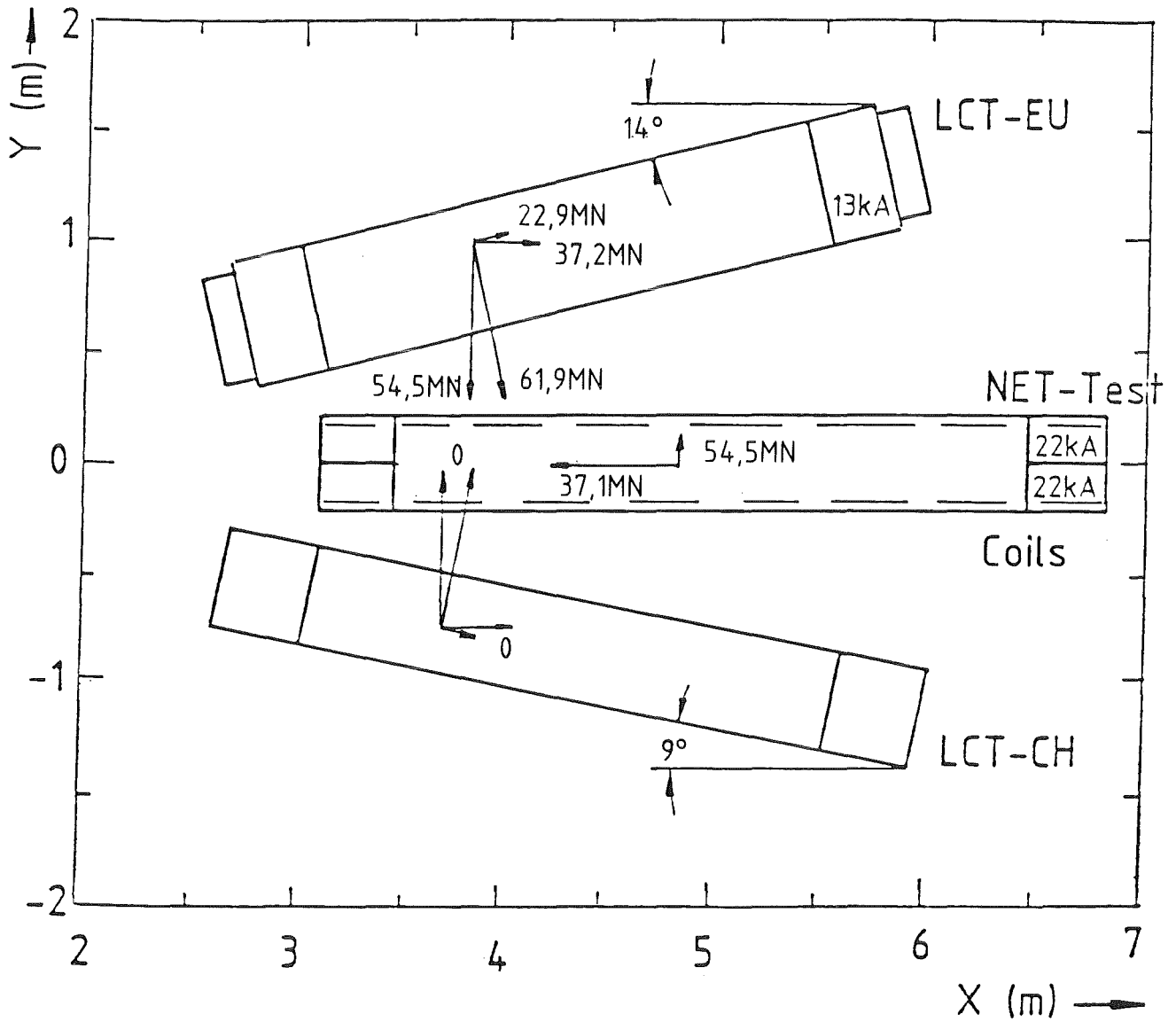


Fig. 5.1-2: Forces between the Coils for Configuration C6; 11T; $I_{CH} = 0$.

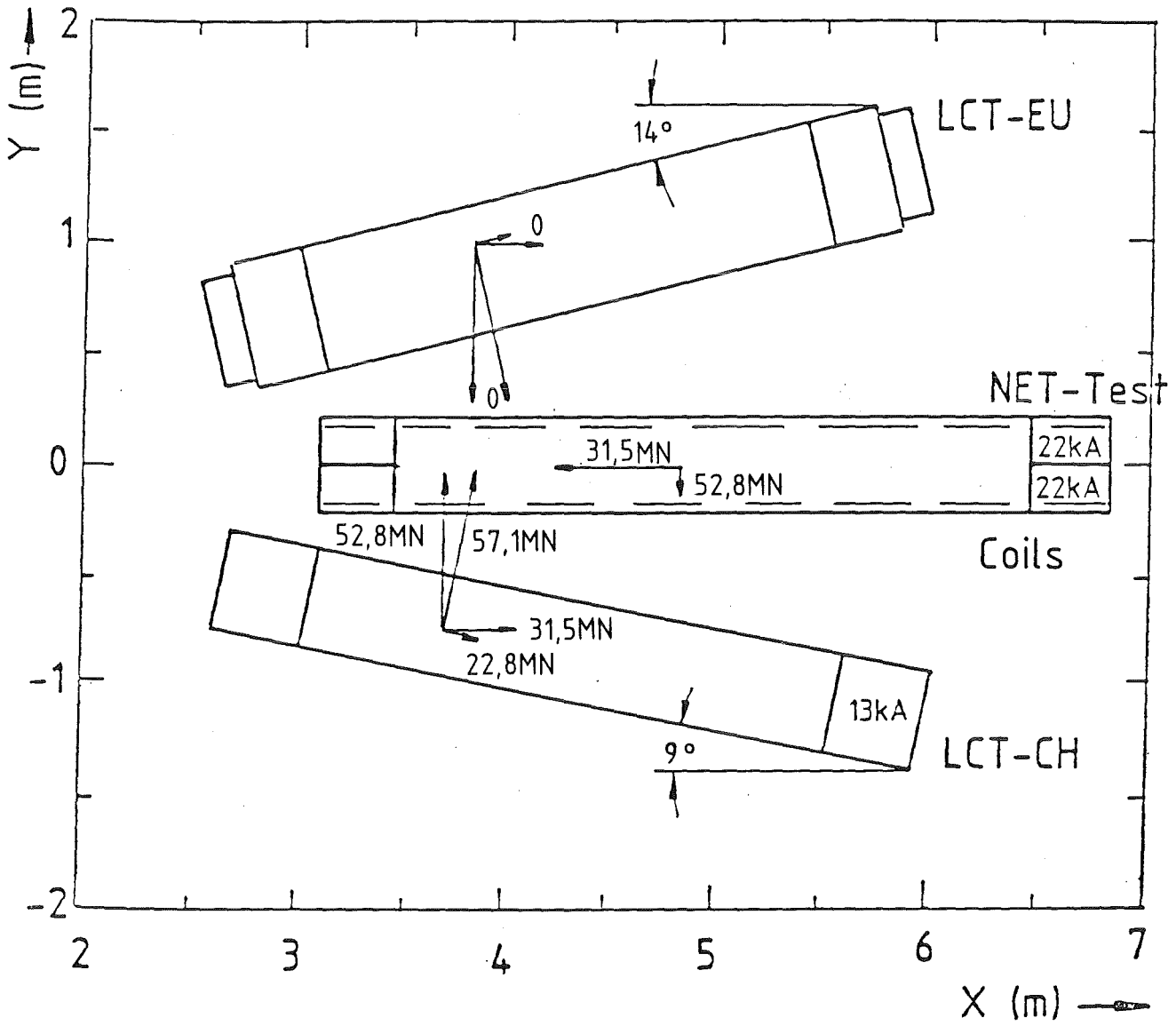


Fig. 5.1-3: Forces between the Coils for Configuration C6; 11T; $I_{EU} = 0$

Table 5.1-1: Comparison of Mechanical Test Facilities Characteristics with NET. The Values for S3 and C6 stem from Lorentz-Force Calculations. The Values given by the NET Team are from FEM Calculations.

Configuration	NET		Solenoid S3			Cluster C6	
Coil	TF	OH	KfK	OH	Sultan	KfK	Sultan
Axial Pressure [MPa]	140	100	50.2	44.3	43.4	17.5	18.5
Radial Pressure [MPa]	40	10	63	51.3	50.3	110	100
Hoop Stresses							
σ_{Hoop} [MPa]	140	200	153	143	118	249	217
τ_{max} [MPa]	30	30	15.5*				

* For this calculation it was assumed that the pancake is supported by a rod at two areas and without a case.

5.1.1 Stresses in the TF-model coils.

For the KFK- and SULTAN-model coil of the cluster configuration C6 the theoretical calculations were performed with the FEM-method to get an impression of the stress distribution, the deformations and the peaks of stresses in the individual coils.

5.1.1.2 Calculation model

The technical and physical data of the arrangement are summerized in table 3.6-1. The following simplifications were taken for the first calculation-model:

1. both coils are modelled without casing
2. both coils are fixed together along their side-faces
3. both coils are supported on a support
4. both supports are fixed together along their side-faces
5. both coils are encircled and fixed with the supports from 90° up to 180° (figure 5.1.1-2)

The geometry and the distribution of the volume loads have been calculated with the program-system HEDO /1/. They are symmetric so that only the half of the whole coil system had to be modelled. The model (figure 5.1.1-1) has been constructed with volume elements of the type HEXE-8. The whole system was subdivided in the following substructures:

- | | | | |
|------------------------|---|-----|----------|
| 1. KFK-coil | - | 384 | Elemente |
| 2. support KFK-coil | - | 96 | " |
| 3. SULTAN-coil | - | 384 | " |
| 4. support SULTAN-coil | - | 96 | " |

As boundary conditions we define the fixation in x- and y-direction from all nodal points of the front of the support and in z-direction from all nodal points of the plane of symmetry $z=0$. They were shown in figure 5.1.1-2.

The material properties of the winding packs (KFK- and SULTAN-coil) were assumed to be orthotropically with the following values:

	Young's modulus	Poisson's ratio
E_1 (radial)	80.0 GPa	0.3
E_2 (axial)	80.0 GPa	0.3
E_3 (longitudinal)	120.0 GPa	0.3
G	20.0 GPa	

For the supports we assume isotropic behaviour with the following value:

	Modulus of elasticity	Poisson's ratio
Support	208.0 GPa	0.3

The stress analysis is performed with the FEM-program PERMAS /2/. By the calculation with orthotropic material the program PERMAS expects the Hooke's matrix between the stresses and the strains for each element as input. The generalized Hooke's law /3/ relating stresses to strains can be written with the notation:

$$\sigma_i = C_{ij} \varepsilon_j \quad i, j = 1, \dots, 3$$

where σ_i are the stress components, C_{ij} is the stiffness matrix, and ε_j are the strain components. The stiffness matrix, C_{ij} , has generally 36 constants. The stress-strain relation for orthotropic material in coordinates aligned with principal material directions is

$$\begin{bmatrix} \sigma_1 \\ \sigma_2 \\ \sigma_3 \\ \tau_{23} \\ \tau_{31} \\ \tau_{12} \end{bmatrix} = \begin{bmatrix} C_{11} & C_{12} & C_{13} & 0 & 0 & 0 \\ C_{12} & C_{22} & C_{23} & 0 & 0 & 0 \\ C_{13} & C_{23} & C_{33} & 0 & 0 & 0 \\ 0 & 0 & 0 & C_{44} & 0 & 0 \\ 0 & 0 & 0 & 0 & C_{55} & 0 \\ 0 & 0 & 0 & 0 & 0 & C_{66} \end{bmatrix} \begin{bmatrix} \varepsilon_1 \\ \varepsilon_2 \\ \varepsilon_3 \\ \gamma_{23} \\ \gamma_{31} \\ \gamma_{12} \end{bmatrix}$$

Principal material directions are parallel to the intersections of the three orthogonal planes of material symmetry. Only nine independent constants in the stiffness matrix must be taken into account.

5.1.1.3 Numerical analysis

We use the element type HEXE-8 of the PERMAS library and introduce a local coordinate system. The x-axis for all elements is in radial direction, the y-axis is in axial direction and the z-axis is perpendicular to the x,y-plane (figure 5.1.1-1). The material and stress directions are parallel to this coordinate system. In the figures of the displacements and stresses of the two coils and of the two supports following conventions have been met:

1. all displacements (mm) in global-system
2. all stresses (MPa) in local-system (figure 5.1.1-1)

To get an impression of the stresses and displacements, the extreme values of the 6 stress components and equivalent stresses (local-system) and of the three displacement components (global-system) in all element layers are given in the tables 5.1.1-1, -2, -3 and -4. The element layers are numbered from 1 (0°) to 25 (180°) for the coils and from 1 (90°) to 13 (180°) for the supports. The deformations and the stress distributions for the KFK-coil are shown in the figures 5.1.1-3 to 5.1.1-9. As expected, the maximum radial stresses $\sigma(x)$ in both coils occur in the region of the support as pressure. The maximum is -65.1 MPa (KFK-coil) and -64.3 MPa (SULTAN-coil) respectively in the section 18 (127.5°). On the side-faces of both coils which are fixed together the axial stresses $\sigma(y)$ are in the range of -19.2 MPa and -27.4 MPa. In tangential direction the maximum tensile stresses $\sigma(z)$ occur in the plane of symmetry $z=0$. The maximum value is 310.7 MPa (KFK-coil) and 309.9 MPa (SULTAN-coil) in the section 1 (0°). The von Mises stresses reach their maximum values in the plane of symmetry $z=0$ like the tangential stresses. The shear stresses in the xy- and yz-plane are in the range of -8.3 MPa and 4.5 MPa. The maximum shear stresses of the zx-plane occur in the region of the support. The maximum is -26.8 MPa (KFK-coil) and -28.8 MPa (SULTAN-coil) in the section 16 (112.5°). The extreme displacements of the KFK-coil are -0.63 mm in x-, 1.14 mm in y- and 3.47 mm in z-direction (global-system) and of the SULTAN-coil -0.84 mm in x-, -1.11 mm in y- and 3.37 mm in z-direction (global-system). In both supports the most interesting stresses are the von Mises' values. The maximum is 311.0 MPa.

For orthotropic material the following relations are valid:

$$\nu_{ij}/E_i = \nu_{ji}/E_j \quad \text{with } i, j = 1, 2, 3$$

With

E_1, E_2, E_3 = Young's moduli in x, y, and z direction

ν_{ij} = Poisson's ration for transverse strain
in the j-direction when stressed
in the i-direction

$$\nu_{ij} = - \epsilon_j / \epsilon_i$$

G_{23}, G_{31}, G_{12} = G - shear moduli in the 2-3, 3-1, and
1-2 planes, respectively we get the following
expression for the C_{ij} :

$$C_{11} = (1 - \nu_{23}\nu_{32})/E_2E_3D$$

$$C_{12} = (\nu_{21} + \nu_{31}\nu_{23})/E_2E_3D \\ = (\nu_{12} + \nu_{32}\nu_{13})/E_1E_3D$$

$$C_{13} = (\nu_{31} + \nu_{21}\nu_{32})/E_2E_3D \\ = (\nu_{13} + \nu_{12}\nu_{23})/E_1E_2D$$

$$C_{22} = (1 - \nu_{13}\nu_{31})/E_1E_3D$$

$$C_{23} = (\nu_{32} + \nu_{12}\nu_{31})/E_1E_3D \\ = (\nu_{23} + \nu_{21}\nu_{13})/E_1E_2D$$

$$C_{33} = (1 - \nu_{12}\nu_{21})/E_1E_2D$$

$$C_{44} = G_{23}$$

$$C_{55} = G_{31}$$

$$C_{66} = G_{12}$$

where

$$D = (1 - \nu_{12}\nu_{21} - \nu_{23}\nu_{32} - \nu_{31}\nu_{13} - 2\nu_{21}\nu_{32}\nu_{13})/E_1E_2E_3$$

The numerical results are:

$$C_{11} = 1.238E+05 \text{ N/mm}^2$$

$$C_{12} = 0.623E+05 \text{ N/mm}^2$$

$$C_{13} = 0.837E+05 \text{ N/mm}^2$$

$$C_{22} = 1.238E+05 \text{ N/mm}^2$$

$$C_{23} = 0.837E+05 \text{ N/mm}^2$$

$$C_{33} = 1.954E+05 \text{ N/mm}^2$$

$$C_{44} = 0.200E+05 \text{ N/mm}^2$$

$$C_{55} = 0.200E+05 \text{ N/mm}^2$$

$$C_{66} = 0.200E+05 \text{ N/mm}^2$$

All important maximal stress values in the model coils and in the NET-TF-coils are summerized in the following table:

		KFK-coil	SULTAN-coil	Target Test Values
Radial stress $\sigma(x)$	(MPa)	-65.1	-64.3	-40.0
Axial stress $\sigma(y)$	(MPa)	-27.4	-26.3	-140.0
(Toroidal stress)				
Tangential stress $\sigma(z)$	(MPa)	310.7	309.9	140.0
(Hoop stress)				
Shear stress $\tau(zx)$	(MPa)	-26.8	-28.8	-30.0

In comparison with the values of the NET-TF-coils and of the KFK-calculation the maximal shear stresses correspond quite well and all other maximal stresses differ considerably. The maximal radial- and tangential-stresses of the KFK-calculation are significant higher and the maximal axial-stresses are significant lower than those of the NET-TF-coils. In order to reduce the radial- and tangential-stresses a casing should be modelled around the coils and the supports reinforced in z-direction. In the first step the reinforcement of the support in z-direction by 130 mm was carried out, but the stress decrease was very small. From the other measure we expect a more significant decrease of the stresses.

Two other variants were calculated additionally:

1. both coils were encircled and fixed with the supports from 135° up to 180°
2. we modelled a gap between the coils and the supports (contact analysis)

Both calculations resulted in an increase of the stress values.

The analysis of these FEM-calculations gives a general impression of the stress distribution and the deformation of both coils and supports. For a better analysis following details are necessary:

1. modelling with volume elements of higher quality, e.g. HEXE-27
2. modelling of the coils with casing
3. contact analysis between the planes of the coils and the corresponding planes of the casing
4. a more detailed FEM-model for a local stress analysis on the conductors

Table 5.1.1-1

KFK-coil

Stress components in circumferential direction
(local-system)

Section	$\sigma(x)$		$\sigma(y)$		$\sigma(z)$	
	MPa		MPa		MPa	
	min.	max.	min.	max.	min.	max.
1	-15.6	26.8	-20.6	3.4	10.9	310.7
2	-15.4	25.8	-20.6	3.2	13.4	306.3
3	-15.1	23.9	-20.4	2.7	19.9	296.0
4	-14.9	20.4	-20.1	1.9	30.7	278.0
5	-16.4	15.4	-19.7	0.9	45.3	253.1
6	-18.4	9.3	-19.2	-0.5	62.9	224.1
7	-20.5	2.9	-19.2	-1.8	82.7	192.7
8	-22.7	-4.0	-19.4	-3.1	102.9	159.6
9	-24.9	-7.5	-19.8	-3.1	100.7	137.0
10	-26.8	-5.6	-21.9	-3.0	66.9	159.6
11	-28.1	0.9	-24.7	0.7	42.0	185.5
12	-28.5	4.5	-27.4	-2.1	32.8	204.9
13	-23.9	21.7	-25.6	17.4	43.9	177.1
14	-31.5	-16.4	-24.2	2.0	56.6	127.5
15	-37.0	-11.6	-20.7	-0.5	31.1	146.2
16	-52.5	-5.9	-19.7	-0.4	21.0	185.9
17	-62.6	-0.7	-21.2	-0.2	26.3	220.7
18	-65.1	3.7	-21.9	-0.8	36.0	246.0
19	-58.2	6.7	-21.9	-0.3	41.4	261.0
20	-53.2	8.2	-21.7	-1.3	44.8	267.3
21	-45.4	8.6	-21.3	-1.7	55.5	268.8
22	-39.9	8.4	-21.2	0.2	73.4	269.4
23	-40.8	7.7	-21.3	13.9	99.5	270.6
24	-48.6	7.1	-22.0	31.9	120.2	272.2
25	-51.1	6.9	-22.4	33.3	122.8	273.1

Table 5.1.1-1

KFK-coil

Stress components in circumferential direction
(local-system)

Section	$\sigma(xy)$		$\sigma(yz)$		$\sigma(zx)$	
	MPa		MPa		MPa	
	min.	max.	min.	max.	min.	max.
1	-1.3	2.0	-0.3	1.1	-8.3	4.1
2	-1.3	1.9	0.0	0.3	1.0	4.2
3	-1.2	1.9	-0.1	0.6	1.9	8.3
4	-1.2	1.7	-0.1	1.0	2.8	12.1
5	-1.1	1.5	-0.1	1.4	3.6	15.3
6	-1.0	1.2	-0.2	1.6	4.2	17.7
7	-0.9	0.9	-0.2	1.8	4.6	19.2
8	-0.9	0.6	-0.2	2.0	4.7	19.6
9	-1.0	0.8	-0.2	2.0	4.6	18.7
10	-1.2	0.9	-0.3	1.8	4.3	16.1
11	-1.4	1.1	-0.7	1.1	3.8	11.4
12	-2.6	1.1	-0.3	1.9	-0.2	8.8
13	-4.7	4.5	-1.2	3.0	-10.9	21.5
14	-0.8	1.7	-2.2	1.8	-20.4	3.8
15	-2.6	2.2	-2.7	0.4	-25.3	-9.5
16	-1.8	1.8	-2.7	0.3	-26.8	-16.2
17	-1.2	1.5	-2.4	0.1	-24.0	-13.4
18	-0.9	1.7	-1.8	-0.1	-19.1	-9.1
19	-0.8	1.7	-1.5	-0.3	-14.5	-5.3
20	-0.8	1.9	-1.3	-0.3	-13.2	-2.7
21	-2.0	2.6	-1.7	-0.2	-14.6	-1.4
22	-2.6	2.1	-1.5	-0.2	-18.7	-1.4
23	-2.5	2.0	-0.9	-0.1	-20.2	-1.5
24	-2.4	3.9	-0.4	0.0	-14.1	-1.0
25	-1.6	4.0	-0.6	0.1	6.7	11.8

Table 5.1.1-1

KFK-coil

Stress components in circumferential direction
(local-system)

Section	$\sigma(\text{eq})$	
	min.	max.
1	27.6	297.5
2	29.1	293.3
3	35.7	283.5
4	46.7	266.8
5	61.5	243.6
6	79.4	215.6
7	99.6	184.8
8	121.2	152.2
9	119.8	141.1
10	90.6	161.5
11	68.3	150.8
12	59.0	139.8
13	69.9	127.2
14	99.3	122.0
15	113.3	138.6
16	116.1	179.3
17	121.2	214.8
18	122.1	240.6
19	120.1	255.8
20	120.6	262.8
21	123.8	265.3
22	132.6	266.9
23	145.2	268.9
24	155.7	271.1
25	173.1	272.8

Table 5.1.1-1

KFK-coil

Displacement components in circumferential direction
(global-system)

Section	x		y		z	
	min.	max.	min.	max.	min.	max.
1	-0.52	-0.05	-1.14	-0.56	0.00	0.00
2	-0.47	-0.03	-1.13	-0.55	0.04	0.33
3	-0.32	0.02	-1.10	-0.53	0.12	0.66
4	-0.13	0.11	-1.06	-0.50	0.26	1.01
5	0.04	0.33	-1.00	-0.46	0.49	1.37
6	0.14	0.60	-0.93	-0.41	0.81	1.75
7	0.23	0.82	-0.85	-0.36	1.20	2.13
8	0.31	0.97	-0.76	-0.30	1.65	2.50
9	0.36	1.01	-0.67	-0.23	2.11	2.85
10	0.37	0.92	-0.57	-0.17	2.53	3.15
11	0.35	0.71	-0.49	-0.10	2.86	3.36
12	0.30	0.45	-0.43	-0.05	3.05	3.47
13	-0.08	0.32	-0.26	0.00	3.07	3.44
14	-0.23	0.21	-0.15	0.04	2.81	3.28
15	-0.27	0.11	-0.09	0.07	2.50	3.03
16	-0.23	0.02	-0.08	0.09	2.12	2.71
17	-0.17	-0.07	-0.10	0.11	1.75	2.39
18	-0.21	-0.09	-0.12	0.11	1.45	2.06
19	-0.27	-0.07	-0.13	0.11	1.22	1.76
20	-0.37	-0.05	-0.14	0.11	1.04	1.46
21	-0.46	-0.06	-0.15	0.10	0.88	1.18
22	-0.54	-0.06	-0.16	0.10	0.69	0.89
23	-0.59	-0.05	-0.17	0.09	0.47	0.59
24	-0.62	-0.03	-0.17	0.09	0.24	0.30
25	-0.63	-0.03	-0.17	0.09	0.00	0.00

Table 5.1.1-2

SULTAN-coil

Stress components in circumferential direction
(local-system)

Section	$\sigma(x)$		$\sigma(y)$		$\sigma(z)$	
	MPa		MPa		MPa	
	min.	max.	min.	max.	min.	max.
1	-15.2	26.7	-20.4	3.6	7.6	309.9
2	-15.0	25.7	-20.4	3.2	10.0	305.1
3	-14.7	23.7	-20.2	2.7	16.5	294.1
4	-14.7	20.0	-19.7	1.5	27.2	274.6
5	-16.3	14.8	-19.2	-0.1	41.5	247.4
6	-18.2	8.4	-18.8	-1.7	58.7	214.5
7	-20.2	1.7	-18.7	-3.3	78.1	178.7
8	-22.3	-5.6	-18.7	-4.5	98.5	140.5
9	-24.5	-6.3	-18.9	-4.6	89.9	126.2
10	-26.3	-4.4	-19.5	-4.5	57.7	148.0
11	-27.5	1.6	-22.1	-1.3	33.3	174.2
12	-27.7	4.4	-26.5	-4.3	23.6	202.9
13	-22.7	22.4	-22.9	19.3	33.9	167.1
14	-31.0	-14.5	-21.4	-0.7	56.6	103.2
15	-35.3	-12.7	-17.9	-1.9	26.9	119.5
16	-50.9	-6.5	-18.6	-1.6	18.2	165.9
17	-61.5	-0.9	-20.3	-1.4	24.7	206.7
18	-64.3	3.9	-21.3	-1.8	36.1	236.6
19	-57.9	7.3	-21.5	-1.3	41.8	254.0
20	-52.8	9.3	-21.5	-2.2	44.8	261.8
21	-42.3	10.4	-21.4	-1.1	57.5	264.3
22	-34.6	10.8	-21.5	1.2	76.8	265.6
23	-38.8	10.5	-22.4	13.7	110.4	267.3
24	-47.0	10.2	-23.3	31.1	119.9	269.2
25	-50.2	10.1	-23.8	34.2	122.4	270.2

Table 5.1.1-2

SULTAN-coil

Stress components in circumferential direction
(local-system)

Section	$\sigma(xy)$		$\sigma(yz)$		$\sigma(zx)$	
	MPa		MPa		MPa	
	min.	max.	min.	max.	min.	max.
1	-2.1	2.3	-1.9	-0.2	-8.2	4.5
2	-2.1	2.3	-0.5	0.3	1.0	4.8
3	-2.0	2.2	-1.0	0.7	2.0	9.4
4	-1.7	2.0	-1.5	1.0	2.9	13.6
5	-1.4	1.8	-1.9	1.2	3.6	17.2
6	-1.0	1.5	-2.2	1.5	4.2	19.9
7	-0.6	1.2	-2.3	1.7	4.6	21.6
8	-0.2	0.9	-2.4	1.8	4.7	22.1
9	-0.2	0.6	-2.2	1.9	4.6	21.0
10	-0.4	0.7	-1.8	2.0	4.3	18.0
11	-0.9	1.1	-0.9	2.7	4.1	12.6
12	-0.4	2.1	0.1	2.0	0.0	8.6
13	-2.4	3.5	-1.7	3.0	-11.4	21.0
14	-2.4	0.8	-1.4	2.5	-22.2	3.8
15	-3.0	1.9	-0.7	2.9	-27.4	-10.4
16	-2.8	1.7	-1.1	2.5	-28.8	-16.3
17	-2.5	2.0	-1.4	1.8	-25.6	-13.4
18	-2.9	2.1	-1.5	0.9	-19.8	-9.2
19	-3.0	2.1	-1.6	0.1	-15.2	-5.3
20	-4.2	2.1	-1.6	0.1	-13.5	-2.8
21	-5.0	1.9	-1.5	0.2	-14.2	-1.4
22	-4.9	1.8	-1.2	0.3	-17.6	-1.2
23	-6.2	1.7	-1.1	0.2	-19.4	-1.3
24	-8.1	1.6	-0.6	0.1	-13.8	-0.9
25	-8.3	1.6	0.0	0.9	6.1	11.6

Table 5.1.1-2

SULTAN-coil

Stress components in circumferential direction
(local-system)

Section	$\sigma(\text{eq})$	
	min.	max.
1	20.0	297.3
2	20.6	293.1
3	26.9	283.3
4	37.2	266.6
5	51.0	243.4
6	67.6	215.4
7	86.2	184.6
8	105.7	152.0
9	119.6	127.6
10	90.4	145.9
11	68.1	130.9
12	58.8	119.1
13	69.7	105.7
14	99.1	101.8
15	97.1	138.3
16	102.6	179.0
17	108.8	214.5
18	110.6	240.4
19	109.8	255.6
20	111.9	262.6
21	116.6	265.1
22	126.2	266.7
23	139.0	268.8
24	149.4	270.9
25	165.3	272.7

Table 5.1.1-2

SULTAN-coil

Displacement components in circumferential direction
(global-system)

Section	x		y		z	
	mm		mm		mm	
	min.	max.	min.	max.	min.	max.
1	-0.84	-0.21	-1.11	-0.23	0.00	0.00
2	-0.78	-0.19	-1.10	-0.22	0.03	0.33
3	-0.63	-0.14	-1.07	-0.22	0.10	0.66
4	-0.43	-0.06	-1.01	-0.21	0.23	1.00
5	-0.26	0.17	-0.94	-0.19	0.45	1.36
6	-0.13	0.44	-0.86	-0.18	0.76	1.73
7	-0.01	0.67	-0.76	-0.16	1.15	2.10
8	0.10	0.82	-0.65	-0.13	1.60	2.46
9	0.17	0.87	-0.54	-0.10	2.06	2.79
10	0.21	0.79	-0.43	-0.07	2.49	3.07
11	0.22	0.60	-0.32	-0.03	2.83	3.27
12	0.19	0.35	-0.23	0.02	3.02	3.37
13	-0.12	0.24	-0.13	0.08	3.02	3.35
14	-0.26	0.17	-0.07	0.15	2.75	3.21
15	-0.28	0.09	-0.03	0.22	2.43	2.97
16	-0.23	0.01	0.00	0.29	2.04	2.68
17	-0.17	-0.06	0.02	0.34	1.69	2.36
18	-0.21	-0.08	0.02	0.37	1.40	2.04
19	-0.26	-0.04	0.02	0.39	1.18	1.74
20	-0.36	-0.02	0.02	0.40	1.01	1.45
21	-0.45	-0.03	0.01	0.40	0.85	1.17
22	-0.53	-0.03	0.00	0.40	0.66	0.88
23	-0.58	-0.03	0.00	0.39	0.46	0.59
24	-0.61	-0.02	0.00	0.39	0.23	0.30
25	-0.62	-0.02	0.00	0.39	0.00	0.00

Table 5.1.1-3

KFK-support
 Stress components in circumferential direction
 (local-system)

Section	$\sigma(x)$ MPa		$\sigma(y)$ MPa		$\sigma(z)$ MPa	
	min.	max.	min.	max.	min.	max.
1	-6.5	142.3	-65.6	7.1	0.0	191.3
2	-21.2	142.2	-24.5	10.3	-12.9	159.0
3	-10.9	105.0	-8.0	6.0	-13.1	112.7
4	-23.6	40.6	-8.3	13.4	-26.6	105.6
5	-106.7	-13.9	-12.8	13.1	-37.5	117.6
6	-136.6	-17.8	-2.1	19.2	-24.9	133.6
7	-130.1	-25.8	-45.9	20.5	-23.0	126.1
8	-27.2	-19.3	-2.2	6.5	19.9	128.8
9	-19.2	-7.4	-6.1	21.7	74.0	140.8
10	-37.1	1.2	-6.5	45.0	132.6	160.8
11	-58.2	20.4	-5.0	75.3	186.3	230.6
12	-71.2	49.1	-10.9	100.5	235.9	285.8
13	-76.6	30.9	1.2	94.0	240.8	300.2

Section	$\sigma(xy)$ MPa		$\sigma(yz)$ MPa		$\sigma(zx)$ MPa	
	min.	max.	min.	max.	min.	max.
1	-37.4	49.2	-20.5	26.5	-72.5	113.5
2	-7.7	0.9	-3.9	7.2	-2.7	15.1
3	-1.7	2.0	-1.7	1.6	2.9	13.1
4	-2.2	1.6	-0.8	1.0	-14.0	28.0
5	-1.4	0.6	-1.9	1.2	-28.2	37.8
6	-2.0	1.5	-4.3	3.6	-31.6	36.8
7	-3.9	7.0	-3.8	2.1	-30.9	43.8
8	-1.9	0.9	-5.0	3.9	-23.1	30.8
9	-8.2	6.6	-7.0	5.0	-26.9	29.3
10	-21.0	10.8	-6.1	4.1	-37.4	24.6
11	-41.1	15.7	-3.8	2.9	-38.4	16.6
12	-64.2	31.0	-2.4	1.8	-30.9	18.7
13	-75.7	22.6	-3.1	6.3	-82.6	3.8

Section	$\sigma(eq)$ MPa	
	min.	max.
1	125.2	310.9
2	120.6	157.1
3	88.4	112.1
4	17.9	110.3
5	84.8	131.4
6	84.6	146.1
7	107.8	150.0
8	78.8	142.9
9	106.6	148.1
10	162.4	176.1
11	222.8	224.6
12	277.7	283.0
13	302.0	305.3

Table 5.1.1-3

KFK-support

Displacement components in circumferential direction
(global-system)

Section	x mm		y mm		z mm	
	min.	max.	min.	max.	min.	max.
1	-0.23	0.01	-0.26	-0.13	3.06	3.10
2	-0.35	-0.16	-0.12	-0.07	2.78	2.82
3	-0.49	-0.22	-0.06	-0.02	2.42	2.50
4	-0.53	-0.20	-0.02	0.00	1.95	2.12
5	-0.45	-0.14	0.00	0.03	1.50	1.76
6	-0.27	-0.09	-0.03	0.04	1.16	1.45
7	-0.09	0.00	-0.01	0.02	0.96	1.22
8	-0.06	0.00	-0.01	0.02	0.94	1.04
9	-0.07	0.00	-0.02	0.01	0.86	0.89
10	-0.07	0.00	-0.04	0.01	0.72	0.74
11	-0.07	0.00	-0.05	0.01	0.53	0.55
12	-0.05	0.00	-0.05	0.02	0.29	0.29
13	-0.05	0.00	-0.05	0.00	0.00	0.03

Table 5.1.1-4

SULTAN-support
Stress components in circumferential direction
(local-system)

Section	$\sigma(x)$ MPa		$\sigma(y)$ MPa		$\sigma(z)$ MPa	
	min.	max.	min.	max.	min.	max.
1	-6.0	123.3	-62.3	-0.2	-2.5	176.6
2	-20.3	125.0	-22.4	7.6	-12.3	121.2
3	-11.5	83.8	-6.3	4.7	-12.0	85.3
4	-24.6	24.5	-8.5	10.9	-26.3	82.9
5	-108.9	-19.3	-11.7	10.6	-37.5	102.1
6	-138.9	-13.3	-2.0	17.3	-27.1	123.2
7	-127.7	-17.5	-45.2	20.1	-22.9	123.1
8	-33.4	-6.4	-5.0	7.3	16.8	123.2
9	-23.4	23.9	-4.4	34.7	70.9	140.2
10	-39.0	40.9	-5.6	61.2	128.8	162.9
11	-58.9	63.0	-4.5	92.6	183.5	245.5
12	-68.6	91.5	-3.4	117.2	237.2	299.0
13	-73.1	70.7	2.7	109.2	240.8	312.1

Section	$\sigma(xy)$ MPa		$\sigma(yz)$ MPa		$\sigma(zx)$ MPa	
	min.	max.	min.	max.	min.	max.
1	-42.1	44.1	-24.0	25.1	-65.1	101.8
2	-1.3	8.0	-5.8	9.0	-3.4	13.3
3	-1.3	2.6	-2.0	2.7	3.0	11.7
4	-3.7	2.1	-1.9	1.1	-13.4	27.8
5	-3.4	2.7	-3.2	1.9	-26.1	38.8
6	-3.2	4.3	-7.2	2.2	-29.3	38.3
7	-7.9	5.3	-5.3	3.2	-29.8	44.3
8	-0.2	5.2	-5.2	4.9	-21.9	30.3
9	-1.9	17.0	-5.3	4.4	-24.1	28.1
10	-8.2	31.3	-4.9	3.9	-33.0	23.1
11	-16.3	51.9	-4.3	3.4	-35.2	15.8
12	-33.3	75.6	-2.4	2.9	-29.4	18.2
13	-30.7	86.8	-6.1	3.0	-85.4	3.6

Section	$\sigma(eq)$ MPa	
	min.	max.
1	125.8	250.1
2	121.1	122.4
3	79.1	90.1
4	19.7	85.2
5	86.1	110.4
6	86.7	127.3
7	109.3	134.2
8	78.5	129.8
9	103.8	138.0
10	159.0	166.3
11	211.6	221.7
12	265.3	280.1
13	289.8	305.3

Table 5.1.1-4

SULTAN-support

Displacement components in circumferential direction
(global-system)

Section	x mm		y mm		z mm	
	min.	max.	min.	max.	min.	max.
1	-0.26	-0.08	-0.13	0.00	3.01	3.07
2	-0.37	-0.23	-0.08	-0.02	2.72	2.81
3	-0.50	-0.27	-0.06	0.00	2.35	2.50
4	-0.54	-0.23	-0.04	0.02	1.89	2.12
5	-0.46	-0.15	-0.05	0.04	1.45	1.75
6	-0.27	-0.08	-0.06	0.05	1.13	1.45
7	-0.09	0.00	-0.01	0.06	0.95	1.22
8	-0.05	0.00	0.00	0.06	0.93	1.04
9	-0.07	0.00	0.00	0.06	0.84	0.89
10	-0.07	0.00	-0.01	0.06	0.71	0.74
11	-0.07	0.00	-0.01	0.07	0.52	0.55
12	-0.05	0.00	-0.02	0.06	0.28	0.29
13	-0.05	0.00	0.00	0.06	0.00	0.04

Literaturhinweis:

/1/ P. Martin, H. Preis

Program Description and User's Manual for the HEDO 2 Magnetic
Computer-Program, IPP-Report II/34, 1975

/2/ K. Bernhard, H. Knapp, E. Schremm

PERMAS-I - Linear Static Analysis, User's Reference Manual
INTES Publication No. 202, Rev. H, Stuttgart 1985

/3/ Robert M. Jones

MECHANICS OF COMPOSITE MATERIALS

Institute of Technology, Southern Methodist University

Dallas, Texas; McGRAW-HILL BOOK COMPANY

- DATA
- EYE
- FINISH
- HELP
- INDEX
- LABEL
- OPTIONS
- PRESENT
- RESULTS
- SET
- VIEW

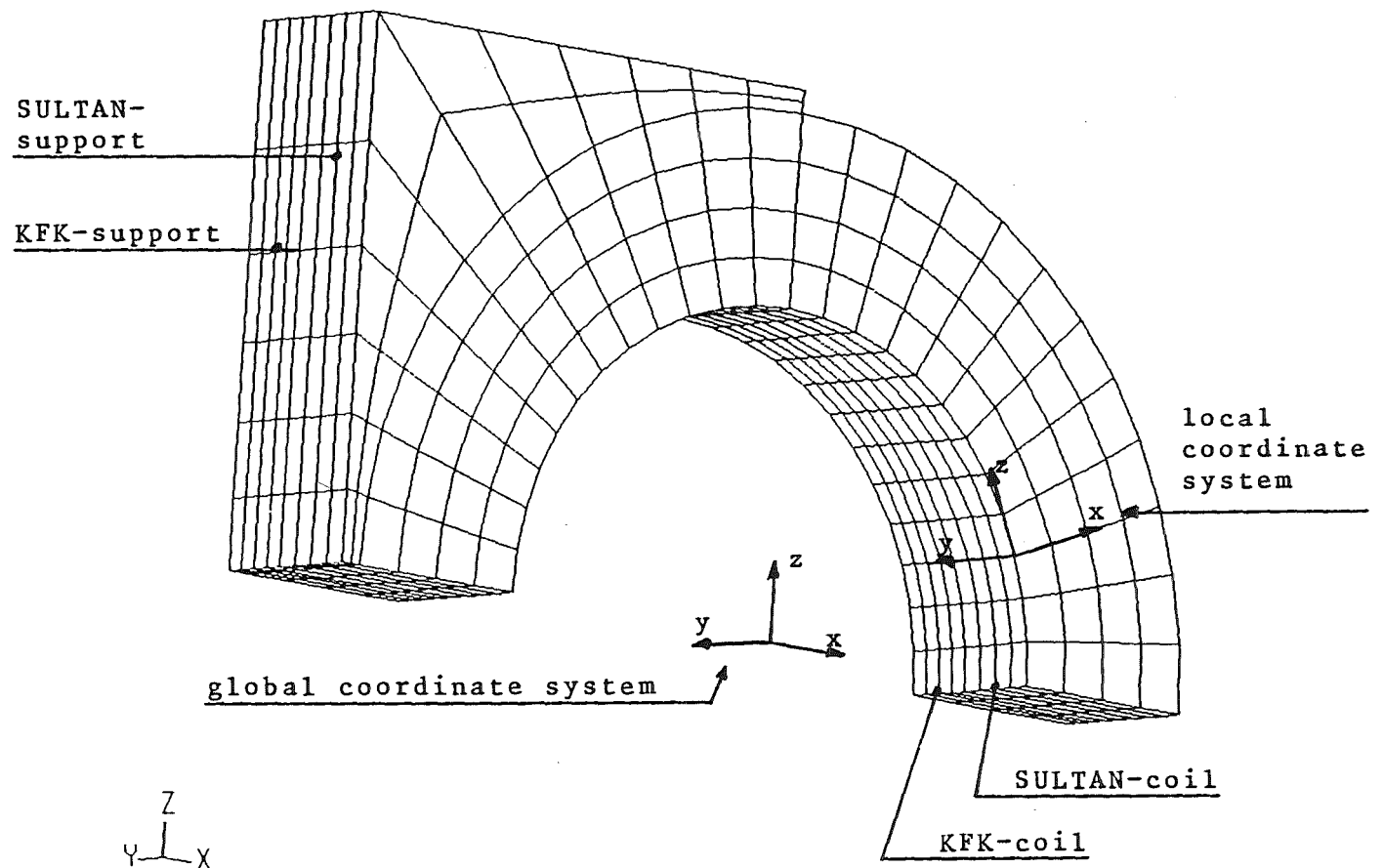


Fig.: 5.1.1-1 - FEM-model of the cluster-configuration
 Presentation of the local- and global-coordinate system

FEMVIEW 3.5

COMMANDS

DATA
EYE
FINISH
HELP
INDEX
LABEL
OPTIONS
PRESENT
RESULTS
SET
VIEW

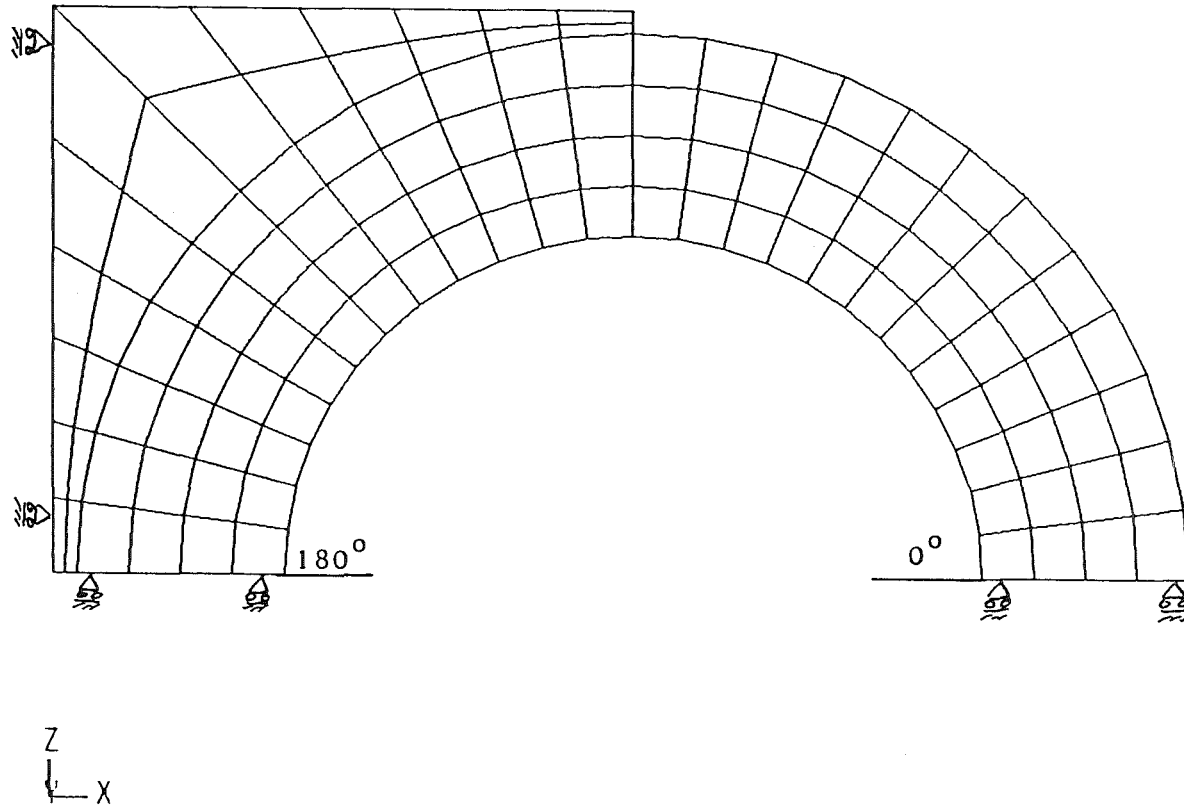


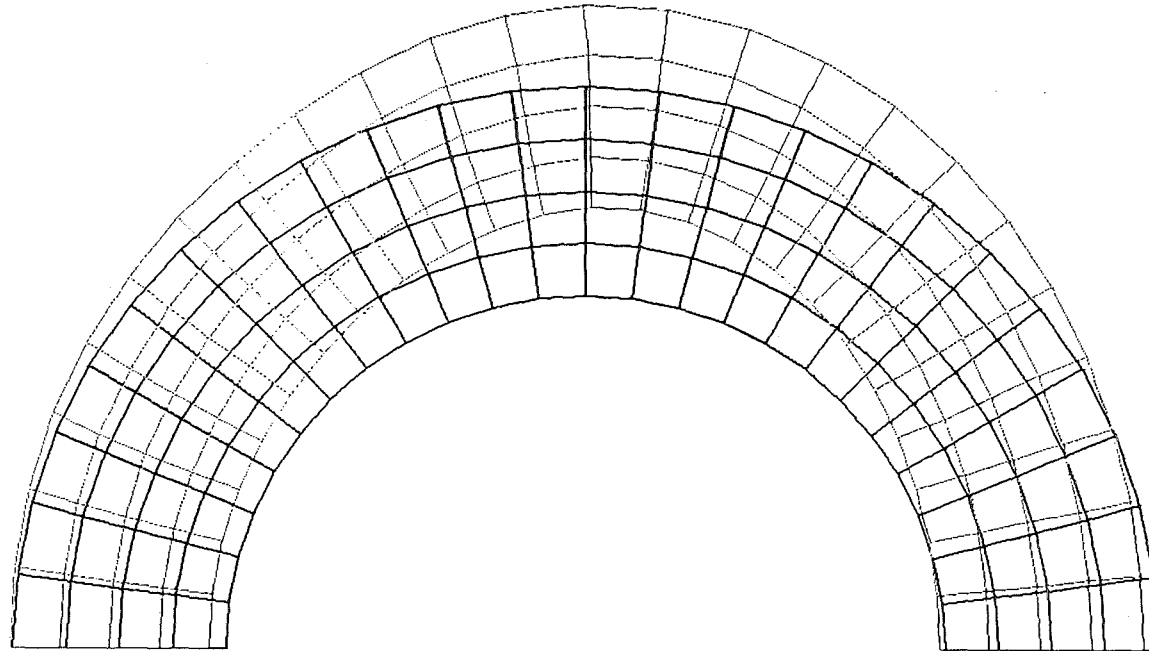
Fig.: 5.1.1-2 - Presentation of the boundary conditions in x- and z-direction

FEMVIEW 3.5

MODEL: KFK
DISPLACEMENTS RESULTANT
LC01
FACTOR = 74.7
MAX = 3.50
MIN = .511E-1

COMMANDS

DATA
EYE
FINISH
HELP
INDEX
LABEL
OPTIONS
PRESENT
RESULTS
SET
VIEW



Z
↓
X

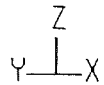
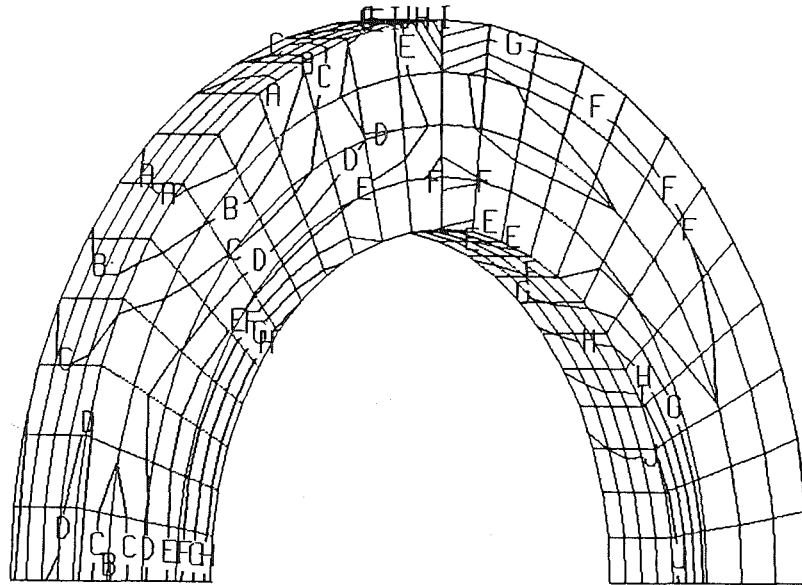
Fig.: 5.1.1-3 - Deformed and undeformed model of KFK-coil

FEMVIEW 3.5

MODEL: KFK
NODAL STRESS XX
LC01

COMMANDS

DATA
EYE
FINISH
HELP
INDEX
LABEL
OPTIONS
PRESENT
RESULTS
SET
VIEW



MAX 26.8
J= 18.4
I= 10.1
H= 1.72
G= -6.62
F= -15.0
E= -23.3
D= -31.7
C= -40.0
B= -48.4
A= -56.7
MIN -65.1

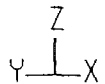
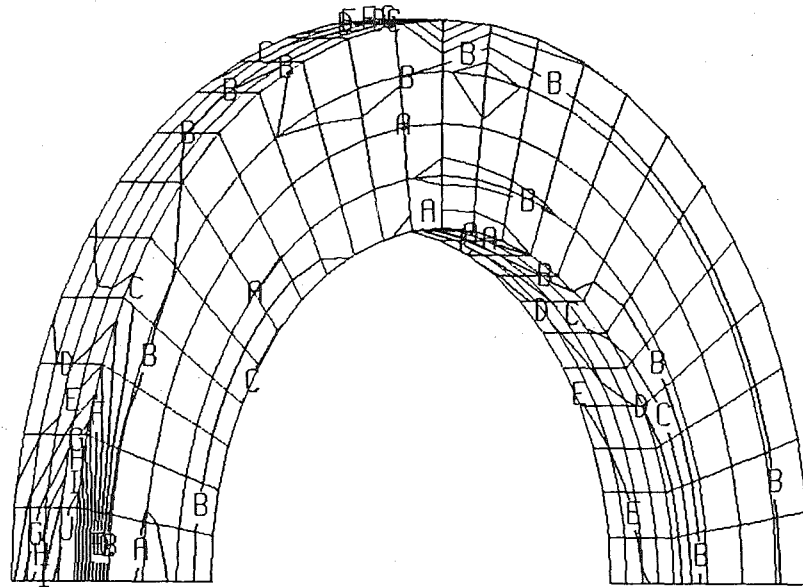
Fig.: 5.1.1-4 - Radial stresses (σ_x /MPa) in KFK-com

FEMVIEW 3.5

MODEL: KFK
NODAL STRESS YY
LC01

COMMANDS

DATA
EYE
FINISH
HELP
INDEX
LABEL
OPTIONS
PRESENT
RESULTS
SET
VIEW



MAX 33.3
J = 27.8
I = 22.3
H = 16.8
G = 11.2
F = 5.73
E = .216
D = -5.30
C = -10.8
B = -16.3
A = -21.8
MIN -27.4

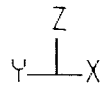
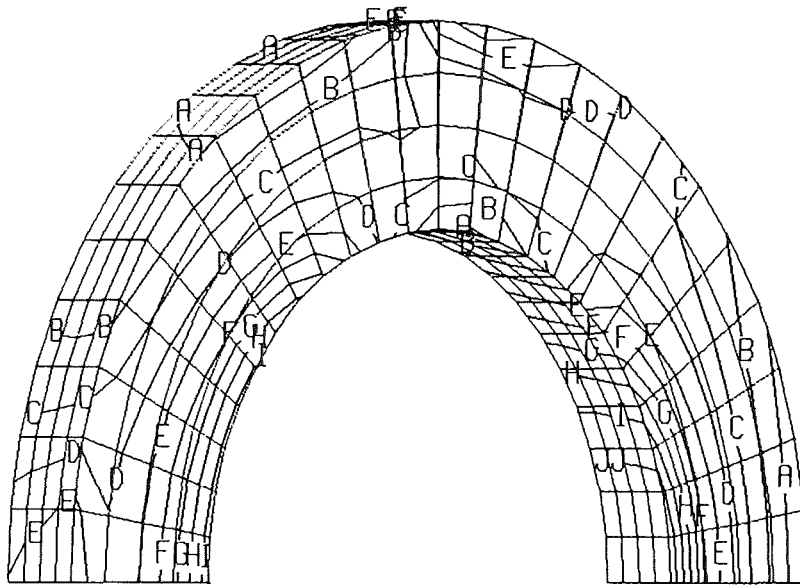
Fig.: 5.1.1-5 - Axial stresses (σ_y /MPa) in KFK-coi

FEMVIEW 3.5

MODEL: KFK
NODAL STRESS ZZ
LC01

COMMANDS

DATA
EYE
FINISH
HELP
INDEX
LABEL
OPTIONS
PRESENT
RESULTS
SET
VIEW



MAX 311.
J = 283.
I = 256.
H = 229.
G = 202.
F = 174.
E = 147.
D = 120.
C = 92.7
B = 65.4
A = 38.2
MIN 10.9

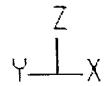
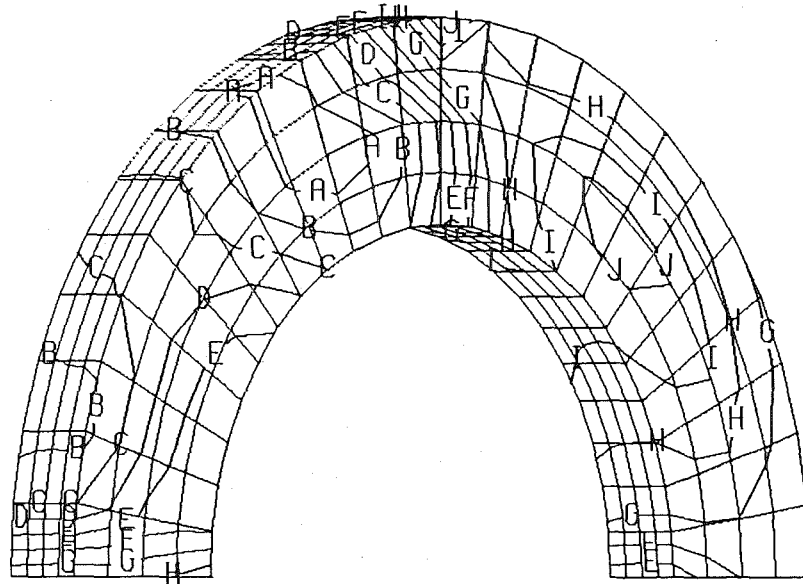
Fig.: 5.1.1-6 - Tang. stresses (σ_z /MPa) in KFK-coin

FEMVIEW 3.5

MODEL: KFK
NODAL STRESS ZX
LC01

COMMANDS

DATA
EYE
FINISH
HELP
INDEX
LABEL
OPTIONS
PRESENT
RESULTS
SET
VIEW



MAX 21.5
J= 17.1
I= 12.7
H= 8.33
G= 3.93
F= -.465
E= -4.86
D= -9.26
C= -13.7
B= -18.1
A= -22.5
MIN -26.8

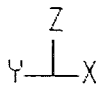
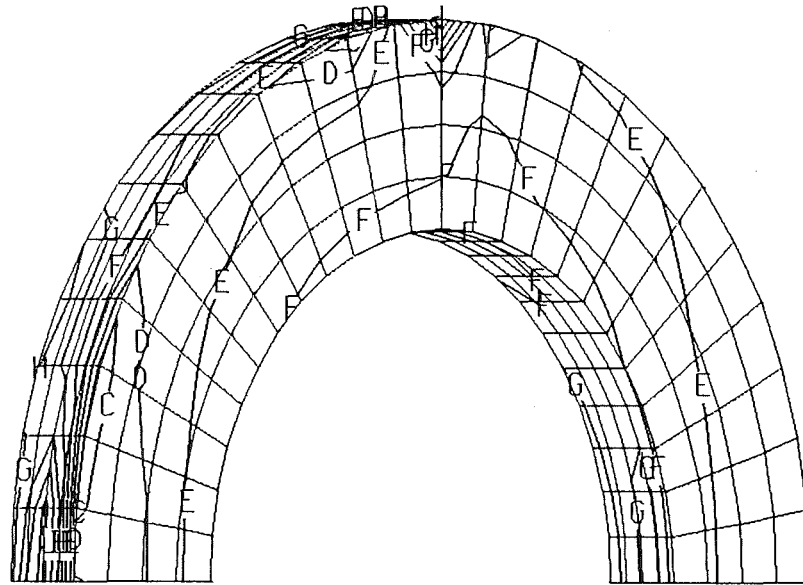
Fig.: 5.1.1-7 - Shear stresses (σ_{zx} /MPa) in KFK-com

FEMVIEW 3.5

MODEL: KFK
NODAL STRESS XY
LC01

COMMANDS

DATA
EYE
FINISH
HELP
INDEX
LABEL
OPTIONS
PRESENT
RESULTS
SET
VIEW



MAX 4.48
J= 3.65
I= 2.82
H= 1.99
G= 1.16
F= .325
E= -.507
D= -1.34
C= -2.17
B= -3.00
A= -3.83
MIN -4.66

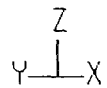
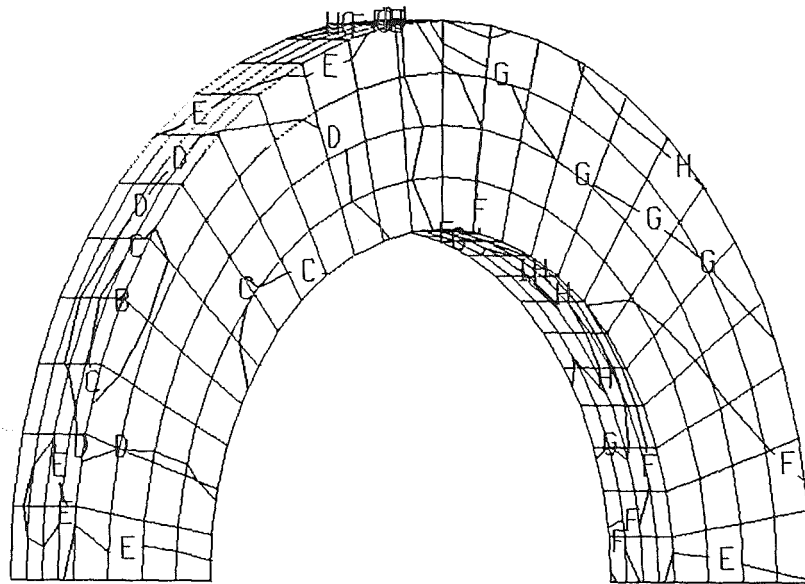
Fig.: 5.1.1-8 - Shear stresses (σ_{xy} /MPa) in KFK-com

FEMVIEW 3.5

MODEL: KFK
NODAL STRESS YZ
LC01

COMMANDS

DATA
EYE
FINISH
HELP
INDEX
LABEL
OPTIONS
PRESENT
RESULTS
SET
VIEW



MAX 3.00
J= 2.47
I= 1.95
H= 1.43
G= .907
F= .385
E= -.137
D= -.659
C= -1.18
B= -1.70
A= -2.22
MIN -2.75

Fig.: 5.1.1-9 - Shear stresses (σ_{yz} /MPa) in KFK-com

5.1.2 Stresses in the EU-LCT Coil

The nominal current of the EU-LCT coil is 11.4 kA, but during the tests in 1987 in the IFSMTF the coil was operated at a current of 15.95 kA. The out-of-plane force was 26.6 MN maximum, which is only about a quarter of the load calculated for the TOSKA-Upgrade cluster configuration.

It must be mentioned that the load conditions in a six coil arrangement are completely different to TOSKA-Upgrade. In the six coil arrangement the in plane force is balanced by the bucking post connected with the straight section of the D-shaped coil. The resulting in plane forces in TOSKA-Upgrade are opposite in direction. Therefore a support structure has to be designed and calculations for these new load conditions are necessary in order to prove whether the coil can withstand this load.

Analytical calculations were performed for the EU-LCT coil for the Cluster Test Facility. Fig. 5.1.2-1 shows the simplified geometry of case and winding pack. This geometry was used everywhere without taking into account the reinforced corners of the coil. Therefore these results can be only preliminarily. The in plane bending moment vs the angle α is shown in Fig. 5.1.2-2. The high positive values in the upper right corner and the high negative values at about $\alpha = 90^\circ$ will be partly balanced in reality by the reinforcement at the corners. Table 5.1.2.-1 shows the bending moments at different angle positions and resulting bending stresses. Table 5.1.2.-2 gives the in plane bending stresses and in addition axial bending stresses and shear stresses. The in plane bending and shear stresses are very high, but according to our experience with the EU-LCT coil the quoted values of the tables obtained using this simplified model are by about 50 % larger than the results of FEM calculations. The maximum axial bending stress occur at $\alpha = 0$. These stresses can be reduced by additional support structure. Therefore the EU-LCT coil is suited for the Cluster Test Facility if an additional support structure is provided.

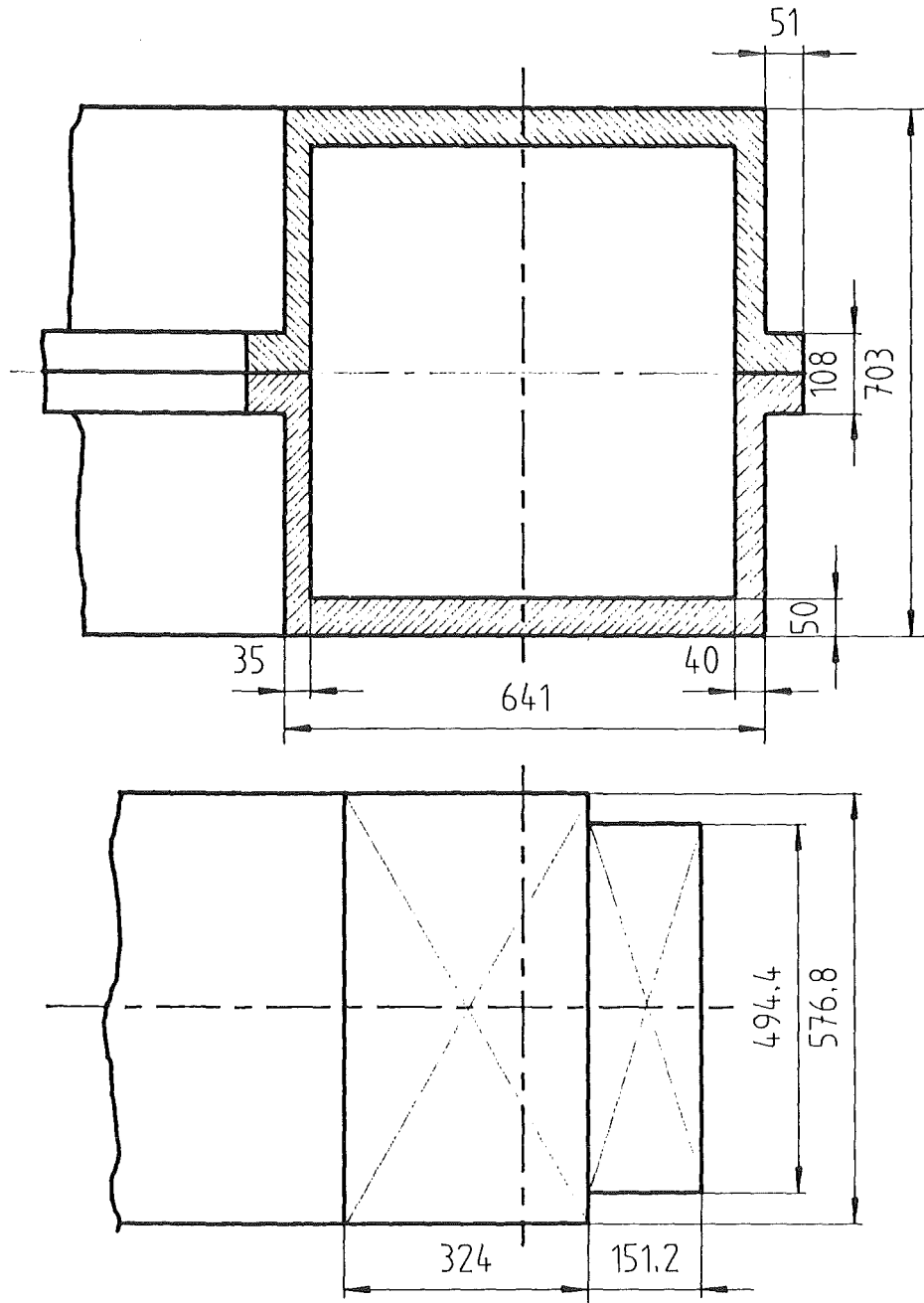


Fig. 5.1.2-1: Cross Section of Case (top) and Winding Pack (bottom) in the x^*y^* -Plane at $\alpha = 0$

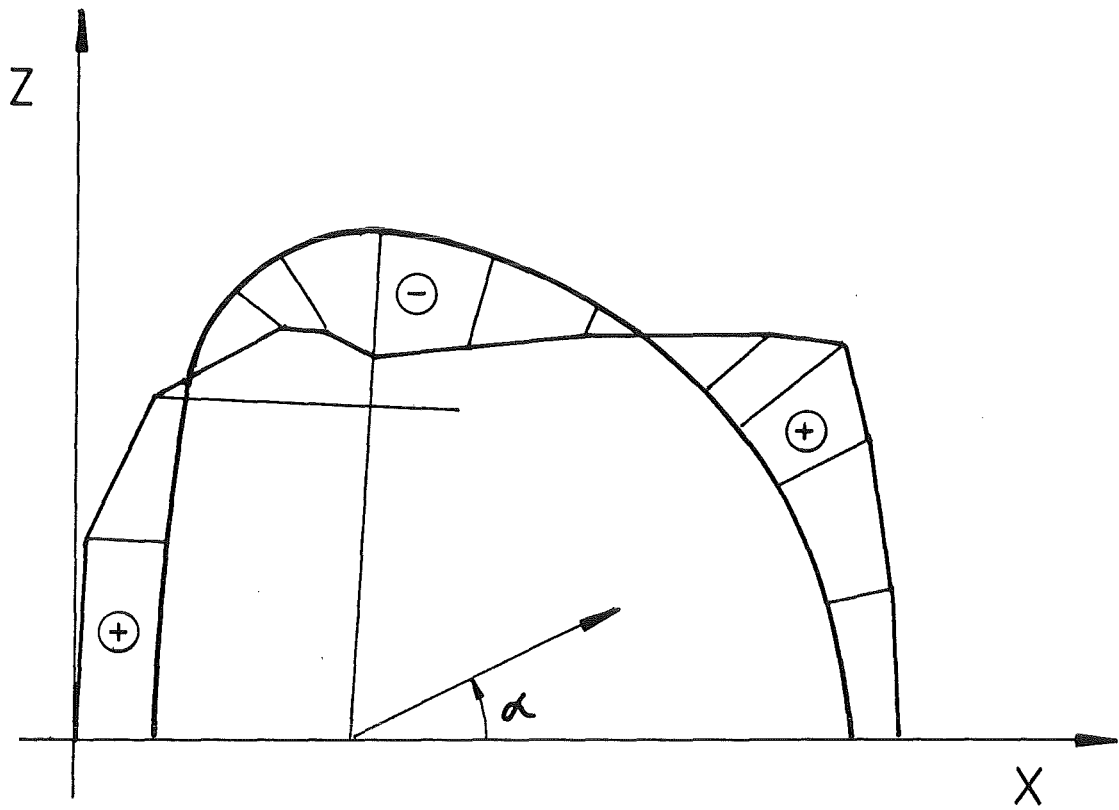
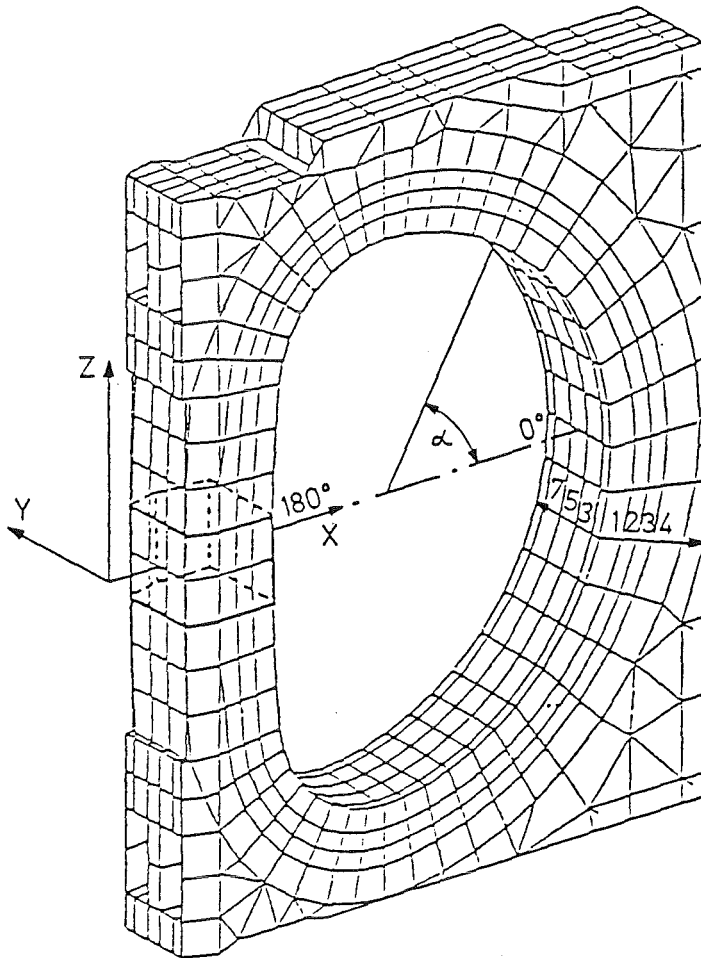


Fig. 5.1.2-2: Bending Moment vs Angle α for the EU-LCT Coil (simplified model)

Table 5.1.2-1: In Plane Bending Moments and Stresses for different values for the EU-LCT Coil in C3.

Angle α /degree	Bending Moment $M(\alpha)$ /MNm	Bending Stress $\sigma_b(\alpha)$ /MPa
0	4,59	193
15	6,46	
30	11,94	
38,1	16,27	685
45	9,07	
60	-3,92	
75	-12,60	
85,74	-15,83	667
105	-15,39	
120	-12,08	
129,9	-8,57	
135	-8,06	
150	-5,15	217
165	-0,35	
174	3,32	
177	9,69	
180	9,49	400

Table 5.1.2-2: Stresses in the EU-LCT Coil Cluster Configuration C3 (simplified model)



In Plane Stresses (X,Z)

$\sigma_{Bmax} = 685 \text{ MPa}$
(only case)

$\sigma_{max} = 100 \text{ MPa}$ (case)
 $\sigma_{max} = 60 \text{ MPa}$ (winding)

Axial Stresses (Y)

$\sigma_{Bmax} = 435 \text{ MPa}$
(only case)

Shear Stress

$\tau_{max} = 35 \text{ MPa}$

5.1.3 Structural feasibility of the Swiss LCT coil

The structural feasibility of the *cluster* solution for the NET Pancake Test Facility was verified at SIN by estimating the stresses in the Swiss LCT coil (LCT-CH). The analysis reported in this Section is of preliminary nature and detailed effects need to be included before conclusive remarks can be made.

5.1.3.1 Model

The stress components at 5 indicative coil locations were estimated using an analytical beam model at the neutral line of the winding pack. Because of symmetry only the upper half of the coil was modeled. A schematic representation of the coil and the beam models is shown in Figure 5.1.3.1. The unknown reaction forces and moments due to in-plane and out-of-plane loads were calculated from translation and rotation equilibrium conditions. In the out-of-plane case the beam is *statically indeterminate*, with 4 unknowns (R_1 , R_2 , M_{XA} and M_{XC}) and 3 equations. The moments M_{ZA} and M_{ZC} are zero for symmetry about the XY plane. The support distributed along the nose D tends to prevent the reaction moment in C and in the limit ($M_{XC} = 0$) the beam becomes *statically determinate*. Both cases have been solved, assuming a constant beam rigidity.

The stainless steel case and the winding pack are included, whereas detailed components such as the insulation layer around the winding pack and the bolts in the case are neglected. Although the LCT-CH coil is made up by several components, some of stainless steel 316L and some of 316LN (Figure 5.1.3.2) only one value of the Young's modulus was used (210 GPa). The Young's modulus of the winding pack was assumed to be 70 GPa [5.1.3.1]. For both components the Poisson's ratio is 0.3.

Because of the lack of a well defined set of supporting structures, the following preliminary boundary conditions for the LCT-CH coil were assumed (Figure 5.1.3.1):

- in the Y-direction, the coil is rigidly supported on the nose E and on the reinforcing bars at the upper right corner;
- an arbitrarily defined cross section D (582 x 550 mm²) provides a rigid support in the X-direction.

Electromagnetic field and forces for the "C-3" cluster configuration (Figure 5.1.3.3) were calculated in collaboration with ENEA-Frascati using the 3-dimensional code MAG3D-WF-6 [5.1.3.2]. The forces integrated along one half coil are $F_X = 10.62$ MN, $F_Y = 51.77$ MN and $F_Z = 31.18$ MN. In this cluster configuration F_X is positive and tends to push the coil radially towards the outside, in the opposite direction of the usual *centering* force in toroidal configurations. In addition to the in-plane forces (X-Y plane), a large out-of-plane resultant F_Y contributes to bending and torsion in the coil. Concentrated electromagnetic loads and reaction forces were used. The distribution of forces and moments in the stainless steel case and in the winding was assumed to be inversely proportional to the stiffness of these components in each section.

5.1.3.2 Results

Stresses due to bending, torsion, normal (hoop) forces and the equivalent vonMises stress were calculated in the coil case and in the winding pack. The results of the statically determinate case ($M_{XC} = 0$) are summarized in the following tables.

Section Fig.5.1.3.1	Stresses [MPa]			
	bending	torsion	normal	vonMises
A	443	0	90	533
B	482	37	43	529
C	0	0	67	67
D	0	0	34	34
E	0	0	107	107

Table 5.1.3.1 - Summary of stresses in the stainless steel case

Section Fig.5.1.3.1	Stresses [MPa]			
	bending	torsion	normal	vonMises
A	117	0	30	147
B	85	15	14	103
C	0	0	22	22

Table 5.1.3.2 - Summary of stresses in the winding pack

In comparison, the LCT-CH coil is considerably less stressed during the test conditions in OakRidge with 5 coils fully energized while one fails. The maximum equivalent stresses in the case and in the winding are 220 MPa and 75 MPa, respectively [5.1.3.1]

With the following working stress limits:

- for the stainless steel, 400 MPa for 316L and 600 MPa for 316LN;
- for the winding pack, 80÷100 MPa,

it appears that in the cross sections A and B the resultant equivalent vonMises stresses exceed the limits of both coil components. In the other cross sections the stresses are not critical.

It must be pointed out that in general the results in section A are pessimistic since the bending moment in section C was neglected. In fact, the solution of the statically indeterminate model, with no moment constraint in section C, have shown a favourable redistribution of stresses between section A ($\sigma_{vonMises} = 417$ MPa) and C ($\sigma_{vonMises} = 180$ MPa), with no change in section B. Moreover, a reduction of the bending moments in section A and B is to be expected because of the higher rigidity of the coil corners, not included in this model. No appreciable effect on these results was shown by the use of concentrated instead of distributed electromagnetic forces.

The results in the cross section B were calculated assuming a continuous outer ring (Figure 5.1.3.4). In order to calculate the stress concentration due to the opening for the current leads, a detailed 3-D finite-element stress analysis of this region is needed.

No substantial change of these results is to be expected for the latest cluster configuration proposed for the NET Pancake Test Facility ($r_{pancake} = 1.0$ m), since the integrated electromagnetic forces are only slightly reduced with respect to those of this study.

5.1.3.3 Summary

From the results of this analysis it appears that, with the conservative assumptions of the model and the given set of supporting structures, the LCT-CH coil in the cluster configuration does *not* withstand the electromagnetic loads during normal operation. To overcome this limitation, however, several solutions are possible. For example:

- To include additional out-of-plane coil supports, in particular to reduce bending due to M_x in section A and due to M_z in section B. Only qualitatively suggestions can be made in this phase of the study, whereas detailed evaluations of each solution will be done when other components of the TOSKA Facility are fully defined.
- To include local reinforcement of the coil case such as, for example, an additional steel thickness in selected areas and a radial steel bar in the equatorial plane. As shown by a parametric study of the cross section A, an additional thickness of 25 mm would be needed to reduce the stresses in the steel and in the winding pack below the limits of these materials (Figure 5.1.3.5).

Details of the analysis presented in this Section will be reported elsewhere [5.1.3.3]

5.1.3.4 References

- [5.1.3.1] LCT-CH Final Report - BBC Report (1982)
- [5.1.3.2] G.Pasotti, M.V.Ricci - Fields and forces distribution on the SIN coil of the TOSKA upgrade facility - ENEA Memo Fus/Tecn/Superc 4.86 (1986)
- [5.1.3.3] C. Marinucci, C. Sborchia, P. Weymuth - Preliminary assessment of the structural behaviour of the Swiss LCT coil in the cluster configuration of the NET Pancake Test Facility - SIN Report [in preparation]

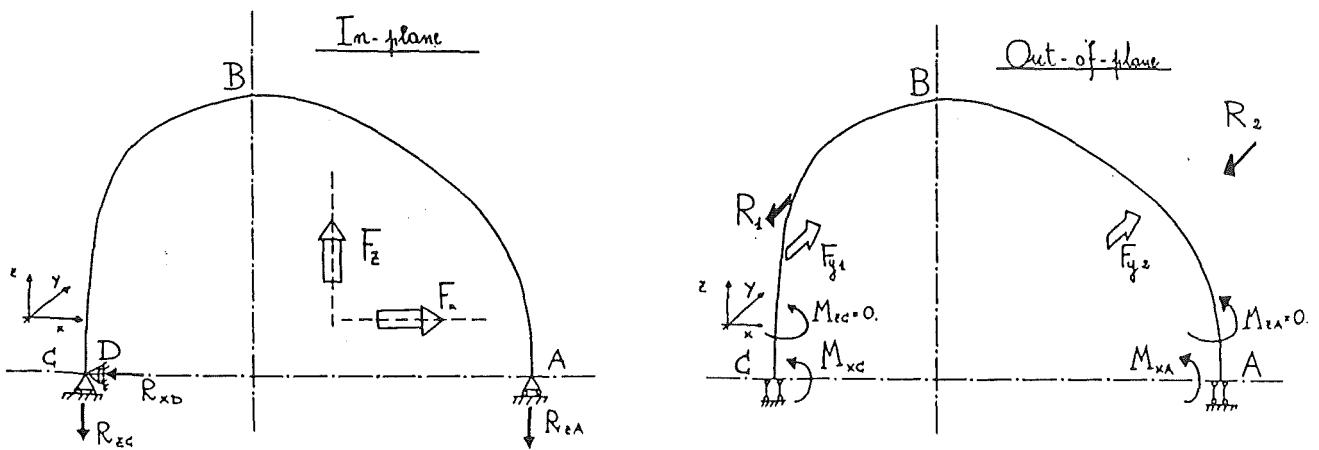
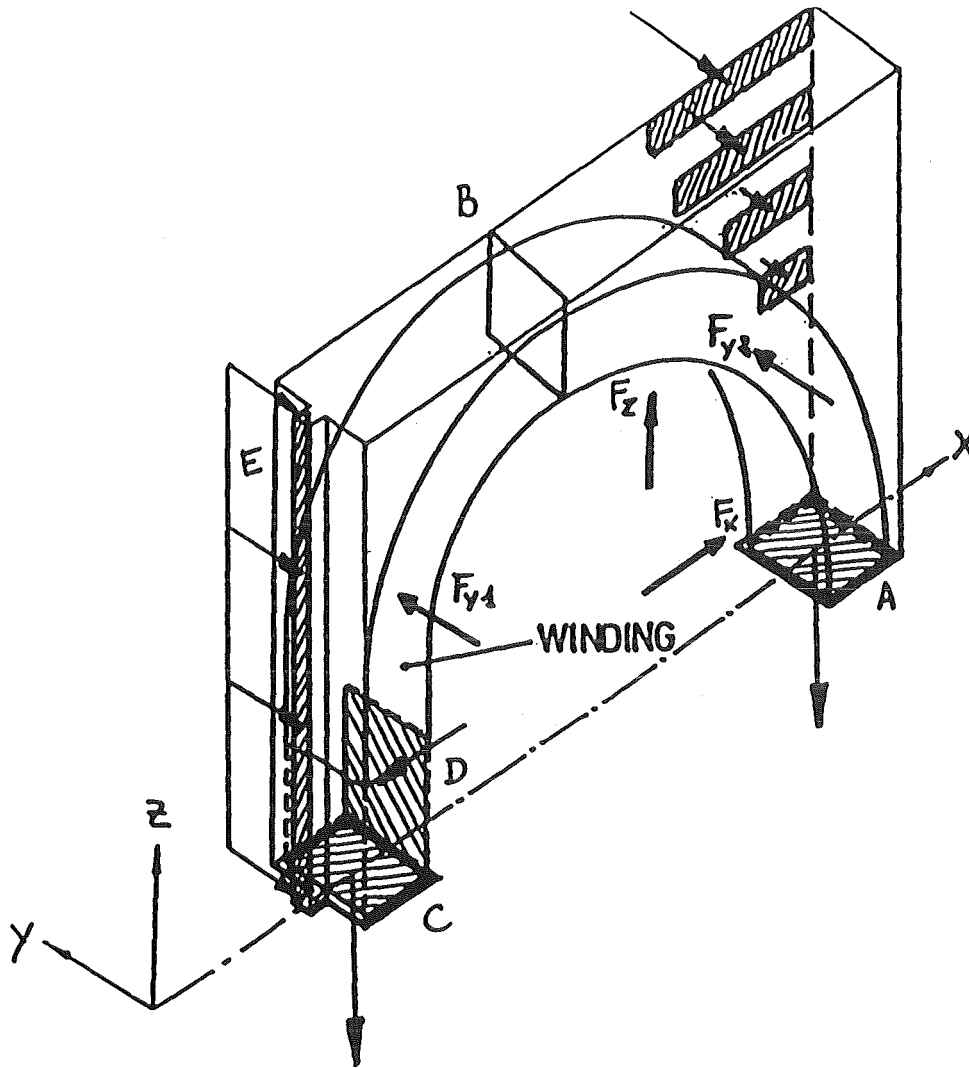




Figure 5.1.3.1 - Schematic representation of the upper half of the LCT-CH coil

316 LN 
316 L 

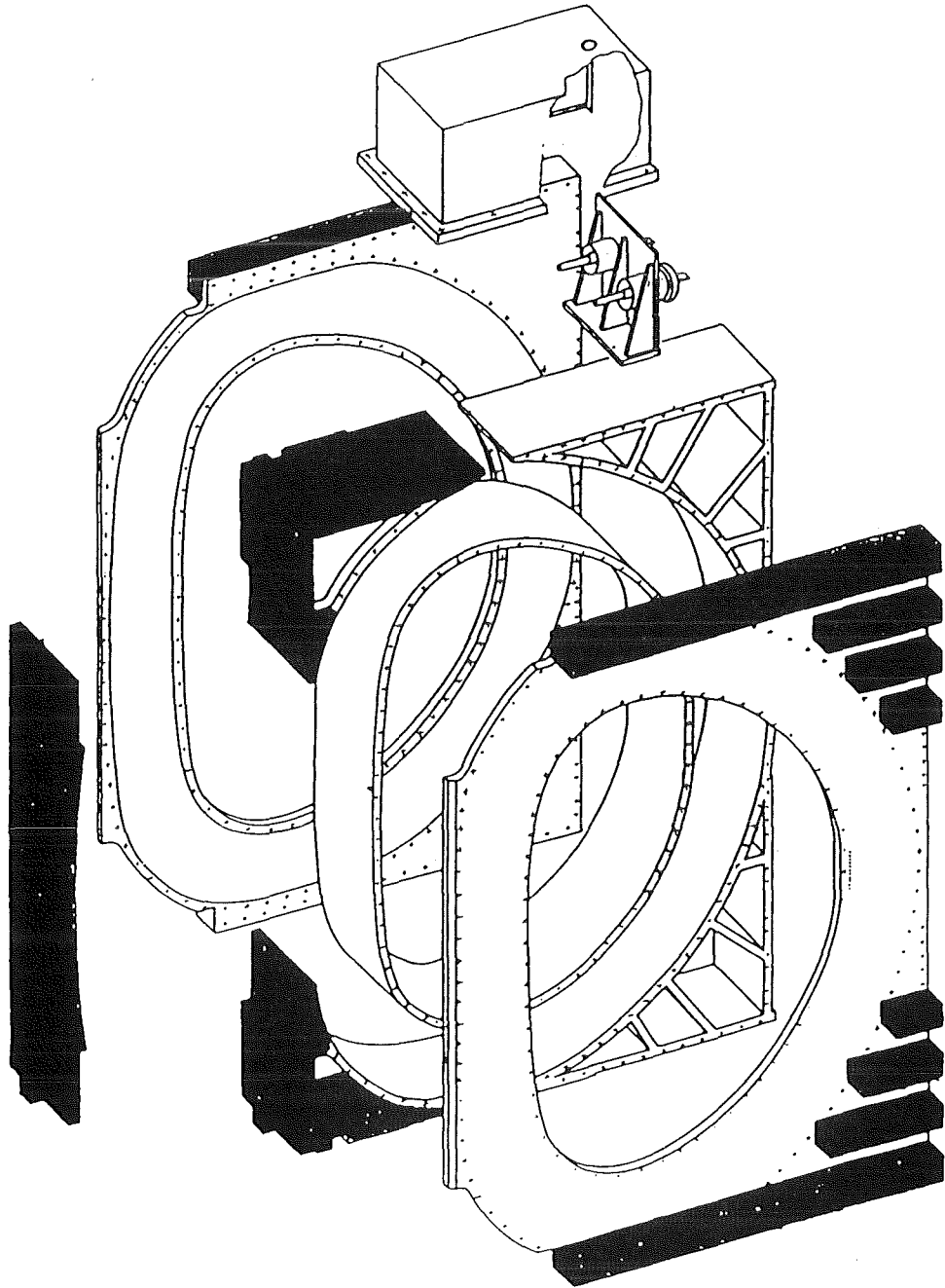


Figure 5.1.3.2 - Exploded view of the LCT-CH coil case

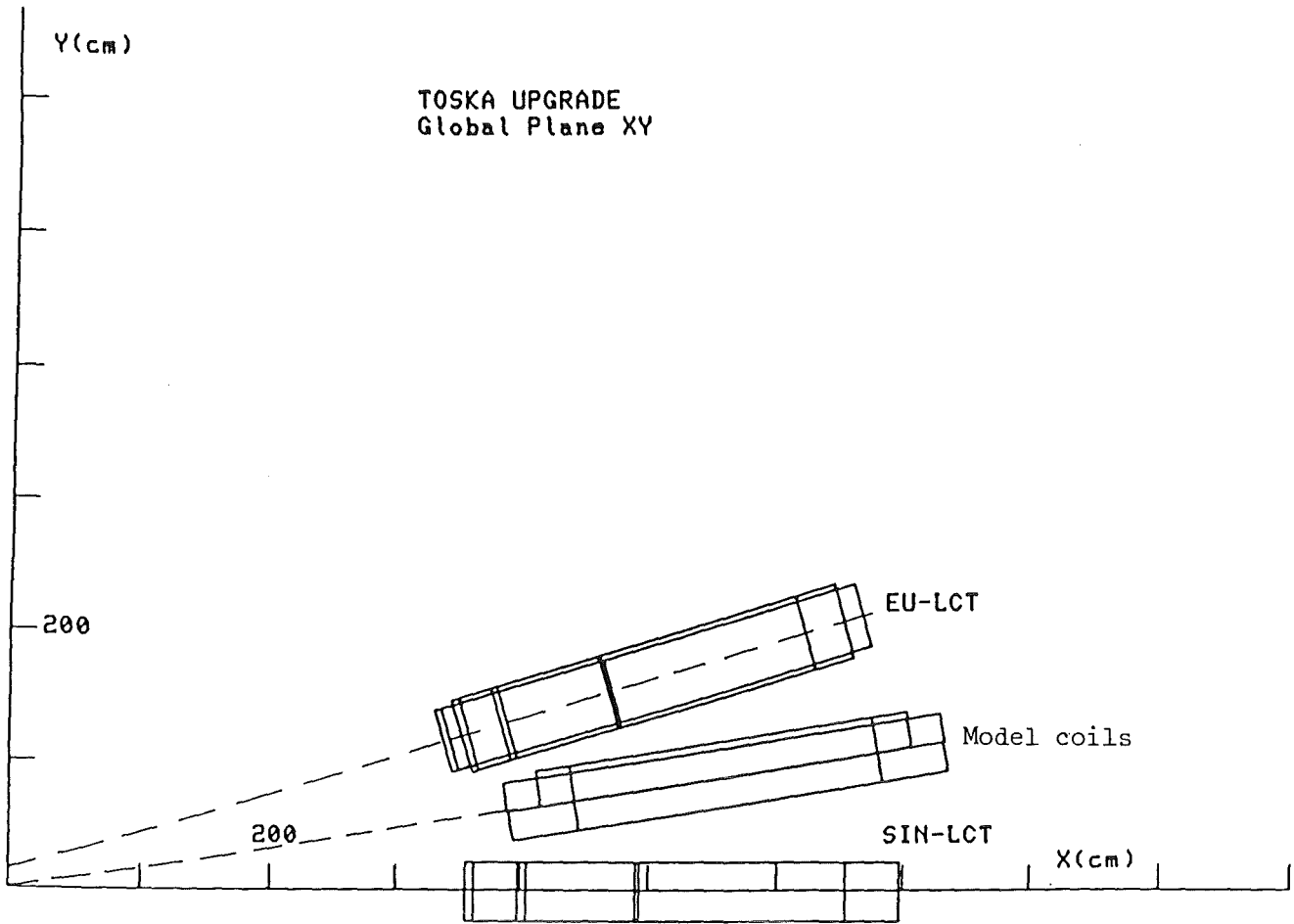


Figure 5.1.3.3 - Configuration used for calculation of electromagnetic fields and forces

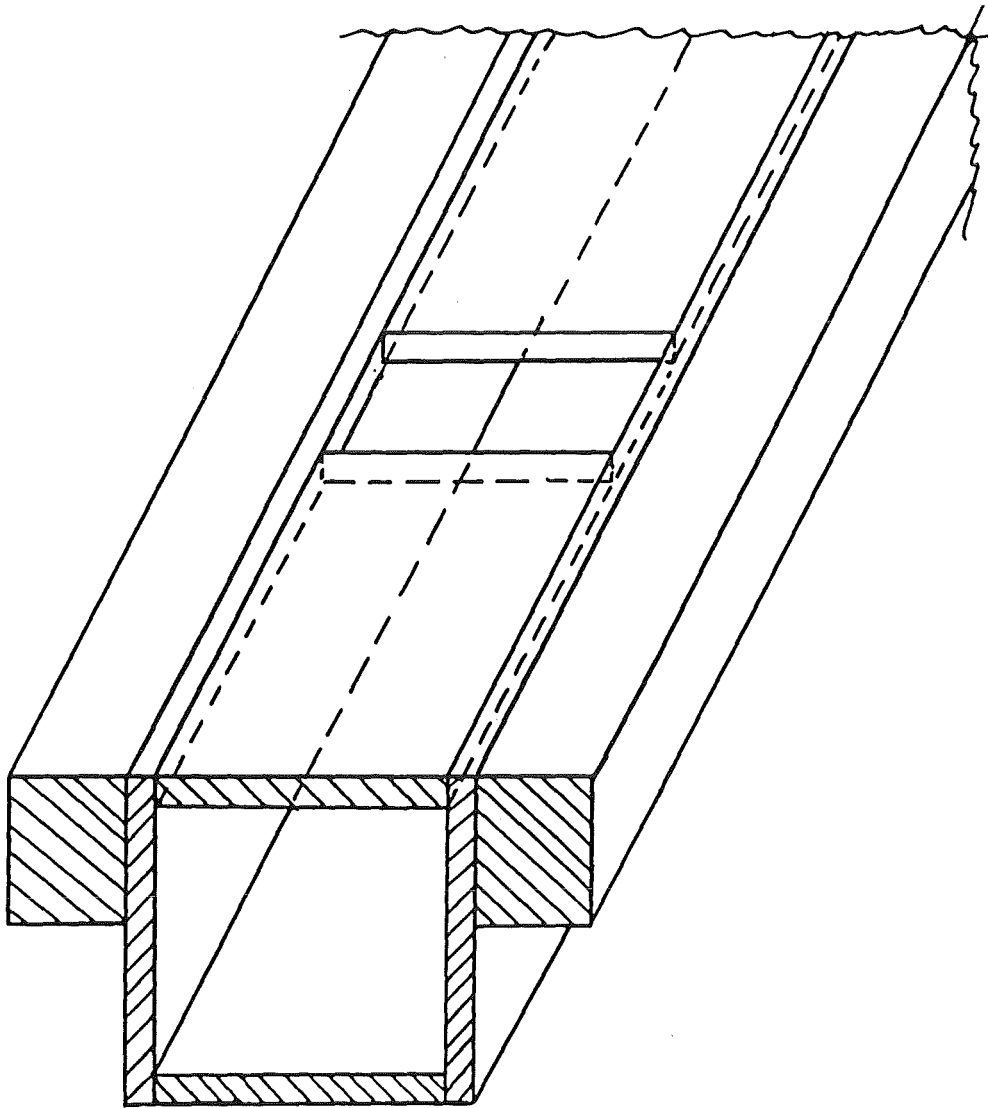
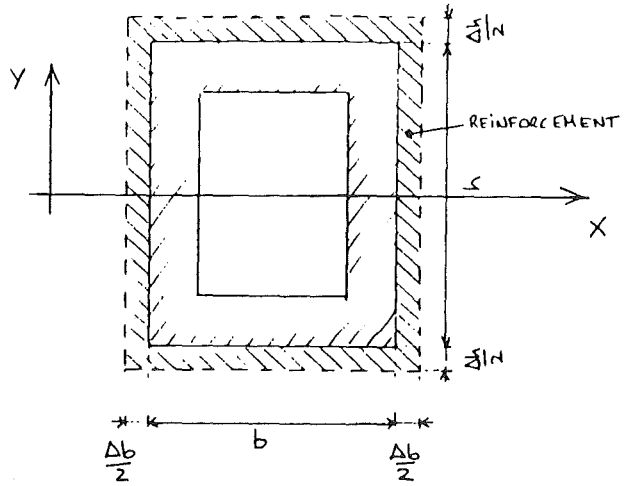


Figure 5.1.3.4 - Details of the coil cross section B



6-AUG-87 vonMises Stresses in Sec. A
Coil case / winding pack

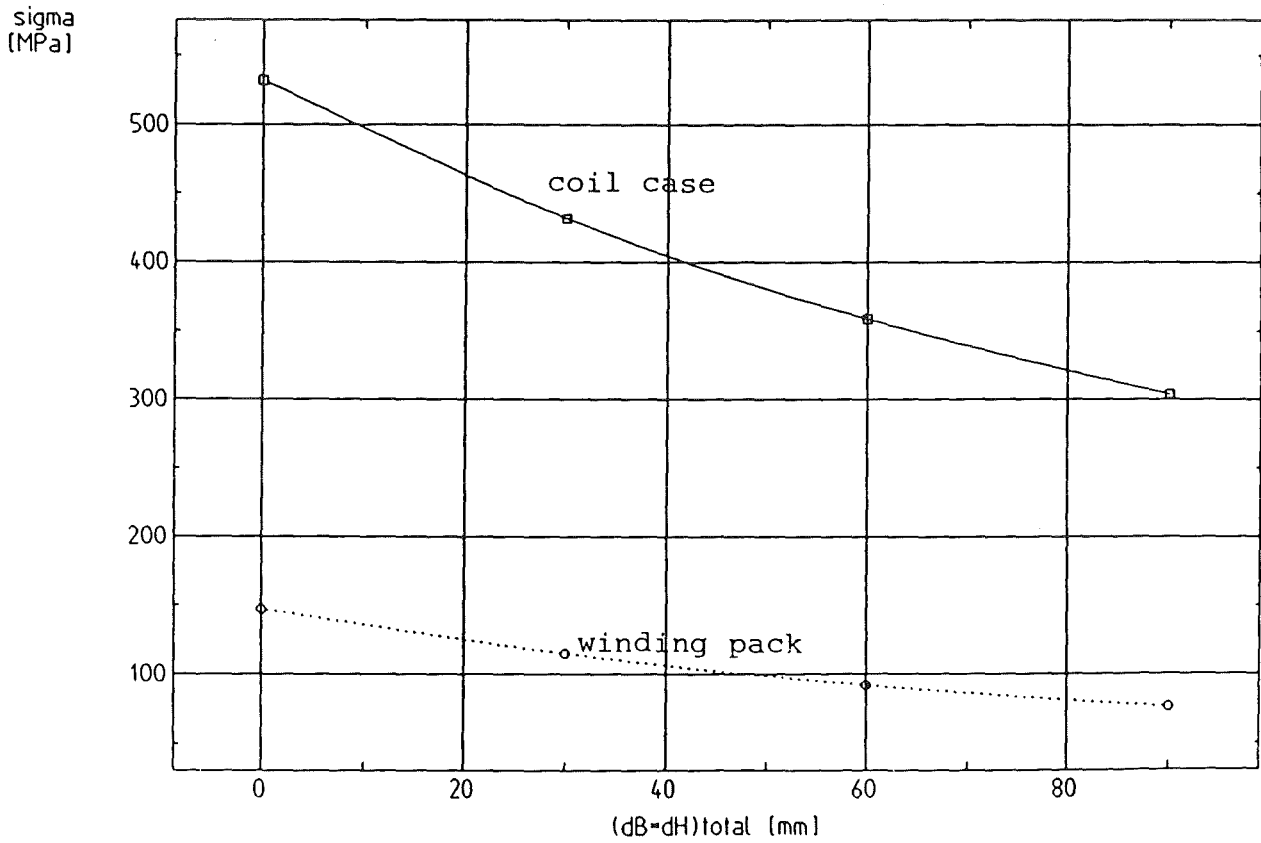


Figure 5.1.3.5 - Dependence of vonMises stresses on steel reinforcement in the cross section A

5.2. Forces and Stresses in the Solenoid Facility

In this section stress analyses, with respect to the solenoid configuration S1, performed at ECN, with the FEM-(Finite Element Method) code ANSYS [5.2.1.], and at KfK, with the FEM-code PERMAS [5.2.2.], are discussed. Former analysis is made by C. Jong and can be found in report [5.2.3.], latter is made by A. Grünhagen and can be found in report [5.2.4.].

The main goals of these analyses were to get an impression of the stress distribution and the stress peaks in the individual coils and to compare these with the stress distribution and the stress peaks in the NET-DN coils.

In the subsections 5.2.1. and 5.2.2. the calculation models will be described and the most important numerical results will be given for the TF-(Toroidal Field) model coils and the OH-(Ohmic Heating) model coil respectively. In subsection 5.2.3. the numerical results will be compared. In subsection 5.2.4. the two models will be discussed and some conclusions will be drawn.

NOTE: All the parameters used in both reports are those belonging to the solenoid configuration S1 (October 1986, $R_1 = 1.2$ m).

5.2.1. TF-Model Coils

With respect to the TF-model coils, FEM-calculations are made by A. Grünhagen only. The configuration of the coils, used for the calculations, is shown in figure 1. The global and local coordinate systems are shown in figure 2.

The simplifications which are introduced are given below:

1. the three coils are modelled without a s.s.-(stainless steel) casing,
2. the three coils are fixed together along their side-faces,
3. the rods, which are supposed to be square, are fixed with the individual coils,
4. only the OH-coil is supported,
5. the winding packs are being regarded as simple continua, which are isotropic.

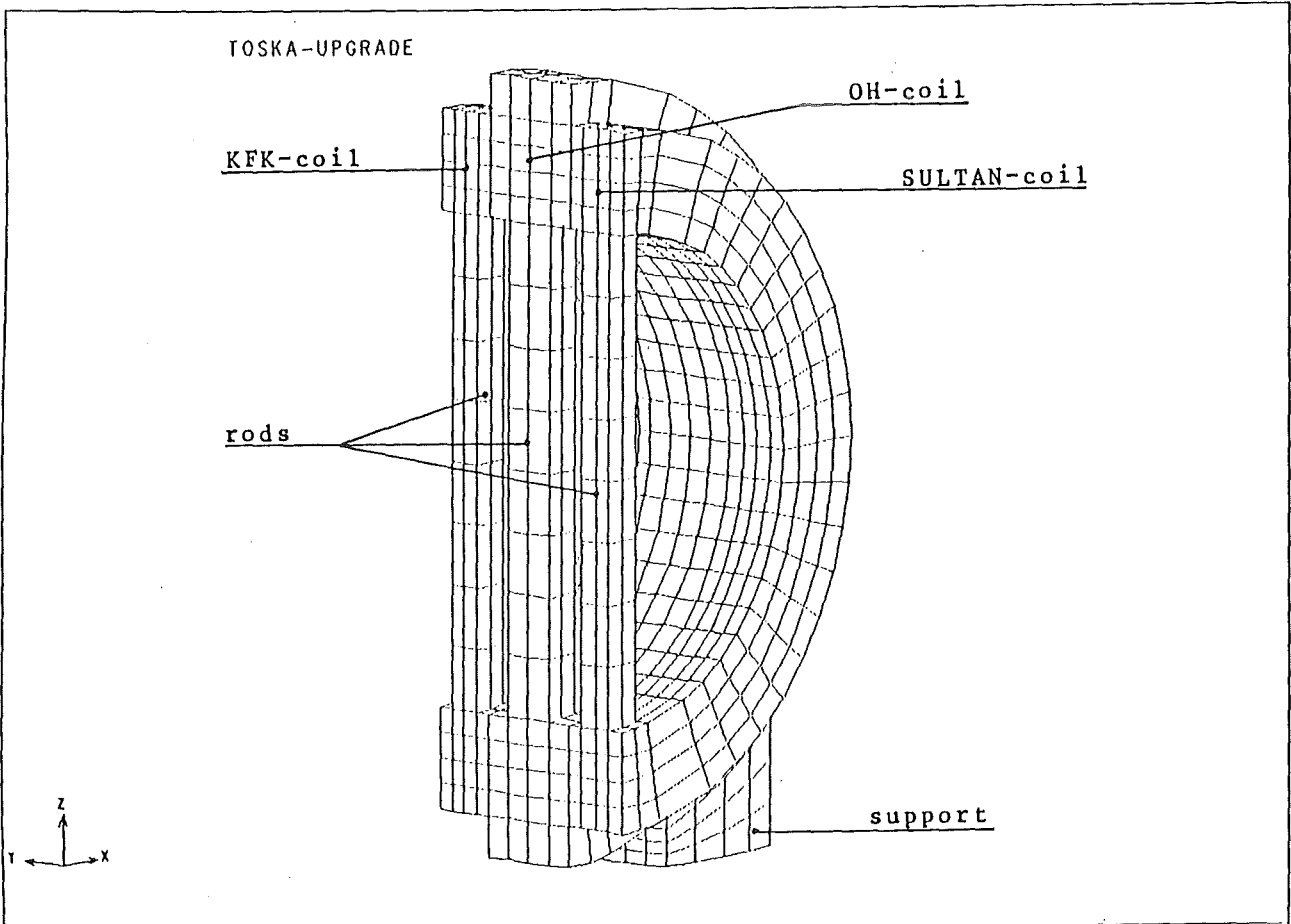


Figure 1 : FEM-model of KFK-, OH-, and SULTAN-coil

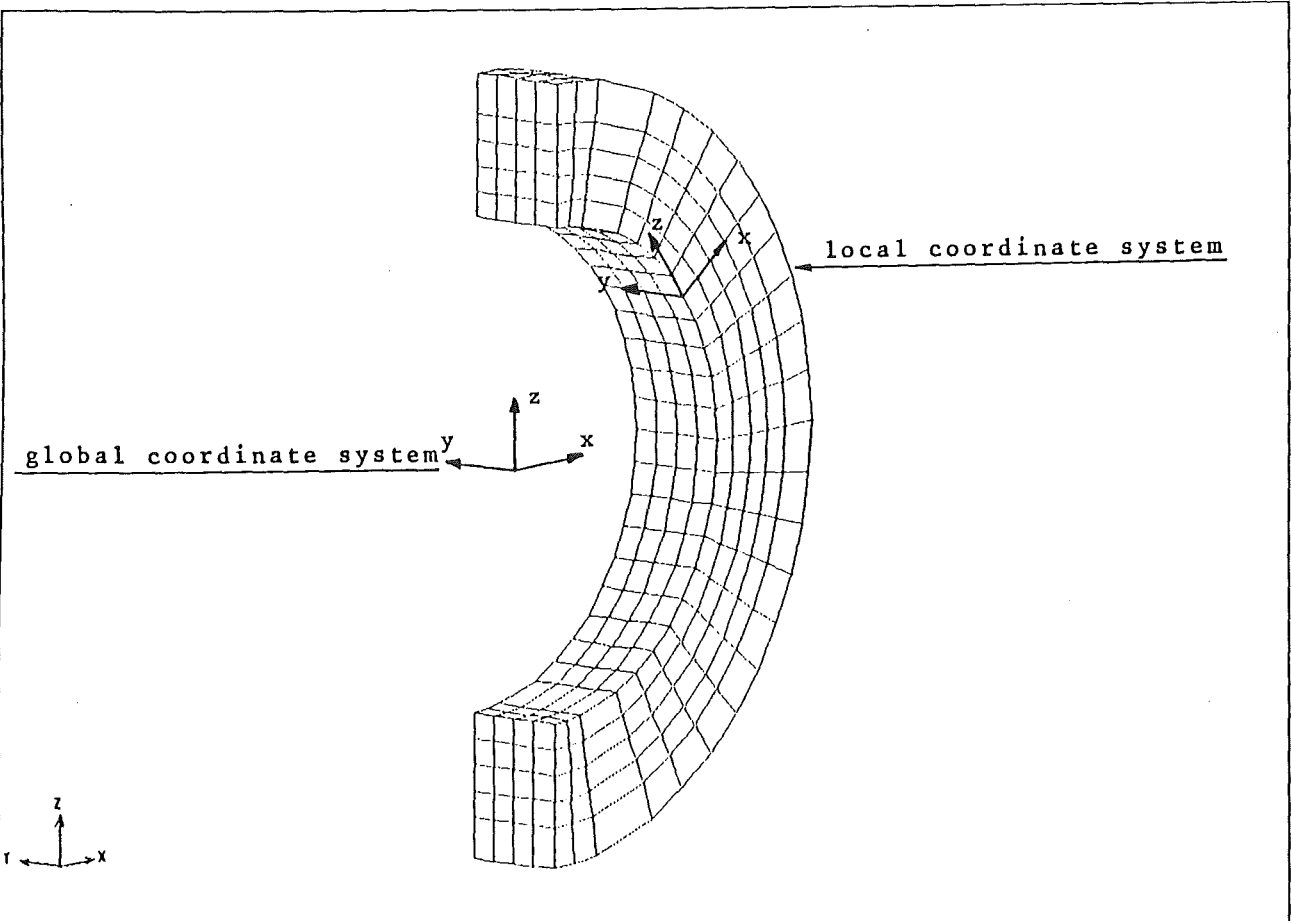


Figure 2 : Presentation of the local- and global-coordinate system

The values of the material properties are tabulated in table 1.

Table 1.
Material properties of the KfK-model.

	Young's modulus	Poisson's ratio
KfK	97.7 GPa	0.3
OH	97.7 GPa	0.3
SULTAN	77.0 GPa	0.3
Rods	208.0 GPa	0.3
Support	208.0 GPa	0.3

Stresses and displacements have been calculated for six cross-sections in circumferential direction. These sections are shown in figure 3.

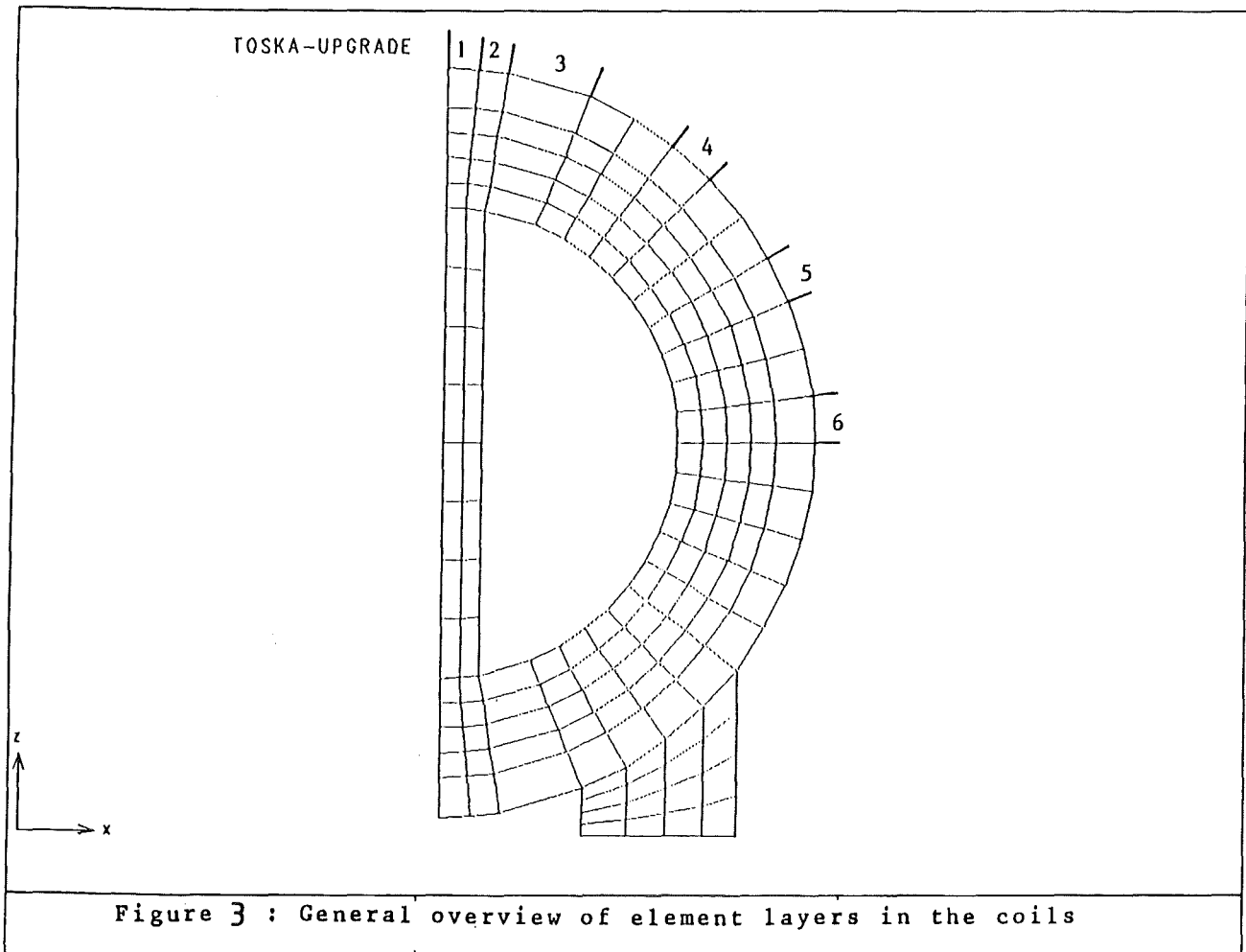


Figure 3 : General overview of element layers in the coils

In the tables 2 and 3 the extreme values of the stresses (local) and of the displacements (global) in all the cross-sections are given for the KfK-coil and the SULTAN-coil respectively.

5.2.2. OH-Model Coil

With respect to the OH-model coil two different FEM-calculations have been performed; one by A. Grünhagen and the other by C. Jong.

1. The model description belonging to the former already has been presented in subsection 5.2.1. Here only the numerical results will be given.

In table 4 the extreme values of the stresses (local) and of the displacements (global) in the six cross-sections are given for the OH-coil.

2. The configuration of the OH-coil, used for the ECN-calculations, is shown in figure 4. In figure 4 one can also find the global and local coordinate systems.

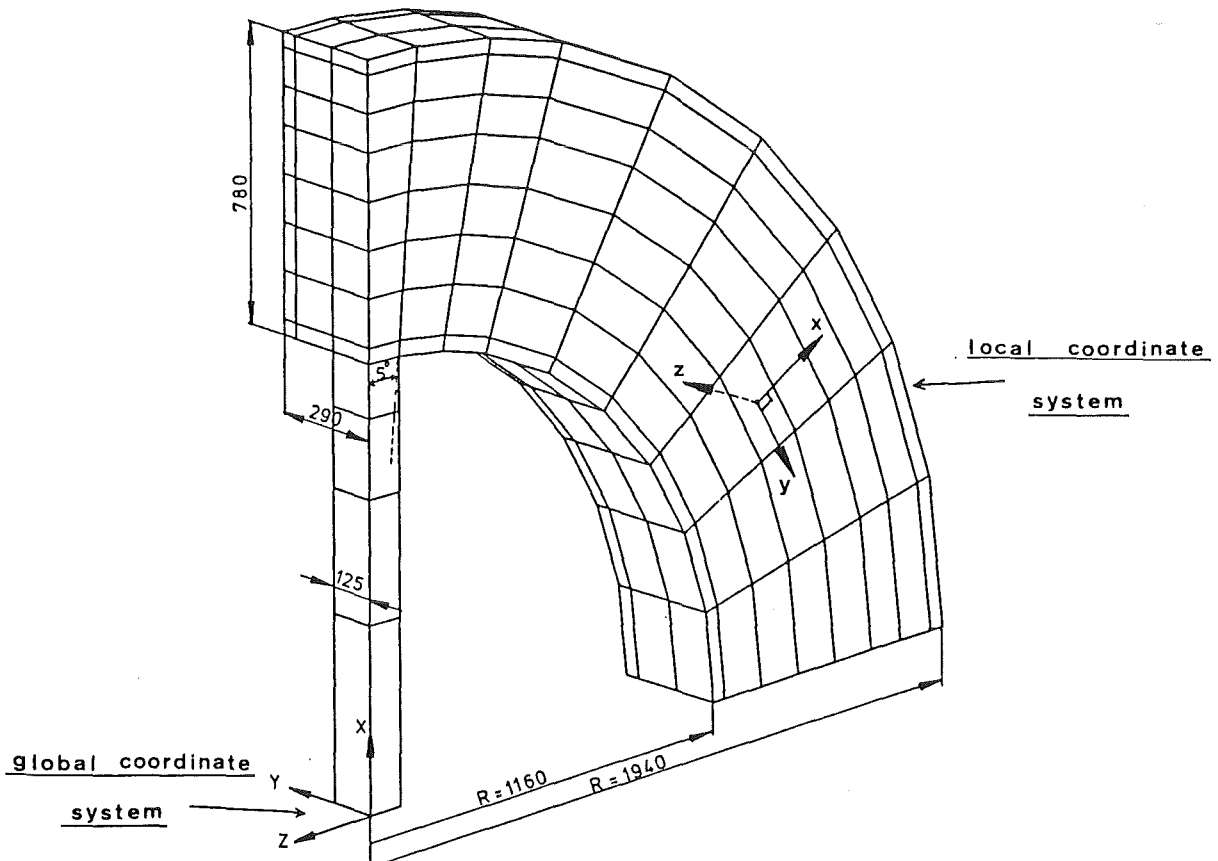


Figure 4: Geometry and element lay-out of OH-coil.

Table 2:

KFK-coil
 Stress components at 6 sections in circumferential direction
 (local-system)

Section	$\sigma(x)$ N/mm ²		$\sigma(y)$ N/mm ²		$\sigma(z)$ N/mm ²	
	min.	max.	min.	max.	min.	max.
1	-38.8	12.1	-70.5	17.9	45.9	247.0
2	-37.4	81.8	-68.3	17.9	46.5	282.0
3	-33.5	81.8	-62.4	7.0	55.4	284.0
4	-40.1	-0.3	-63.3	-6.6	89.4	209.0
5	-42.5	-5.9	-65.5	-8.2	114.0	155.0
6	-43.3	-5.2	-66.4	-8.1	99.1	164.0

Section	$\tau(xy)$ N/mm ²		$\tau(yz)$ N/mm ²		$\tau(zx)$ N/mm ²	
	min.	max.	min.	max.	min.	max.
1	-18.7	14.1	-13.1	40.4	-16.5	5.5
2	-45.3	28.1	-60.4	95.8	-72.9	3.9
3	-45.3	28.1	-60.4	95.8	-72.9	3.9
4	-0.6	16.6	-5.7	16.6	-19.3	-3.8
5	-1.1	19.7	-3.4	10.6	-11.2	-1.8
6	-1.3	20.6	-1.8	1.4	-1.2	2.3

Section	$\sigma(eq)$ N/mm ²	
	min.	max.
1	60.5	296.0
2	60.5	343.0
3	67.5	343.0
4	115.0	228.0
5	132.0	185.0
6	120.0	191.0

Displacement components at 6 sections in circumferential direction
 (global-system)

Section	x mm		y mm		z mm	
	min.	max.	min.	max.	min.	max.
1	0.0	0.24	-0.34	0.22	0.92	1.37
2	0.09	0.54	-0.41	0.22	0.93	1.37
3	0.16	1.36	-0.45	0.23	0.97	1.51
4	1.34	2.86	-0.33	0.24	1.51	2.16
5	2.96	3.98	-0.24	0.23	1.50	2.15
6	3.94	4.33	-0.27	0.16	0.90	1.34

Table 3:

SULTAN-coil

Stress components at 6 sections in circumferential direction
(local-system)

Section	$\sigma(x)$ N/mm ²		$\sigma(y)$ N/mm ²		$\sigma(z)$ N/mm ²	
	min.	max.	min.	max.	min.	max.
1	-34.9	17.6	-73.3	20.2	39.2	221.0
2	-33.6	85.8	-70.9	20.2	39.8	246.0
3	-31.5	85.8	-61.1	14.6	48.9	249.0
4	-39.0	0.0	-63.3	-5.8	71.8	185.0
5	-41.4	-5.2	-65.6	-7.4	94.1	139.0
6	-42.1	-4.6	-66.5	-7.3	83.3	145.0

Section	$\tau(xy)$ N/mm ²		$\tau(yz)$ N/mm ²		$\tau(zx)$ N/mm ²	
	min.	max.	min.	max.	min.	max.
1	-12.6	22.7	-38.3	14.9	-17.8	4.7
2	-29.8	44.7	-87.7	61.2	-73.4	4.7
3	-29.8	44.7	-87.7	61.2	-73.4	4.7
4	-16.6	0.9	-21.8	10.2	-20.7	-3.7
5	-19.5	1.2	-13.5	5.8	-11.6	-1.7
6	-20.3	1.4	-1.4	3.0	-0.9	2.8

Section	$\sigma(eq)$ N/mm ²	
	min.	max.
1	59.8	260.0
2	59.8	300.0
3	65.9	300.0
4	109.0	194.0
5	124.0	158.0
6	113.0	162.0

Displacement components at 6 sections in circumferential direction
(global-system)

Section	x mm		y mm		z mm	
	min.	max.	min.	max.	min.	max.
1	0.0	0.26	0.50	0.85	1.19	1.51
2	0.11	0.58	0.50	0.91	1.21	1.51
3	0.21	1.49	0.51	0.95	1.26	1.69
4	1.60	3.12	0.43	0.82	1.82	2.45
5	3.28	4.41	0.34	0.86	1.69	2.44
6	4.26	4.80	0.27	0.83	1.04	1.51

Table 4:

OH-coil
Stress components at 6 sections in circumferential direction
(local-system)

Section	$\sigma(x)$ N/mm ²		$\sigma(y)$ N/mm ²		$\sigma(z)$ N/mm ²	
	min.	max.	min.	max.	min.	max.
1	-29.3	22.8	-91.5	1.0	21.0	263.0
2	-26.9	105.0	-84.4	9.1	21.0	299.0
3	-31.7	105.0	-61.9	9.1	31.6	307.0
4	-34.2	-1.8	-57.9	-1.5	88.8	222.0
5	-38.1	-6.3	-56.0	-1.9	112.0	166.0
6	-39.1	-5.7	-55.5	-2.0	96.4	177.0

Section	$\tau(xy)$ N/mm ²		$\tau(yz)$ N/mm ²		$\tau(zx)$ N/mm ²	
	min.	max.	min.	max.	min.	max.
1	-16.2	15.2	-21.3	24.2	-19.2	3.7
2	-32.6	30.5	-57.2	63.9	-86.6	6.0
3	-32.6	30.5	-57.2	63.9	-86.6	6.0
4	-10.0	9.5	-7.4	10.2	-18.0	-3.5
5	-9.5	8.9	-4.7	5.8	-10.1	-1.6
6	-9.5	8.9	-1.4	1.0	-0.9	2.3

Section	$\sigma(eq)$ N/mm ²	
	min.	max.
1	35.4	316.0
2	35.4	335.0
3	46.0	344.0
4	102.0	244.0
5	145.0	182.0
6	132.0	188.0

Displacement components at 6 sections in circumferential direction
(global-system)

Section	x mm		y mm		z mm	
	min.	max.	min.	max.	min.	max.
1	0.0	0.26	-0.08	0.53	1.08	1.51
2	0.05	0.58	0.09	0.54	1.10	1.51
3	0.09	1.45	-0.10	0.55	1.16	1.70
4	1.17	3.04	-0.08	0.58	1.66	2.47
5	2.83	4.21	-0.05	0.62	1.56	2.45
6	3.88	4.57	-0.10	0.58	0.92	1.46

The simplifications which are introduced are given below:

1. only the OH-coil is analysed,
2. the OH-coil is modelled with a s.s.-casing,
3. the s.s.-casing and the winding pack are fixed together,
4. the rod, which is supposed to be square, is fixed with the s.s.-casing,
5. the OH-coil is not supported,
6. the winding pack is being regarded as a simple continuum, which is orthotropic.

The values of the material properties are tabulated in table 5.

Table 5: Material properties of OH-coil

	STAINLESS STEEL	EQUIVALENT PROPERTIES FOR WINDING PACK		
		x-dir.	y-dir.	z-dir.
E [GPa]	208.	106.	140.	106.
ν	.3	xy-plane	xz-plane	yz-plane
		.3	.3	.3
G [GPa]	80.	25.	25.	25.

An overview of the selected cross-sections is shown in figure 5. In table 6 the extreme values of the stresses (local) in the different cross-sections are given. The extreme values of the displacements are not tabulated. The maximum displacements are: 1.57 mm in radial direction and 0.23 mm in axial direction.

5.2.3. Comparison of the numerical Results

The numerical results of both reports, with respect to the stresses in the OH-coil, are globally in good agreement with each other. This becomes obvious if one compares the extreme stresses in table 4 (KfK)

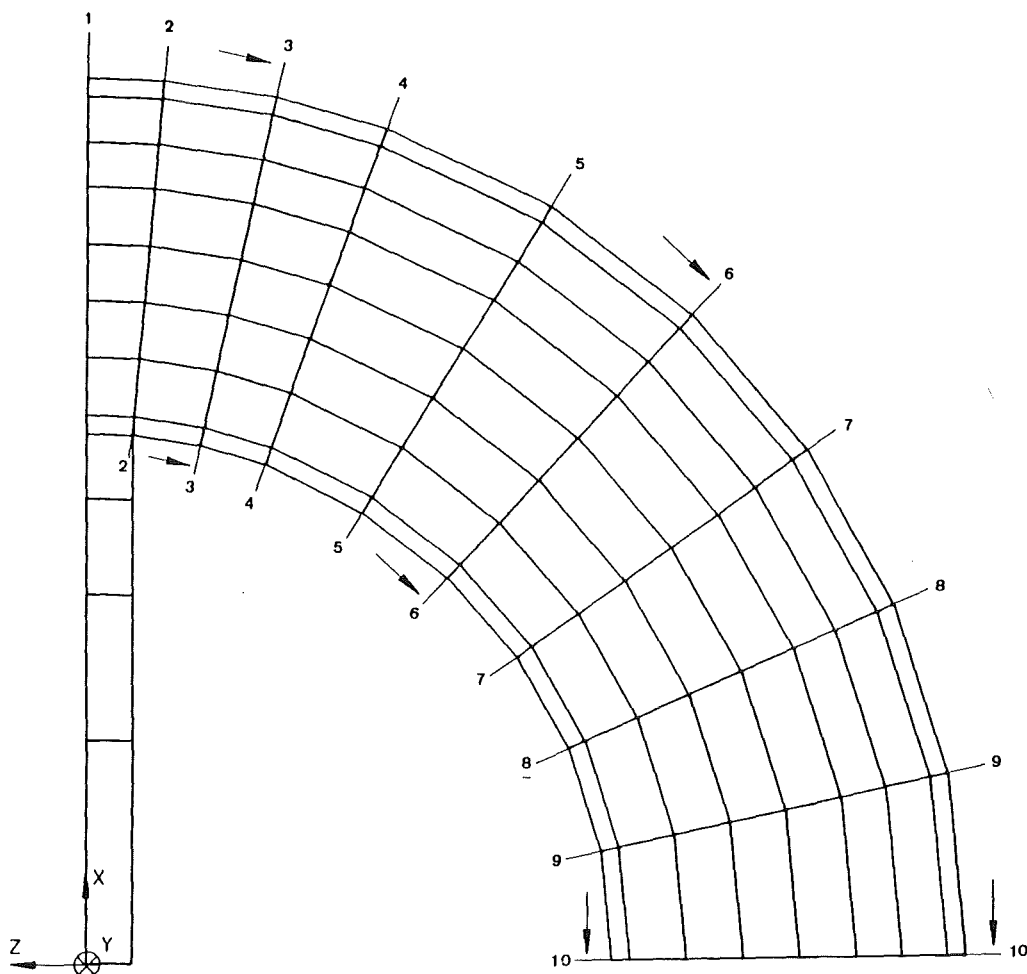


Figure 5: General overview of cross-sections in OH-coil.

Table 6: Stress components at 10 cross sections in circumferential direction

CROSS SECTION	σ_x [MPa]		σ_y [MPa]		σ_z [MPa]		τ_{xy} [MPa]		τ_{yz} [MPa]		τ_{xz} [MPa]		σ_{eq} [MPa]	
	min.	max.	min.	max.	min.	max.	min.	max.	min.	max.	min.	max.	min.	max.
1	-24.9	86.2	54.2	270.3	-80.22	5.8	-17.05	18.9	-7.7	2.2	-9.9	1.8	63.8	309
2	-25.3	88.3	54.9	259.5	-64.8	4.6	-19.8	23.5	-9.2	2.2	-7.4	4.3	65.9	295.5
3	-28.8	1.5	57.2	286.6	-101.0	4.1	-17.7	5.5	-5.2	3.3	-5.1	2.0	70.8	351.3
4	-32.7	12.0	61.0	227.0	-118.2	5.5	-21.7	0.3	-1.5	1.1	-7.2	1.5	75.6	287.5
5	-35.9	6.7	66.0	211.4	-114.4	3.6	-20.9	-2.9	-1.8	1.1	-6.3	1.7	81.2	281.5
6	-37.9	9.3	69.7	192.5	-112.6	3.6	-18.9	-3.7	-2.2	1.5	-6.5	1.6	86.8	257.7
7	-39.1	8.0	72.2	176.7	-112.6	3.7	-18.0	-4.8	-2.5	1.7	-6.4	1.6	91.6	244.1
8	-39.4	8.8	72.7	164.2	-112.5	3.8	-19.6	-5.9	-2.8	2.11	-6.5	1.7	94.9	231.6
9	-39.4	8.9	71.8	162.4	-108.5	3.9	-22.2	-7.5	-2.3	1.9	-6.5	1.6	97.4	224
10	-39.4	6.6	70.7	166.4	-103.5	3.9	-27.0	-10.1	-2.1	1.6	-5.1	3.3	97.6	221.9

with those in table 6 (ECN); "corresponding" cross-sections are given below.

KfK	1	3	4	5	6
ECN	2	4	6	8	10

Large differences, for instance a minimal axial stress of -103.5 MPa in cross-section 10 (table 6) versus a minimal axial stress of -55.5 MPa in cross-section 6 (table 4), are due to the presence/absence of the s.s.-casing in the models. Color prints of the stress distributions, inserted in the original reports, support this view.

Due to the presence/absence of the s.s.-casing or the support in the models, there are local differences.

Comparing the maximum displacements in radial and in axial direction for the OH-coil, it turns out that for the KfK-model these are about a factor 3 larger than those for the ECN model (see table 7).

Table 7.

	max. rad. displ. (mm)	max. ax. displ. (mm)
KfK	4.57	0.62
ECN	1.57	0.23
factor	2.91	2.70

The explanation for this difference must be sought mainly in the presence of the s.s.-casing and the larger Young's modulus in the ECN-model and furthermore in the fact that the KfK-model includes the complete set-up, with the KfK-coil and the SULTAN-coil being fixed with the OH-coil.

Taking these arguments into consideration one can make plausible that the displacements calculated by ECN are a factor of about 2.63 smaller than the displacements calculated by KfK. Hence, we may conclude that also the numerical results of both reports, with respect to the displacement in the OH-coil, are globally in good agreement with each

other. The effect of the OH-coil support on the stresses is relatively small.

5.2.4. Discussion and conclusion

The results of the comparison in the preceding subsection give, from a global point of view, a good confidence in the used models. However, from a local point of view the used models do not give a good impression of the stress distribution and the stress peaks (the two models differ too much, which makes it impossible to compare them locally).

In addition attention has been paid to the effect of the radius reduction from $R = 1.2$ m to $R = 1.0$ m. The magnetic field components have been calculated for the solenoid configuration S3 (May 1987), with the changed set-up OH-KfK-SULTAN. Simple analytical calculations showed that the tangential stresses will increase about 0.5 percent and that the radial displacements will decrease about 20 percent. The difference in the tangential stresses is very small. The large decrease in the radial displacements should be expected, because the radius reduction is about 17 percent. For these two reasons no further FEM-calculations have been performed for the solenoid configuration S3. Nevertheless it is, for design purposes, advisable to make more elaborate stress calculations later on, but then with a more sophisticated model.

Finally the peak stresses in the winding packs of the model coils will be compared with the target test values in table 2.1 of this report.

The target test values for the TF-model coils can be found in column 4 of table 8. The peak stresses in the columns 5 and 6 are taken from the tables 2 and 3 of this report (only the cross-sections 4, 5 and 6 have been taken into consideration, because the very high stresses in the neighbourhood of the rod appear only in very small areas and are considered not to be characteristic). In ECN-report [5.2.5] stress analyses on the winding pack at the central vault of TF-coils for NET-DN have been performed. The peak stresses in the winding park at the central vault of TF-coils are tabulated in column 7 (they are taken from figure 10 on page 47-48 of that report).

Table 8.

Peak stresses in TF-coils

NET	TOSKA		Target test values	KfK-model coil	SULTAN-model coil	NET-TF-coils
σ_{tor}	$\sigma_{\text{ax}} = \sigma_y$	MPa	-140	- 67	- 67	-130
σ_{rad}	$\sigma_{\text{rad}} = \sigma_x$	MPa	- 40	- 44	- 43	- 50
σ_{hoop}	$\sigma_{\text{tang}} = \sigma_z$	MPa	140	210	185	200
τ	σ_{xz}	MPa	- 30	- 20	- 21	- 29

From table 8 follows that the axial stresses in the TF-model coils are much too small. The target test value for the peak hoop stress is too small compared with the peak hoop stresses in the TF-model coils and in the central vault of NET-TF-coils. The other stresses are in good agreement with each other.

The target test values for the OH-model coil can be found in column 4 of table 9. The values of the peak stresses in the OH-model coil for the KfK-model and the ECN-model can be found in the columns 5 and 6 respectively. The former are taken from table 4 of this report (again only cross-sections 4, 5 and 6), the latter from the color prints in ECN-report [5.2.3].

Table 9.

Peak stresses in OH-coil

NET	TOSKA		Target test values	KfK-model	ECN-model
σ_{tor}	σ_{ax}	MPa	-100	- 58	- 66
σ_{rad}	σ_{rad}	MPa	- 10	- 40	- 39
σ_{hoop}	σ_{tang}	MPa	200	222	206
τ	$\sigma_{\text{xz}} \quad \sigma_{\text{xy}}$	MPa	- 30	- 18	- 20
	KfK ECN				

From table 9 follows that the axial stresses in the OH-model coil are too small and that the radial stresses in the OH-model coil are too large. The other stresses are in good agreement with each other.

So for the TF-model coils as well as for the OH-model coil steps have to be undertaken to increase the axial stresses. Finally it has to be remarked that by varying the thickness of the rod or its Young's modulus, all the stresses, except the axial stresses, in the model coils can be changed so that they come up to the NET-requirements.

References 5.2.

- [5.2.1.] De Salvo G.J., Swanson J.A.;
ANSYS Rev. 4.1 B; Swanson Analysis Systems
Incorporation, Houston, Pennsylvania, USA.
- [5.2.2.] Bernhard K., Knapp H., Schremm E.;
PERMAS-I- Lin. Stat. An., User's Reference
Manual; Intes Publication No 202, Rev.H;
Stuttgart, 1985.
- [5.2.3.] Jong C.; Stress analysis of the OH-coil
on behalf of the Toska-Upgrade;
ECN nr. 4.377.00 - GR3 (OD 84-51), May 1987.
- [5.2.4.] Grünhagen A.; Stress analysis of the
KfK-, OH- and SULTAN-coil of the
Toska-Upgrade; Primary Report KfK
nr. 03.03.02/33 A; 16-6-1987 (unpublished).
- [5.2.5.] Klok J.; Stress analysis on the winding
pack and conductor at the central
vault of TF-coils for NET-22 B;
ECN nr. 86-137, September 1986
(unpublished).

6. Installation of the Test - Rig

6.1 Cluster Configuration

6.1.1 Cluster Configuration C3 with a minimum Bending Radius of 1.2 m

The different design options of the Cluster Configuration are already explained in Chapter 3. In the first design option which is described in Reference [3.1] the minimum bending radius was 1.5 m with the consequence that the Test-Rig was too large for installation into the existing vacuum vessel. A new vessel with an inner diameter of at least 5.5 m would be required, that means additional costs of about 3 Mio. DM.

In order to reduce the investment costs and use the existing TOSKA - facility as much as possible the bending radius was reduced to 1.2 m and the options C2 - C4 developed. An installation of the Test Rig of option C2 - C4 into the existing vacuum vessel seems to be possible but requires additional installation work and modifications of the vacuum vessel. The following steps and modifications are necessary:

- * remove all helium and nitrogen transfer lines including the vacuum insulated ones,
- * remove the liquid nitrogen shield from the vacuum vessel,
- * lift upper and lower part of the vessel out of the pit,
- cut the bottom of the vessel from the lower part of the wall section,
- weld additional support structure to the bottom,
- weld a special flange (diameter = 5 m) to the bottom and lower wall section,
- install the test configuration (LCT coils, model coils, piping, support structure) onto the bottom of the vessel,
- perform leak testing of coils and piping,

- install and test the instrumentation of coil and facility,
- modify nitrogen supply and exhaust lines,
- * reinstall the nitrogen shield wall and connect supply and exhaust lines,
- * reinstall the vacuum vessel wall sections,
- * reinstall helium and nitrogen transfer lines and connect the lines inside the vessel,
- * install the current leads and connect the helium lines,
- * close the lid and evacuate the vessel for final leak tests.

For exchange of a test coil (TF - coil , OH - coil), modifications or maintenance work , the vessel wall has to be removed and the steps marked by an " * " must be performed , because the distance between nitrogen shield and coils is too small for access as shown in Fig. 6.1 - 1. Consequently this configuration is expensive and the installation work is very time consuming . Therefore this configuration is not advised from an engineering point of view .

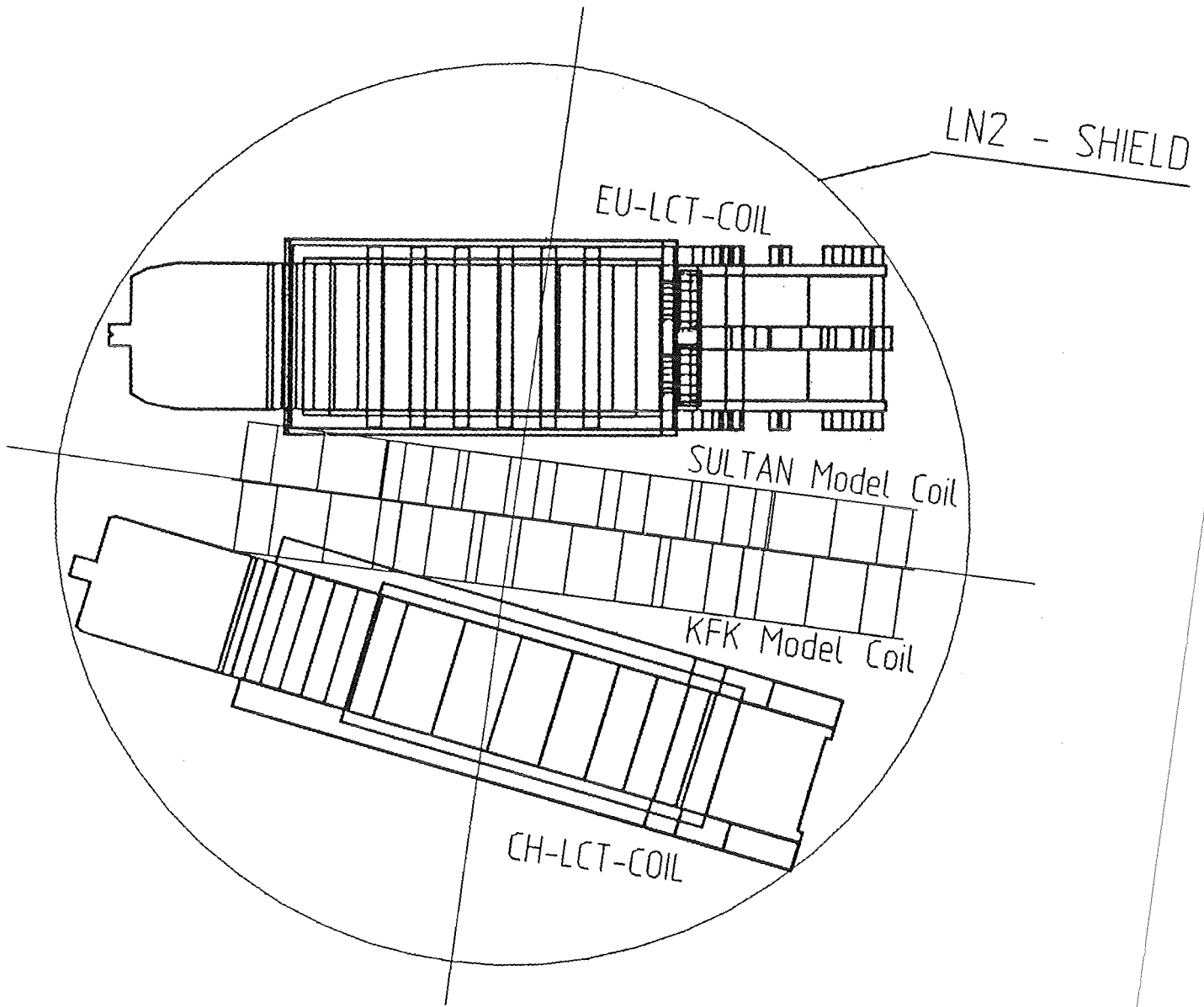


Fig. 6.1-1 Top View of the Cluster Configuration C3.

6.1.2 Cluster Configuration C6 with a minimum Bending Radius of 1.0 m

The restrictions listed above and the possibility to reduce the necessary amount of conductor led to a further reduction of the bending radius to 1 m , as already mentioned in Chapter 3 . An increase of the angle between the EU - LCT - coil and the model coil from 9 deg. to 14 deg. was mandatory to reduce the maximum field at the conductor below 8.3 T.

Due to this modifications and an enlargement of liquid nitrogen shield , an installation into the existing vacuum vessel seems to be possible without a removal of the vessel wall. The enlargement of the liquid nitrogen shield is possible , because it is mounted out of 36 individual panels , each of about 3.1 m length and 1.1 m width.

As shown in Fig. 6.1 - 2 the LCT - coils can be installed first , including the support structure. As second step the model coils will be mounted in between . The distance between liquid nitrogen shield and test rig is still small (350 mm) but sufficient for installation and maintenance. Modifications of the vacuum vessel have been reduced to additional ports for the current leads . Pretests of the cryogenic system including leak tests can be performed in advance . Compared with version C3 , the installation should be faster and the modifications not so expensive .

In order to avoid an overloading of the LCT - coils additional support structure will be installed especially at the rear side of the coils.

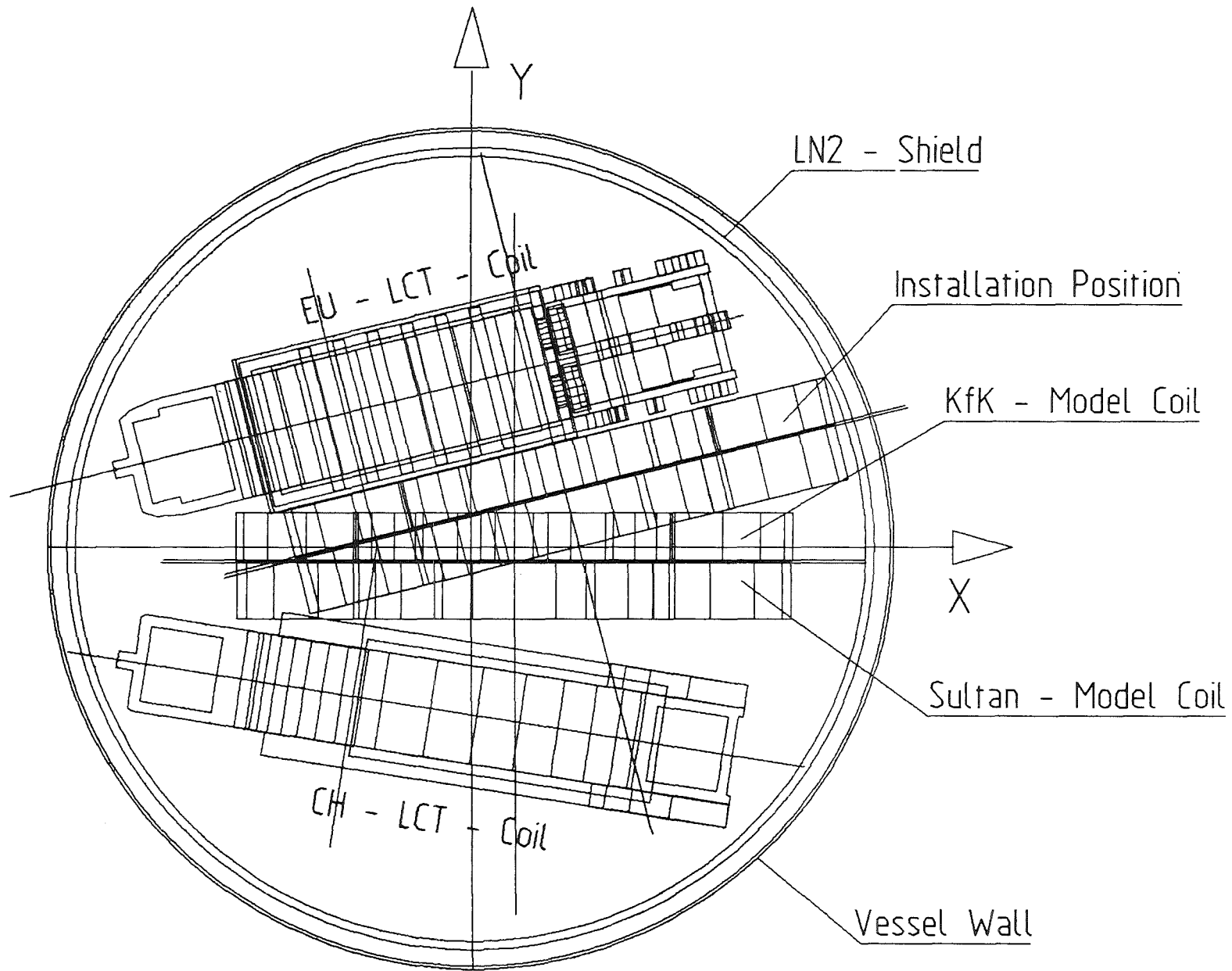


Fig. 6.1-2 Top View of the Cluster Configuration C6

The calculated mechanical pressure in axial direction is far below the pressure in the NET - TF - coils . Consequently we have to apply artificial forces to reach the NET requirements . Different means for applying additional forces were considered :

- use of wedges ,
- thermal contraction ,
- helium cylinders.

The disadvantage of wedges and thermal contraction is ,that the additional forces will be applied during energizing the coils or during cool down in an uncontrollable manner. Due to the possibility to apply the artificial force in well defined steps at the end of the test program, it was decided to use helium cylinders. In order to achieve an axial pressure similar to NET values we have to apply a mechanical load of 130 MPa, but the helium pressure has to be kept below about 10 MPa to avoid helium solidification inside the cylinder as shown in Fig. 6.1-3. Consequently the ratio between helium cylinder and pressure area at the model coils must be at least 13. Under these constraints and taking into account the limited space in the test rig, a device was preliminarily designed as shown in Fig.6.1-4 . A movement of the piston of less than 1 mm leads to a diaphragm as seal between piston and cylinder. One problem is still the relatively small pressure area at the model coils (595 mm x 30 mm) and especially the transition zone between high and low pressure region. Further investigations and pretests are necessary for the development of this device.

Fig. 6.1-5, a CAD - generated view of the Cluster Test Rig , gives the impression how the test device installed into the vacuum vessel would look like.

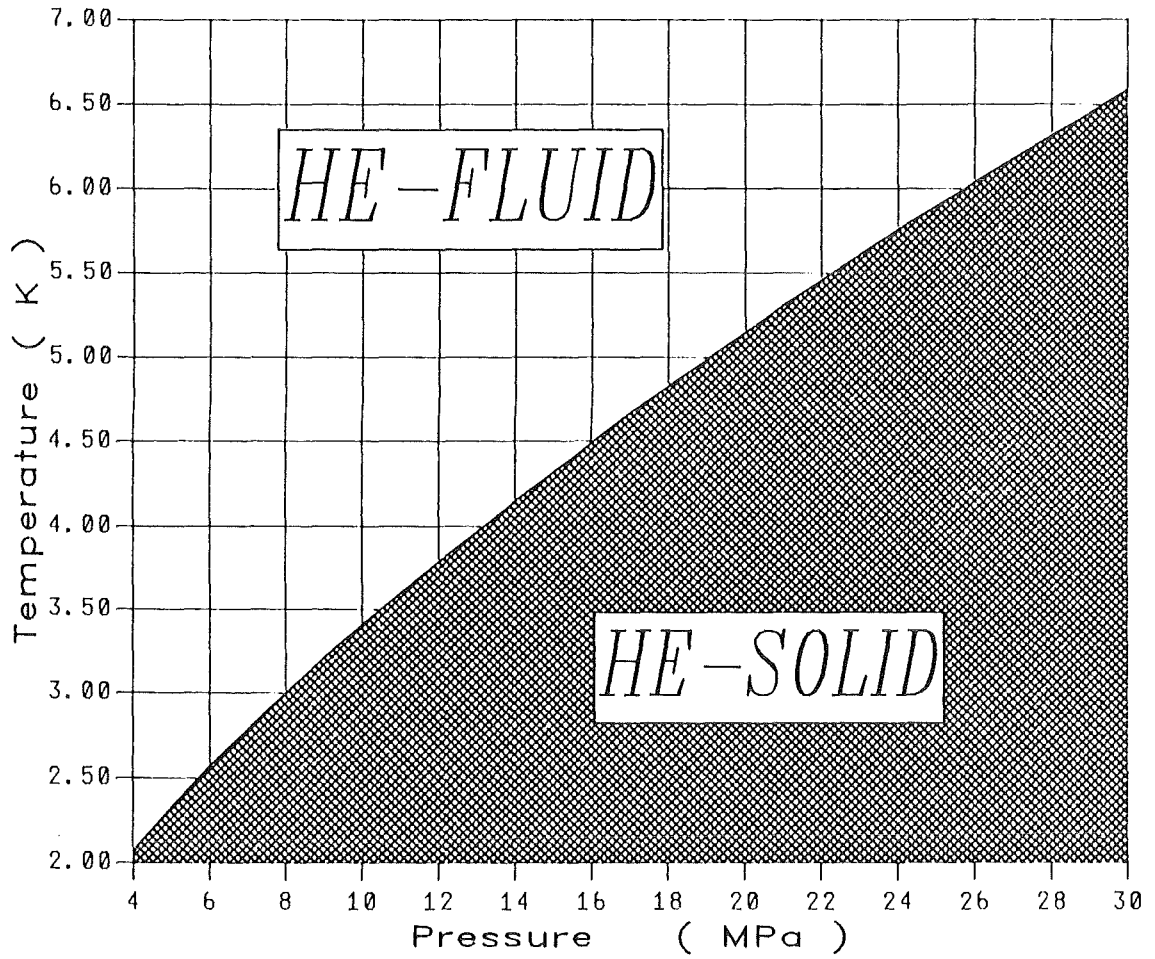


Fig. 6.1-3 Solidification of Helium

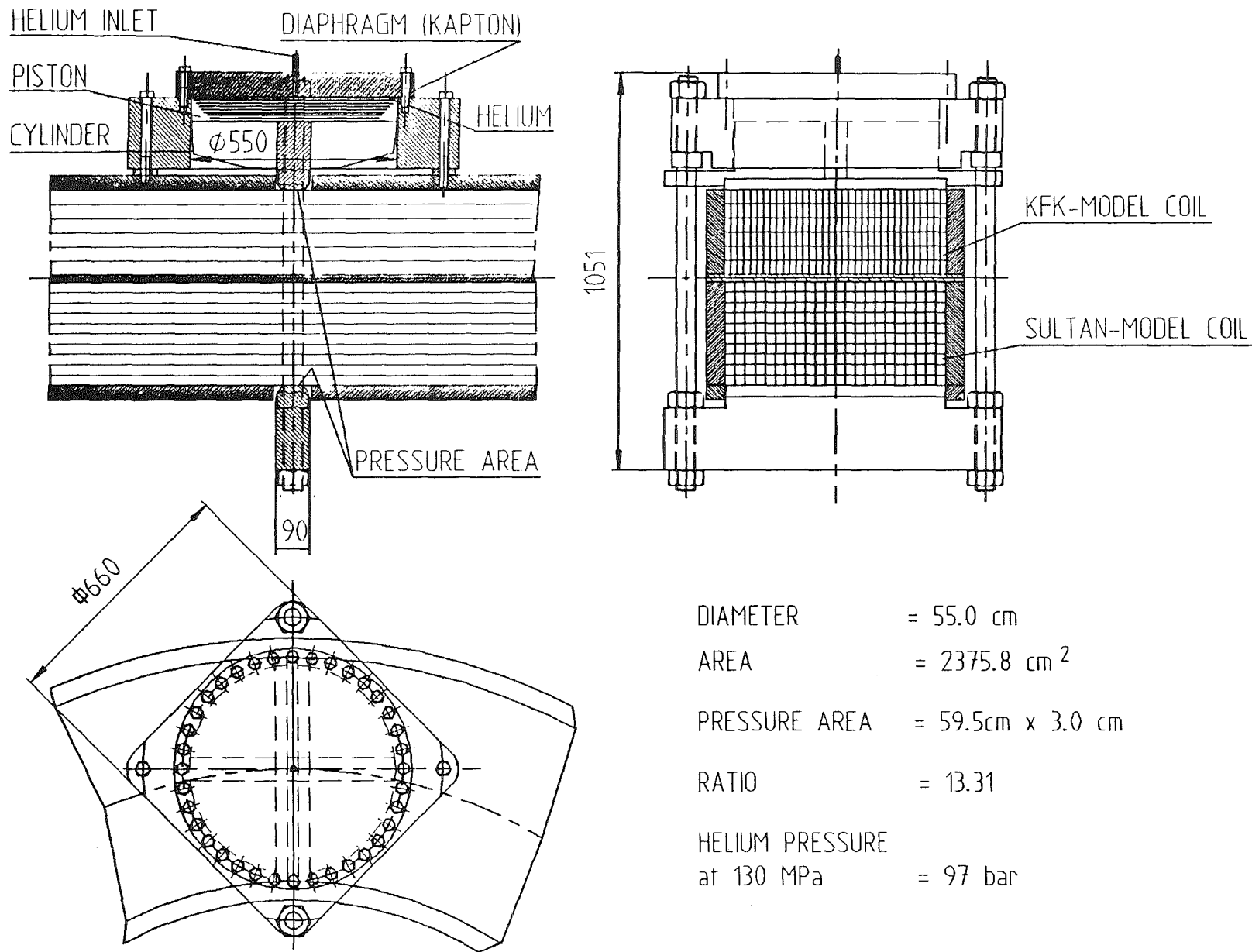


Fig. 6.1-4 HELIUM CYLINDER TO APPLY ARTIFICIAL LOAD TO THE MODEL COILS

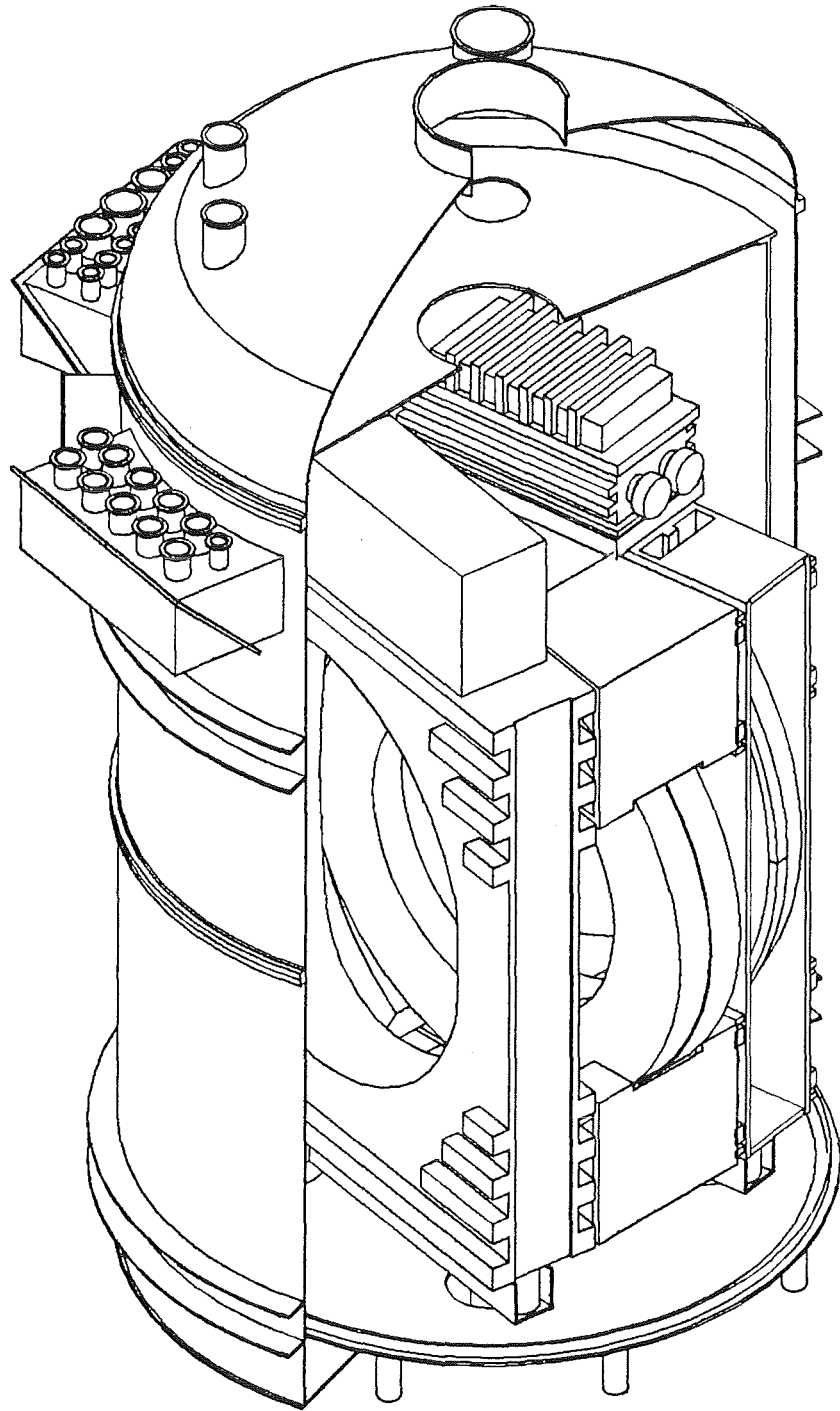


Fig. 6.1-5 CAD generated View of the Cluster Test Rig installed into the Vacuum Vessel.

6.2 Installation of the Solenoid Configuration

In case of the solenoid configuration , all versions fit properly into the existing vacuum vessel and liquid nitrogen shield without larger modifications at the vessel or shield. Only additional ports have to be installed for the current leads. Installation, pretests and maintenance are possible without space restrictions. As in the cluster case the mechanical pressure in axial direction is too low by a factor of about 3 compared with NET operational values . However , helium cylinders to apply additional axial pressure to the model coils can be integrated into the pedestals .

A pulse coil for AC loss measurements or/and quench detector tests can also be mounted onto the model coils if it is desired . The Solenoid Configuration S1 with an inner diameter of 2.4 m installed into the vacuum vessel is shown in Fig. 6.1 - 1 and 6.2 - 2 .

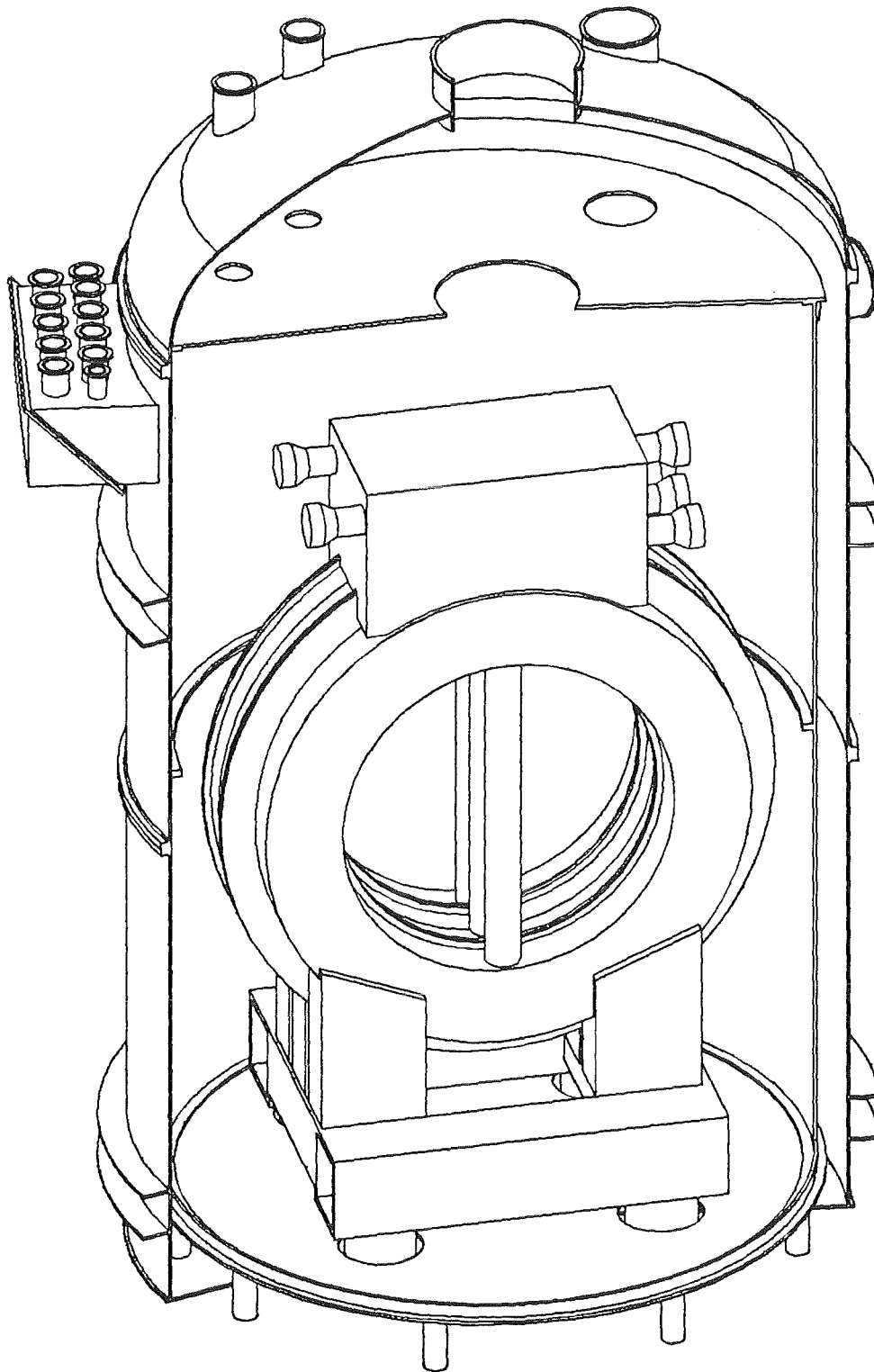


Fig. 6.2-1 CAD generated View of the Solenoid Test Rig installed into the Vacuum Vessel .

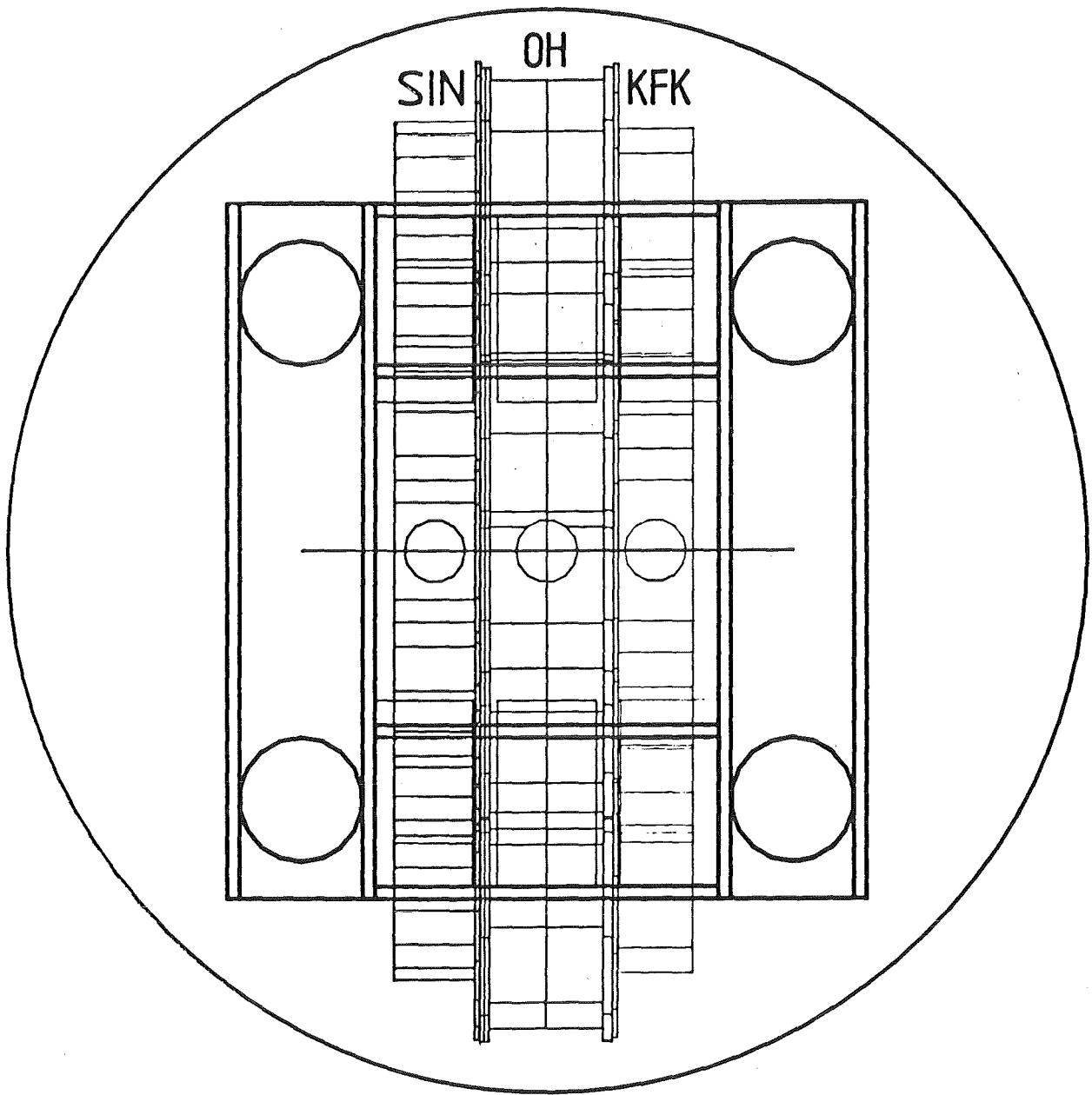


Fig. 6.2-2 Projection of the Solenoid Test Rig into the Midplane.

7. Cooling Considerations

A preliminary cooling system was designed for the Cluster and Solenoid Configuration under the following constraints:

- use as much as possible the existing TOSKA- facility,
- a new refrigeration system will be required for both configurations,
- allow cooling conditions which are flexible and independent of the refrigeration system,
- avoid a disturbance of the refrigeration system during quench or dump of model coils,
- helium losses during quench and dump have to be kept as low as possible.

The conditions listed above and the positive experience gained during the LCT - Coil Test in TOSKA led to a secondary cooling system for the test coils in TOSKA-Upgrade. In such a cooling system pressure and helium mass flow can be chosen independently of the refrigeration system.

Reactions during quench or dump to the refrigeration system are negligible. The helium mass flow in the secondary loop will be circulated with a piston pump as developed for the LCT-Coil Test [7.4].

7.1 Cluster Facility

The Cluster Facility can be built up for helium supply to the forced flow magnets with the following temperature options:

- Model coils and LCT-coils are cooled at 3.5 K inlet temperature,
- Model coils are cooled at 3.5 K to 4.5 K,
LCT-coils are cooled at 1.8 K inlet temperature if desired for LCT-coil tests at higher magnetic fields.

7.1.1 Cooling of the LCT-coils at 3.5 K

A simplified flow diagram of the cooling circuit for the Cluster Facility is shown in Fig. 7.1-1. The main components are the control dewar B250 with two helium pumps ($\dot{m}_{\max} = 2 \times 150 \text{ g/s}$), two heat exchangers to remove the heat load from the coils, transfer lines, and the compression work of the helium pumps.

Inside the vacuum vessel B300 there are the 4 coils, lower part of 6 current leads, and a cold storage vessel (B310). Both vessels are connected together and to the refrigerator by vacuum insulated transfer lines. All 4 coils will be forced flow cooled in parallel with a helium mass flow rate each of 50 g/s at 6 bar and 3.5 K except the KfK model coil with only 30 g/s. The mass flow rate of the LCT-coils is chosen from the operational experience with these coils in the IFSMTF [7.1]. The mass flow rate for the model coils is optimized to a minimum outlet temperature as shown in Fig. 7.1-2. To reach a coil inlet temperature of 3.5 K the control dewar has to be operated at subatmospheric pressure corresponding to a temperature of 3.3 K.


Heaters on the inlet lines of one or two model coil pancakes allow a rise of the temperature up to the value required by NET and for current sharing tests.

A part of the helium return flow (120 g/s) will be used to cool the coil cases. So the total helium flow can be kept low.

Cool down from room temperature to $\sim 100 \text{ K}$ will be done through mixing of cold and warm helium in a three-way-valve. The coil inlet temperature will be controlled by a computer system similar to the EU-LCT-coil test in TOSKA [7.2]. A summary of the cooling data for the 3.5 K version is given in table 7.1-1.

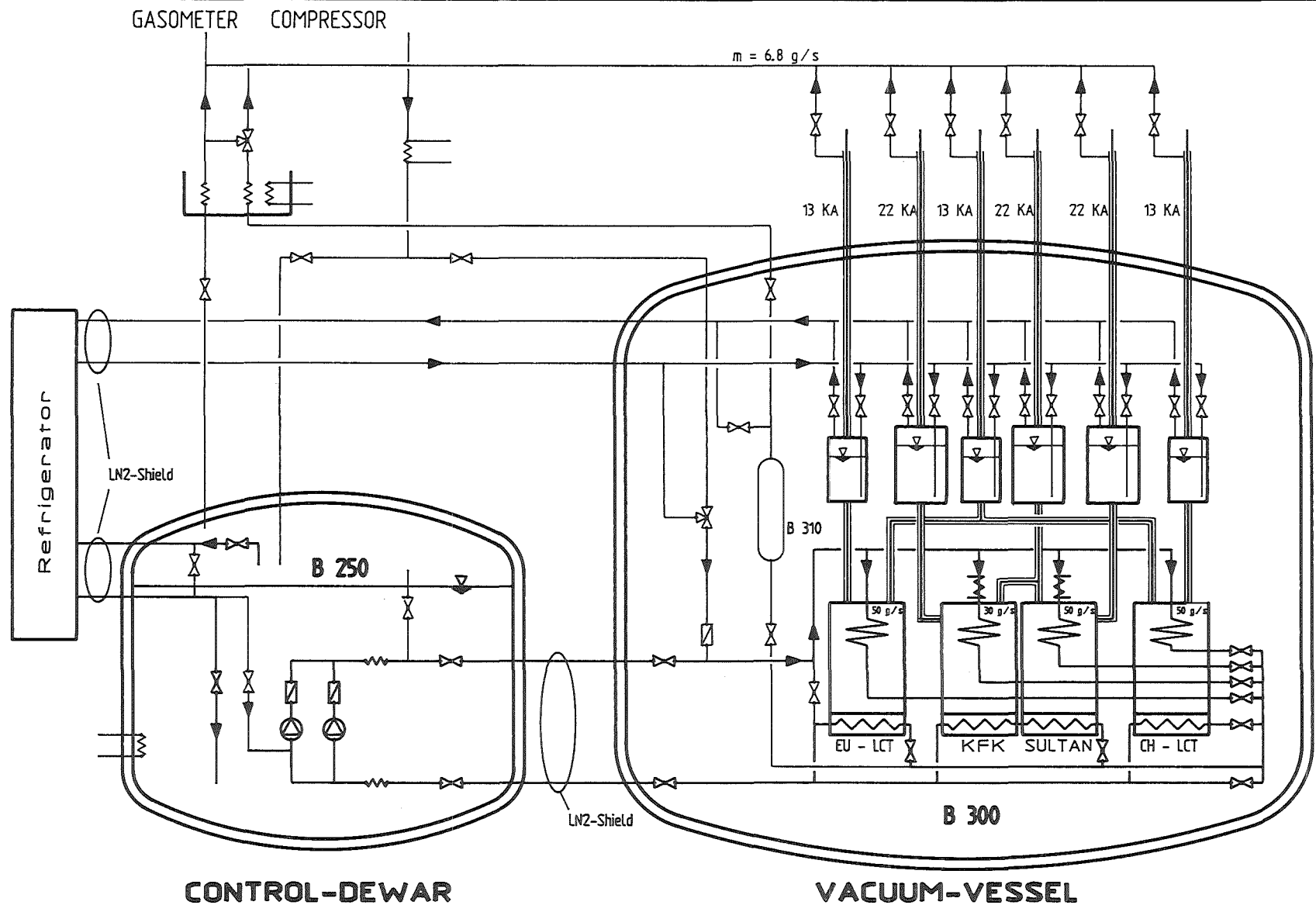


**Fig. 7.1-1 Cryogenic System of the Cluster Configuration
(3.5 K Version)**

 CAM
CAD

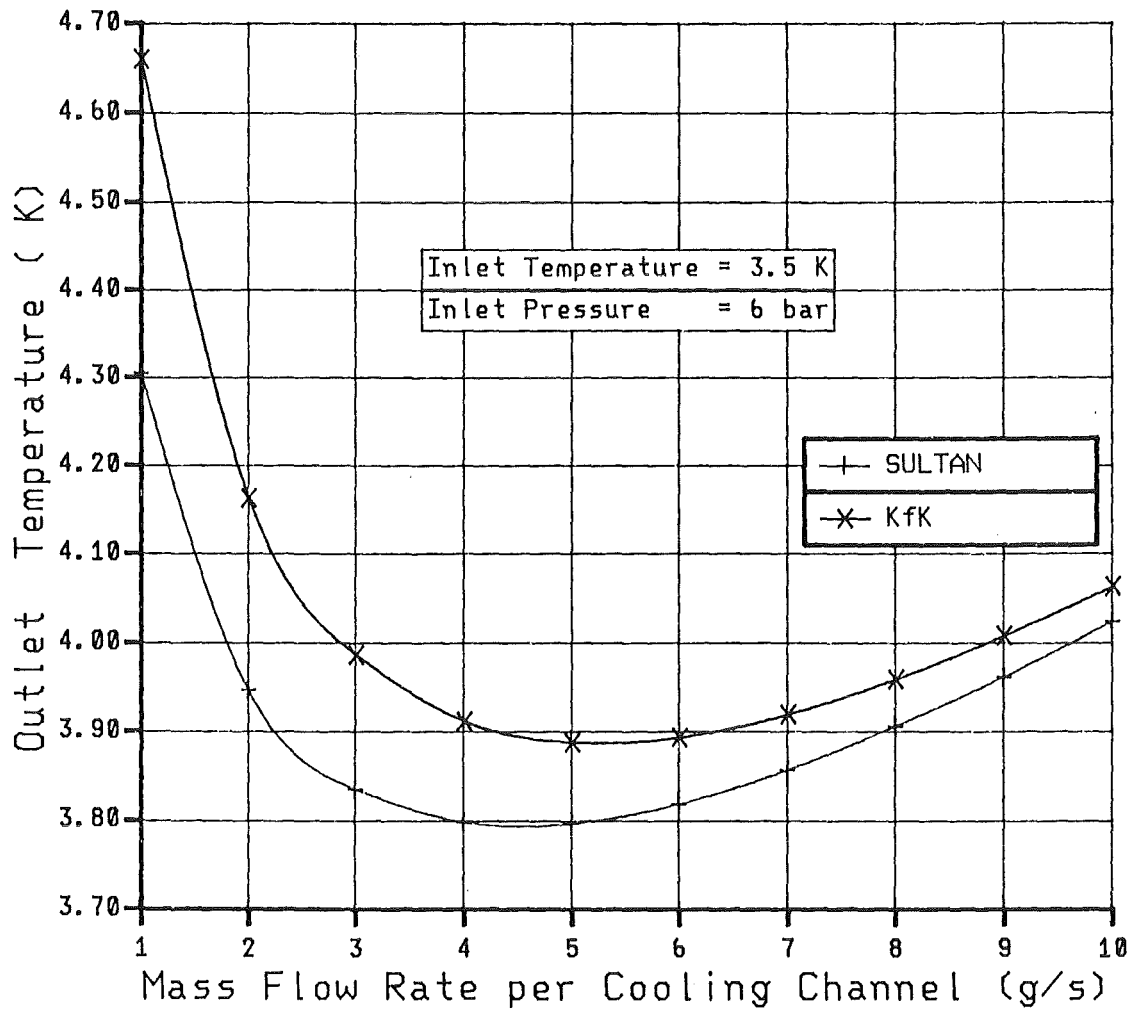


Fig. 7.1-2 Mass Flow Optimization for the Cluster Version C6

Table 7.1-1: Cooling Conditions of the Cluster Configuration C6, Version 3.5 K

		KfK	Sultan	LCT-CH	LCT-EU	Total
Conductor						
Width x height (insulated)	[mm]	38 x 17.5	27.7 x 26.8	18.5x18.5	40x10	
Cooling channel cross section	[mm ²]	83	51.2	15.9	95	
Coil						
Cooling length	[m]	277	179	250	250	
No. of pancakes per coil		3x2	5x2	11	14	
Mass flow rate per cooling channel	[g/s]	5	5	2.3	1.8	
Mass flow rate per coil	[g/s]	30	50	50	50	180
Pressure drop (coil and transfer lines)	[bar]	0.75	0.6	1.0	0.1	
He inlet temperature	[K]	3.5	3.5	3.5	3.5	
He outlet temperature	[K]	3.9	3.8	3.75	3.6	
Pumping power ($\Delta p = 1.0$ bar, $\eta = 0.5$)	[W]	40	70	70	70	250
Heat load	[W]	10	10	15	15	50
Case						
Surface	[m ²]					174
Heat load	[W]					210
Mass flow rate	[g/s]					120
Current leads						
Warm gas flow rate	[g/s]					6.8
Refrigeration power (T = 4.5 K)	[W]					210
Refrigeration power (T = T _{coil})	[W]					25
Facility						
Dewar, valves,	T = 4.5 K	[W]				50
pumps, transfer lines	T = T _{coil}	[W]				160
Theor. cooling power						
	T = 4.5 K	[W]				260
	T = T _{coil}	[W]				695
Cooling power with a safety margin of 30%						
	T = 4.5 K	[W]				338
	T = T _{coil}	[W]				904

7.1.2. An 1.8 K Cooling Option for the LCT-Coils

In order to test the LCT-coils up to 11 T as described in Chapter 11.1 it is mandatory to cool the winding to an inlet temperature of 1.8 K. For this we need a second control dewar B260 which can be connected to the existing Linde 1.8 K - refrigerator. This refrigerator has a cooling capacity of 380 W at 1.8 K. The dewar B260 contains the flow loop equipments immersed into the superfluid He-bath. A simplified flow circuit is shown in Fig. 7.1-3.

The 1.8 K helium pump loop provides a flow rate of 50 g/s to each winding of the LCT-coils. The inlet pressure is rated to 2.2 bar. More cryogenic data are listed in table 7.1-2. The model coils and the coil cases of the LCT-coils will be cooled in the same manner as described in chapter 7.1.1.

The existence of a second control dewar offers an additional cooling option to cool the model coils at 3.5 K to 4.5 K and the LCT-coils with 3.5 K forced flow helium.

This option was worked out regardless the stiffness of the LCT-coils. For both coils FEM-calculation must be performed to find weak areas where additional support structure must be applied. In case of the EU-LCT-coil the FEM-calculation is already started.

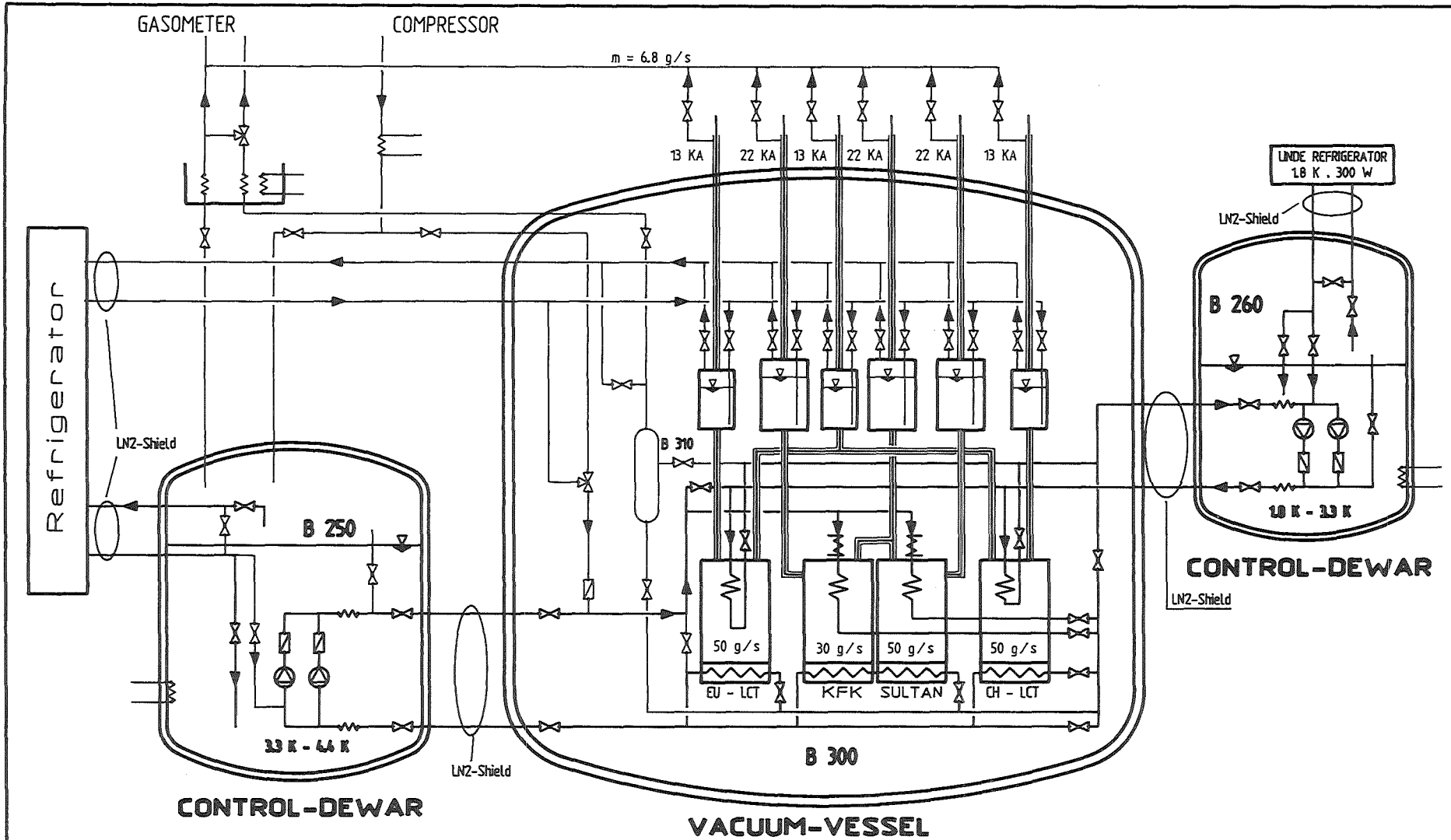


**Fig. 7.1-3 Cryogenic System of the Cluster Configuration
(1.8 K COOLING OPTION FOR THE LCT-COILS)**

KfK CAM
CAD

Table 7.1-2: Cooling Conditions of the Cluster Configuration C6, 1,8 K Option

		KfK	Sultan	LCT-CH	LCT-EU	Total
<u>Conductor</u>						
Width x height (insulated)	[mm]	38 x 17.5	27.7 x 26.8	18.5x18.5	40x10	
Cooling channel cross section	[mm ²]	83	51.2	15.9	95	
<u>Coil</u>						
Cooling length	[m]	277	179	250	250	
No. of pancakes per coil		3x2	5 x 2	11	14	
Mass flow rate per cooling channel	[g/s]	5	5	2.3	1.8	
Mass flow rate per coil	[g/s]	30	50	50	50	180
Pressure drop (coil and transfer lines)	[bar]	0.75	0.6	1.0	0.1	
He inlet temperature	[K]	3.5	3.5	1.8	1.8	
He outlet temperature	[K]	3.9	3.8	2.37	2.12	
Pumping power ($\Delta p = 1.0$ bar, $\eta = 0.5$)	[W]	40	70	70	70	110/140*
Heat load	[W]	10	10	15	15	20/30*
<u>Case</u>						
Surface	[m ²]					174
Heat load	[W]					210
Mass flow rate	[g/s]					80
<u>Current leads</u>						
Warm gas flow rate	[g/s]					6.8
Refrigeration power (T = 4.5 K)	[W]					210
Refrigeration power (T = 3.5 K)	[W]					15
Refrigeration power (T = 1.8 K)	[W]					10
<u>Facility</u>						
Dewar, valves,	T = 4.5 K	[W]				50
pumps, transfer lines	T = 3.5 K	[W]				160
	T = 1.8 K	[W]				70
<u>Theor. cooling power</u>						
	T = 4.5 K	[W]				260
	T = 3.5 K	[W]				515
	T = 4.8 K	[W]				250
<u>Cooling power with a safety margin of 30%</u>						
	T = 4.5 K	[W]				338
	T = 3.5 K	[W]				670
	T = 1.8 K	[W]				325

* heat load at 1.8 K

7.2 Cooling Considerations of the Solenoid Facility

For this configuration , a cooling system was designed under the same constraints as for the cluster configuration . A simplified flow diagram of the cooling circuit is shown in Fig.7.2-1.

The three model coils of the solenoid configuration with a total number of 30 pancakes in the version S1 and 32 pancakes in the version S3 will be cooled in parallel with a helium mass flow rate of 140 g/s resp. 146 g/s. The mass flow rate through cooling channels of the different conductors was optimized for version S1 and S3 to a minimum outlet temperature as shown in Fig. 7.2-2 and 7.2-3. A conservative heat load of 13 mW/m was assumed for this calculation. The computer code used for optimization is explained in [7.3].

For case cooling the return gas is partly used to avoid an additional mass flow. This gives the advantage to use the existing equipment (helium pump, heat exchanger and transfer lines).

An inlet temperature of 4.2 K in version S1 and of 3.5 K in version S3 is necessary, as shown in Fig. 4.4-2, to get sufficient safety margin to the current sharing temperature. In order to achieve a coil inlet temperature of 4.2 K resp. 3.5 K the control dewar has to be operated at subatmospheric pressure and a temperature of 3.8 K resp. 3.3 K. For heat load calculations the test results gained during the LCT coil test in TOSKA and helium pump test in HELITEX [7.4] has been used. The cooling requirements of the current leads has been calculated by means of conservative data (warm gas 0.065 g/s kA ,refrigeration power 2 W/kA), because there are very different values published so far. The results of this calculation and the cooling conditions are summarized in Table 7.2-1.

The cooldown will be done by mixing of helium at 77 K with helium at 300 K in a three-way-valve similar to the cooldown of the EU-LCT-Coil in TOSKA. In order to avoid helium losses during quench or dump , a cold storage vessel (B 310) is foreseen.

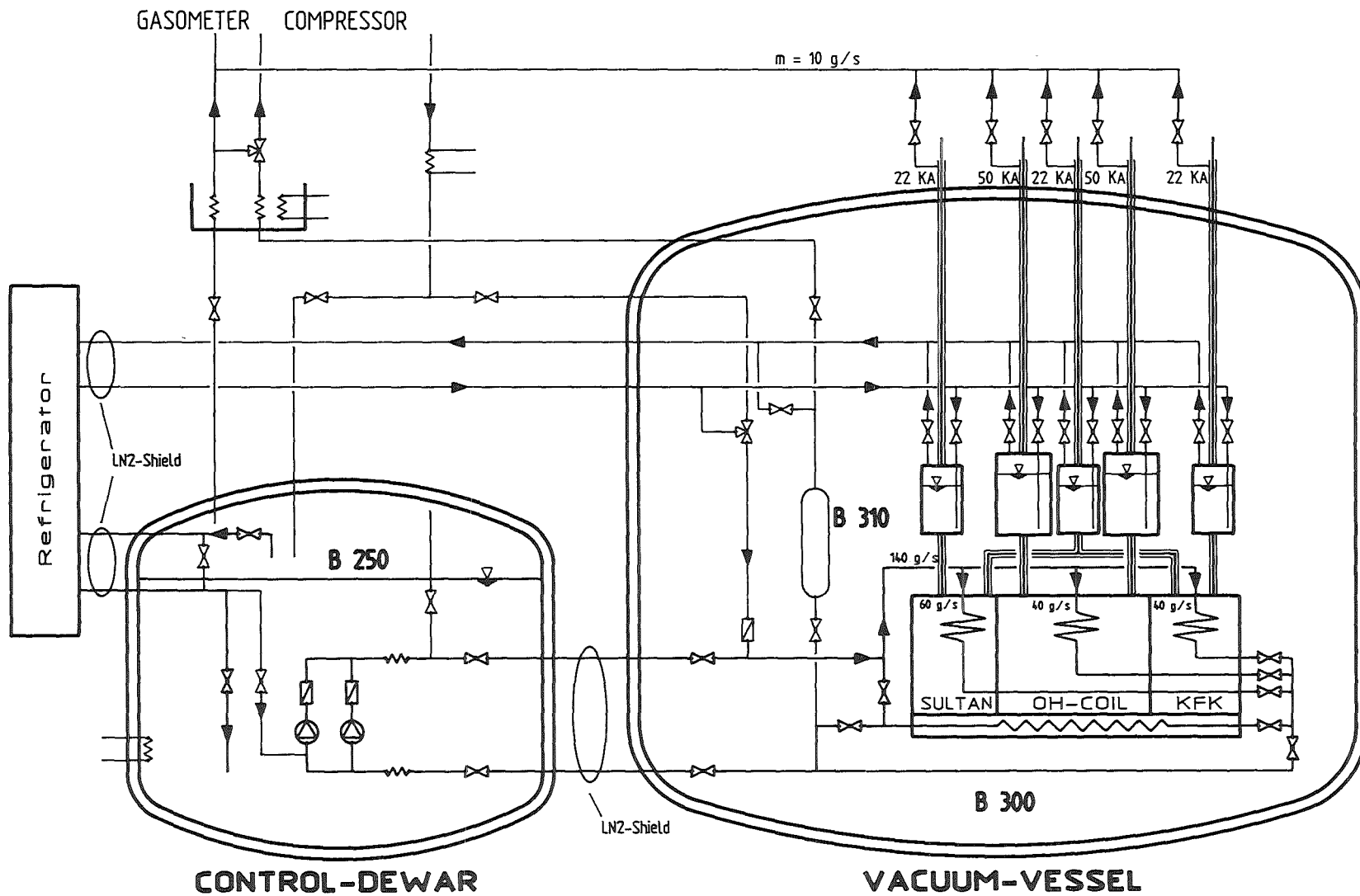


**Fig. 7.2-1 Cryogenic System
of the Solenoid Configurations S1 and S3**

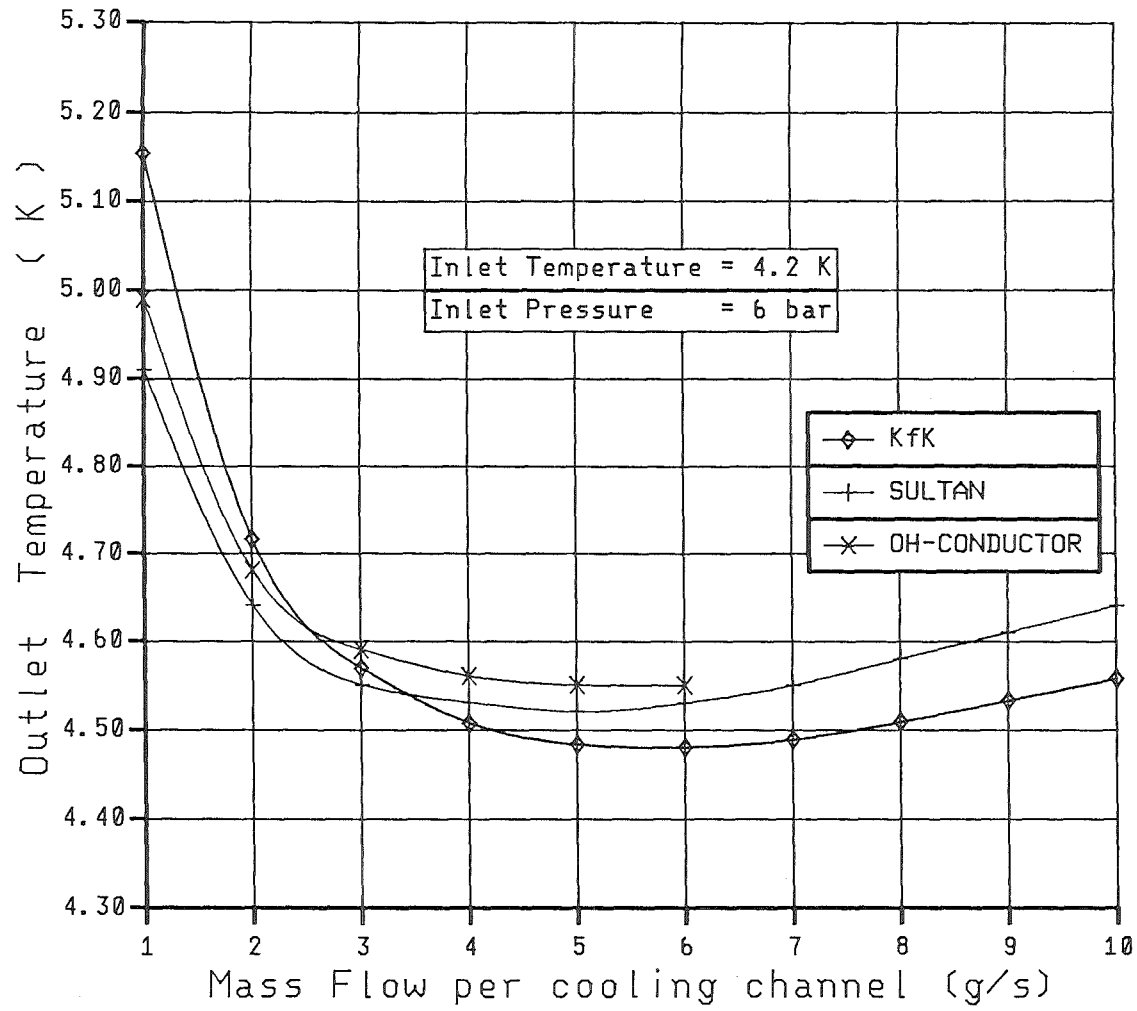


Fig. 7.2-2 Mass Flow Optimization for the Solenoid Version S1

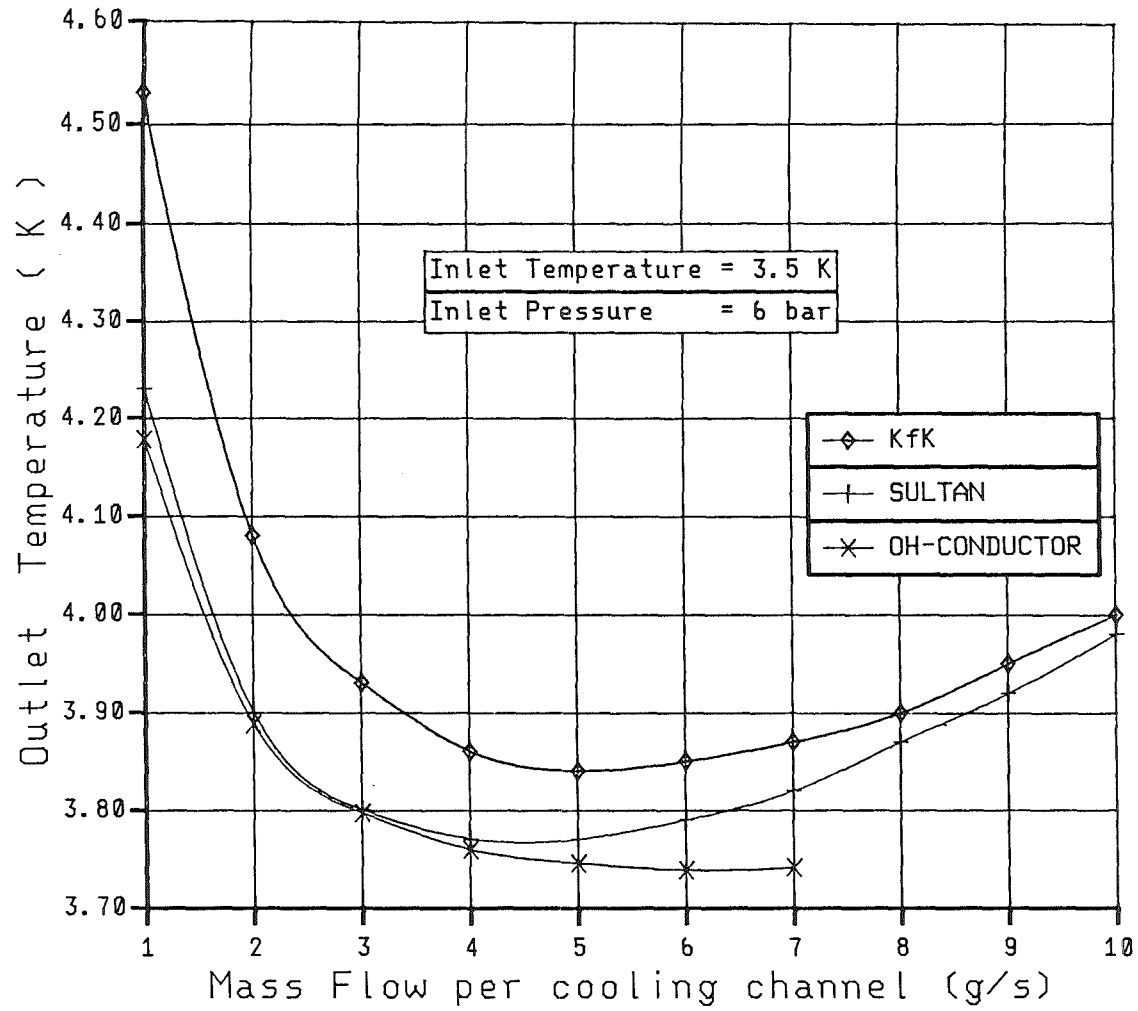


Fig. 7.2-3 Mass Flow Optimization for the Solenoid Version S3

Table 7.2-1: Cooling Conditions of the Solenoid Configuration

	Version S1				Version S3			
	KfK	OH	Sultan	Total	KfK	OH	Sultan	Total
<u>Conductor</u>								
Width x height (insulated) [mm]	38.0 x 17.5	50 x 33.3	27.7 x 26.8		38x17.5	49x32,3	27.7x268	
Cooling channel cross section [mm ²]	83	232	51.2		83	311	51.2	
<u>Coil</u>								
Cooling length [m]	255	205	174		238	127	160	
No. of pancakes per coil	4 x 2	5 x 2	6 x 2		5x2	4x2	7x2	
Mass flow rate per cooling channel [g/s]	5	4	5		5	5	4	
Mass flow rate per coil [g/s]	40	40	60	140	50	40	56	146
Pressure drop (coil and transfer lines) [bar]	0.6	1.4	0.7		0.6	0.5	0.5	
He inlet temperature [K]	4.2	4.2	4.2		3.5	3.5	3.5	
He outlet temperature [K]	4.48	4.56	4.52		3.84	3.77	3.74	
Pumping power ($\Delta p = 1.4/0.6$ bar, $\eta = 0.5$) [W]	86	86	129	301	40	32	45	117
Heat load [W]	10	10	10	30	10	10	10	30
<u>Case</u>								
Surface [m ²]				40				40
Heat load [W]				80				80
Mass flow rate [g/s]				50				50
<u>Current leads</u>								
Warm gas flow rate [g/s]				10				10
Refrigeration power T = 4.5 K [W]				332				332
Refrigeration power T = T _{coil} [W]				20				20
<u>Facility</u>								
Dewar, valves, pumps, transfer lines T = 4.5 K [W]				50				50
T = T _{coil} [W]				160				160
Pulse coil T = T _{coil} [W]				50				50
<u>Theor. cooling power</u>								
T = 4.5 K [W]				382				382
T = T _{coil} [W]				641				457
<u>Cooling power with a safety margin of 30%</u>								
T = 4.5 K [W]				496				496
T = T _{coil} [W]				833				594

7.3 Summary

The total cooling power requirements including the equivalent cooling power at 4.4 K of the Cluster and Solenoid Configuration are summarized in table 7.2-2 for comparison . As shown in this table an equivalent cooling power at 4.4 K between 2.2 and 2.8 kW is necessary for the different options .The cooling capacity of the existing refrigerator system at KfK is only (400 + 600) W and consequently a new powerful refrigeration system is mandatory in any case .

A test of the LCT - coils (NbTi conductor) at 1.8 K and 11 T is possible in the cluster configuration with minor modifications of the facility.

References to Chapter 7

- [7.1] W. Herz et al., Testing of the EURATOM- LCT-Coil, a Forced-Flow Cooled NbTi Coil, in the International Fusion Superconducting Magnet Test Facility (IFSMTF). Applied Superconductivity Conference ASC-86, Baltimore, Maryland, USA, Sept. 28-Oct. 3, 1986.

- [7.2] W. Herz et al. Test of the EURATOM LCT-Coil in the Karlsruhe Test Facility TOSKA. ICEC, Helsinki, 1984 .

- [7.3] R. Flükiger et al., An A15 Conductor Design and its Implications for the NET-II TF Coils. Final Study Report, KfK 3937, June 1985.

- [7.4] W. Lehmann, J. Mingos, Operating Experience with a High Capacity Helium Pump under Supercritical Conditions, Proceedings of the Cryogenic Engineering Conf., Colorado Springs, August 15 - 17, 1983, Plenum Press.

Table 7.2-2: Comparison of the Total Cooling Power

	Solenoid-Configuration S1			Solenoid-Configuration S3			Cluster Config. C6, Version 3.5 K			Cluster Config. C6, 1.8 K Option			
	Q[W] 3.8 K*	Q[W] 4.5 K	\dot{m} [g/s] 4.5-300K	Q[W] 3.3 K*	Q[W] 4.5 K	\dot{m} [g/s] 4.5-300K	Q[W] 3.3 K*	Q[W] 4.5 K	\dot{m} [g/s] 4.5-300K	Q[W] 1.8 K*	Q[W] 3.3 K*	Q[W] 4.5 K	\dot{m} [g/s] 4.5-300K
<u>Background Coils</u>													
Heat load	-	-	-				160			30	130		
Pumping power	-	-	-				140			140			
<u>Test Coils</u>													
Heat load winding	30			30			20				20		
Heat load case	80			80			80				80		
Pumping power	301			117			110				110		
<u>Current Leads</u>													
Solenoid 166 kA/Cluster 105 kA (0,065 g/s kA + 2 W/kA)	20	332	10	20	332	10	25	210	6.8	10	15	210	6.8
<u>Facility</u>													
Dewar, valves, transfer lines, pumps	160	50		160	50		160	50		70	160	50	
<u>Pulse Coil</u>													
Pulse Coil	50			50									
<u>Theor. cooling power</u>													
Theor. cooling power	641	382	10	457	382	10	695	260	6.8	250	515	260	6.8
Cooling power with a safety margin of 30%	833	496	13	594	496	13	904	338	8.8	325	670	338	8.8
<u>Cooling power 4.4 K equivalent</u>													
Cooling power 4.4 K equivalent		2.8 kW			2,7 kW				2,6 kW	Linde Refrig.		2,2 kW	

*Temperature in the Control Dewar

8. Costs Estimate

It is difficult to estimate the costs of the model coils and the facility without a completed development and a detailed design . However , based on the costs of the EU-LCT coil and the offers for the POLO model coil [2.5], average specific manufacturing costs of 460 DM/kg have been evaluated for large superconducting coils. Another uncertainty is still a different design for components (e. g. joints) and the handling of the brittle Nb₃Sn conductor.

In the following approximate costs of the model coils are included the costs for material, manufacturing, pretests, detail design, development of components and calculations but not the costs of the conductor and installation into the facility. The conductor development and manufacturing costs are in task M5 and therefore not in this estimation. Only the amount of conductor necessary for the model coils is included in the tables for comparison.

The facility costs are estimated on the base of the TOSKA- facility and include the installation at KfK, pretests, and acceptance tests.

The operating costs contain mainly electricity, cooling water, helium losses, maintenance and repair but not manpower and interests.

8.1 Costs of the Cluster Configuration C6

In case of the Cluster Configuration the costs and manpower requirements are presented only for the version C6 because the difference to version C3 is within the accuracy margin . The results are summarized in table 8.1-1 , 8.1-2 and 8.1-3 without the OH-model coil.

Table 8.1-1 Approximate Costs and Manpower Requirements for the Model Coils of the Cluster Configuration Version C6.

	Quantity	Costs Mio. DM	Manpower				
			1st year 1988	2nd year 1989	3rd year 1990	4th year 1991 (1/2 year)	Man x a
Goal			1988	1989	1990	1991	
Sultan-Conductor * (task M5)	1790 m						
KfK - Conductor * (task M5)	1664 m						
Manufacturing of the Sultan - Coil	9.3 to	4.3					
Manufacturing of the KfK - Coil	7.8 to	3.6					
Tooling		3.0					
Design at Sultan and KfK side			2	2	2	2 x 0.5	7
Magnet and FEM - Calculations			1	1			2
Diagnostic			2	2	2	2 x 0.5	7
Quench Detection and High Voltage			1	1	1	2 x 0.5	4
Cooling System			2 x 0.5	2 x 0.5	2 x 0.5	2 x 0.25	3.5
Quality Assurance				1	2	2 x 0.5	4
Support Staff			6	8	6	4 x 0.5	22
Total Costs		10.9					
Total Manpower Requirements			13	16	14	6.5	~50

* Without spare length

Table 8.1-2 Approximate Costs and Manpower Requirements for the Facility Modifications of the Cluster Version 3.5 K.

	Quantity	Costs Mio. DM	Manpower				Man x a (1/2 year)
			1st year 1988	2nd year 1989	3rd year 1990	4th year 1991	
<u>Facility</u>							
Coordination			1	1	1	1 x 0.5	3.5
Transfer Lines and Piping		1.5					
He - Pumps	2 pcs	0.3	1	1	1	1 x 0.5	3.5
Vacuum Pump System		0.2					
Vacuum Vessel Modification		1.0	1	1	1	1 x 0.5	3.5
Current Leads	6 pcs	0.5	1	1	1	1 x 0.5	3.5
Support Structure and Helium Cylinder		2.0	2	2	2	2 x 0.5	7
Pretests and Operation	0.5 a	1.0				7 x 0.5	3.5
Support Staff			2	3	2	5 x 0.5	9.5
<u>Power Supply</u>							
13 kA / 20 V - Power Supply	260 kW	0.4	1 x 0.5	1	1	1 x 0.5	3
13 kA / 5 kV Switch and Dump System		0.5					
22 kA / 2 x 4.5 kV Switch and Dump Sys.		0.3	1 x 0.5	1	1	1 x 0.5	3
Support Staff			2 x 0.5		2 x 0.5	2 x 0.5	3
<u>Diagnostic</u>							
Data Acquisition System		0.5	1 x 0.5	1	1	1 x 0.5	3
Software			1 x 0.5	1	1	1 x 0.5	3
Control System		0.5	1 x 0.5	1	1	1 x 0.5	3
<u>Total Costs</u>		8.7					
<u>Total Manpower Requirements</u>			11.5	14	14	25 x 0.5	52

Table B.1-3 Approximate Costs and Manpower Requirements for Installation of the Model Coils and carrying out the Test.

	Time	Costs Mio. DM	Manpower			
			4th year (1/2 year)	5th year	6th year	Man x a
<u>Goal</u>			1991	1992	1993	
<u>Installation and Pretest of the Model Coils</u>	1 year					
Coordination			1 x 0.5	1 x 0.5		1
Representative of the Model Coils			4 x 0.5	4 x 0.5		4
Cryogenic System			2 x 0.5	2 x 0.5		2
Diagnostic			3 x 0.5	3 x 0.5		3
Support Structure and Helium Cylinder			1 x 0.5	1 x 0.5		1
Power Supply , Switch and Dump System			2 x 0.5	2 x 0.5		2
Support Staff			10 x 0.5	10 x 0.5		10
<u>Test of the Model Coils</u>	1 year					
Coordination				1 x 0.5	1 x 0.5	1
Representative of the Model Coils				6 x 0.5	6 x 0.5	6
Cryogenic System				2 x 0.5	2 x 0.5	2
Diagnostic				3 x 0.5	3 x 0.5	3
Power Supply , Switch and Dump System				2 x 0.5	2 x 0.5	2
Operation		2.0		7 x 0.5	7 x 0.5	7
Support Staff				7 x 0.5	7 x 0.5	7
<u>Result Evaluation</u>	0.5 year					
Coordination					1 x 0.5	0.5
Representative of the Model Coils					2 x 0.5	1
Cryogenic System					1 x 0.5	0.5
System Performance					1 x 0.5	0.5
Magnet and FEM - Calculation				1 x 0.5	2 x 1.0	2.5
Support Staff					4 x 0.5	2
<u>Total Costs</u>		2.0				
<u>Total Manpower Requirements</u>			11.5	26	20.5	58

8.2 Costs of the Solenoid Configuration S3

In case of the Solenoid Configuration the costs and manpower requirements are presented only for the version S3 because the difference to version S1 is also within the accuracy margin. The results are summarized in tables 8.2-1 , 8.2-2 and 8.2-3. Main differences, compared with the Cluster Facility, are the additional costs and manpower requirements for manufacturing and test of the OH-model coil. But this has to be compared with the requirements of a solitary test.

The total costs of the Cluster and Solenoid configuration are summarized in table 8.2-4. These costs have to be compared with the total costs of $1000 \cdot 10^6$ DM of the NET-Magnet system.

Table 8.2-1 Approximate Costs and Manpower Requirements for the Model Coils of the Solenoid Configuration Version 53.

Goal	Quantity	Costs Mio. DM	Manpower				Man x a (1/2 year)
			1st year 1988	2nd year 1989	3rd year 1990	4th year 1991	
Sultan-Conductor * (task M5)	2231 m						
KfK - Conductor * (task M5)	2380 m						
OH - Conductor * (task M5)	1019 m						
Manufacturing of the Sultan - Coil	11.6 to	5.4					
Manufacturing of the KfK - Coil	11.1 to	5.1					
Manufacturing of the OH - Coil	11.9 to	5.5					
Tooling		3.5					
Design at Sultan , KfK and OH side			3	3	3	3 x 0.5	10.5
Magnet and FEM - Calculations			1.5	1.5			3
Diagnostic			3	3	3	3 x 0.5	10.5
Quench Detection and High Voltage			1.5	1.5	1.5	3 x 0.5	6
Cooling System			3 x 0.5	3 x 0.5	3 x 0.5	3 x 0.25	5.25
Quality Assurance				1.5	3	3 x 0.5	6
Support Staff			9	12	9	6 x 0.5	33
Total Costs		19.5					
Total Manpower Requirements			19.5	24.0	21	9.75	~ 75

* Without spare length

Table B.2-2 Approximate Costs and Manpower Requirements for the Facility Modifications of the Solenoid Version S3.

	Quantity	Costs Mio. DM	Manpower				
			1st year	2nd year	3rd year	4th year (1/2 year)	Man x a
<u>Goal</u>			1988	1989	1990	1991	
<u>Facility</u>							
Coordination			1	1	1	1 x 0.5	3.5
Transfer Lines and Piping		1.0					
He - Pumps	2 pcs	0.3	1	1	1	1 x 0.5	3.5
Vacuum Pump System		0.1					
Vacuum Vessel Modification		0.2	1	1	1	1 x 0.5	3.5
Current Leads	5 pcs	0.5	2	2	2	2 x 0.5	7.0
Support Structure and Helium Cylinder		0.5	1	1	1	1 x 0.5	3.5
Pretests and Operation	0.5 a	1.0				7 x 0.5	3.5
Support Staff			2	3	3	5 x 0.5	10.5
<u>Power Supply</u>							
50 kA / 10 V - Power Supply	500 kW	0.6	1 x 0.5	1	1	1 x 0.5	3
50 kA / 20kV Switch and Dump System		1.7					
22 kA / 2 x 4.5 kV Switch and Dump Sys.		0.3	1 x 0.5	1	1	1 x 0.5	3
Support Staff			2 x 0.5		2 x 0.5	2 x 0.5	3
<u>Diagnostic</u>							
Data Acquisition System		0.5	1 x 0.5	1	1	1 x 0.5	3
Software			1 x 0.5	1	1	1 x 0.5	3
Control System		0.5	1 x 0.5	1	1	1 x 0.5	3
<u>Puls. Coil</u>							
		0.5	1 x 0.5	1	1	1 x 0.5	3
Power Supply		0.4	1 x 0.5	1	1	1 x 0.5	3
<u>Total Costs</u>							
		8.1					
<u>Total Manpower Requirements</u>							
			12.5	16	17	27 x 0.5	~ 60

Table 8.2-3 Approximate Costs and Manpower Requirements for Installation of the Model Coils and carrying out the Test (Solenoid S3).

	Time	Costs Mio. DM	Manpower				
			4th year (1/2 year)	5th year	6th year	7th year	Man x a
<u>Goal</u>			1991	1992	1993	1994	
<u>Installation and Pretest of the Model Coils</u>	1 year						
Coordination			1 x 0.5	1 x 0.5			1
Representative of the Model Coils			6 x 0.5	6 x 0.5			6
Cryogenic System			2 x 0.5	2 x 0.5			2
Diagnostic			3 x 0.5	3 x 0.5			3
Support Structure and Helium Cylinder			1 x 0.5	1 x 0.5			1
Power Supply , Switch and Dump System			2 x 0.5	2 x 0.5			2
Support Staff			10 x 0.5	10 x 0.5			10
<u>Test of the Model Coils</u>	1.5 year						
Coordination				1 x 0.5	1		1.5
Representative of the Model Coils				6 x 0.5	6		9
Cryogenic System				2 x 0.5	2		3
Diagnostic				3 x 0.5	3		4.5
Power Supply , Switch and Dump System				2 x 0.5	2		3
Operation		3.0		7 x 0.5	7		10.5
Support Staff				7 x 0.5	7		10.5
<u>Result Evaluation</u>	0.5 year						
Coordination						1 x 0.5	0.5
Representative of the Model Coils						3 x 0.5	1.5
Cryogenic System						1 x 0.5	0.5
System Performance						1 x 0.5	0.5
Magnet and FEM - Calculation				2 x 0.5	2 x 1	3 x 0.5	4.5
Support Staff						6 x 0.5	3
<u>Total Costs</u>		3.0					
<u>Total Manpower Requirements</u>			12.5	27.5	30	7.5	~ 78

Table 8.2-4 Comparison of the Costs for the Cluster and Solenoid Configuration

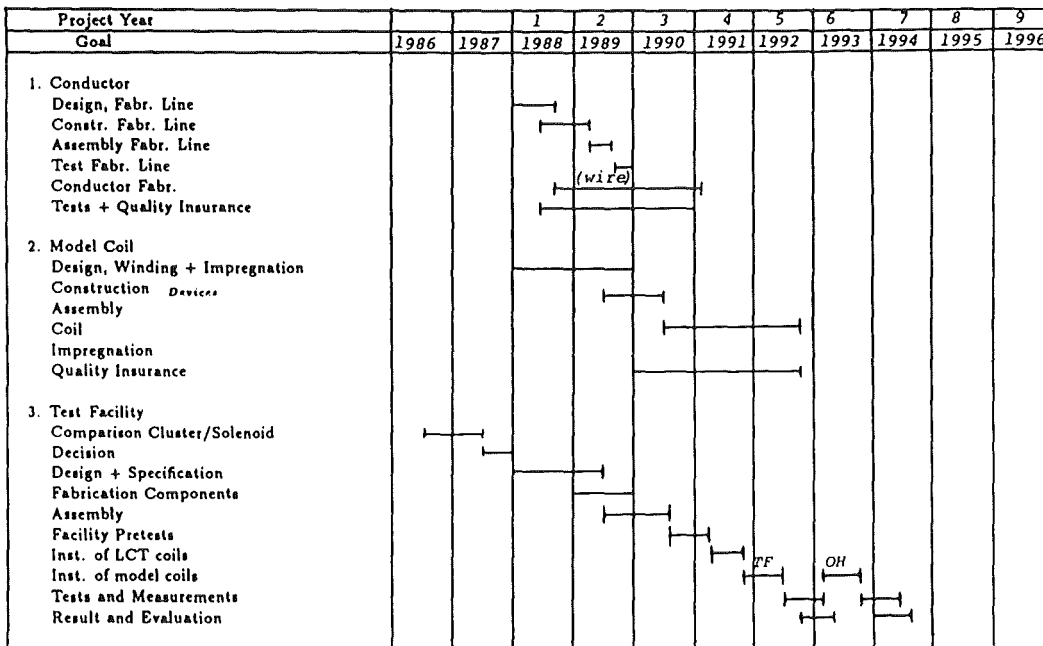
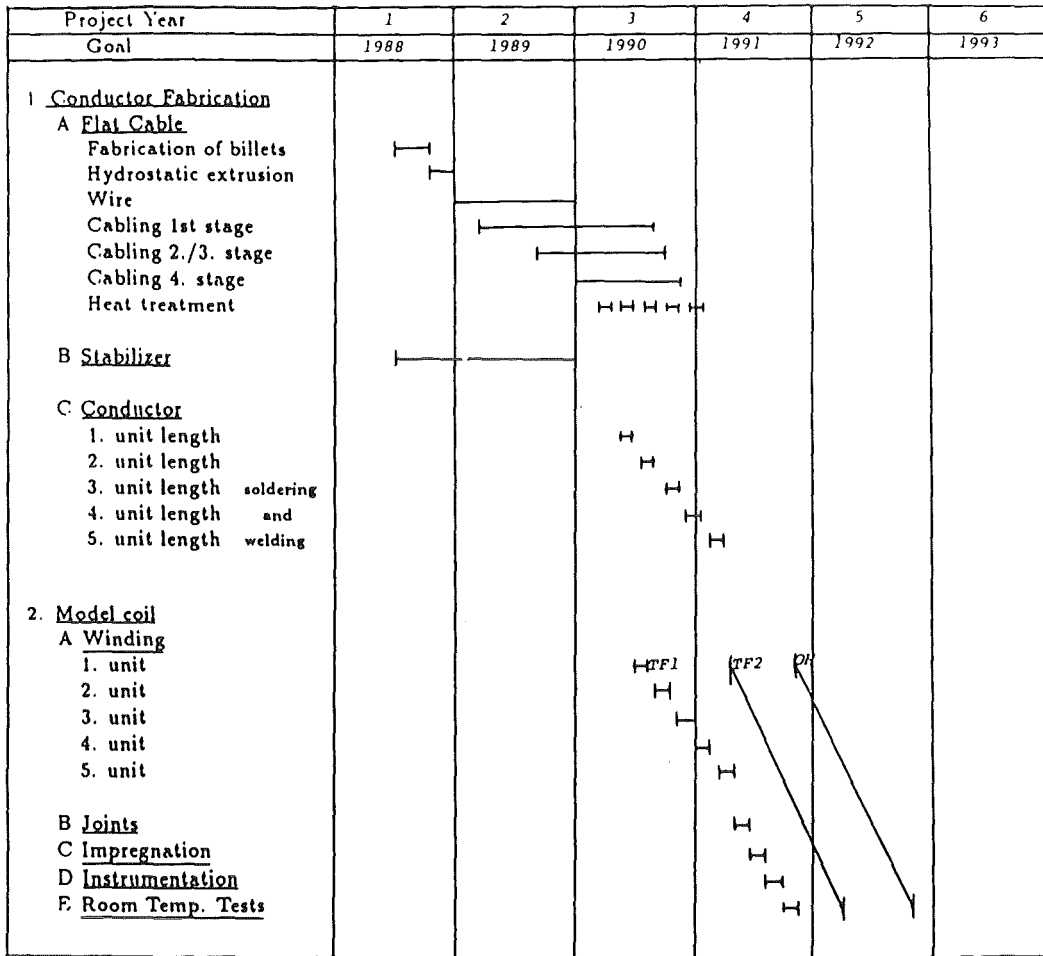
Configuration	Model Coils	Facility and Test	Total Costs
Cluster	10.9 Mio. DM (2 x TF)	10,7 Mio. DM	21.6 Mio. DM
Solenoid	19.5 Mio. DM (2 x TF + 1 x CH)	11.1 Mio. DM	30.6 Mio. DM

9. Time Schedule

Detailed time schedules of the two possible test facilities are given. In both cases the schedule is based on the assumption of an 8 hour working day. A speeding up for example of the conductor fabrication by 2 shifts may be possible. Furthermore, on request of the NET-Team it was assumed that one manufacturer will make all pancakes and only one set of winding tools will be available.

In both facility options the test results are available in 1993 if industrial contracts for conductor fabrication (M-5/M-13) are placed before 1988. A delay of that action would result in a delay of the testing.

9.1 Time Schedule for the Cluster Facility



9.3 Comparison of Time Schedule of M7

a) Cluster Facility

Project Year	4	5	6	7
Goal	1991	1992	1993	1994
3. Facility				
Installation				
Test of Coils				
Result Evaluation				

b) Solenoid Facility

Project Year	4	5	6	7
Goal	1991	1992	1993	1994
3. Facility				
Installation				
Test of Coils				
Result Evaluation				

10. Model Coil Test Programme (NET)

10.1 Design Approach

The model coil test program should estimate as close as possible (within physical and cost boundaries) the actual operating conditions of the NET TF and OH coils, including peak field at the winding, peak stresses and ac operation. It should be carefully studied whether the TF- and OH-coils can be tested in same test facility or whether separate tests are needed.

The best way for proving proper operation of the OH-coil can be done by an experiment in which fast ramp-up of coil current can be performed. Only in such a test arrangement clear data about the most critical situation are obtained where coil current and magnetic field are increasing while the critical current (and therefore also the energy margin) is decreasing quite fast. The extrapolation of data measured during a fast discharge of the OH-coil to operating conditions is difficult.

The model coil test program should verify the manufacturing process and conductor and coil performance of the NET-TF and OH-coil designs. It should prove the feasibility of the entire conductor and coil manufacture process including coil termination, coil winding, insulation and vacuum impregnation of double pancakes. The conductor and coil performance should be verified not only by measurement of the steady state nominal operating characteristics but also for mechanical and AC-behaviour.

10.1.1 Test Programme for the TF-Model Coils in TOSKA-Upgrade

Testing of the Toroidal Field Coils should specifically include:

1. stress/strain - because of the size and geometry of the test configuration it is difficult to simulate the actual operating stress/strain of the coils. Therefore additional external mechanical loads should be applied, if needed to approach these conditions of transverse, hoop and shear stresses. Strain measurements on the outer surface of the coil should be made to estimate the global winding pack mechanical characteristics,
2. ac-loss - an ac field should be applied from an external field source while the coil is energized at the standard condition. The goal is not to perform an exhaustive ac loss test but to verify the predicted performance. The energy dissipated can be measured from the thermodynamic states of the helium at inlet and outlet,
3. quench tests - the behaviour of the coils during quenching should be studied to determine the He temperature and pressure, and pressure drop, and coil voltages as a function of time for different operating currents, dump delay times, and dump time constants, and also the quench propagation velocity. Proposed quench detection systems have to be developed and tested on these coils,

4. standard operation - energize coils to an operating current to achieve the nominal peak field at the conductor (16 kA, 11.4T). Measure steady state values of pressure drop, flow rate, helium inlet and outlet temperatures, pancake joint and termination resistance and heat loads,
5. critical/current temperature - the operating margins should be determined either by individually raising the current in each coil until a predetermined voltage is measured or by individually raising the inlet helium temperature at constant current to reach the normal transition point; this is the determination of the magnet load line.

These kind of tests could deliver results which are needed for the construction of NET TF-coils. Information on the last two items can also be obtained from simple short sample tests.

10.1.2 Test Procedure

In general, testing is to be accomplished by increasing operating parameters continuously. At each step sufficient data will be taken and critical measured parameters will be compared to the corresponding values predicted by the coil supplier.

The test procedure itself can be divided into three phases:

- I Initial Checkouts
- II Single Coil Tests
- III Full Array Tests

These three testing phases are described in more detail below. This has to be taken as a first base for future discussions.

I. Initial Checkouts

A. Room Temperature

1. Coil characterization
2. Connection - Sensors, Coil, Facility
3. Facility Systems
4. Pumpdown
5. Safety and Interlocks
6. Coil Self and Mutual Inductances
7. Leak Rates

B. Slow Cooldown

1. Facility Systems, Coils, Test Stand

C. Low Current Checks

1. Facility Systems
2. Instrumentation Calibration
3. Data Acquisition
4. Field Direction (of each coil)
5. Leads
6. Coils (resistances, inductance, insulation)
7. Exercise Interlocks
8. Exercise Heaters
9. Exercise Dump Circuits - Manual, Simulated Automatic
10. Set Voltage Tap Compensations

II Single Coil Tests (to be performed with all three coils separately)

A. Single Coil Test (coil 1) to $I = 1.0$ ($I = \frac{\text{operating current}}{\text{design current}}$)

1. Raise I to $1/4$ in steps, and reduce to $I = 0$ using power supply reversed voltage.
2. Exercise manual dump at $I = 1/4$.
3. Prove automatic dump, using moderate heater power and increased circuit sensitivity.
4. Raise I to 1.0 in steps, repeating 3 at $I = 0.5, 0.7, 0.8, 0.9, 1.0$

B. Repeat (A) with coil 2 as the test coil, except dump levels in 4 are $I = 0.5, 0.8, 1.0$.

C. Repeat (B) with coil 3 as the test coil.

III Full Array Tests

- A. Repeat II with all three coils simultaneously
- B. Measurement of critical current of NET model coils by heating helium flow
- C. AC-loss measurements
- D. Mechanical Experiments.

10.1.3 Instrumentation and Quench Detection

The minimum instrumentation requirements for the NET TF-coil described in this Section is of preliminary nature. It is shown in Figure 10.1.1 and is partly based on the experience gained with the Swiss and EU LCT-coils.

At least the inlet and outlet temperatures and the total mass flow, especially for cooldown and warmup, should be measured. For helium density and mass flow calculation, the helium pressure in front of the flowmeter has to be measured. The differential temperature of the coils will be used to control the inlet temperature by mixing warm and cold helium. In normal operation mode the outlet temperature of each cooling channel should be measured in addition to the inlet conditions and mass flow. On the 12T points two hall generators and Pick-Up-Coils will be installed to measure the magnetic and pulse field. In regions where stress concentrations were calculated, strain gauge Rosettes should be used to check the maximum stresses and direction. Displacement transducer should be installed in order to measure the movement of the winding, and also the overall deformation of the coil. A list of minimum required sensors is given in tables 10.1.1 and 10.1.2

Sensor types. The calibrated *carbon glass or carbon temperature* sensors could be used for a highly reproducible temperature measurement in high magnetic field in the temperature range $4 \div 10$ K. For cooldown and warmup ($300 \div 4$ K) a cryogenic linear temperature sensor CLTS-2 can be used. This is a small surface-thermometer gauge consisting of grids laminated into a glassfiber reinforced epoxy resin matrix. This sensor has a linear resistance vs. temperature characteristic and can be used together with commercial resistance - current transducers.

For mass flow measurement, an *orifice or venturi flowmeter* measuring the differential pressure over the orifice at $4 \div 300$ K helium temperature can be used. If the flowmeter dimension are in good agreement with the DIN 1952 (Deutsche Industrie-Normen) standards, then the calibration will not be necessary.

Hall generators are available for low temperature and high magnetic field. They were used in the Swiss and EU LCT coils.

Quench Detection. The high energy, stored in the magnet requires a very quick detection of normal conducting zones. The only way to reach this goal is by measuring the ohmic voltage drop across each pancake. For compensating of the inductive voltage there are two methods for choice.

The first possibility is a bridge circuit. One branch of the bridge is a dual in hand wound double pancake, the other branch consists of two resistors. For each double pancake a separate quench detector is necessary. This system was used for the EU-LCT coil in the IFSMTF and has demonstrated, that it is the most sensitive quench detection system in this experiment. Unfortunately the system in his actual state was disturbed dumps of an adjacent coil.

The second method uses an insulated compensating wire, either integrated into the superconducting cable or fixed on his outside. Superconductor and compensating wire are connected at one end. Balancing is unnecessary and for the whole magnet only one quench detector is needed. Compensating wires are insensitive to field gradients and displacement of the winding. Up to now there are no experiences of such a quench detection system. Therefore both systems should be installed in the model coil and tested in order to obtain a reliable system for the NET-coils.

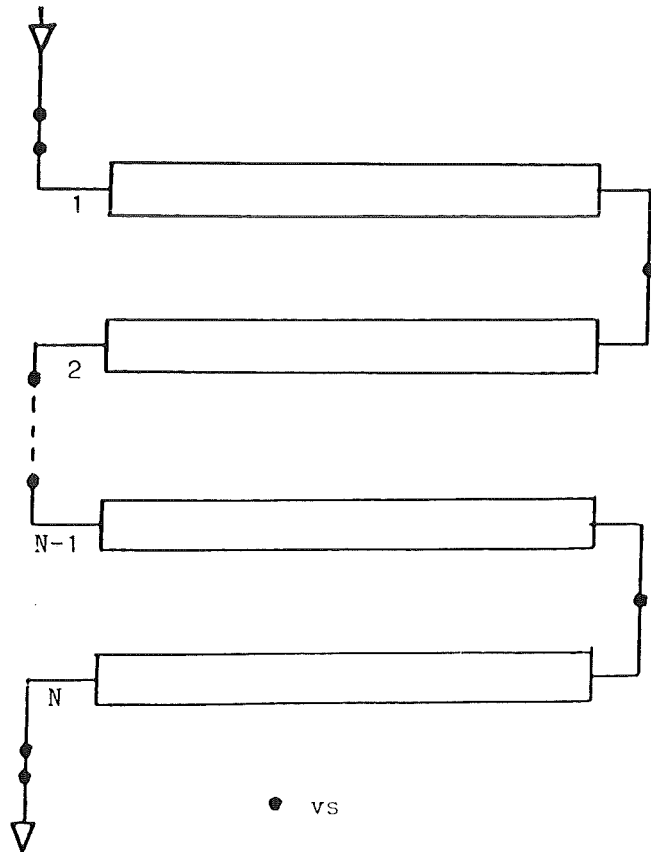
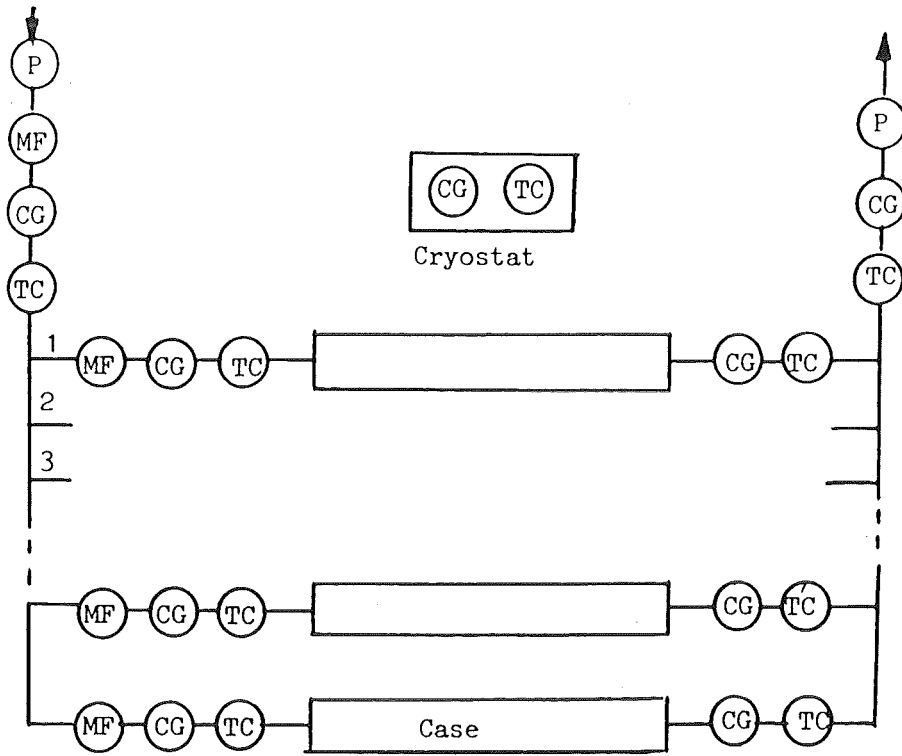


Figure 10.1.1 Scheme of TF model coil instrumentation

Symbol	Description
VS	Voltage sense wire
TC	Temperature Sensor 300-20K
CG	Temperature Sensor 4-40K
SG	Straingauge (Rosettes)
HG	Hall generator
P	Pressure transmitter
MF	Flowmeter

Table 10.1.1 - Sensor nomenclature

Sensor	Qt.	Physical units	
		Full scale	Resolution (\pm)
a) <u>winding</u>			
VS	N+3	250 mV	1 mV
TC	2N+2	300 \div 20 K	0.25 K at 300K
CG	2N+2	40 \div 4 K	0.01 K at 4 K
P	2	0 \div 10 bar	0.1 bar
MF	1	4N gs^{-1} at 5000 Pa	0.33 gs^{-1} at max flow
MF	N	4 gs^{-1} at 5000 Pa	0.015 gs^{-1} at max flow
b) <u>case</u>			
SG		< 0.01	10 ⁶
HG	4	0 \div 12 T	0.1 T
MF	1	\approx 20 g/sec	0.33 gs^{-1} at max flow
CG	2N+2	40 \div 4 K	0.01 K at 4 K
TC	2N+2	300 \div 20 K	0.025 K at 300 K

Table 10.1.2 - List of minimum instrumentation requirements

11. Further Use of TOSKA

11.1 Magnet Test Facility

The TOSKA-facility existing now has served for the domestic LCT-test in 1984 and is now modified in order to allow a test of a pulsed model coil (POLO, M4) of about 3m diameter. This is part of the NET development programme for poloidal field coils.

Further use of TOSKA is to modify the facility in order to perform the TF model coil test. How the facility would look like is discussed in previous chapters. This TOSKA-Upgrade facility would mainly allow to test:

- NET relevant TF model coils,
- NET relevant PF model coils, but with certain restrictions
- 1.8 K high field tests of the NbTi LCT coils, and
- other magnets.

The 1.8 K high field tests of the NbTi LCT coils can lead to a backup solution for NET. Such a solution is proposed in Ref. [11.1]. NbTi cables cooled by internal flow of superfluid helium are considered for fusion reactor TF coils with 11 T peak magnetic induction. The He II flow is driven by fountain effect pumps, which are driven by the thermal load absorbed in the coil (self-driven FEP). It is shown in [11.1] that the NET specifications with 11 T peak field at a 16 kA cable can be met with basically the same set-up as the EU-LCT conductor.

Beside these considerations to use TOSKA as a magnet test stand, a proposal was made to use TOSKA as a test stand for nuclear components of NET where LCT coils deliver only the background field.

11.2 Blanket Test Facility

Forces and stresses in the blanket structure caused by electric currents induced during plasma disruptions are very difficult to calculate due to the complicated geometries. Three-dimensional models have to be developed and qualified by comparing with suitable experimental results. In view of the uncertainties involved in such models, it is necessary to test real blanket geometries (ceramic

blankets, liquid metal blankets) under realistic conditions. The values to be determined are:

- forces to the supporting structure,
- stresses in blanket and first wall,
- liquid metal pressure (for liquid breeder blankets only).

Test in real geometries including boundary conditions have to be very similar in order to allow the application of computer codes for predicting the blanket behaviour in NET.

As a part of the test program for liquid breeder blankets a modification of the existing TOSKA facility was proposed. This modified facility allows blanket testing in nearly half scale with a magnetic field strength of 4 - 5 T. If a disruption simulation coil is added, disruption tests for all blanket concepts can be performed in this facility. This arrangement can be seen in Fig. 11.2-1. The figure shows the arrangement using the existing D-shaped LCT-magnets. A similar test is possible in the solenoid configurations discussed in this report, but then the warm bore is smaller (~ 2 m), but higher fields can be reached if necessary. The disruption coil has to simulate the fast decay of the electric current in the plasma. A suitable power supply and a very fast acting switch are available from the magnet development program. The power circuit for the disruption simulation coil is shown in Fig. 11.2-2.

The design parameter of the proposed facility are:

- magnetic field strength 4-5 T,
- maximum height of blanket segment 3 m
(scaling factor 0.4),
- maximum current in simulation coil 30 kA,
- time constant for current decay 1-100 ms
(resulting in $(dI/dt)_{t=0} = 30 \cdot 10^6 \text{A/s} \div 0.3 \cdot 10^6 \text{A/s}$),
- maximum change in magnetic field strength as caused by the current in the disruption simulation coil (0.5 m distance) $(dB/dt)_{\text{max}} = 12 \text{T/s}$.

Scoping calculation have shown, that in the case of a selfcooled liquid metal breeder blanket, forces up to 20 kN are caused by the current decay in the disruption coil.

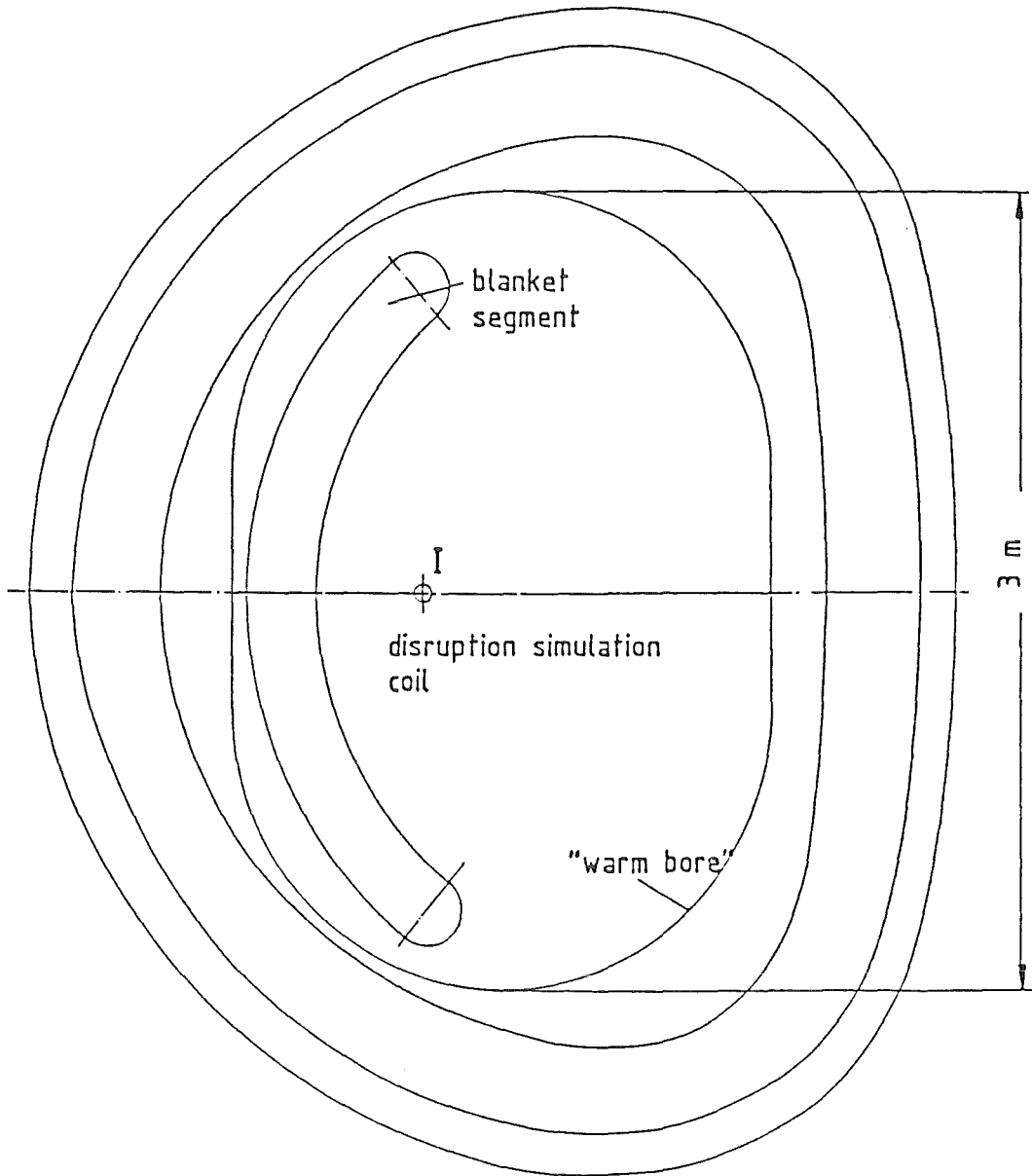
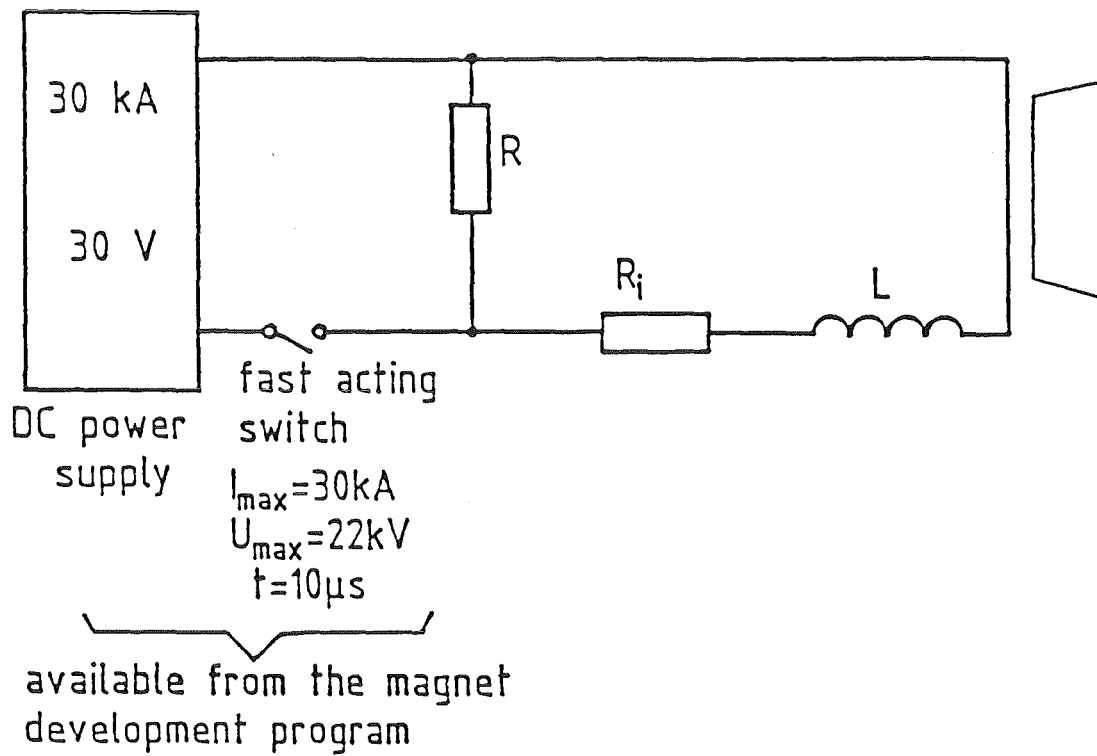


Fig. 11.2-1: Disruption Test in the modified TOSKA Test Facility



Example:

$$L = 0.5 \cdot 10^{-3} \text{ H}$$

$$R_i = 0.5 \cdot 10^{-3} \Omega$$

$$0.5 \cdot 10^{-2} \Omega \leq R \leq 0.5 \Omega$$

$$100 \text{ ms} \leq T_{\text{decay}} \leq 1 \text{ ms}$$

$$0.3 \cdot 10^{-6} \frac{\text{A}}{\text{S}} \leq \frac{dI}{dt} \leq 30 \cdot 10^{-6} \frac{\text{A}}{\text{S}}$$

Fig. 11.2-2: Power Circuit for Disruption Simulation Coil

11.3 Non Nuclear Component Test Stand

Another possible use of TOSKA is as a general test facility for big non nuclear components, especially for such with rotating or moving parts e.g. turbomolecular pumps as proposed for NET [11.2] If two LCT coils would stand upright in parallel as shown in Fig. 11.3-1 then a usable volume of approximately 1 m x 3 m x 2 m would be available with fields in the order of 5 T. In the case of the solenoids, discussed in Chapt. 4, the warm bore would have a smaller diameter but the attainable fields were higher (8 - 10 T). A study about the general use of such a magnet test facility should be envisaged.

References to Chapt. 11:

- [11.1] A. Hofmann et al., Considerations on Magnet Design based on forced flow of He II in internally cooled Cables, Contribution to the INTOR-Report (Nov. 1986).
- [11.2] J. Hanauer et al., KfK, Nov. 1985, unpublished.

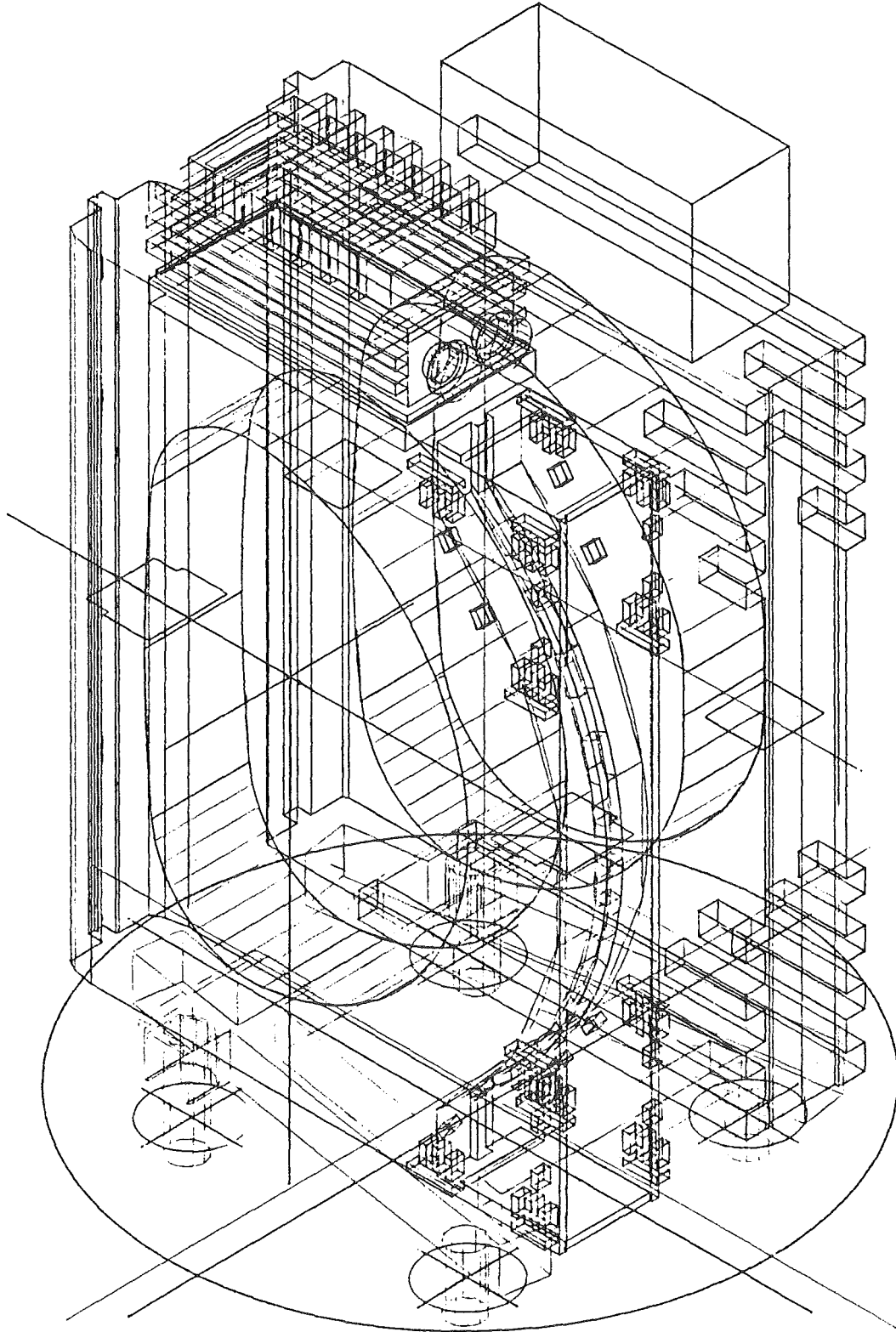


Fig. 11.3-1: CAD View of Blanket Test Stand using LCT Coils.

12. Other Possibilities for Testing

12.1 Solitary OH-Model Coil Test

Beside the possibility of testing the OH model coil in the Cluster Test Facility or in the Solenoid Test Facility a solitary test should be investigated. One reason is the necessity of a 50 kA power supply, another the difficulty to apply a $dB/dt = 3T/s$ in the test facilities discussed above.

A study about the solitary OH-Model Coil Test is going on at Cadarache, France. Therefore, no further discussion will be given here in this study.

12.2 Pancake Tests in SULTAN III

12.2.1 Introduction

The major goal of this very preliminary study is to investigate possibilities of pancake testing in the proposal SULTAN III split coil system.[12.2.13]

With the installation of a split coil system, where the 8T section of SULTAN II will be replaced by two A-15 coils the facility can be used for NET-conductor prototype and acceptance tests.

In the SULTAN III a gap as shown in Figure 12.2.1 between the background coils could be envisaged. The middle flange can be designed in such a way that a plate of 8cm thickness (containing a vertical hole of 8cm in diameter for the conductor samples) can be replaced by a double pancake made of a NET-conductor (see Figure 12.2.2). Such a solution would be most flexible if SULTAN III has to be used for conductor and pancake tests.

The sections in this chapter are mainly based on the assumption to test only NET-TF conductors and pancakes, although DC-tests on short samples and pancakes of an OH-conductor could be performed too. But OH-pancake tests would require an additional 50 kA power supply.

12.2.2 Assumptions and Calculations

a) Magnetic field

Magnetic field calculations were performed assuming the geometrical data as shown in Figure 12.2.1. Coil currents are given in Table 12.2.1 [12.2.2]

Figure 12.2.3 shows the field distribution in the split coil gap. It can be seen that the maximum field is about 11T. However, if the sample is made (as suggested in the SULTAN II proposal) of two parallel conductors that produce a self field of 0.4 T, the maximum total field experienced by the conductor is 11.4T.

Replacing of the 6cm plate in the middle flange by a double pancake with 2×9 windings of NET conductor would enhance the gap of the split coil system by 4cm (see Figure 12.2.4). As a consequence the magnetic field in the center of the split coil system would decrease by ~ 0.4 T. However, this lower field will be compensated by the self field of the pancake which is 0.8T assuming 17kA operating current (see Figure 12.2.5). This has to be compared with 0.4T of the conductor sample.

b) Forces

The forces acting on each of the seven coils has been calculated using the local value of the field and the current. Each coil has been divided into 256 elements and the field calculated in the middle point of each element when all the coils are energized. The total forces FX and FZ acting on each coil are schematically reported in figure 12.2.6. Since the X axis is the vertical one there are no net forces on the coils in the Y direction because of symmetry.

c) Strain Effects

Due to high temperature differences during cooldown after heat treatment of the sc cable, fabrication of the compound conductor, coil manufacturing and coil cooldown to operating temperature mechanical strain and stress will occur because of the different expansion coefficients of the various conductor components. To estimate the mechanical behaviour of such a conductor it is important to calculate the contributions of the different effects in the correct sequence:

- cooldown of the Rutherford cable from heat treatment to room temperature
- wind off of the Rutherford cable from the heat treatment drum
- soldering of flat cable with stabilizing parts
- welding of cable into steel jacket
- coil winding
- coil cooldown from room temperature to 4K

For the SIN-NET Prototype cable these estimations were performed [12.2.4]. Based on these calculations one can summarize the results one obtains for the various test arrangement as follows.

The conductor of the NET-TF coil has a minimum bending radius of 2m. In the SULTAN III pancake test one has to assume a minimum bending radius of 0.8m. The I_c - degradation for these two bending radii with the SIN NET conductor have been checked:

- | | |
|-------------------------|-----------------|
| (a) NET TF-coil | 20% degradation |
| (b) SULTAN-Pancake Test | 30% degradation |

This has to be compared with the values one has to expect in TOSKA-Upgrade with minimum bending radius of 1 to 1.2m:

I_c - degradation of 25% .

12.2.3 Budget (in kSFr.)

The following budget figures are based on the assumption that three times 500m of conductor would be fabricated for pancake tests only. This is the minimum required length to develop conductor manufacturing process. A double pancake for tests in SULTAN-III would only need 150m of conductor. A combination of pancake tests in SULTAN-III and model coil tests in TOSKA-Upgrade would decrease this investment costs to 2 Mio SFr. (conductor, winding equipment and 20kA power supply already included in TOSKA-Upgrade budget).

12.2.3.1 Double Pancakes

	1 double Pancake	3 double Pancakes	
Conductor	1000	3000	500m each 2000 SFr./m
Winding	300	900	winding at the same factory
Winding equip.	2000	2000	
Instrumentation	150	450	
Total	3450	6350	

12.2.3.2 Facility

Pancake installation system	300 kSFr.
Data Acquisition System	100 kSFr.
20 kA Power supply	400 kSFr.
20 kA Current leads	200 kSFr.
<u>TOTAL</u>	<u>1'000 kSFr.</u>

12.2.3.3 Additional Costs

In the above mentioned figures the following items are not included:

- conductor development (joints, bending etc.)
- investment for AC-loss measurements
 - (possible AC-loss measurements of the pancake in the high field and low field region have to be investigated in more detail).
- investment for mechanical experiments
 - (Although it is difficult to simulate the actual operating stress/stream of the pancake, detailed analysis of possible application, external, mechanical loads would be worthwhile to be investigated).

12.2.3.4 Manpower Requirements (MY)

	1989	1990	1991	1992	Total
<u>1. Pancake Manufacture</u>					
a) Professionals	6 × 1	6 × 1			12
b) Support Staff	6 × 1	6 × 1			12
<u>2. Facility</u>					
<u>2.1 Pancake Installation</u>					
a) Professionals			5 × 0.5	3 × 0.5	4
b) Support Staff			9 × 0.5	6 × 0.5	7.5
<u>2.2 Operation</u>					
a) Professionals			2 × 0.5	2 × 0.5	2
b) Support Staff			4 × 0.5	4 × 0.5	4
<u>3. Pancake Test</u>					
a) Professionals			4 × 0.5	2 × 0.5	3
b) Support Staff			8 × 0.5	4 × 0.5	6
<u>4. Result Evaluation</u>					
a) Professionals			2 × 0.5	4 × 0.5	3
b) Support Staff			2 × 0.5	4 × 0.5	3
TOTAL	12	12	18	14.5	56.5

12.2.4 Time Schedule

	1987	1988	1989	1990	1991	1992	1993
Design	-----						
Conductor fabr. 9T coil							
-strands	-----						
-composite cond.		-----					
Coil fabrication		-----					
6T-coil splitting		-----					
Assembly			-----				
Test				-----			
Conductor Tests (NET)				----->			
Short Sample				----->			
NET Cond. Fabr.		-----					
Winding Pancake				1 2 3			
Installation Pancake					1. ----- 2. ----- 3. -----		
Test Pancake					1. ----- 2. ----- 3. -----		
Result Evaluation					1. ----- 2. ----- 3. -----		

Coil No	I[kA]	ℓ [cm]	r_i [cm]	r_e [cm]	δ_C [cm]	δ_{PC} [cm]
1	4.9	66	65.6	99.6	20	24
2	12	67	54.0	64.0	16	20
3	6	35	30.0	50.2	12	16
Pancake	17	7.6	80.0	104.5	-	-

Table 1 - Currents and Geometrical Data of Split-Coil-System

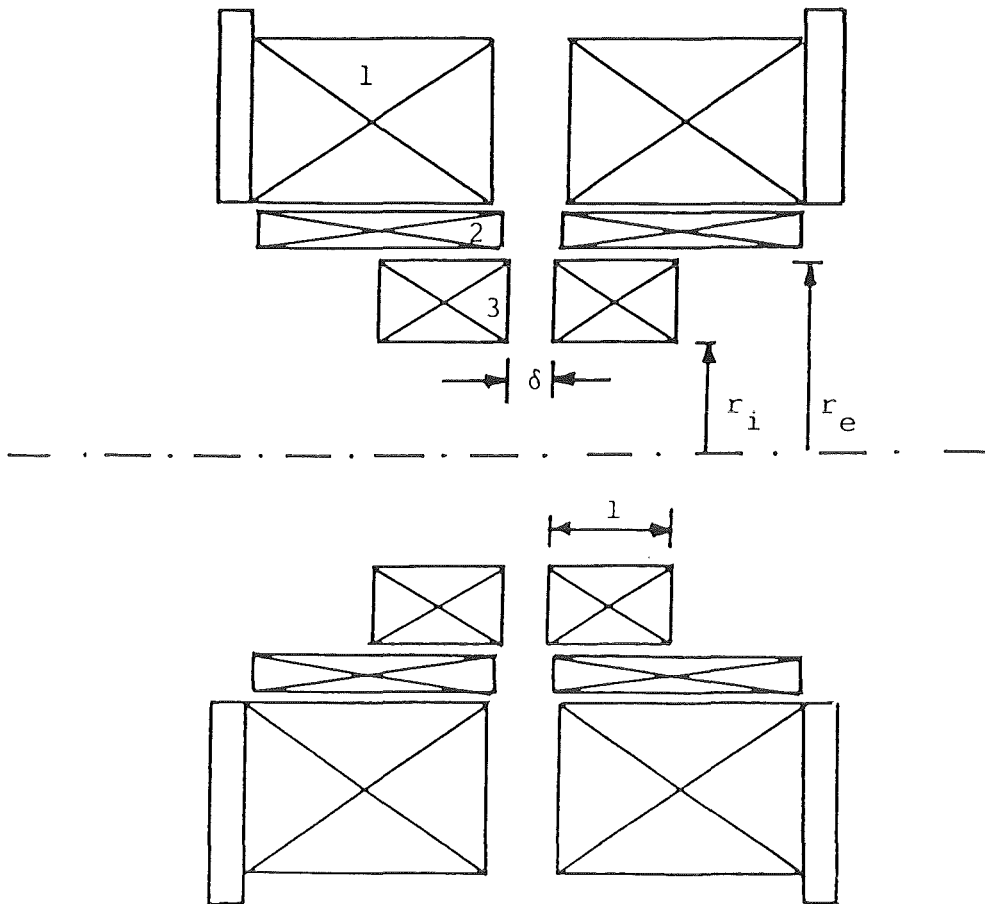


Figure 12.2.1

Magnet System for NET
Conductor and Pancake-Test

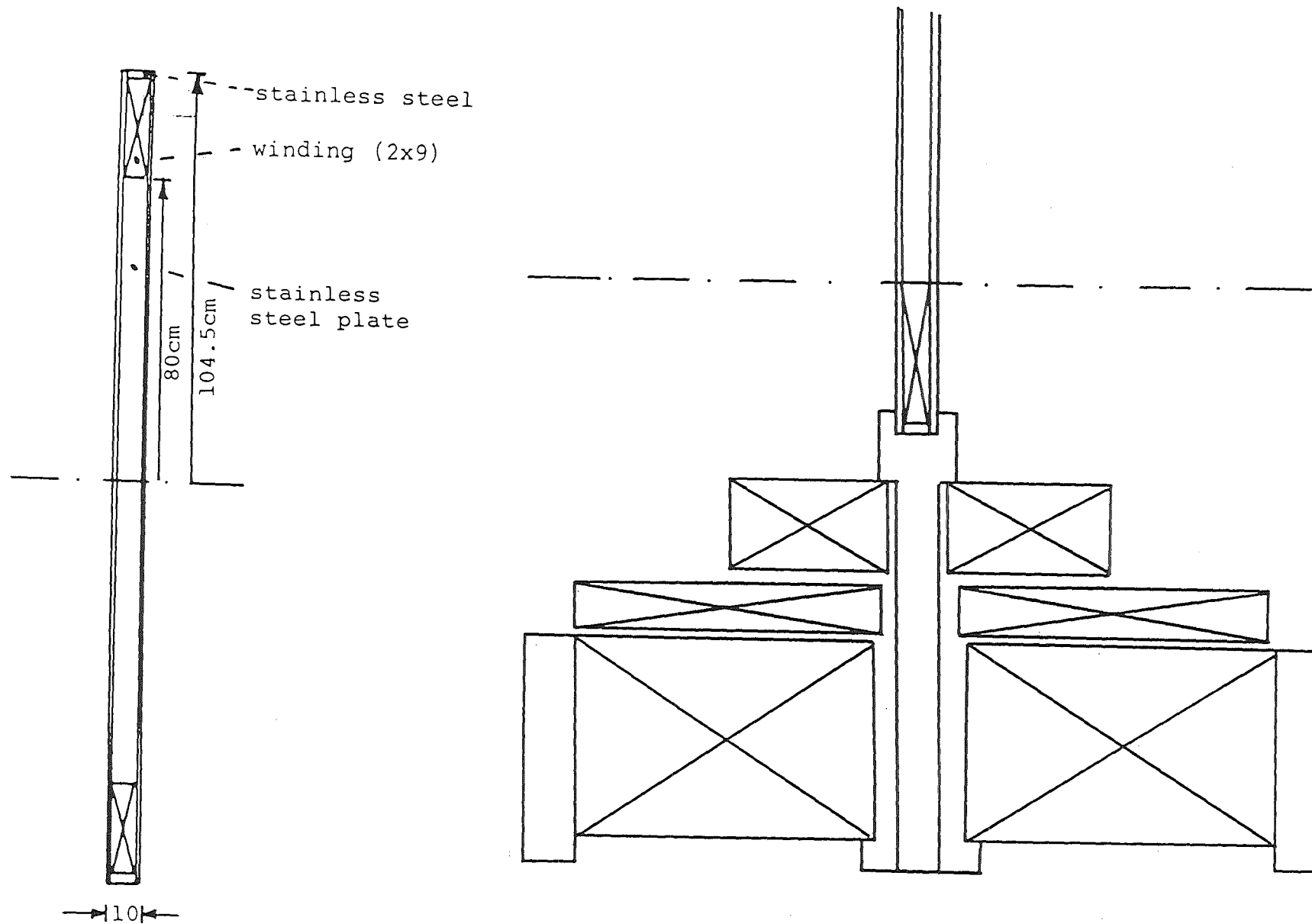


Figure 12.2.2 - NET - Test Pancake

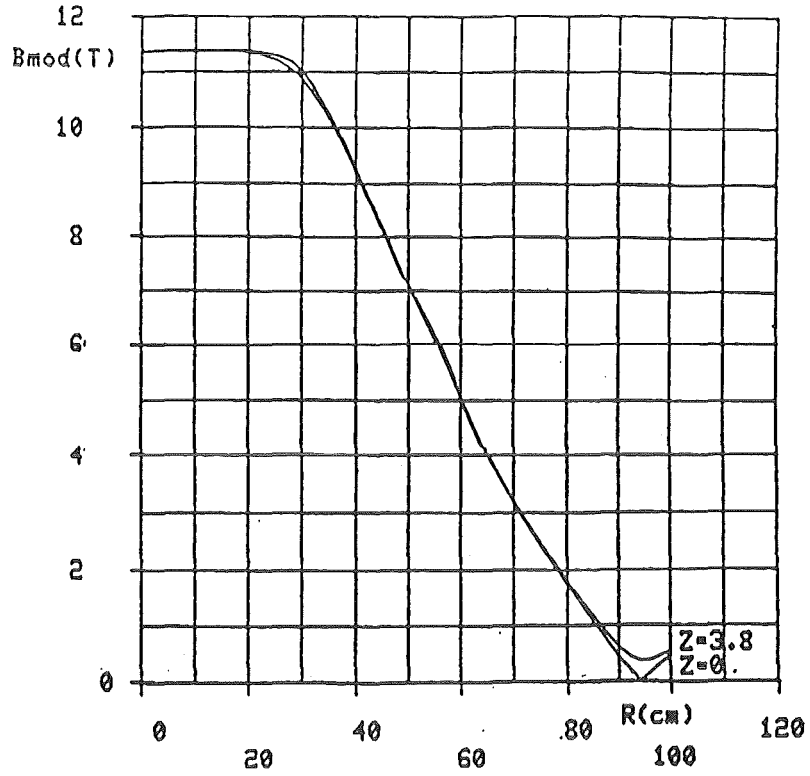


Figure 12.2.3.1 - Field distribution in the GAP

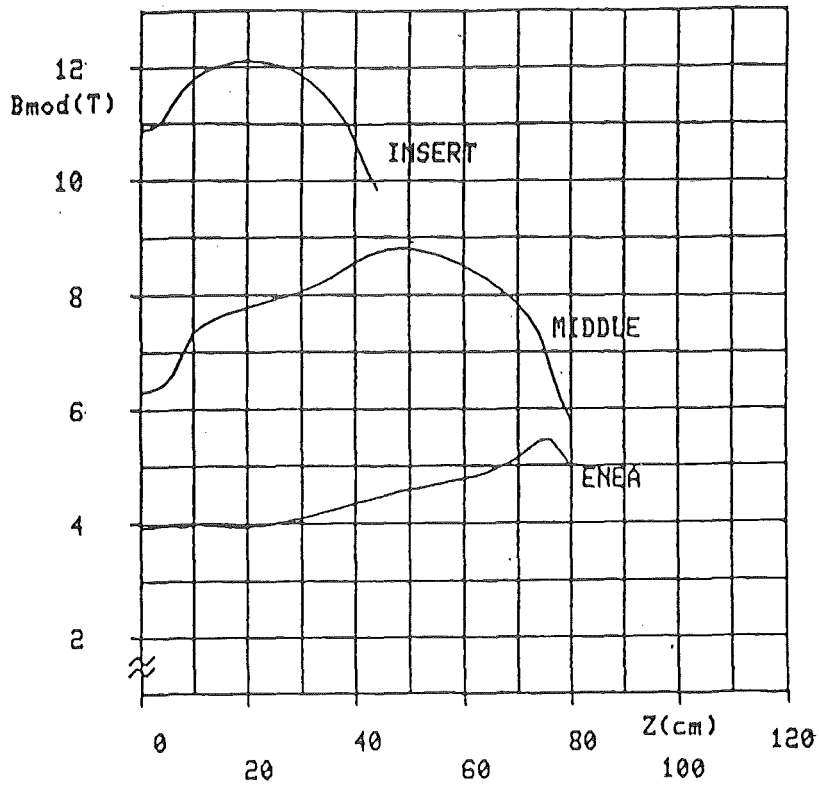


Figure 12.2.3.2 - Field distribution on the external surface of the three coils

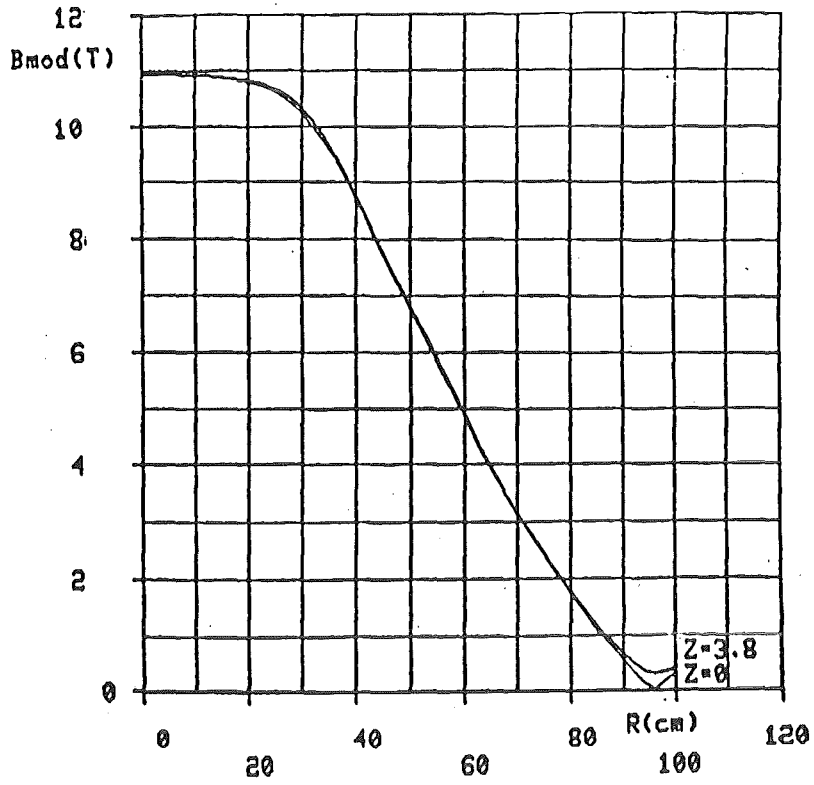


Figure 12.2.4.1 - Field distribution in the GAP

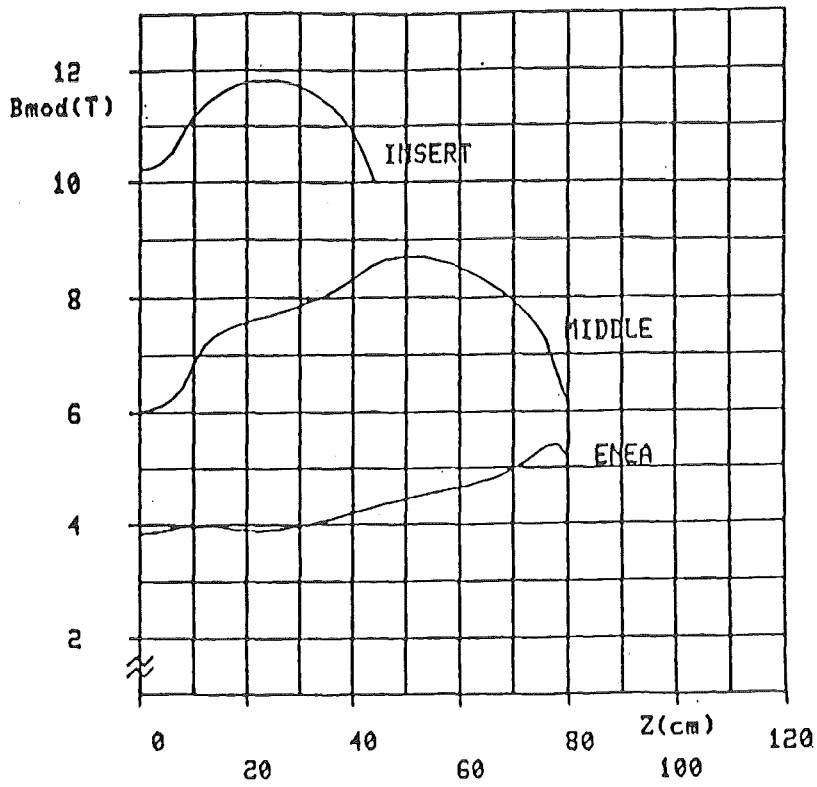


Figure 12.2.4.2 Field distribution on the internal surface of the three coils

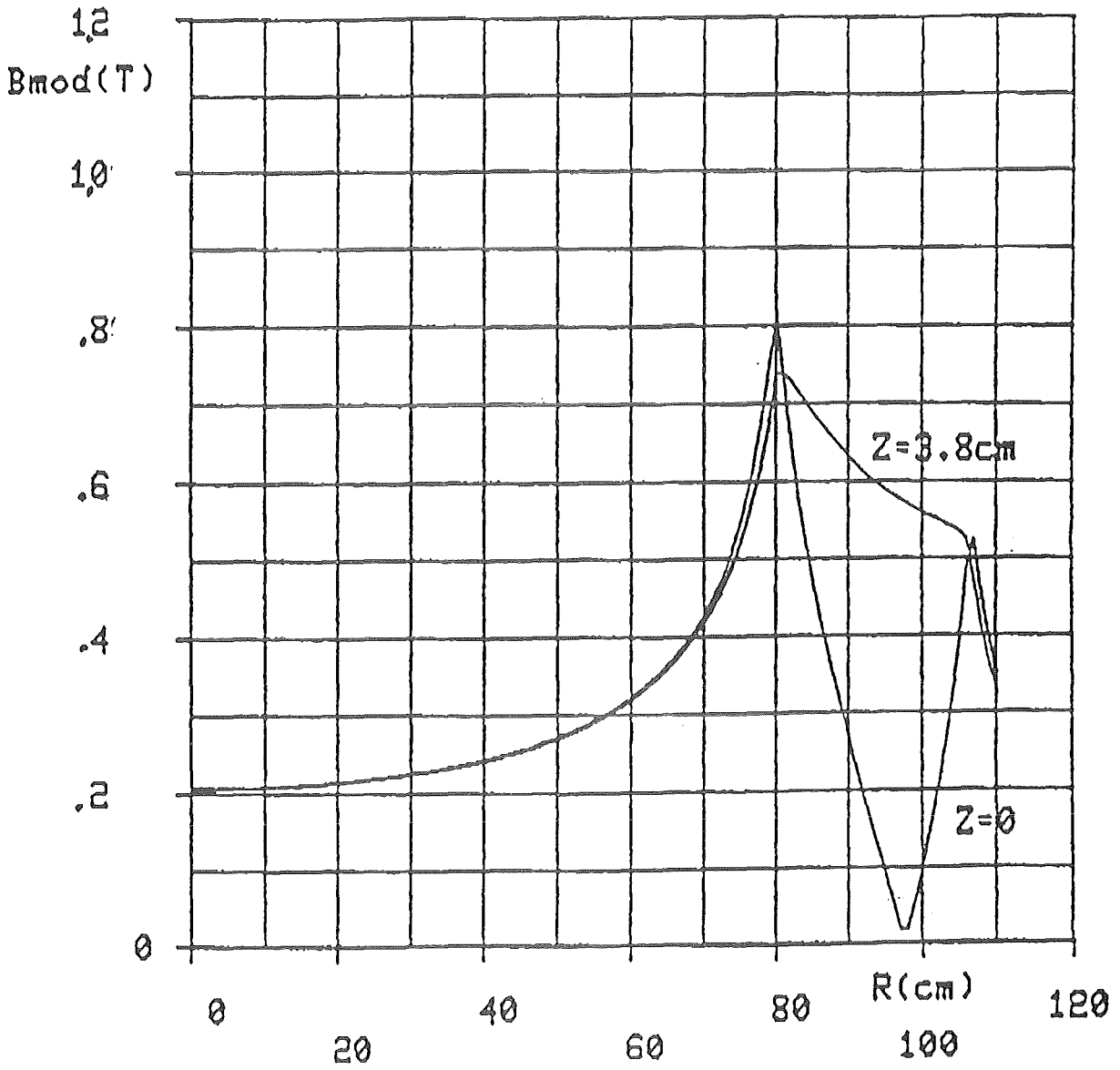


Figure 12.2.5 Self Field of the Pancake (I=17 kA)

Coil	Force	F_x	F_z
1		108.3	2450
2		54.3	1298
3		35.9	160
Pancake		-400	-

Table 2 - Forces acting on the different coils

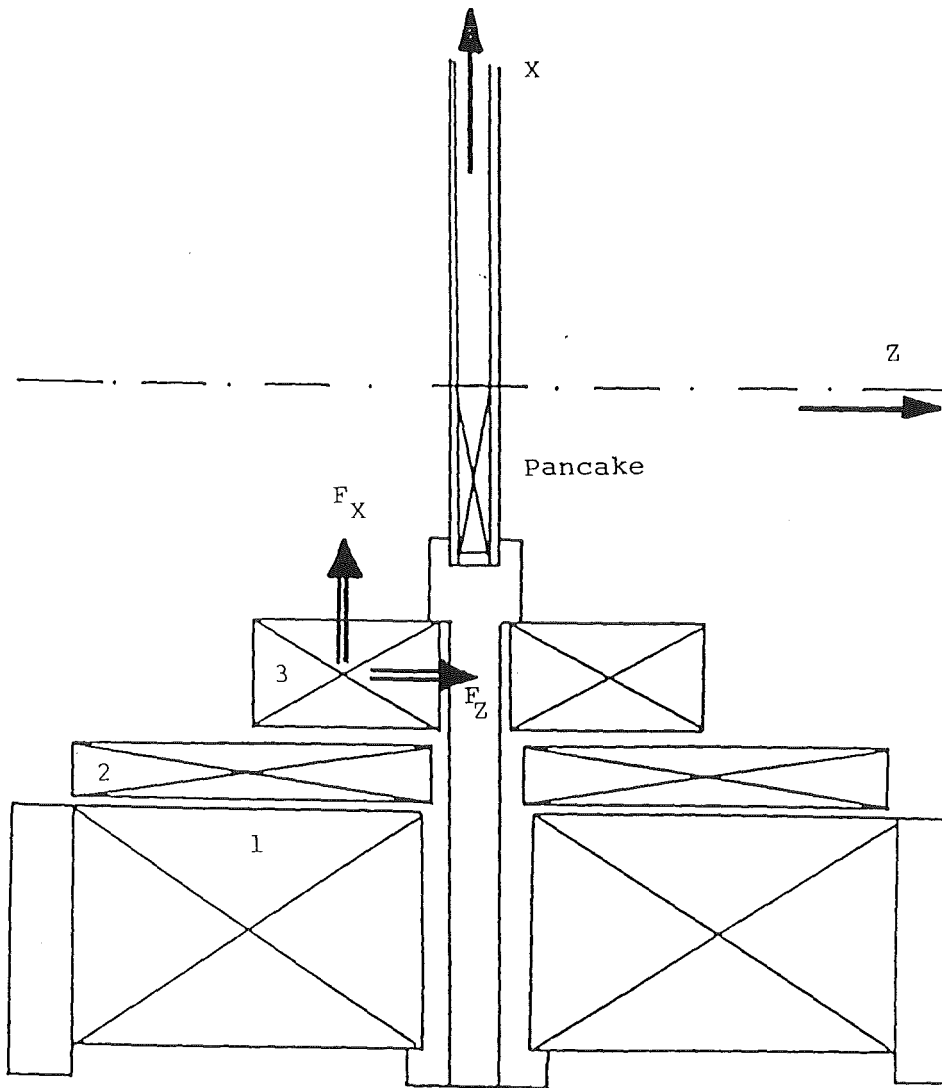


Figure 12.2.6 - Forces (in tons) acting on the different coils

12.2.5 References

- [12.2.1] J.D.Elen, N.Sacchetti, G.Vécsey
Project Proposal; 12T Split Coils for the SULTAN Test Facility,
August 25, 1986
- [12.2.2] G.Pasotti, ENEA internal note, July 2, 1987
- [12.2.3] G.Pasotti, ENEA internal note, August 1987
- [12.2.4] C.U.Wassermann, Mechanische Spannungen und Dehnungen im SIN-NET
Leiter während der Herstellung und Abkühlung, December 1986 (unpublished).
- [12.2.5] J.D.Elen, N.Sacchetti, P.Weymuth,
Feasibility of Pancake Tests in SULTAN-III, May 11, 1987 (unpublished).

13. Technical Comparison of the Cluster and Solenoid Test Facilities

Table 13.1 (identical with Table 3.6-1) contains the main technical data of three cluster configurations C3, C5, and C6. The main difference is seen in bending radius and current:

- C3 has 1.2m and 22 kA,
- C5 has 1.0m and 16 kA,
- C6 has 1.0m and 22 kA.

C5 operates at the NET nominal current, but has a winding length which is not reconcilable with conductor lengths foreseen for the model coil test. In order to keep conductor lengths relatively low the current is risen to 22 kA, which is about 5% below the critical current of the KfK-NET conductor at 12T and 4.2 K, if a degradation of 35% due to bending strain and handling is taken into account.

The Cluster Test Facility is foreseen mainly for the test of TF-conductors. But the OH conductor can also be tested to a certain extent by replacing the TF-model test coils by an OH-model test coil. The main restrictions for that case are given by the limits on dB/dt for the LCT coils.

The cluster configuration C6 is better than C3 and C5 with respect to overall requirements of the model coils, the LCT-background field coils, and the modification amount of the TOSKA facility. Therefore this configuration is the favoured Cluster Test Configuration.

Table 13.1: Comparison of Test Coil Characteristics for three different Versions of the Cluster Test Facility.

Winding pack characteristics	Unit	C3		C5		C6	
		KfK	SULTAN	KfK	SULTAN	KfK	SULTAN
Model coil current	kA	22	22	16	16	22	22
Current density	kA/cm ²	3.308	2.958	2.406	2.151	3.308	2.958
Kind of winding		double		pancake		winding	
Number of pancakes		2 x 3	2 x 5/2 x 4	2 x 4	2 x 5	2 x 3	2 x 5
Number of layers/pancake		30	10/10	50	33	34	22
Total number of turns		180	100/80	400	330	204	220
Inner radius, R _i	m	1.2	1.2	1.0	1.0	1.0	1.0
Axial winding width, DA	m	0.228	0.277/0.222	0.304	0.277	0.228	0.277
Radial winding thickness, DR	m	0.525	0.268/0.268	0.875	0.884	0.595	0.5896
Average winding radius, R _{av}	m	1.462	1.334/1.602	1.4375	1.442	1.2975	1.2948
Average turn length	m	9.189	8.382/10.06	9.05	9.06	8.15	8.14
Average pancake conductor length (= cooling length)	m	276	~ 200	451	290	277	179
Total conductor length *	m	1654	838/805	3613	2990	1664	1790
Winding cross section	m ²	0.120	0.0744/0.059	0.266	0.245	0.13566	0.16332
Winding volume	m ³	1.1	1.22	2.402	2.219	1.11	1.33
Estimated winding weight (ρ ~ 7 t/m ³)	t	7.7	8.54	16.8	15.5	7.8	9.3
Ampère-meters	10 ⁶ Am	36.4	18.44/17.71	57.92	47.84	36.608	39.38
Total coil current	10 ⁶ A	3.96	2.2/1.76	6.4	5.28	4.488	4.84
Stored Self Energy	MJ					34	38
B _{max}	T	11.5	11.5	11.7	11.5	12.1	12.0

* not including spare lengths for fabrication and joints (~ 10 %)

Table 13.2 (identical with Table 4.4-1) contains the main technical data of three different solenoid test configurations. There is a fundamental difference between cluster and solenoid configuration:

- in the cluster TF-winding packs and PF-winding packs would be tested in sequence,
- in the solenoid TF-winding packs and PF-winding packs must be tested simultaneously in one arrangement.

This means that all 3 conductors (2 TF + 1 OH) have to be available at approximately the same time in order to construct the solenoid test facility.

Again, the main difference is seen in bending radius and current:

- S1 has 1.2m and 22 kA (TF) and 50 kA (PF)
- S2 has 1.0m and 16 kA (TF) and 40 kA (PF)
- S3 has 1.0m and 22 kA (TF) and 50 kA (PF).

The configuration S2 is eliminated due to the very high conductor length necessary for the production of the model coils. S3 is the best suited solenoid test configuration and therefore the favoured one.

In the following only the cluster C6 and solenoid S3 configuration are compared. Table 13.3 contains a qualitative comparison of both configurations with respect to modifications of the already existing TOSKA-facility, and installation and maintenance work.

The modifications of the existing facility are moderate if the solenoid solution is chosen. If the cluster solution is chosen, the expenditure is higher for the LN₂-shield, support structure, and the cooling system.

If all considered conductors (2TF and 1PF) should be tested in one facility, then a 50 kA power supply is needed in any case.

Table 13.2: Comparison of the different Solenoid Test Configurations.

Configuration		S1			S2			S3		
Winding pack characteristics	Unit	KfK	OH	SULTAN	KfK	OH	SULTAN	KfK	OH	SULTAN
Model coil current	kA	22	50	22	16	40	16	22	50	22
Current density	kA/cm ²	3.308	3.003	2.958	2.406	2.435	2.18	3.308	3.003	2.958
Kind of winding		double	pancake	winding	double	pancake	winding	double	pancake	winding
Number of pancakes		2 x 4	2 x 5	2 x 6	2 x 6	2 x 4	2 x 10	2 x 5	2 x 4	2 x 7
Number of layers/pancake		28	21	19	40	21	26	30	16	20
Total number of turns		224	210	228	480	168	520	300	128	280
Inner radius, R _i	m	1.2	1.2	1.2	1.0	1.0	1.0	1.0	1.0	1.0
Axial winding width, DA	m	0.304	0.5	0.3324	0.456	0.4	0.554	0.38	0.4	0.3878
Radial winding thickness, DR	m	0.49	0.6993	0.5092	0.700	0.699	0.696	0.525	0.5328	0.536
Average winding radius, R _{av}	m	1.445	1.55	1.455	1.350	1.349	1.348	1.2625	1.2664	1.268
Average turn length	m	9.08	9.74	9.14	8.48	8.48	8.47	7.94	7.98	7.97
Average pancake conductor length (= cooling length)	m	255	205	174	339	178	220	238	127	160
Total conductor length *	m	2034	2045	2084	4070	1424	4400	2380	1019	2231
Winding cross section	m ²	0.149	0.35	0.17	0.32	0.28	0.39	0.2	0.213	0.208
Winding volume	m ³	1.353	3.405	1.547	2.71	2.37	3.30	1.584	1.7	1.66
Estimated winding weight (ρ ~ 7 t/m ³)	t	9.5	24	11	18.97	16.61	23.12	11.1	11.9	11.6
Ampère-meters	10 ⁶ Am	45	103	46	65	57	71	53	51	49
Total coil current	10 ⁶ A	4.93	10.5	5.02	7.68	6.72	8.32	6.6	6.4	6.16
Stored Self-Energy	10 ⁶ J	49	200	50				67	40	58
B _{max}	T	11.65	12.38	11.5	11.65	12.25	11.65	12.27	11.62	11.54

* not including spare lengths for fabrication and joints (~ 10 %)

Table 13.3: Qualitative Comparison of Solenoid and Cluster Configuration concerning Facility Modification, Installation and Maintenance

	Solenoid S3 KfK/OH/Sultan	Cluster C6/3.5 K KfK/Sultan (OH)
<u>Modifications:</u> Vacuum vessel LN ₂ -shield	moderate negligible	moderate must be enlarged
Transfer lines Heat Exchanger Pump	Transfer lines to the new refrigerator	Transfer lines to the new refrigerator
Current leads (30 kA power supply available)	3 x 22 kA 2 x 50 kA	3 x 22 kA (2 x 50 kA) 3 x 13 kA (3 x 13 kA)
Support structure	simple	difficult and expensive
Distance between winding and LN ₂ - shield	sufficient	sufficient
Installation	possible without any larger modification (40 to)	more extensive
Installation of a pulse coil	possible	space restrictions; questionable, but not investigated in detail.
Maintenance	without obvious problems	difficult, but possible
OH coil testing	included as a "must"	in sequence possible; time consuming

It is indisputable that the support structure for the solenoid solution is simple compared with that of the cluster solution. In the latter arrangement, where the LCT-coils are placed prone to each other by an angle of 23° , the support structure has to balance the forces between the coils. First considerations lead to the conclusion, that the construction of the support structure is complicate, eg. the cooling channels and the helium headers onto the case of the LCT coils prevent a continuous support system.

The distance between the coil windings and the LN_2 -shield is about half a meter for the solenoid solution, however, in the cluster solution this space is filled up by the coil case. Therefore an enlargement of the LN_2 -shield is envisaged, and that is also feasible because the LN_2 -shield consists of panel elements. This construction allows an easy enlargement.

The installation of the cluster arrangement is unquestionably much more difficult than in the solenoid case, but it seems feasible.

An open question is still the installation of a pulse coil, especially in the cluster configuration. Possible pulse coil arrangements are:

- two solenoids like in the IFSMTF in Oak Ridge,
- a pair of saddle coils,
- use of the POLO model coil.

Another open question is whether the LCT coil can sustain the pulse load during testing. Test results for the EU-LCT coil and for the Swiss-LCT-coil up to $\text{dB}/\text{dt} = 0.16 \text{ T/s}$ are available. It is difficult to extrapolate from $\text{dB}/\text{dt} = 0.16 \text{ T/s}$ to about 1 T/s , but according to [3.5] a rise of the losses by a factor of about 6 is expected. If the background field LCT-coils do not sustain the pulse load, a test without energized LCT-coils is possible, but then the maximum field is only about 7.5 T at the test coil conductor. Whether this is sufficient, has to be discussed. In any case, a comprehensive conductor pulse test seems to be questionable in the Cluster Test Facility.

A similar situation exists in the Solenoid Test Facility. Although the installation of a pulse coil is simpler, a comprehensive conductor pulse test for the OH conductor is questionable. This is due to the fact that the TF model coils are designed for $\text{dB}/\text{dt} = 1 \text{ T/s}$, but the OH model coil for 3 T/s . Due to the strong

coupling of the model coils, the latter value can not be reached without pulse overloading of the TF model coils.

A final solution of this problem is not given in this study. The question whether it is necessary to perform AC-loss measurements in the test facility or to use only short sample tests in auxiliary small test facilities is still under discussion. An intensive evaluation of the AC-loss measurements in the IFSMTF should help answer this question.

Maintenance work is possible without problems in the solenoid facility; it will be difficult, but possible in the cluster. The cluster configuration is mainly devoted for TF-model coil tests, and therefore a test coil exchange is not on the main line of the tasks of this test facility. However, it would be feasible to replace the TF-model coils by an OH-model coil for a test in sequence.

With respect to cooling, a new refrigerator is necessary for both facilities. As explained in Chapter 7, the 4.4 K equivalent cooling power requirements are between 2.2 and 2.8 kW.

The primary guide during the numerical evaluation was the magnetic field level to be achieved in the test facility. Both facilities fulfil the magnetic field requirements by NET. However the operation at the NET nominal current of 16 kA led to too high conductor lengths for both facilities. To stay in reasonable limits (given by M5) the current was raised to 22 kA. This is certainly an acceptable compromise from a technical point of view as short sample tests and pancake tests in SULTAN-III can be performed either at NET operating conditions (11 T, 16 kA) or/and at TOSKA-Upgrade conditions (11 T, 22 kA). These tests can deliver a solid, experimental basis for reliable extrapolation of data obtained from model coil tests in TOSKA-Upgrade to NET-operating conditions.

With respect to operation flexibility to reach the required field levels, there is the following difference between Cluster and Solenoid Test Facility:

Solenoid Test Facility:

- If OH model coil fails, then the maximum field at the KfK coil is 10.06 T and 9.81 T at SULTAN.
- If KfK model coil fails, then the maximum field at the OH coils is 8.04 T and 7.89 T at SULTAN.
- If SULTAN model coil fails, then the maximum field at the KfK model coil is 10.16 T and 9.96 at OH.

Cluster Test Facility:

- If KfK model coil or SULTAN model coil fails, then the other TF model coil has 9.2 T maximum field at conductor.
- If the EU-LCT coil fails, the maximum field at the model coils is 10.06 T.
- If the CH-LCT coil fails, the maximum field at the model coils is still 10.55 T.

If one coil fails, only a rise of current in the model coils is possible in case of the Solenoid Test Facility to reach the required field levels.

However, there are several means in the Cluster Test Facility in case of failure of one coil:

- if one model coil fails, the field at the LCT-coils decreases, and this decrease can be balanced by enhancement of the current in the LCT coils leading to a higher field at the survived model coil.
- if one LCT-coil fails, then the other experiences a lower conductor field, and again a current rise would balance that leading to higher field at the model coils.
- if one LCT-coil fails, the other can be cooled down to 1.8 K, if this can be provided in advance and support structure is added to the LCT-coils; again a current rise would lead to a higher field at the model coils.

It should be mentioned that the performance of the LCT coil is already proven. Therefore the risk of a Cluster Test failure is diminished compared with the Solenoid Test Facility.

Relevant stress and pressure data are given in table 13.4. Both test facilities don't hit in their characteristics all the NET requirements. Therefore additional preventive measures are considered to fulfil the NET requirements.

At a first glance, the solenoid solution seems to be the technically simpler one of both solutions. However, the important disadvantage of the solenoid solution is the constraint to a simultaneous test of TF- and PF-model coils leading to a higher risk.

Table 13.4 shows a comparison of characteristic test values required by NET (see table 2.1) and the values which can be reached in the Cluster and Solenoid Test Facilities.

Test costs estimate and man power requirements are discussed in Chapt. 8. A clear preference of one facility is not seen, if an OH test in the Cluster Test Facility is foreseen. If, however, the Test Facility is only devoted to TF model coil test, then only the Cluster Test Facility is meaningful.

The time schedule is discussed in Chapt. 9 and fits approximately in the NET development programme, if industrial contracts for conductor fabrication are placed and the tasks M6 and M7 are started before 1988.

Table 13.4: Comparison of Values required by NET and attainable Values in the Cluster and Solenoid Test Facilities.
All Values given in this Table are from FEM-Calculations.

	NET		Solenoid-Configuration S1			Cluster-Configuration C6	
	TF-Coil	OH-Coil	KfK-Coil	OH-Coil	Sultan-Coil	KfK-Coil	Sultan-Coil
Maximum Field [T]	11.4	11.5	12.27	11.62	11.54	12.1	12.0
Current [kA]	16	40	22	50	22	22	22
Axial Pressure [MPa]	140	100	66.4	57.9	66.5	27.4	26.3
Radial Pressure [MPa]	40	10	43.3	39.1	42.1	65.1	64.3
Hoop Stresses							
σ_{Hoop} [MPa]	140	200	209	222	185	310.7	309.9
τ_{max} [MPa]	30	30	19.3*	18*	20.7*	26.8	28.8

* For this calculation it was assumed that the pancake is supported by a rod at two areas and without a case.

14. Conclusions and Proposals

14.1 General

A study was undertaken in order to define a test facility for NET-TF-model coils. During the study the NET team proposed to investigate also the possibility to include an OH-(PF) model coil into the tests.

Two possible test facilities for NET-TF-(and also PF-) conductors were investigated and compared with each other from a technical point of view. The design was made under the constraint to use as much as possible the existing facility TOSKA at KfK, especially the installed vacuum vessel. Several alternatives were considered with different boundary conditions for both facilities.

One solution, using two LCT-coils as background field coils, is called Cluster Test Facility. The other one is called Solenoid Test Facility; here the conductors to be tested are wound to solenoids and use only their self-field as test field. Both facilities reach the required NET fields, but not all the pressure and stress levels. The main characteristics are compared and the solenoid solution seems to be the technically simpler one from an engineering point of view determined by modifications of the existing facility, installation, maintenance, and operation of the facility. However, the risk to reach the goal of the test is much higher because all pancakes made from different conductors must work altogether to get the design values.

The Cluster Test Facility has a higher operation flexibility compared with the Solenoid Test Facility as explained in Chapt. 13. It copes easier with a failure of a magnet. The performance of the LCT magnets is already proven. Therefore the risk to reach the test goals for NET is lower in the Cluster Test Facility.

Costs were estimated and a time schedule was worked out. The test programme and procedure were also outlined as also a further use of TOSKA and other test possibilities.

14.2 Conclusions

Some conclusions can be drawn:

- In both test facilities the required maximum magnetic field is reached but only operating the model coils with a conductor current of 22 kA (see Configuration C6 and S3), well above the NET nominal current of 16 kA. Otherwise the required total length of conductor is much longer, a few extra kilometers are needed (see Configuration C5 and S2).
- The Solenoid Configuration is technically simpler (easier accommodation in TOSKA, installation, maintenance, and operation of the facility). It does allow a simultaneous test of TF conductor and OH conductor and the model coils manufactured with them, but there are restrictions with respect to the test of the OH-Model coil due to the different dB/dt (3 T/s for PF and 1 T/s for TF). On one hand it means adding the risks of the manufacture of the TF and OH conductor and model coils - one of these may not be available in time. On the other hand, the Euratom and the Swiss coils have not been tested under the full operating conditions of TOSKA-Upgrade, C6. Main differences are: the much higher dB/dt required for NET TF coils than applied during the LCT tests (only 0.16 T/s), and the much higher out-of-plane loads in TOSKA-Upgrade (LCT 26.6 MN, TOSKA-Upgrade 93.1).
- The Cluster Test Facility has a higher operation flexibility in order to overcome a coil failure and make it possible to test the LCT-coils at 1.8 K in the same facility.
- Both facilities have to have additional preventive measures to apply forces to meet NET requirements.
- AC-loss measurements with added pulse coils are easier in a solenoid configuration than in a cluster configuration.
- Both facilities need in any case a new refrigeration system if built up in KfK.
- The costs of the model coils and the Facility seems to be enormous, but compared with the total costs of the NET-magnet system are they only in the order of 2 or 3 percent.

14.3 A Proposal to meet the Test Goals

One should assure oneself of a viable and working superconducting magnet solution for the NET-TF coils. This implies according to the opinion of the authors of this report:

- the pursuit of a Nb₃Sn-conductor concept for NET-TF magnets which includes small sample tests and single pancake tests and model coil tests:
Small sample tests should proof the feasibility of manufacturing basic Nb₃Sn strands with predicted superconducting properties. Single pancake tests should proof that the manufacture of one to one conductor is possible and the winding process is feasible without loosing superconducting properties. Model coil tests should proof the feasibility of manufacturing coils from these conductors and the operation under NET load conditions.
- the pursuit of a backup solution with NbTi-conductors subcooled to 1.8 K.

To reach this goal we propose:

- the construction of a Cluster Test Facility at KfK (TOSKA-Upgrade), because it is the most flexible configuration in order to overcome a coil failure, and has therefore the lowest risk to reach the goals required by NET.
- double pancake tests in SULTAN III, because this step in between conductor tests and model coil tests confirms (or not) conductor performance after producing pancakes with a few windings and lowers the risk for model coil construction.
- a NbTi-1.8 K test of a LCT magnet in order to have a backup solution. This test can be either eventually integrated into the Cluster Test Facility or performed as single coil test.